

เคมีซูปราโมเลคิวลาร์ของไดทอปิกแอนไอออนเซ็นเซอร์และโมเลกุลแอมฟิฟิลิก



นางสาว จอมใจ สุกใส

สถาบันวิทยบริการ

จุฬาลงกรณ์มหาวิทยาลัย

วิทยานิพนธ์นี้เป็นส่วนหนึ่งของการศึกษาตามหลักสูตรปริญญาวิทยาศาสตรดุษฎีบัณฑิต

สาขาวิชาเคมี ภาควิชาเคมี

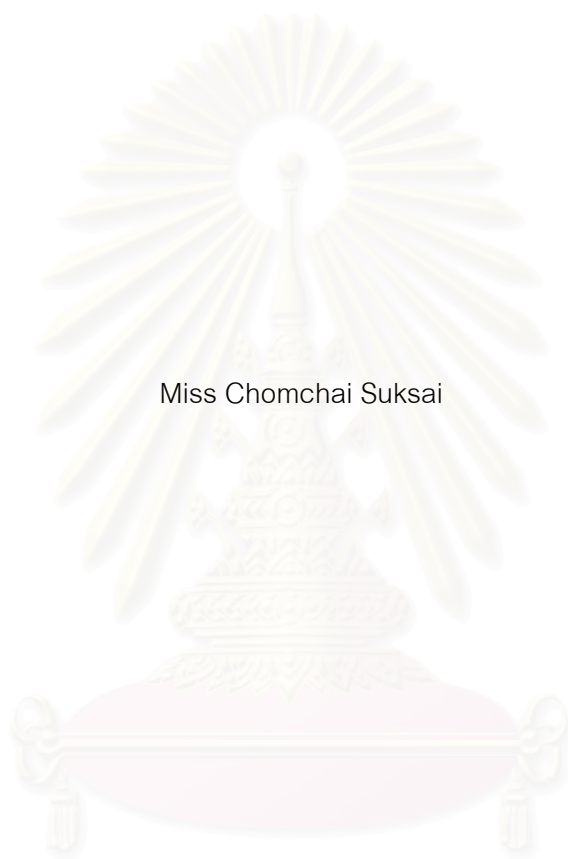
คณะวิทยาศาสตร์ จุฬาลงกรณ์มหาวิทยาลัย

ปีการศึกษา 2549

ISBN 974-14-3905-9

ลิขสิทธิ์ของจุฬาลงกรณ์มหาวิทยาลัย

Supramolecular Chemistry of Ditopic Anion Sensors and Amphiphilic Molecules



Miss Chomchai Suksai

สถาบันวิทยบริการ

A Dissertation Submitted in Partial Fulfillment of the Requirements
for the Degree of Doctor of Philosophy Program in Chemistry

Department of Chemistry

Faculty of Science

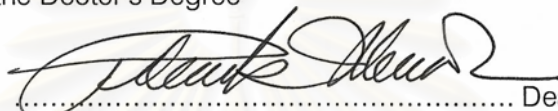
Chulalongkorn University

Academic year 2006

ISBN 974-14-3905-9

Thesis Title Supramolecular Chemistry of Ditopic Anion Sensors and
 Amphiphilic Molecules
By Miss Chomchai Suksai
Filed of study Chemistry
Thesis Advisor Associate Professor Thawatchai Tuntulani, Ph.D.

Accepted by the Faculty of Science, Chulalongkorn University in Partial Fulfillment of
the Requirements for the Doctor's Degree


..... Dean of the Faculty of Science
(Professor Piamsak Menasveta, Ph.D.)

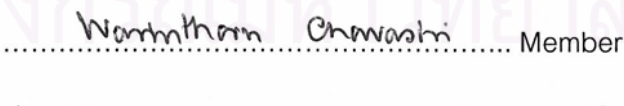
THESIS COMMITTEE

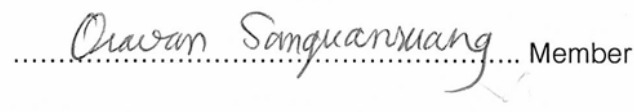

..... Chairman
(Professor Sophon Roengsumran, Ph.D.)

T. Tuntulani
..... Thesis Advisor
(Associate Professor Thawatchai Tuntulani, Ph.D.)


..... Member
(Assistant Professor Tienthong Thongpanchang, Ph.D.)


..... Member
(Associate Professor Orawon Chailapakul, Ph.D.)


..... Member
(Assistant Professor Warinthorn Chavasiri, Ph.D.)


..... Member
(Oravan Sanguanruang, Ph.D.)

จอมใจ สุกใส : เคมีซูพราโมเลกุลาร์ของไดทอปิกแอนไอออนเซ็นเซอร์และโมเลกุลแอมฟิฟิลิก (SUPRAMOLECULAR CHEMISTRY OF DITOPIC ANION SENSORS AND AMPHIPHILIC MOLECULES) อ. ที่ปรึกษา: รศ. ดร. ธวัชชัย ตันฑุลานี, 174 หน้า. ISBN 974-14-3905-9.

ได้ทำการสังเคราะห์เฮเทอโรไดทอปิกเซนเซอร์ทางเคมีไฟฟ้าที่มีควานอ์เธอร์สำหรับจับกับแคทไอออนและอะมิโนเฟอรโรซีนสำหรับจับกับแอนไอออนโมเลกุล (2d) และ (3d) โดยที่ส่วนประกอบทั้งสองอยู่บนโครงสร้างของไดเอซา-18-คราวน์-6และพาราเทอร์เทียรีบิวทิลคาลิกซ์[4]อารีน และทำการศึกษาความสามารถในการจับกับเฮไลด์แอนไอออนโดยใช้เทคนิค $^1\text{H-NMR}$ และเทคนิคทางเคมีไฟฟ้าทั้งในสถานะที่ปราศจากและมีไอออนของโลหะ Na^+ และ K^+ อยู่ในระบบโดยทำการเปรียบเทียบกับโมโนทอปิกรีเซปเตอร์ (1) จากการทดลองพบว่าเมื่อมีโซเดียมไอออนอยู่ในระบบจะส่งผลให้เซนเซอร์ทั้งสองโมเลกุลมีความเฉพาะเจาะจงอย่างสูงในการจับกับโบรไมด์ไอออน นอกจากนี้ยังพบว่าโมเลกุลของเซนเซอร์ทั้งสองดังกล่าวสามารถนำมาใช้เป็นเฮเทอโรไดทอปิกแอนไอออนเซ็นเซอร์ทางเคมีไฟฟ้าของคลอไรด์ไอออนเมื่อมี Na^+ หรือ K^+ อยู่ในระบบ

ได้ทำการสังเคราะห์แอมฟิฟิลิกรีเซปเตอร์ (8b) ที่มีลักษณะเป็นโมเลกุลที่มีขนาดใหญ่ โดยมีแอนไอออนอยู่ที่ส่วนหัวของโมเลกุลและมีสายโซ่อัลคิลชนิดเดี่ยวอยู่ที่ส่วนปลายของโมเลกุล และได้ทำการศึกษาสมบัติการเข้ารวมตัวกันและสมบัติทางเคมีของโฮสต์-เกสต์ของสารประกอบดังกล่าว จากการทดลองพบว่าในสถานะที่ไม่มีโมเลกุลของเกสต์ ปลายของสายโซ่ยาวของ (8b) จะสอดเข้าไปในช่องว่างของโมเลกุลและทำให้เกิดกระบวนการเชลฟี-แอสเซมบลีโดยมีรูปร่างของโมเลกุลเป็นหลอดขนาดเล็กที่มีความยาวอยู่ในระดับไมโครเมตร นอกจากนี้ยังพบว่าสายโซ่ดังกล่าวสามารถถูกแทนที่ได้โดยอะครีลิคซีเนียมโบรไมด์เกสต์ซึ่งทำให้โมเลกุลของ (8b) ที่เกิดการเชลฟี-แอสเซมบลีมีการเปลี่ยนแปลงทั้งขนาดและรูปร่างของโมเลกุล จากผลการทดลองโดยใช้การละลายของไนล์เรดพบว่าการรวมตัวที่เกิดขึ้นใหม่ดังกล่าวคือไมเซลล์ โดยมีค่า cmc อยู่ที่ประมาณ $35 \mu\text{M}$ จากผลการทดลองดังกล่าวเป็นครั้งแรกที่แสดงให้เห็นว่าสมบัติทางเคมีของโฮสต์-เกสต์ที่มีลักษณะเฉพาะสามารถควบคุมการเปลี่ยนแปลงทั้งขนาดและรูปร่างของโมเลกุลขนาดเล็กที่อยู่รวมกันได้

ภาควิชา.....เคมี..... ลายมือชื่อนิสิต.....จอมใจ.....สุกใส.....
 สาขาวิชา.....เคมี..... ลายมือชื่ออาจารย์ที่ปรึกษา.....ธวัชชัย ตันฑุลานี.....
 ปีการศึกษา ...2549..... ลายมือชื่ออาจารย์ที่ปรึกษาร่วม.....

4573806123 : MAJOR CHEMISTRY

KEY WORD: SUPRAMOLECULAR CHEMISTRY / HETERODITOPIC SENSORS / ELECTROCHEMICAL ANION SENSORS / HOST-GUEST INTERACTIONS / SELF-ASSEMBLY

CHOMCHAI SUKSAI: SUPRAMOLECULAR CHEMISTRY OF DITOPIC ANION SENSORS AND AMPHIPHILIC MOLECULES. THESIS ADVISOR: ASSOC. PROF. THAWATCHAI TUNTULANI, Ph.D. 174 pp. ISBN 974-14-3905-9.

Two heteroditopic electrochemical anion sensors (**2d**) and (**3d**) comprised of crown ether for cation recognition and amidoferrocene for anion complexation using diaza-18-crown-6 and *p-tert*-butylcalix[4]arene as scaffold have been developed. Halide binding abilities of those two receptors in the presence and absence of Na⁺ and K⁺ cations have been investigated by ¹H NMR and electrochemical techniques compared to the monotopic receptor (**1**). From NMR studies, the proposed receptors presented the highest selectivity for Br⁻ in the presence of Na⁺. In addition, they can act as electrochemical sensors for Cl⁻ in the presence of Na⁺ and K⁺.

A new amphiphilic receptor containing a macrocyclic anionic headgroup and a single alkyl chain was prepared through an efficient templated synthesis, receptor (**8b**). The interdependence of the aggregation behavior and the host-guest chemistry was studied. In the absence of any guest the terminus of the alkyl chain of the receptor is included inside the hydrophobic cavity of the macrocycle leading to self-assembly into micrometer-long nanotubes. The alkyl chain can be displaced by an acridizinium bromide guest, which leads to a dramatic change in aggregate size and morphology. Studies of the solubilization of Nile red suggest that the resulting aggregates are micelles having a cmc of around 35 μM. These results represent one of the first examples in which specific host-guest chemistry controls the size and shape of nanoscale aggregates.

Department.....Chemistry.....Student's signature.....*Chomchai Sukasai*.....
 Field of study.....Chemistry..... Advisor's signature.....*Dr. Tuntulani*.....
 Academic year2006..... Co-advisor's signature.....

ACKNOWLEDGEMENTS

I would like to express highest appreciation to my Ph.D. thesis supervisor, Associate Professor Thawatchai Tuntulani, for his guidance throughout the Ph.D. process, and all of the hard work involved in supervising me. I would also like to thank Dr. Sijbren Otto, my second supervisor, who has been able to devote large amounts of time and effort to provide me with advice, support and training with many of the techniques involved in my research. In addition, I would like to thank and pay my respect to Professor Jeremy Sanders, Professor Sophon Roengsumran, Assistant Professor Tienthong Thongpanchang, Associate Professor Orawan Chailapakul, Assistant Professor Warinthorn Chavasiri and Dr. Orawan Sanguanruang for their valuable suggestions and comments as committee members and thesis examiners.

Nevertheless, I would like to thank the members of the Supramolecular Chemistry Research Unit at the Department of Chemistry Chulalongkorn University and the members of Sanders and Otto groups at the Department of Chemistry University of Cambridge for all the helps. There are too many to list here, but I would like to single a few of them out for various reasons. A lot of people outside of the group have been helpful. I would like to thank Dr. Jeremy N. Skepper and people at Multi-Imaging Center (MIC) at the Department of Anatomy University of Cambridge for Transmission Electron Microscope experiments, Associate Professor Narongsak Chaichit, Assistant Professor Nongnuj Muangsin, Assistant Professor Chaveang Pakawatchai and Associate Professor Palangpon Kongsaree for X-ray crystallography experiments and many useful suggestions.

I would like to express my deepest gratitude to my parents and family for their love, kindness, encouragement, and financial support throughout my life. Finally, I would like to thank the Thailand Research Fund and EPSRC and my parents for financial support.

CONTENTS

	Page
ABSTARCT IN THAI.....	iv
ABSTRACT IN ENGLISH.....	v
ACKNOWLEDGEMENTS.....	vi
CONTENTS.....	vii
LIST OF TABLES.....	xii
LIST OF FIGURES.....	xiv
LIST OF SCHEMES.....	xxi
LIST OF ABBREVIATIONS AND SIGNS.....	xxiii
CHAPTER I SUPRAMOLECULAR CHEMISTRY.....	1
1.1 Concept of Supramolecular Chemistry.....	1
1.2 Molecular Recognitions to Chemical Receptors and Chemical Sensors....	3
1.3 Non-covalent Interactions to Molecular Assembles.....	4
CHAPTER II HALIDE ANIONS SENSING BY HETERODITOPIC ELECTROCHMICAL ANION SENSORS.....	6
2.1 Introduction.....	6
2.1.1 Chemistry of Anions.....	6
2.1.2 Chemical Receptors for Anions.....	8
2.1.3 Chemical Sensors for Anions.....	14
2.1.4 Electrochemical Anion Sensors.....	16
2.1.5 Hetroditopic Receptors and Sensors.....	19
2.1.6 Ion-Pair receptors and Sensors.....	20
2.1.7 Literature Review of Ion-Pair Receptors and Sensors.....	21
2.1.8 Objectives of this Research.....	26
2.2 Experimental Section.....	28
2.2.1 Synthesis of Diaza Crown Ether and Calix[4]arene Derivatives Containing Amidoferrocene.....	28
2.2.1.1 General Procedure.....	28

	Page
2.2.1.1.1 Analytical Measurements.....	28
2.2.1.1.2 Materials.....	29
2.2.1.2 Synthesis.....	30
2.2.1.2.1 Preparation of 1,1'-bis(phenylamino carbonyl)ferrocene (1).....	30
2.2.1.2.2 Preparation of diaza-18-crown-6 (2a).....	31
2.2.1.2.3 Preparation of <i>N,N'</i> -di-(3-nitrobenzyl)-4,13- diaza-18-crown-6 (2b).....	32
2.2.1.2.4 Preparation of <i>N,N'</i> -di-(3-aminobenzyl) - 4,13-diaza-18-crown-6 (2c).....	33
2.2.1.2.5 Preparation of <i>N,N'</i> -di-(3-amidoferrocenyl benzyl)-4,13-diaza-18-crown-6 (2d).....	34
2.2.1.2.6 Preparation of 5,11,17,23- tetra- <i>tert</i> -butyl - 25,27-dihydroxycalix[4] arene[4]-crown-6 (3a).....	35
2.2.1.2.7 Preparation of 5,11,17,23- tetra- <i>tert</i> -butyl - 25,27-di-(3-nitrobenzyl) calix[4]arene- crown-6 (3b).....	36
2.2.1.2.8 Preparation of 5,11,17,23- tetra- <i>tert</i> -butyl - 25,27-di-(3-aminobenzyl) calix[4]arene- crown-6 (3c).....	37
2.2.1.2.9 Preparation of 5,11,17,23- tetra- <i>tert</i> -butyl - 25,27-di-(3-amidoferrocenyl benzyl) calix [4]arene-crown-6 (3d).....	39
2.2.2 Binding Studies by NMR Titrations.....	41
2.2.2.1 General Procedure.....	41
2.2.2.1.1 Apparatus.....	41
2.2.2.1.2 Chemicals.....	41

	Page
2.2.2.2 Experimental Procedure.....	41
2.2.2.2.1 Anion Binding Studies of Receptors 1 , 2d and 3d	41
2.2.2.2.2 Cation Binding Studies of Receptors 2d and 3d with NaClO ₄ and KPF ₆	43
2.2.2.2.3 Simultaneous Cation and Anion Binding Studies of Receptors 2d and 3d	44
2.2.3 Electrochemical Studies.....	45
2.2.3.1 General Procedure.....	45
2.2.3.1.1 Apparatus.....	45
2.2.3.1.2 Chemicals.....	45
2.2.3.2 Experimental Procedure.....	46
2.2.3.2.1 Anion Bindings Studies of Receptors 1 , 2d and 3d	46
2.2.3.2.1 Cation Bindings Studies of Receptors 2d and 3d	47
2.2.3.2.3 Simultaneous Cation and Anion Binding Studies of Receptors 2d and 3d	48
2.3 Results and Discussion.....	49
2.3.1 Synthesis and Solid State Structure of 1,1'-bis(phenylamino carbonyl)ferrocene 1	49
2.3.2 Synthesis and Characterization of Receptor 2d	62
2.3.3 Synthesis and Characterization of Receptor 3d	63
2.3.4 Binding Properties of Receptors 2d and 3d towards Alkali Metal Cations by NMR Studies.....	65
2.3.5 Binding Properties of Receptors 1 , 2d and 3d with Anionic Guests in the Absence and Presence of Alkali Metal Cations by NMR Studies.....	70
2.3.6 Solid State Structure of [2d .NaCl] Complex.....	84

	Page
2.3.7 Electrochemical Properties of Receptors 1 , 2d and 3d and their Electrochemical Sensing Towards Cationic and Anionic Guests.	87
2.3.8 Electrochemical Studies of Receptors 2d and 3d towards Cationic Guests.....	94
2.3.9 Electrochemical Studies of Receptors 1 , 2d and 3d towards Anionic Guests in the Absence and Presence of Alkali Metal Cations.....	98
CHAPTER III CONTROLLING THE MORPHOLOGY OF AGGREGATES OF AN AMPHIPHILIC SYNTHETIC RECEPTOR THROUGH HOST-GUEST INTERACTIONS.....	108
3.1 Introduction.....	108
3.1.1 Template Effect : Thermodynamic and Kinetic Approaches.....	108
3.1.2 Oxidation of Thiols to Disulfides.....	111
3.1.3 Dynamic Combinatorial Chemistry(DCC).....	112
3.1.4 Aggregation of Amphiphiles : Micelles Formation.....	119
3.1.5 Objectives of this Research.....	121
3.2 Experimental Section.....	123
3.2.1 Synthesis of Dithiols Building Blocks and Guest Molecules.....	123
3.2.1.1 General Procedure.....	123
3.2.1.1.1 Analytical Measurements.....	123
3.2.1.1.2 Materials.....	123
3.2.1.2 Synthesis.....	123
3.2.1.2.1 Preparation of 3,5-bis-dimethylcarbamoylsulfanyl benzoic acid (2).....	123
3.2.1.2.2 Preparation of 3,5-bis-dimethylcarbamoylsulfanyl benzoyl chloride (3).....	124
3.2.1.2.3 Preparation of <i>N</i> -dodecyl-3,5-dimethylcarbamoyl sulfanyl benzamide (4).....	125

	Page
3.2.1.2.4 Preparation of <i>N</i> -dodecyl-3,5-dimercapto benzamide (5).....	126
3.2.2 Preparation and Purification of Receptor 8b	127
3.2.3 Analytical HPLC.....	128
3.2.4 LC-MS Method and Parameters.....	128
3.2.5 Isomers Discrimination of Receptor 8b	128
3.2.6 Isothermal Titration Calorimetry.....	129
3.2.7 Dynamic Light Scattering Studies	129
3.2.8 Transmission Electron Microscopy (TEM).....	130
3.2.9 Nile red Solubilization.....	130
3.2.10 NMR Titrations : Micelles Formation.....	130
3.3 Results and Discussion.....	131
3.3.1 Preparation of Macrocyclic Receptor 8b	131
3.3.2 Isomers Discrimination of Receptor 8b	133
3.3.3 Binding Studies of Receptor 8b	135
3.3.4 Self-Assembly of Amphiphilic Receptor 8b	137
3.3.5 Micelles Formation.....	141
CHAPTER IV CONCLUSIONS	144
4.1 Halide Anions Sensing by Hetroditopic Electrochemical Anion Sensors...	144
4.2 Controlling the morphology of Aggregates of an Amphiphilic Synthetic Receptor through Host-Guest Interactions.....	146
4.3 Suggestions for Future Works.....	147
REFERENCES	148
APPENDICES	164
APPENDIX A	165
APPENDIX B	168
VITA	174

LIST OF TABLES

Tables	Page
2.1 Volume and concentration of guests (as tetrabutylammonium salts) which have been used in the experiments.....	42
2.2 Volume and concentration of metal salts (NaClO ₄ and KPF ₆) which have been used in the experiments.....	43
2.3 Volume and concentration of guests (as tetrabutylammonium salts) which have been used in the experiments.....	44
2.4 Volume and concentration of guests (as tetrabutylammonium salts) which have been used in the experiments.....	46
2.5 Volume and concentration of metal salts (NaClO ₄ and KPF ₆) which have been used in the experiments.....	47
2.6 Volume and concentration of guests (as tetrabutylammonium salts) which have been used in the experiments.....	48
2.7 Crystallographic data and structure refinement of compound 1.....	51
2.8 Selected bond lengths [Å] and angles [°] for compound 1.....	52
2.9 Hydrogen bond length [Å] and angles [°] for compound 1.....	53
2.10 Crystallographic data and structure refinement of compound 1 after recrystallization in MeOH.....	60
2.11 Selected bond lengths [Å] and angles [°] for compound 1 after recrystallization in MeOH.....	61
2.12 Binding constants (<i>K</i>) for Na ⁺ and K ⁺ cations complexes with receptors 2d and 3d in 5% CD ₃ CN/CDCl ₃	69
2.13 Binding constants (<i>K</i>) for receptors 1, 2d and 3d with anionic guests (as tetrabutylammonium salts) in 5% CD ₃ CN/CDCl ₃	72
2.14 Crystallographic data and refinement of [2d.NaCl].CHCl ₃	85
2.15 Selected bond lengths [Å] and angles [°] for compound [2d.NaCl].CHCl ₃	86

Table	Page
2.16 Electrochemical data (Fc/Fc^+) for receptors 1 , 2d and 3d in 40% $CH_3CN:CH_2Cl_2$ with 0.1 M $TBAPF_6$ at scan rate 100 mV/s.....	89
2.17 Cyclic voltammetric data and calculated binding constants (K_f) of the co-bound complexes 2d and 3d with Na^+ and K^+ in 40% $CH_3CN:CH_2Cl_2$ with 0.1 M $TBAPF_6$ at scan rate 100 mV/s.....	97
2.18 Electrochemical recognition data (ΔE) for receptors 1 , 2d and 3d towards Cl^- and Br^- in 40% $CH_3CN:CH_2Cl_2$ with 0.1 M $TBAPF_6$ at scan rate 100 mV/s.....	102
3.1 HPLC conditions for isomers discrimination of receptor 8b	129
3.2 Thermodynamic data for the binding of macrocycles 8a and 8b with guest 9 and 10 in 10 mM borate buffer pH 9 at 298 K.....	136

LIST OF FIGURES

Figure	Page
2.1 Geometries of various anions.....	7
2.2 Types of interactions available for receptor and anion binding.....	7
2.3 Functional groups providing hydrogen bonding interactions.....	9
2.4 Redox-active molecules for electrochemical sensing (a) ferrocene, (b) cobaltocenium, (c) tetrathiafulvalene and (d) anthraquinone.....	16
2.5 Structure of receptor 2.46 and the X-ray crystal structure of 2.46 with CsF.....	24
2.6 ¹ H-NMR spectrum of compound 1 in CDCl ₃	49
2.7 X-ray structure of compound 2.51 in 50% probability ellipsoids shows the intramolecular hydrogen bonds of amidoferrocene and hydroxyl groups at the lower rim of calix[4]arene. Hydrogen atoms of phenyl rings and cyclopentadienyl rings are omitted for clarity.....	50
2.8 Part of the polymeric chain of receptor 1 . Ellipsoids represent 50% probability, hydrogen bonds are omitted for clarity.....	53
2.9 Plot of polymeric structures of (a) LiCp and (b) KCp.....	54
2.10 Presented the helical structure and pseudo hexagonal structure of compound 1	56
2.11 ORTEP plots of (1) with 50% probability thermal ellipsoids. Hydrogen atoms of phenyl rings and cyclopentadienyl rings are omitted for clarity...	59
2.12 ¹ H-NMR spectrum of receptor 2d in CDCl ₃	63
2.13 ¹ H-NMR spectrum of receptor 3d in CDCl ₃	65
2.14 ¹ H-NMR spectra of receptor 2d with NaClO ₄ and KPF ₆ at 1 equivalent in 5% CD ₃ CN/CDCl ₃ , where ★ is NH protons, ▲ and △ are H _a and H _b protons of ferrocene. The peaks in the square refer to CH ₂ of crown ether part.....	67

Figure	Page
2.15 $^1\text{H-NMR}$ spectra of receptor 2d with NaClO_4 and KPF_6 at 1 equivalent in 5% $\text{CD}_3\text{CN}/\text{CDCl}_3$, where \star is NH protons, \blacktriangle and \triangle are H_a and H_b protons of ferrocene and \blacklozenge is CH_2 bridging methylene protons. The peaks in the square refer to CH_2 of crown ether part.....	68
2.16 Proposed the complex structures of (a) 2d and (b) 3d with alkali metal cations	69
2.17 Proposed the binding structures of amidoferrocene unit with halide anionic guests.....	70
2.18 Titration curves of receptors (a) 1 , (b) 2d and (c) 3d with various halide anions (as tetrabutylammonium salts) in 5% $\text{CD}_3\text{CN}/\text{CDCl}_3$	71
2.19 Cobaltocenium receptor 2.52 and crystal structure of 2.52 complex with Br^-	73
2.20 Change in NH chemical shift (ΔNH) of receptor 2d as a function of increasing amount of TBA chloride, where \blacklozenge free 2d , \blacksquare presence of Na^+ and \triangle presence of K^+ 1 equivalent in 5% $\text{CD}_3\text{CN}/\text{CDCl}_3$	74
2.21 $^1\text{H-NMR}$ titration spectra of $[\text{2d.Na}^+]$ with TBA bromide at room temperature in 5% $\text{CD}_3\text{CN}/\text{CDCl}_3$, where \star is NH protons, \bullet is <i>ortho</i> protons to amide groups and \blacktriangle is H_a protons of cyclopentadienyl rings.....	75
2.22 Change in NH chemical shift (ΔNH) of receptor 2d as a function of increasing amount of TBA bromide, where \blacklozenge free 2d , \blacksquare presence of Na^+ and \triangle presence of K^+ 1 equivalent in 5% $\text{CD}_3\text{CN}/\text{CDCl}_3$	76
2.23 $^1\text{H-NMR}$ titration spectra of $[\text{2d.Na}^+]$ with TBA iodide at room temperature in 5% $\text{CD}_3\text{CN}/\text{CDCl}_3$, where \star is NH protons and \blacktriangle is H_a protons of cyclopentadienyl rings.....	76
2.24 $^1\text{H-NMR}$ titration spectra of $[\text{2d.K}^+]$ with TBA iodide at room temperature in 5% $\text{CD}_3\text{CN}/\text{CDCl}_3$, where \star is NH protons and \blacktriangle is H_a protons of cyclopentadienyl rings.....	77

Figure	Page
2.25 Change in NH chemical shift (Δ NH) of receptor 2d as a function of increasing amount of TBA iodide, where \blacklozenge free 2d , \blacksquare presence of Na^+ and \triangle presence of K^+ 1 equivalent in 5% $\text{CD}_3\text{CN}/\text{CDCl}_3$	77
2.26 $^1\text{H-NMR}$ titration spectra of $[\mathbf{3d.Na}^+]$ with TBA bromide at room temperature in 5% $\text{CD}_3\text{CN}/\text{CDCl}_3$, where \star is NH protons	78
2.27 Change in NH chemical shift (Δ NH) of receptor 3d as a function of increasing amount of TBA bromide, where \blacklozenge free 3d and \blacksquare presence of Na^+ 1 equivalent in 5% $\text{CD}_3\text{CN}/\text{CDCl}_3$	78
2.28 $^1\text{H-NMR}$ titration spectra of $[\mathbf{3d.Na}^+]$ with TBA acetate at room temperature in 5% $\text{CD}_3\text{CN}/\text{CDCl}_3$, where \star is NH protons	79
2.29 Change in NH chemical shift (Δ NH) of receptor 3d as a function of increasing amount of TBA acetate, where \blacklozenge free 3d and \blacksquare presence of Na^+ 1 equivalent in 5% $\text{CD}_3\text{CN}/\text{CDCl}_3$	79
2.30 The proposed structure of the contact ion-pair complexes of receptors (a) 2d and (b) 3d	80
2.31 X-ray structure of bridge-cobaltoceniumamido calix[4]arene upon complexes with chloride anion.....	81
2.32 Partial $^1\text{H-NMR}$ spectra of co-bound metal complexes of receptor 2d in the presence of 4 equivalents of halide anions at room temperature in 5% $\text{CD}_3\text{CN}:\text{CDCl}_3$	82
2.33 Partial variable temperature $^1\text{H-NMR}$ spectra of co-bound receptor $[\mathbf{2d.Na}^+]$ in the presence of TBA chloride 4 equivalents in 5% $\text{CD}_3\text{CN}:\text{CDCl}_3$	82
2.34 Front and side view of the X-ray crystal structure of $[\mathbf{2d.NaCl}]\cdot\text{CHCl}_3$	84
2.35 Cyclic voltammograms of receptors 1 , 2d and 3d in 40% $\text{CH}_3\text{CN}:\text{CH}_2\text{Cl}_2$ with 0.1 M TBAPF_6 at scan rate 100 mV/s.....	88
2.36 Cyclic voltammograms of receptors (a) 1 and (b) 3d with 0.1 M TBAPF_6 in 40% $\text{CH}_3\text{CN}:\text{CH}_2\text{Cl}_2$ at scan rate 20, 100, 200, 500 and 1000 mV/s.....	90

Figure	Page
2.37 Plots of currents (I_p) and square root ($V^{1/2}$) of receptors (a) 1 and (b) 3d with 0.1 M TBAPF ₆ in 40% CH ₃ CN:CH ₂ Cl ₂	91
2.38 Cyclic voltammograms of receptors 2d with 0.1 M TBAPF ₆ in 40% CH ₃ CN:CH ₂ Cl ₂ at scan rate 50, 100 and 200 mV/s.....	92
2.39 Cyclic voltammograms of receptor 2d in the presence of 1 equivalent of NaClO ₄ and KPF ₆ in 40% CH ₃ CN:CH ₂ Cl ₂ with 0.1 M TBAPF ₆ at scan rate 100 mV/s.....	95
2.40 Cyclic voltammograms of receptor 3d in the presence of 1 equivalent of NaClO ₄ and KPF ₆ in 40% CH ₃ CN:CH ₂ Cl ₂ with 0.1 M TBAPF ₆ at scan rate 100 mV/s.....	96
2.41 Receptor 2.53 and proposed the binding structure of its complex with alkali metal cations.....	97
2.42 Cyclic voltammograms of receptor 1 with TBA chloride 4.0 equivalent in 40% CH ₃ CN:CH ₂ Cl ₂ with 0.1 M TBAPF ₆ at scan rate 100 mV/s.....	100
2.43 Cyclic voltammograms of receptor [2d.Na⁺] with TBA chloride 1.0 and 4.0 equivalent in 40% CH ₃ CN:CH ₂ Cl ₂ with 0.1 M TBAPF ₆ at scan rate 100 mV/s.....	102
2.44 Cyclic voltammograms of receptor [2d.K⁺] with TBA chloride 0.5 and 4.0 equivalent in 40% CH ₃ CN:CH ₂ Cl ₂ with 0.1 M TBAPF ₆ at scan rate 100 mV/s.....	104
2.45 Square voltammograms of [2d.K⁺] with TBA chloride 1.0 and 4.0 equivalent in 40% CH ₃ CN:CH ₂ Cl ₂ with 0.1 M TBAPF ₆ at scan rate 100 mV/s.....	104
2.46 Square voltammograms of [3d.Na⁺] with TBA acetate 1.0 and 4.0 equivalent in 40% CH ₃ CN:CH ₂ Cl ₂ with 0.1 M TBAPF ₆ at scan rate 100 mV/s.....	105
3.1 Reversible reactions used in dynamic combinatorial chemistry.....	114

Figure	Page
3.2 HPLC analyses of the DCL made from dithiols 3.15 , 3.16 and 3.17 . (A) in the absence of any templates, (B) in the presence of 3.18 inducing the amplification of host 3.20 , and (C) in the presence of morphine derivative 3.19 leading to the amplification of host 3.21	117
3.3 HPLC analysis of the solution obtained 24 h after mixing building blocks 6 (6.67 mM), 5 (3.33 mM) and template 9 (10 mM) in DMSO.....	132
3.4 A mass spectrum retention time 31 min (top) and 36.5 min (bottom) for receptor 8b meso and 8b rac , respectively.....	132
3.5 HPLC chromatograms of the product mixture obtained upon re-equilibration of (a) receptor 8b (major <i>rac</i> isomer; 0.1 mM) and (b) receptor 8b (minor <i>meso</i> isomer; 0.1 mM) in the building block 7 (1 equivalent) in H ₂ O(pH 9):CH ₃ CN 1:1. the top traces represent the HPLC analysis of an independently generated mixture made from building blocks 6 rac and 7 , which contains all stereoisomers of macrocycle 8a which we have assigned previously.....	134
3.6 Isothermal titration isotherms of receptor 8b with guest 9 (left) and guest 10 (right) in 10 mM borate buffer pH 9.....	136
3.7 Part of ¹ H-NMR spectra of amphiphilic receptor 8b in (a) D ₂ O:CD ₃ CN 1:1, (b) D ₂ O(pD 8.7) and (c) D ₂ O(pD 8.7):MeOD- <i>d</i> ₄ 2:1 at room temperature.....	137
3.8 Part of the ¹ H-NMR titration of MeOD- <i>d</i> ₄ into a solution of receptor 8b rac (1 mM in D ₂ O (pD 8.7)). The volume ratio of D ₂ O (pD 8.7) to MeOD- <i>d</i> ₄ was : (a) 1:0, (b) 1:0.16, (c) 1:0.32, (d) 1:0.5, (e) 1:0.64, (f) 1:0.8, (g) 1:1, and (f) 1:1.16.....	138
3.9 Part of the VT- ¹ H-NMR of receptor 8b rac 1 mM in D ₂ O pD 8.7.....	138
3.10 Part of the TOCSY NMR spectrum of receptor 8b rac 0.6 mM in D ₂ O (pD 8.7):MeOD- <i>d</i> ₄ 2:1 ratio.....	139

Figure	Page
3.11 Transmission electron micrograph of negatively stained (2% PTA:phosphotungstic acid) assemblies receptor 8b (0.1 mg/mL) in 0.10 mM borate buffer pH 9, scale bar represents 1 μm	140
3.12 Cartoon representation of different modes of inclusion of the alkyl chain in the cavity of receptor 8b	141
3.13 Part of the ^1H -NMR spectrum of amphiphilic receptor 8b upon addition guest 10 at 330 K in D_2O pD 8.7.....	142
3.14 (a) Absorption spectra of Nile Red in the solution of 0.1 mM of 8b in the absence of 0.4 mM of 10 . (b) Emission intensity of different saturated solutions of Nile Red at 640 nm ($\lambda_{\text{ex}} = 570 \text{ nm}$) versus concentration of 8b • 10 in 10 mM borate buffer pH 9.....	143
A1 ^1H NMR spectra of <i>N,N'</i> -di-(3-aminobenzyl) 4,13-diaza-18-crown-6 (2c)...	166
A2 ^1H -NMR spectra of 5,11,17,23-Tetrakis(1,1-dimethyl ethyl)-25,27-di(3-nitro benzyl) calix[4]arene-crown-6 (3b).....	166
A3 ^1H NMR spectra of 5,11,17,23-Tetrakis(1,1-dimethyl ethyl)-25,27-di(3-amino benzyl) calix[4]arene-crown-6 (3c).....	167
B1 ^1H NMR spectrum of 3,5-bis-dimethylcarbamoylsulfanyl benzoic acid....	169
B2 ^{13}C NMR spectrum of 3,5-bis-dimethylcarbamoylsulfanyl benzoic acid.....	169
B3 ^1H NMR spectrum of <i>N</i> -dodecyl-3,5-dimethylcarbamoyl sulfanyl benzamide.....	170
B4 ^{13}C NMR spectrum of <i>N</i> -dodecyl-3,5-dimethylcarbamoyl sulfanyl benzamide.....	170
B5 ^1H NMR spectrum of <i>N</i> -dodecyl-3,5-dimercaptobenzamide.....	171
B6 ^{13}C NMR spectrum of <i>N</i> -dodecyl-3,5-dimercaptobenzamide.....	171
B7 ^1H NMR spectrum of receptor 8b <i>rac</i> isomer.....	172
B8 Dynamic Light Scattering data for a solution of 8b (0.1 mg/mL in 10 mM borate buffer pH 9). The graph represents the volume average taken over 14 measurements.....	172

Figure	Page
B9 Dynamic Light Scattering data for a solution of 8b · 10 (0.1 mg/mL of 8b and 4 equivalent of guest 10) in 10 mM borate buffer pH 9. The graph represents the volume average taken over 14 measurements.....	173



สถาบันวิทยบริการ
จุฬาลงกรณ์มหาวิทยาลัย

LIST OF SCHEMES

Scheme	Page
1.1 The complementary shape and size of the host and guest as they interact, non-covalently.....	2
2.1 A cartoon representation for chemical receptors.....	8
2.2 A cartoon representation for chemical sensors.....	14
2.3 The oxidation process of ferrocene to ferrocenium ion.....	17
2.4 Proposed sequential binding of Na^+ and Cl^- by receptor 2.42	20
2.5 Schematic view of the Phe-Phe interactions in the crystal of peptides. The centroid distances (Å) are indicated.....	57
2.6 Schematic view in the crystal packing of 1 shows the aromatic-aromatic interactions between the interhelix arrays.....	58
2.7 Synthetic pathway for receptor 2d	62
2.8 Synthetic pathway for receptor 3d	64
2.9 Proposed binding steps for negative binding of heteroditopic receptor 2d	74
2.10 Schematic representation for guest binding (G) and electron transfer in electrochemical sensing of ferrocene containing receptor (Fc).....	93
2.11 The mechanism of electrochemical process during metal cation (M^+) binding through a ferrocenyl receptor (Fc).....	96
2.12 The mechanism of electrochemical response during anion binding through a ferrocenyl receptor (Fc).....	98
3.1 A cyclic double helicate templated by chloride anion.....	108
3.2 A template effect from porphyrin oligomers.....	109
3.3 Formation of imprinted polymers.....	110
3.4 Schematic representation of (a) traditional combinatorial chemistry and (b) dynamic combinatorial chemistry.....	112
3.5 A small dynamic combinatorial library and its free energy landscape showing the effect of adding a template that strongly and selectively binds to one of the equilibrating species.....	113

Scheme	Page
3.6 Reversible disulfide exchange from dithiols building blocks.....	115
3.7 Diels-Alder reaction, catalysed by a library member from a DCL.....	118
3.8 Thiol oxidation to form receptor 8b as a mixture of stereoisomers.....	131
3.9 Correlation between the diastereoisomers of 8b with those of 8a that are formed in the early stages of re-equilibration of receptor 8b with building block 7.....	133



สถาบันวิทยบริการ
จุฬาลงกรณ์มหาวิทยาลัย

LIST OF ABBREVIATIONS AND SIGNS

$^{\circ}\text{C}$	Degree Celsius
$^{13}\text{C-NMR}$	Carbon-13-Nuclear Magnetic Resonance
$^1\text{H-NMR}$	Proton-1-Nuclear Magnetic Resonance
α	Alpha
\AA	Angstrom
cmc	Critical Micelle Concentration
COSY	Correlation Spectroscopy
d	Doublet
δ	Chemical Shift
DCL	Dynamic Combinatorial Library
DCM	Dichloromethane
ΔG°	Standard Gibbs Free Energy
ΔH°	Standard Enthalpy
DLS	Dynamic Light Scattering
DMF	Dimethylformamide
DMSO	Dimethylsulfoxide
DNA	Deoxyribunuclic Acid
ΔS°	Standard Enthropy
F	Faraday Constants
g	Gram
HMBC	Heteronuclear Multiple Bond Correlation
HMQC	Heteronuclear Multiple-Quantum Coherence
HPLC	High Performance Liquid Chromatography
Hz	Hertz

J	Coupling Constant
K	Kelvin
K	Association Constant
kJ	Kilojule
LC-MS	Liquid Chromatography Mass Spectrometry
m	Multiplet
m/z	Mass per Charge Ratio
mg	Milligram
MHz	Mega Hertz
μL	Microliter
mL	Milliliter
μM	Micrometer
mmol	Millimol
mV	Millivolt
NEt ₃	triethylamine
NMR	Nuclear Magnetic Resonance
R	Gas Constant
RNA	Ribonucleic Acid
s	Singlet
T	Temperature
t	Triplet
TBA	Tetrabutylammonium
TEM	Transmission Electron Microscopy
THF	Tetrahydrofuran
TOCSY	Total Correlated Spectroscopy
UV-Vis	Ultraviolet-Visible
VT- ¹ H-NMR	Variable Temperature Proton-1-Nuclear Magnetic Resonance

CHAPTER I

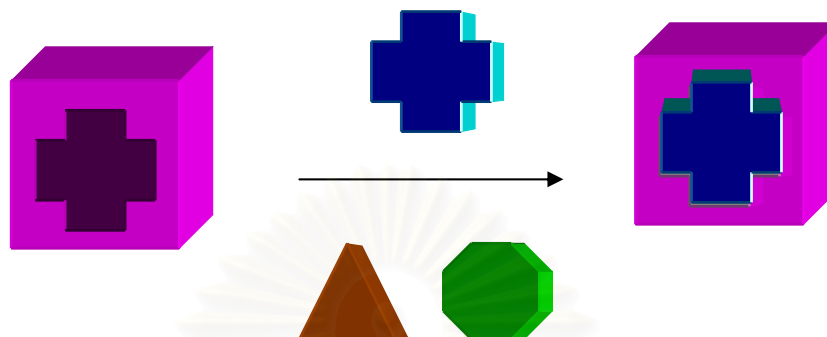
SUPRAMOLECULAR CHEMISTRY

1.1 Concept of Supramolecular Chemistry

Supramolecular chemistry [1,2] is a young discipline dating back to the late 1960s and early 1970s. Jean-Marie Lehn, who won the Noble prize in 1987, has defined the term of “*supramolecular chemistry*” as “the chemistry of molecular assemblies and of the intermolecular bond”. However, many attempts have tried to mention *supramolecular chemistry* as “chemistry beyond the molecule” or “the chemistry of the noncovalent bond” as well as “nonmolecular chemistry”.

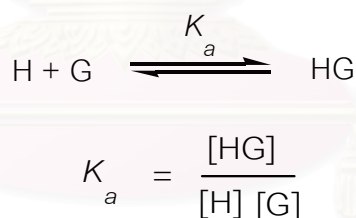
Non-covalent interactions for examples electrostatic interactions, hydrogen bonding and metal-ligand coordination have a profound importance in chemistry and biochemistry. Where these interactions occur with strength and selectivity, *molecular recognition* may occur allowing highly complex systems consisting of discrete molecules to form and operate. Furthermore, non-covalent interactions may be used to control and accelerate the formation and breaking of covalent bonds [3-5].

In supramolecular chemistry, the interactions between two or more molecules in a unique structural arrangement is known to be *host-guest* chemistry [6]. A *host* molecule is one that contains a cavity or a hole within the molecule. This cavity must be complementary to its *guest*, which can be fit inside the cavity. Typically, the host is a larger molecule with a pocket or cavity possessing convergent binding sites for selectivity of a specific guest. The guest molecule possesses divergent binding sites and can vary in size from a single atom to a complex biological assembly (Figure 1.1). An advanced and challenging target in host-guest chemistry is the construction of a host molecule having the ability of specific recognition with a guest molecule.



Scheme 1.1 The complementary shape and size of the host and guest as they interact, non-covalently.

In host-guest systems, the stability of a host-guest complex at equilibrium may be described in term of the *association constant*, K_a .



Ideally, construction of supramolecular chemistry host-guest complexes must be concerned the stability of complex which is being formed. In addition, in the complicated system not only the interaction between host and guest are considering but also many molecular recognition events, involving the making and breaking of many interactions between them and the solvent, and within the solvent itself and effect to conformational changes, makes predicting binding affinity difficult, should not be forgotten. Consequently, the synthesis of successful artificial host-guest systems is still the challenging.

1.2 Molecular Recognitions to Chemical Receptors and Chemical Sensors

One of the current challenges in the area of supramolecular chemistry involves the preparation of chemical receptors [7] and chemical sensors [8] with high selectivity for specifically targeted guest molecules. The systems could have an important role to play in a variety of applications, including sensing [9], analysis [10], waste remediation [11], and drug development [12]. The area continues as a vigorous area of research and is yet to be fully explored. However, the extremely goal to develop chemical receptors and sensors is to achieve a higher level of control over recognition than that obtainable from simple ion binding. Up to date, many strategies have been approached to construct host molecules.

The development of synthetic receptors and sensors has attracted much attention in recent years. Such molecules exhibit a range of interesting and potentially useful molecular recognition properties. Most of the earliest examples were homoditopic receptors that contained two identical binding sites connected by linkers [13,14]. These compounds can chelate a structurally symmetric guest or alternatively bind two very similar guests simultaneously. More recently, attention has turned to heteroditopic receptors that contain two quite different sites [15,16]. These compounds are able to bind a single heteroditopic guest or simultaneously bind two non-identical guests. The invention of convergent heteroditopic host is a challenging problem in molecular design because the binding sites have to be incorporated into a suitable preorganized scaffold that holds them in close proximity, but not so close that the sites interact.

To date, there are few systems capable of selectively reporting simultaneous binding by absorption [17,18], fluorescence [19] and electrochemistry [20]. Herein, in Chapter 2 we described the design, synthesis and binding properties of two heteroditopic electrochemical anion sensors which demonstrate a dramatic enhancement of anion binding by a co-bound cation.

1.3 Non-covalent Interactions to Molecular Assemblies

Millions of years of evolution have produced tremendously complex organisms which are born, live and die as a consequence of an intricate interplay between many (macro)molecular components. Non-covalent interactions play a fundamental role in the build-up of such complexity [21]. Where nature manages to construct organisms such as blue whales and redwood pines from (macro)molecular components, chemists' control over assembly processes is as yet limited. Whereas we are now beginning to understand life's toolbox of noncovalent interactions, using these for the controlled assembly of molecules with the size of a few Angstroms into structures many thousands of times larger than that is posing a considerable challenge.

There have been several attempts in the literature to define the term "self-assembly": Whiteside defined it as "the spontaneous assembly of molecules into structured, stable, non-covalently joined aggregates" [22], while Hamilton defined it as "the non-covalent interaction of two or more molecular subunits to form an aggregate whose novel structure and properties are determined by the nature and positioning of the components" [23]. Self-assembled supramolecules are normally favored thermodynamically over oligomeric or polymeric systems, profiting from enthalpic as well as entropic effects.

For chemists, the host-guest interaction motif offers an alternative to the biological motif allowing for unique design features in the assembly of discrete supramolecular species. The precise control over the size and shape of the assemblies, coupled with a large variety of available building blocks, allows the regulation of their sizes to within a few angstroms. Control of the polarity and charge state of the desired macrocycles is typically achieved via formation of charged, neutral, and mixed macrocycles; the presence of polar or lipophilic groups provides the ability to create water or organic-soluble macromolecular hosts with hydrophilic or hydrophobic cavities. The use of optically active components allows relatively easy, simple access to chiral

supramolecules with controlled stereochemistry. The next step in controlling the size and shape of nanoscale self-assembled systems will involve introducing elements of specific molecular recognition. However, progress in this area is limited.

Early work in the area of self-assembly of nanoscale structures from relatively simple synthetic molecules was inspired on the ability of phospholipids to self-assemble to form biological membranes [24]. The self-assembly of amphiphilic molecules (low molecular weight or macromolecular) of various architectures has been studied extensively and has resulted in assemblies with a great variety of shapes and sizes. The morphology of these assemblies is often dictated by the structure of the constituent molecules. In some cases changes in morphology can be induced by changes in pH [25], concentration [26] or temperature [27]. Some interesting reports have appeared in which host-guest interactions drive the formation of amphiphilic molecules from constituents that are themselves non-amphiphilic. These noncovalent amphiphiles then self-assemble just like their covalent counterparts. However, there was no example that the morphology transformation of the aggregate amphiphile molecules can be directed by host-guest interaction. Then, the next question is, is it feasible to do or not? The answer of this question will be described in Chapter 3.

สถาบันวิทยบริการ
จุฬาลงกรณ์มหาวิทยาลัย

CHAPTER II

HALIDE ANIONS SENSING BY HETERODITOPIC ELECTROCHEMICAL ANION SENSORS

2.1 Introduction

2.1.1 Chemistry of Anions

Anions have an ubiquitous role in the world; they have biological, chemical, industrial and environmental implications. Some examples include: i) over 70% of enzyme substrates in the human body contain anions, for example adenosine triphosphate (ATP) and deoxyribonucleic acid (DNA), ii) chloride anions make up a large fraction of extracellular ions and the transport of chloride ions across the cell membrane is an extremely important process that is thought to lead to cystic fibrosis when the channel is not functioning correctly, iii) from an industrial standpoint by-products such as TcO_4^- are derived from the manufacturing of nuclear fuel reprocessing and iv) lakes and ponds are at risk due to the runoff of fertilizers from crops where the nitrates and phosphates cause eutrophication [28].

The sizes of anions are large compared to their isoelectronic cation counterparts. Therefore, the charge density of anions is more diffuse which lessens their ability to interact electrostatically. The 'in solution' existence of an anion in its charged form is often pH dependent, for example H_2PO_4^- can be H_3PO_4 ($\text{p}K_b = 11.8$), and consequently the receptor must function at the appropriate pH. The design of the receptor must also be suitable for a specific geometry since anions can vary in shape from spherical to octahedral, as shown in Figure 2.1. Therefore, the synthetic receptor should provide a binding site that complements the size and shape of the larger ion in order to overcome the higher solvation energies [29].

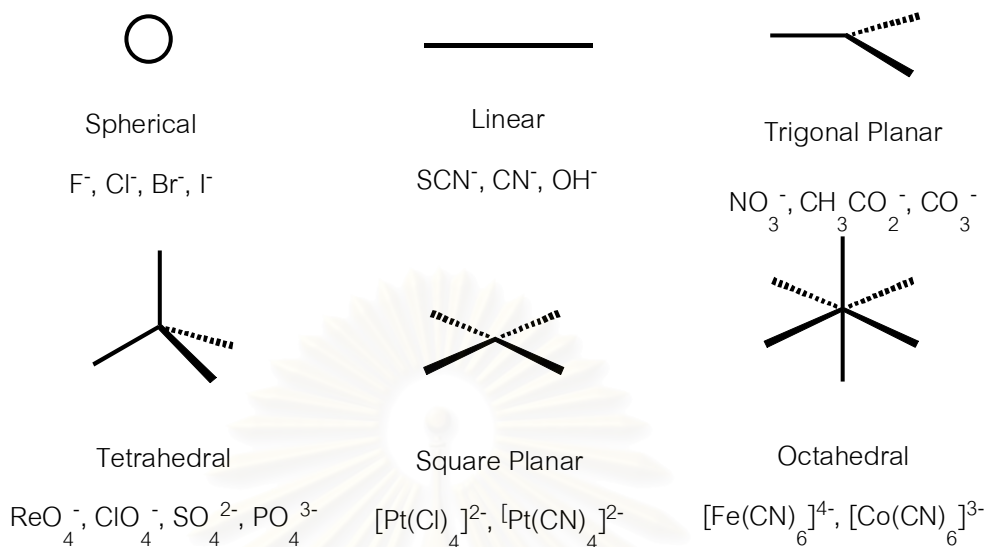


Figure 2.1 Geometries of various anions.

Several types of interactions are available for the coordination of anions into host binding sites. These interactions can be incorporated through either the functional groups or the framework of the receptor. The broad categories of interactions include hydrogen bonds, electrostatics, metal ion coordination and hydrophobicity, as shown in Figure 2.2. The hydrogen bond interactions occur between a relatively acidic hydrogen atom, due to its coordination to an electronegative atom (oxygen or nitrogen), and an electron rich atom, ion or molecule. This interaction involves directionality with an X-H...A⁻ angle of 150 ° - 160 ° being typical.

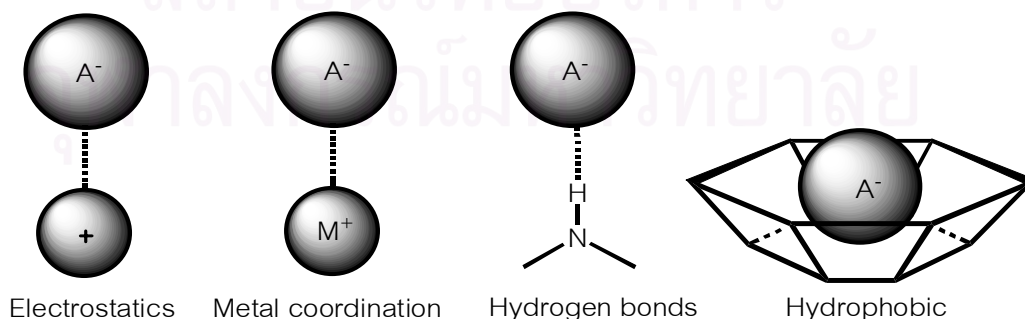
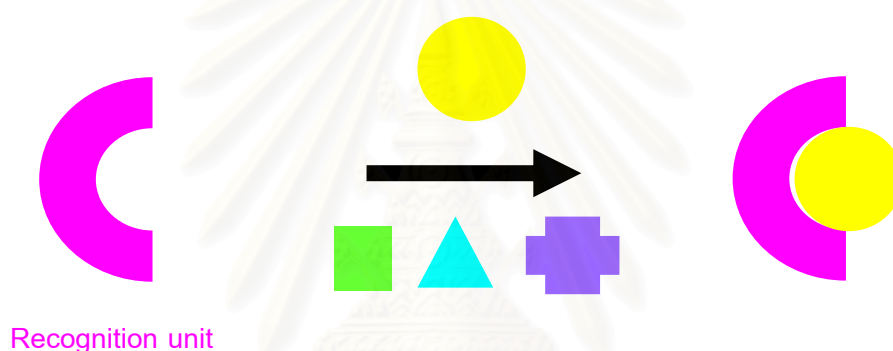


Figure 2.2 Types of interactions available for receptor and anion binding.

2.1.2 Chemical Receptors for Anions

In supramolecular chemistry approach, the chemical receptor must possess structural and chemical features suitable for guest recognition (Scheme 2.1). Chemists have addressed the challenge of designing and building concave receptors having shapes and dimensions suitable for hosting with any kind of guests and ability of establishing guest interactions, for examples hydrogen bonds, electrostatic interactions and π - π interactions.



Scheme 2.1 A cartoon representation for the chemical receptor.

Chemical receptors for anions are frequently incorporate of (i) hydrogen bond donor groups, (ii) a positively charged component for effective electrostatic interactions and (iii) a suitable framework onto which these structural components can be assembled [30-32]. Functional groups provide, for the most part, the hydrogen bonding interactions [33,34], while the framework usually provides the metal coordination [35] and or hydrophobic effects. Electrostatic interactions can be observed through either the functional groups or the framework. The functional groups for hydrogen bonding such as amides [36], sulphonamides, ureas, thioureas and pyrroles [37] possess electron-deficient hydrogen atoms and are therefore capable of acting as hydrogen bond donors (Figure 2.3).

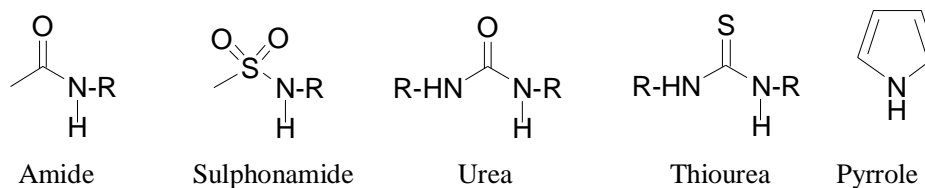
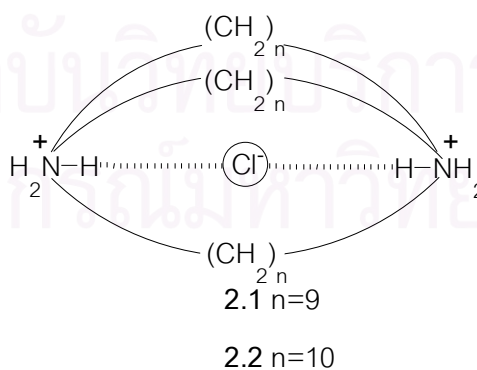


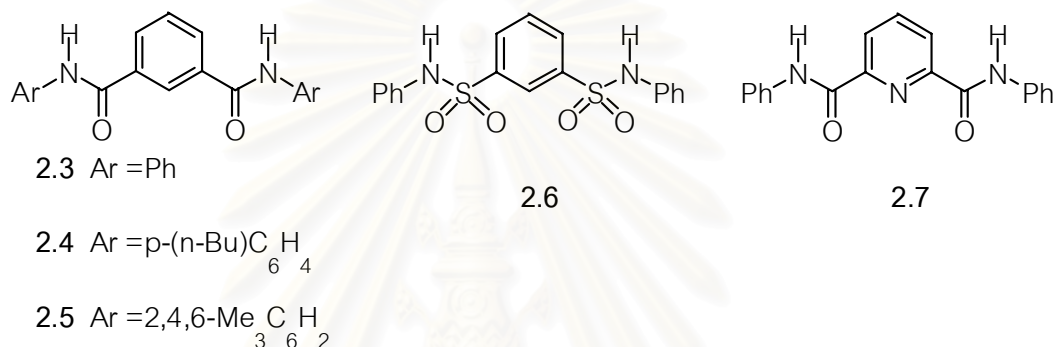
Figure 2.3 Functional groups providing hydrogen bonding interactions.

Moreover, electrostatic interactions are a non-directional mutual attraction between oppositely charged species (ion-ion, ion-dipole and dipole-dipole). For example, metal ion coordination involves an electron deficient metal center coordinating to an anion through orbital overlap and the hydrophobic effect is association of non-polar molecules in aqueous solution.

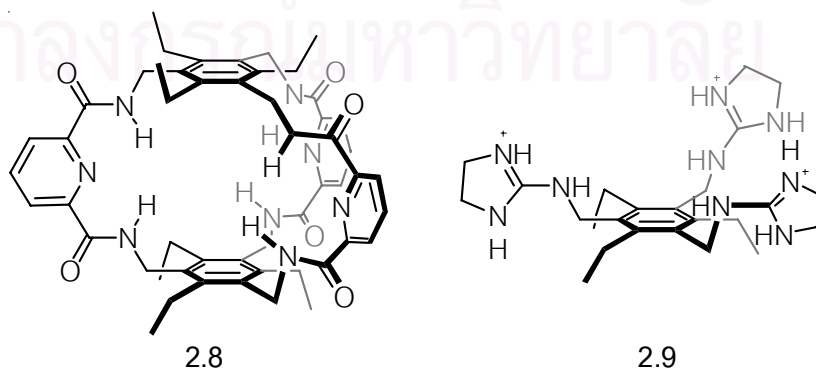
The first synthetic anion receptors were reported in 1968 by Park and Simmons, compounds 2.1 and 2.2 [37]. However, host-guest chemistry involving anion binding did not come into prominence until the late 1980s. The delay in the development of synthetic anion receptors was likely due to the innate properties of anions. As shall be seen, designing receptors for these negatively charged guests can be a challenging task.



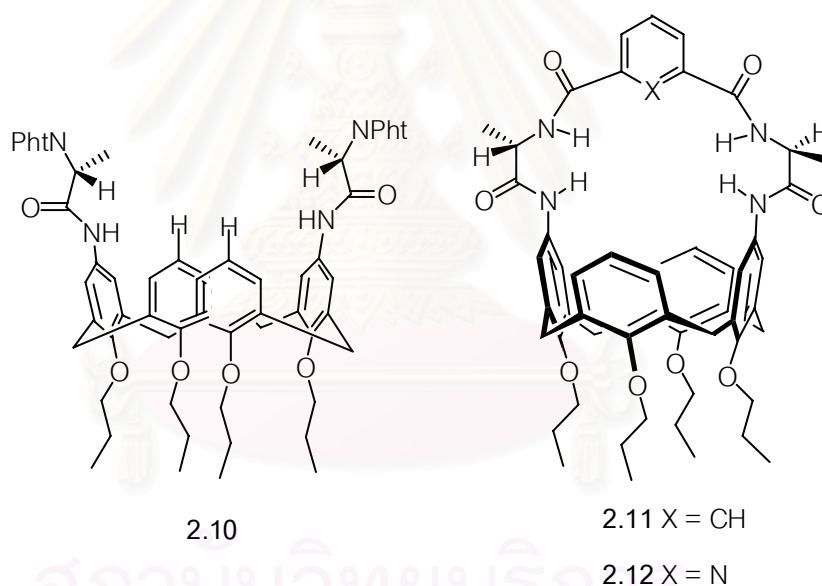
Organic frameworks can be as simple as a single, rigid aromatic ring used to append functional groups. Crabtree [39] has used a very simple example where a *bis*-amide or sulphonamide substituted phenyl or pyridine ring, 2.3-2.7, can bind anions in a 1:1 stoichiometry. Both amide N-H groups rotate to point into the cavity forming a cleft for the anion to bind. Receptor 2.4 binds Cl^- with the highest association constant of $6.1 \times 10^4 \text{ M}^{-1}$ in a CD_2Cl_2 solution.



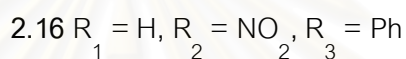
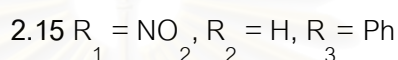
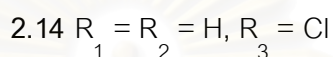
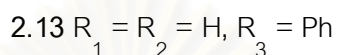
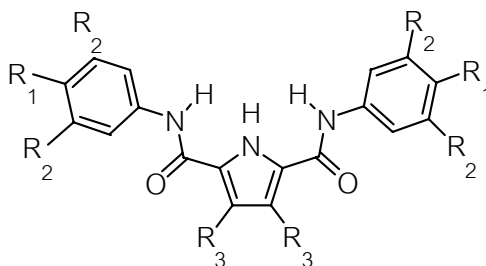
A slight modification of the *di*-substituted aromatic ring is a 1,3,5-*trisubstituted* benzene ring used by Anslyn [40,41]. The bicyclic receptor, 2.8, possesses 3-fold symmetry where the placement of the six hydrogen bonding amides provides the correct placement for the interaction with the anion's π system. Initial studies showed good binding with CH_3CO_2^- (770 M^{-1}) and the enolate (3060 M^{-1}) anions which have the ideal planar geometry for interaction of the receptor with their π -electron system. The guanidinium receptor, 2.9, was designed to complement the geometry of citrate which bound very strongly ($7 \times 10^3 \text{ M}^{-1}$) in pure water.



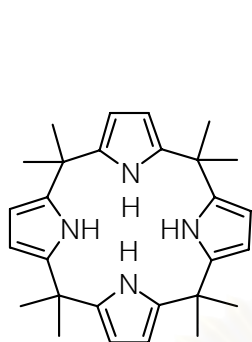
Calixarenes have been used as the framework for many different anion receptors. The flexibility of this framework allows four different conformations to be attained; cone, partial cone, 1,2-alternate and 1,3-alternate. Ungaro [42,43] used this motif in several receptors including a calix[4]arene with the upper rim substituted by C-linked peptides, **2.10**. This receptor binds CH_3CO_2^- with an association constant of 33 M^{-1} in $\text{DMSO-}d_6$. The strapped C-linked peptide calix[4]arenes, **2.11** and **2.12**, locks the receptor in a cone conformation. The binding site formed provides four hydrogen bonds through the N-H units and π - π stacking through the phenyl or pyridine ring. Receptor **2.12** shows less flexibility and higher association constants than **2.11** with binding constants for $\text{C}_6\text{H}_5\text{CO}_2^-$ of $4.0 \times 10^4 \text{ M}^{-1}$ in $\text{acetone-}d_6$.



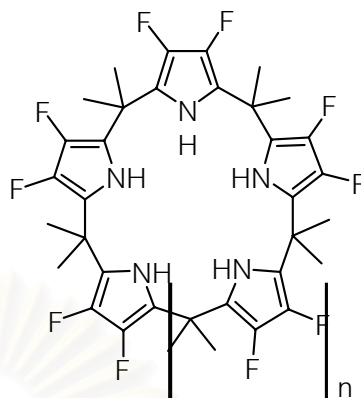
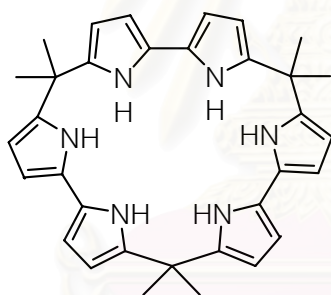
Gale [44-48] and co-workers have used pyrroles as the framework with amide functional groups, see Figure 1.10, in their study of anion recognition. The single pyrrole receptors, **2.13-2.16**, show a semi-cleft arrangement in the solid state in which both amide protons are pointing away from the binding site. Upon addition of anions, the amide groups rotate so the amide N-H groups are now pointing into the binding site forming a cleft.



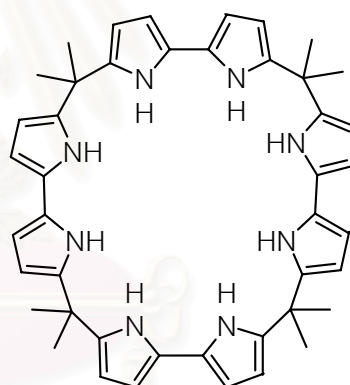
Subsequently, a wide variety of calixpyrroles have been used as receptor frameworks by Sessler [49-51]. By using the pyrrole functional group as part of the macrocycles, these receptors are able to bind halides. The number of pyrroles incorporated into the macrocycle can vary between four and eight, 2.17-2.20, and the substituents can vary between electron-donating and electron-withdrawing groups. Electron-withdrawing groups increase the acidity of the pyrroles and therefore increase the overall affinity of the receptor for the anions. Receptor 2.17 binds F^- preferentially with an association of $1.7 \times 10^4 \text{ M}^{-1}$ in $\text{CH}_2\text{Cl}_2-d_2$. The calix[5]pyrrole, 2.18, binds Cl^- preferentially over the calix[8]pyrrole, 2.20, with a binding of $4.1 \times 10^4 \text{ M}^{-1}$ in $\text{MeCN}-d_3$ 0.5% D_2O . Calixbipyrroles 2.21 and 2.22 have also been studied and the calix[4]bipyrrole, 2.22, binds Cl^- very strongly with an association constant of $2.9 \times 10^6 \text{ M}^{-1}$, obtained by isothermal titration calorimetry (ITC).



2.17 Calix[4]pyrrole

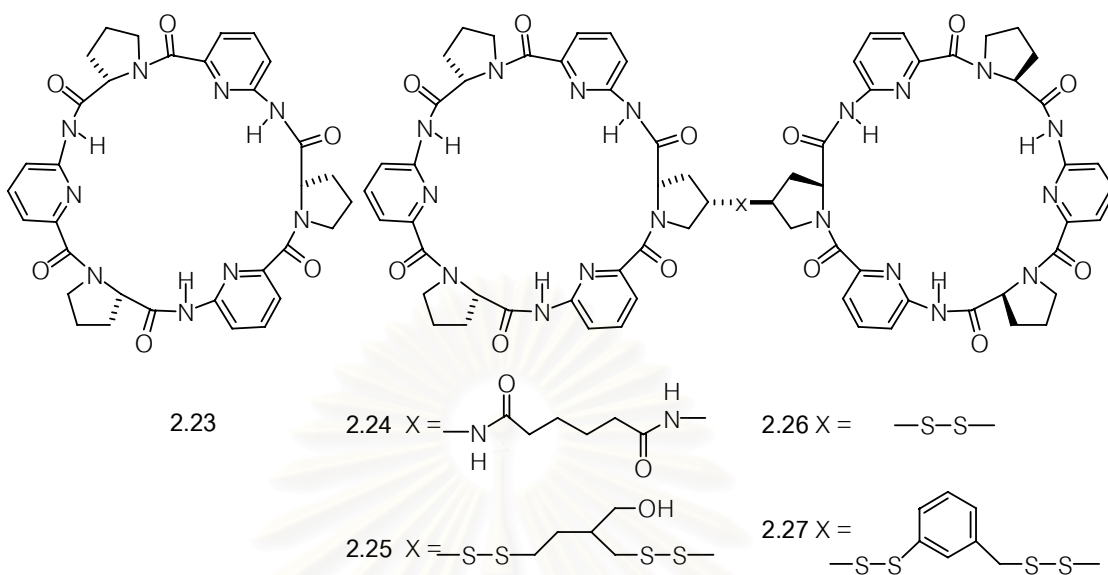
2.18 Calix[5]pyrrole when $n = 1$ 2.19 Calix[6]pyrrole when $n = 2$ 2.20 Calix[8]pyrrole when $n = 4$ 

2.21 Calix[3]bipyrrole



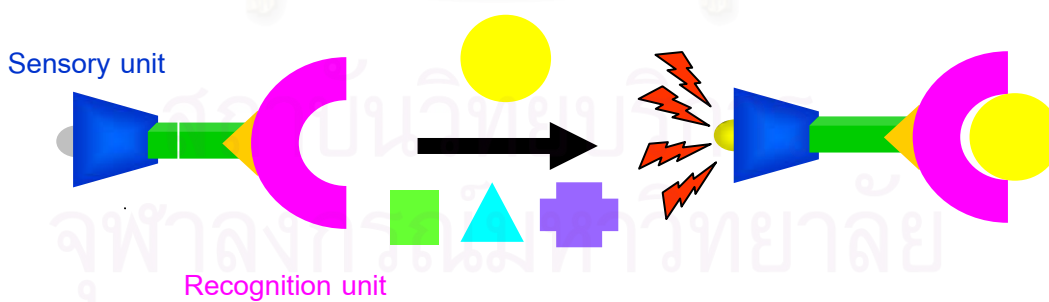
2.22 Calix[4]bipyrrole

Peptides are another feasible framework for an anion receptor. Peptides consist of many amide functional groups and work by Kubik [52] showed the anion binding ability of these backbones. The single macrocycle, **2.23**, is a hexapeptide which has the ability to complex a variety of anions in a very polar 80% $D_2O/MeOH-d_4$ solution. The solid state structure with I^- shows two receptors sandwiching the anion and interacting through six N-H hydrogen bonds. When two of these macrocycles, **2.24-2.27**, are tethered together they act as a molecular oyster upon binding anions [53,54].



2.1.3 Chemical Sensors for Anions

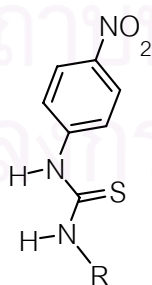
Like chemical receptors, chemical sensors consist of recognition unit incorporating with the sensory unit. The sensory unit can be chromophores for chromogenic sensors or redox-active molecules for electrochemical sensors, which converts the binding event or recognition phenomena to their signals upon binding with guest molecules (Scheme 2.2).



Scheme 2.2 A cartoon representation for chemical sensors.

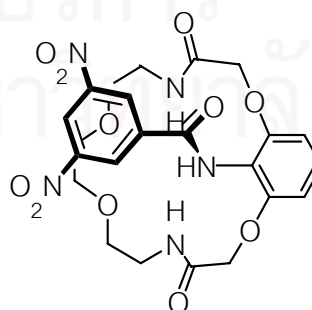
One basic design principle in these new multicomponent systems is that the sensing event has to be related with an easy-to-measure signal. In fact, many chemosensors display changes in either color [55,56] or fluorescence [57] in the presence of a certain guest although changes in electrochemical properties such as the oxidation potential of redox active groups have also been widely used [58]. In this sensing process, information at the molecular level, such as the presence or not of a certain guest in solution, is amplified to a macroscopic level. Hence, sensing might open the door to the determination (qualitative or quantitative) of certain guests [59]. These ideas connect in some way with supramolecular concepts such as that of molecular devices (in this case sensor devices) in which the final operation (anion signaling) performed by the device results from the sum of the basic functions of the components, the binding site (coordination), and the reporting unit (transduction of the coordination event).

For example, incorporate chromophore nitrobenzyl group to acyclic thiourea **2.28-2.29** receptors [60] or cyclic amide-base receptor **2.30** [61] have found to be a potent optical anion sensors. In 1%water : 99% MeCN, sensors **2.28** and **2.29** showed the dramatic colour change from yellow to red in the presence of acetate anion. Upon addition of fluoride anion, a colorless solution of sensor **2.30** turned to dark blue solution in CH₃CN or DMSO.



2.28 R = Me

2.29 R = *p*-nitrophenyl



2.30

2.1.4 Electrochemical Anion Sensors

Electrochemical recognition of anions is an expanding research area at the interface of electrochemistry and supramolecular chemistry. Some of these systems have been applied as molecular devices for converting molecular recognition processes in molecular level into macroscopically measurable electronic signals. A variety of redox-active centers have been incorporated into various host frameworks and been shown to electrochemically detect charged and neutral guests as shown in Figure 2.4. Normally, the redox-responsive molecules contain two components: (i) an electroactive group and (ii) binding sites. As a consequence of the electrochemical shift effect, molecular redox receptors are able to transform chemical information into electronic signals, which can be used for the development of new specific sensors.

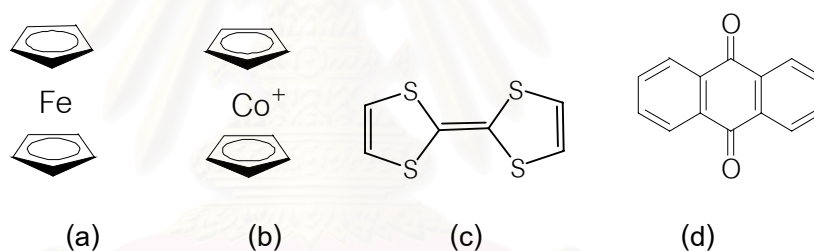
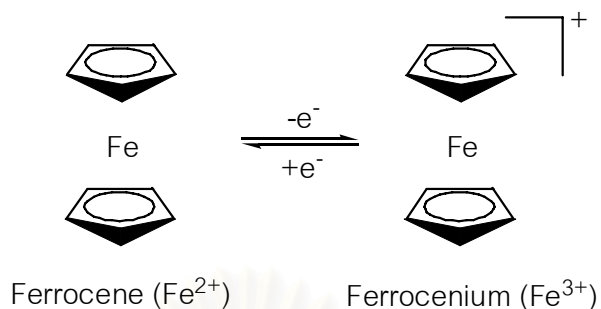


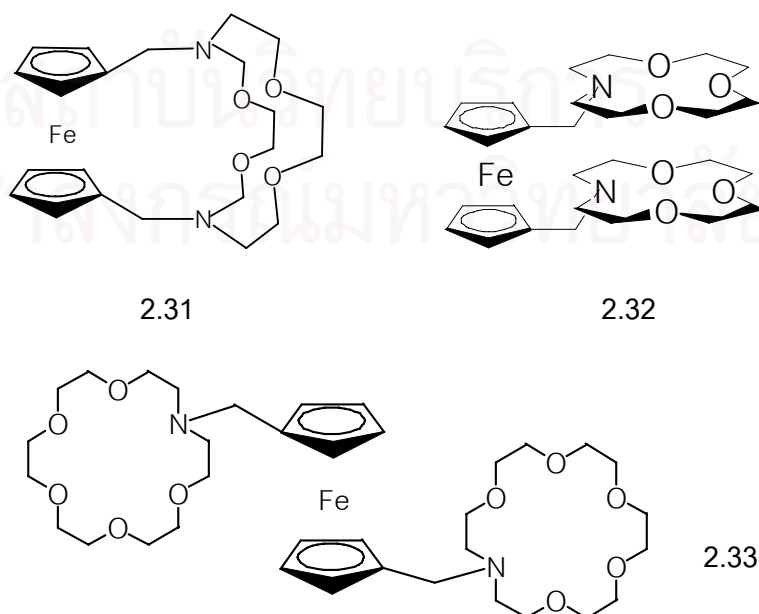
Figure 2.4 Redox-active molecules for electrochemical sensing (a) ferrocene (b) cobaltocenium [62,63], (c) tetrathiafulvalene [64] and (d) anthraquinone [65].

In this chapter only ferrocene redox-active center will be mentioned. Because, it has long been known that the ferrocene molecule has been employed in the electrochemical sensing of cations, anions and neutral molecules in both organic and aqueous media. The ferrocene unit exhibits good reversibly electrochemical signals. Furthermore, cyclopentadiene ring is easy to functionalize. Basically, ferrocene can be oxidized to ferrocenium ion involving one electron transfer process (Scheme 2.3). Consequently, the magnitudes of oxidation potential shifts depend on the interaction between the ferrocenium ion and incoming guest species.

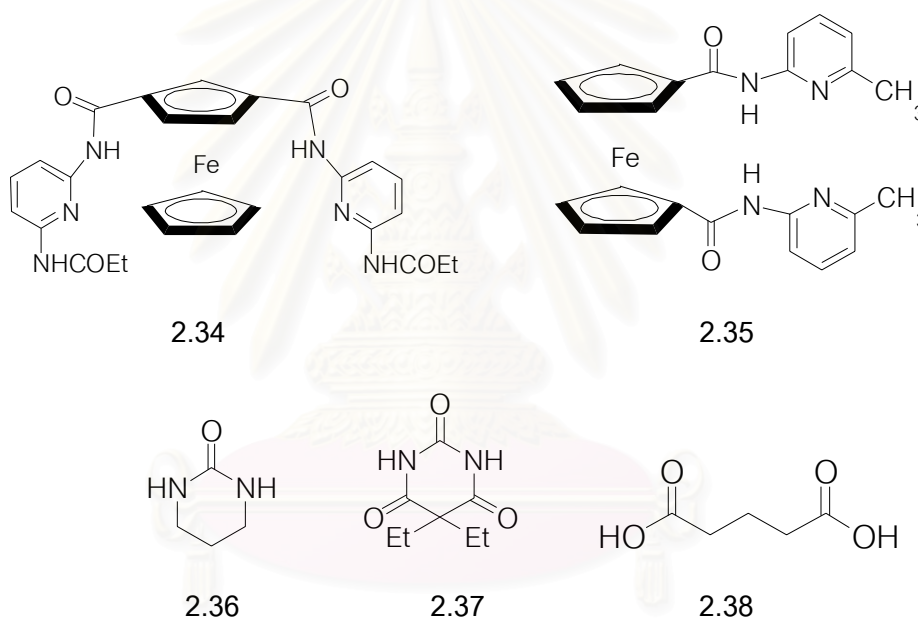


Scheme 2.3 The oxidation process of ferrocene to ferrocenium ion.

For cation sensing, the anodic shifts will be observed in any systems [66]. Because the ferrocene unit becomes harder to oxidize due to the electrostatic repulsion between ferrocenium cation and metal cation, therefore the ferrocene-ferrocenium couple shifts to a higher potential. Several ferrocene cryptand molecules, 2.31-2.33, have been employed as electrochemical cation sensing. Compound 2.31 [67,68] showed the strong binding affinity toward Na^+ whereas 2.32 presented the highly selective for Li^+ in the presence of large excess of other Group 1 metal cations. Moreover, the detection of two different cations simultaneously by a single redox-active receptor has been reported by Beer and co-workers [69]. The receptor 2.33 containing two metal binding sites could be used to sense the presence of barium, magnesium, or a mixture of barium and magnesium *via* a through space interaction [69].

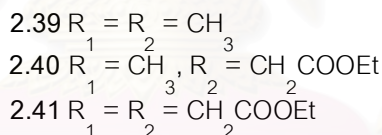
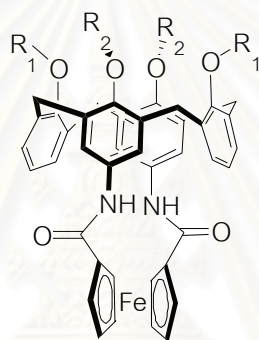


A series of ferrocene-containing amidopyridyl receptors **2.34** and **2.35**, in two regioisomeric forms (1,1'- and 1,3'-), have been shown to bind cyclic organic molecules, urea **2.36** for **2.34** and barbiturate **2.37** for **2.35**, in chloroform through complementary hydrogen-bonding interactions [70]. The magnitude of the host-guest binding strength and the redox response to complexation depend on the relative position of the amidopyridyl groups on the cyclopentadienyl rings of the ferrocene. Moreover, receptor **2.35** was found to be an electrochemical sensor for glutaric acid **2.38** in CH_2Cl_2 in which the observed anodic shifts was found to be -85 mV [71].



For anion sensing, amidoferrocene, ferrocene units appended with amide group, have also been widely used for anion recognition through hydrogen bonding formation between NH amide proton couple with electrostatic interaction with ferrocenium ion [72,73]. Then the cathodic shifts will be observed due to the ferrocene moiety will be easy to oxidize. These behaviors will significantly enhance the binding strength towards anions and also exhibit the interesting electrochemical anion recognition.

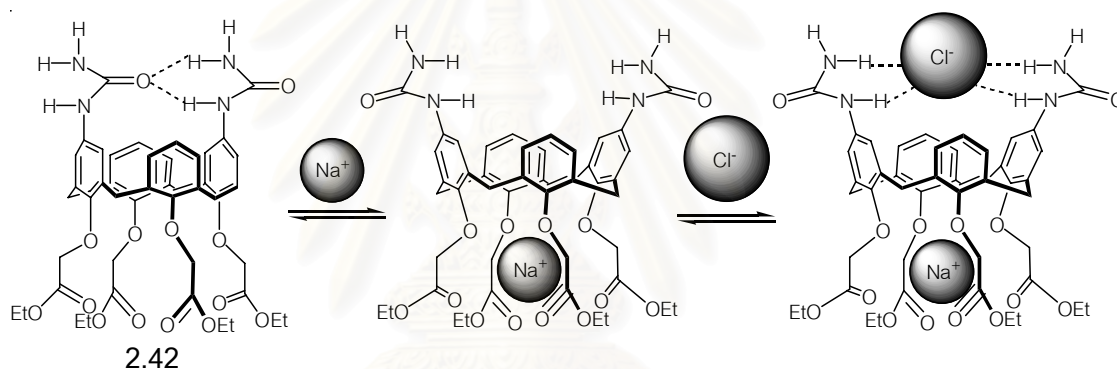
Interestingly, calix[4]arene derivatives containing amidoferrocene at the wide rim and ethyl ester groups at the narrow rim, **2.39-2.41**, have been synthesized and their anion binding and sensing properties were investigated by NMR and electrochemistry [74]. ^1H NMR titrations in CD_3CN showed that compounds **2.39-2.41** were able to bind selectively with carboxylate anions. Consequently, cyclic voltammetry and square wave voltammetry illustrated that the proposed receptors were able to act as electrochemical sensors for carboxylate anions as well.



2.1.5 Heteroditopic Receptors and Sensors

The receptors which contained two binding recognition units for either the same or different ions named “*ditopic receptor*”. All of them are designed in order to enhance the binding ability of one species by another one. The ditopic receptor which can bind two same guest species are defined as “*homoditopic receptor*”.[13,14] In contrast, the receptors that bind two different guest species are categorized as “*heteroditopic receptor*” [15,16]. Normally, the ditopic host molecules often exhibit cooperative effects whereby the association of one ion influences the binding affinity of the other being either enhanced or reduced. The cooperative behavior can result from several factors, such as through-space or through-bond electrostatic interactions between bound guest molecules or conformational changes induced by binding.

For example, Reinhoudt group generated a calix[4]arene scaffold with cation-binding ester groups on the narrow rim and anion-binding urea groups on the wide rim [75]. In CDCl_3 receptor **2.42** adopts a pinched cone conformation due to intramolecular hydrogen bonding between the *trans*-like urea groups, thus preventing anion binding. However, when sodium ions are added, cation complexation at the lower rim alters the calix conformation, thereby breaking the hydrogen bonds between the urea groups. As a result, halide ions, such as Cl^- and Br^- , can be recognized at the upper rim, as evidenced by downfield shifts in the ^1H NMR signals of the urea hydrogens. This chemistry is summarized in Scheme 2.4.



Scheme 2.4 Proposed sequential binding of Na^+ and Cl^- by receptor **2.42**.

2.1.6 Ion-Pair Receptors and Sensors

“*Ion pair*” means a pair of oppositely charged ions held together by coulomb attraction without formation of a *covalent bond* [76]. An ion pair, the constituent ions of which are in direct contact (and not separated by an intervening solvent or other neutral molecule) is designated as a ‘tight ion pair’ (or ‘intimate’ or ‘contact ion pair’) [77]. By contrast, an ion pair whose constituent ions are separated by one or several solvent or other neutral molecules is described as a ‘loose ion pair’. The members of a loose ion pair can readily interchange with other free or loosely paired ions in the solution. A further conceptual distinction has sometimes been made between two types

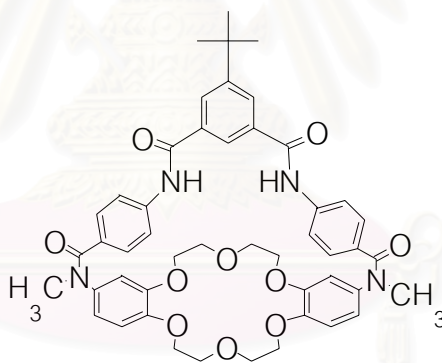
of loose ion pairs. In 'solvent-shared ion pairs' the ionic constituents of the pair are separated by only a single solvent molecule, whereas in 'solvent-separated ion pairs' more than one solvent molecule intervenes. However, the term 'solvent-separated ion pair' must be used and interpreted with care since it has also widely been used as a less specific term for 'loose' ion pair. Such systems have potential as new selective extraction and transportation reagents for metal salt ion-pair species of environmental importance. In addition, ion-pair receptors can be used to mimic important biological functions and coordinate biologically significant species such as amino acids and peptides [78].

Ion-pair receptors to date have been based on hydrogen bonding, positively charged or Lewis acidic groups to coordinate the anions, and crown ether or modified calixarenes to bind cations [79]. Smith and co-workers have been reported the ion-sequestering ability of the Group 1 metal cations was in the order of $\text{Cs}^+ < \text{K}^+ < \text{Na}^+$ matching their ion-pairing ability [80]. Basically, the anion binding ability of the receptor was either enhanced or suppressed depending upon the nature of the receptor and the ion-pairing ability of the cationic guest.

2.1.7 Literature Reviews of Ion-pair Receptors and Sensors

The development of ion-pair receptors or sensors [81], with the goal of achieving a higher level of control over recognition than that obtainable from simple ion binding, has intrigued researchers in supramolecular chemistry over the past decade. The utility of ion-pair receptors has been demonstrated in several systems incorporating engineered steric constraints. Particular success has been encountered with receptors bearing cavities of limited dimensionality and directionality of contact ion pairs as well as with receptors that embody allosteric effects such that the binding of one ion organizes the receptor to accept the counterion. Some examples of ion-pair receptors and sensors have been described below.

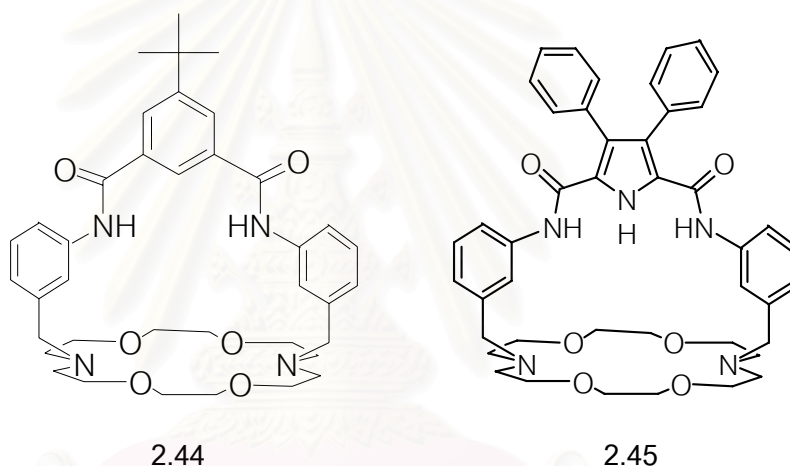
Smith and co-workers combined dibenzo-18-crown-6 and 1,3-phenyldicarboxamide subunits to form the preorganized macrobicyclic receptor **2.43** [80]. Receptor **2.43** is capable of coordinating alkali metal and chloride ions simultaneously. The binding studies showed that in the presence of 1 molar equivalent of Na^+ or K^+ , chloride affinities are enhanced (for Na^+ , $K = 410 \text{ M}^{-1}$; for K^+ , $K = 470 \text{ M}^{-1}$) relative to what is seen in the absence of the cation ($K = 50 \text{ M}^{-1}$). Furthermore, the crystal structure of the NaCl complex shows that in the solid state compound **2.43** binds NaCl as a “*solvent separate ion pair*”. As expected, the Na^+ ion is bound within the dibenzocrown unit, with an axial water molecule completing the coordination sphere, whilst the Cl^- anion is hydrogen-bonded to the two NH residues. The central cavity is occupied by either a CHCl_3 molecule or two molecules of water, with the ion-ion separation being 7.31 Å.



2.43

Subsequently, receptor **2.44**, an analogue of **2.43** was synthesized [82]. It was designed to compare the effect of distance between the cobound cations and anions. From complexation studies, it was found that the binding constants of **2.44** with Cl^- ($K = 35 \text{ M}^{-1}$) are significantly increased in the presence of K^+ ($K = 460 \text{ M}^{-1}$) but not Na^+ ($K = 50 \text{ M}^{-1}$). Single crystal X-ray diffraction structures were obtained for the NaCl and KCl complexes of **2.44**. In order to accommodate the Na^+ ion, the diazacrown unit in $\text{NaCl} \cdot \mathbf{2.44}$ adopts a structure which the effective cavity size is reduced relative to the KCl complex (average K-O distance is 2.77 Å vs. 2.45 Å for Na-O). Additionally, in

NaCl•**2.44**, the average Cl-O distance is 4.20 Å, significantly shorter than that observed in KCl•**2.44** (average Cl-O distance is 4.7 Å). The implication is that once K⁺ cation is bound, receptor **2.44** forms a contact ion-pair with Cl⁻ more favourably than NaCl•**2.44**. Furthermore, this research group synthesized receptor **2.45** by changing the anionic binding site from phenyldicarboxamide to amidopyrrole [83]. Likewise, receptor **2.45** showed a high selective binding of chloride anion in the presence of alkali cation as compared to **2.44** (Na⁺, $K = 128$ and K⁺, $K = 540$). The increased affinity is due to the ability of NH pyrrole to form an additional hydrogen bond with chloride.



Surprisingly, Gale and co-workers have found that calix[4]pyrroles, a well-organized class of anion receptors, could be a successful ion-pair receptor as well [84]. Extraction of cesium salts with octamethylcalix[4]pyrrole **2.46** which suggested especially strong ion-pairing of Cs⁺ ions with complexes formed between **2.46** and Cl⁻ and Br⁻ ions in the organic phase. It should be noted that Cs⁺ ions include in the electron rich cone-like cavity and halide anions bind to the four NH groups of the calix[4]pyrroles. Notably, the halide ion is associated with the Cs⁺ ion within the same complex as contact ion-pair. The Cs⁺ also contacts to the Cl⁻ ion of the adjacent unit of the complex. Thus leading to the formation of a one-dimensional coordination polymer (Figure 2.5).

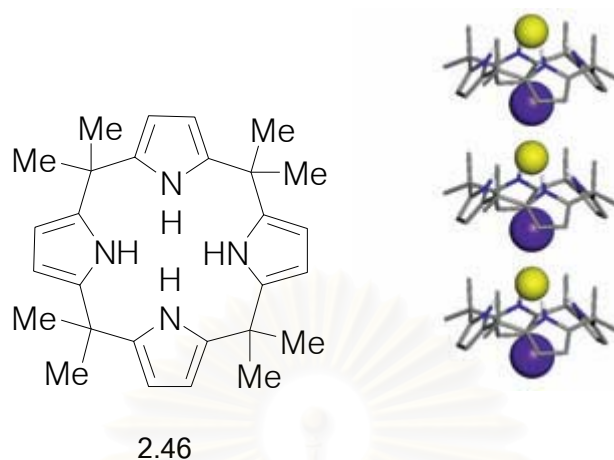
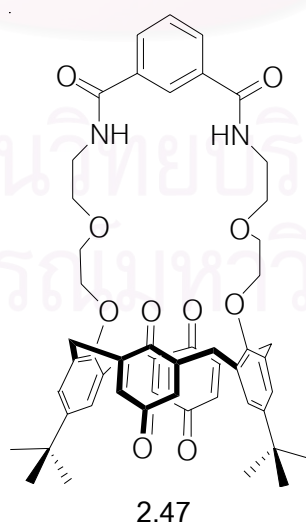
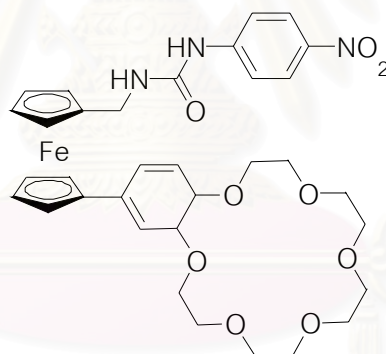


Figure 2.5 Structure of 2.46 and the x-ray crystal structures of 2.46 with CsF.

Recently, Beer and co-workers [18] reported heteroditopic receptor calix[4]diquinone 2.47 capable of binding a cation and anion simultaneously in a cooperative fashion is shown only to recognize halide anions in the presence of a suitable cobound cationic guest species, and displays affinity for certain contact ion-pairs where no affinity for either of the free ion is observed. It was found that this receptor showed the “switch on” chloride, bromide in which $K > 10^4 \text{ M}^{-1}$ and iodide ($K = 380 \text{ M}^{-1}$) bindings in the presence of potassium cation in CD_3CN .

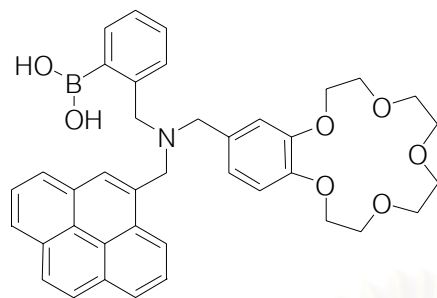


In the progress of construction of anion sensors, Miyaji and co-workers reported chromogenic molecular switch **2.48** as a new ditopic ferrocene receptor for anions and cations [85]. Upon addition of F^- to a colourless solution of **2.48** in acetonitrile, the colour was changed to yellow. In contrast, addition of K^+ to the solution of **2.48** caused a reverse behavior in which the colour of the solution turned to colourless. This implied that the colour change was controlled by F^- 'switches on' and K^+ 'switches off'. This result was confirmed by NMR studies in CD_3CN . When K^+ was added to the solution of **2.48**, large upfield shifts of the proton of the urea-NH occurred and shifted to the position of the free receptor. The results from 1H NMR and UV-Vis studies, therefore, supported the assumption that it was the presence of K^+ in close proximity to the fluoride binding center of **2.48** that caused the colour quenching process. This receptor may thus be applied as an optical device at the molecular level.

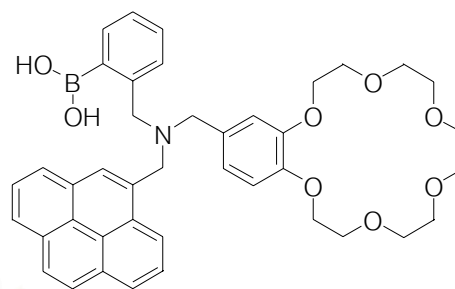


2.48

A heteroditopic fluorescense sensors **2.49** and **2.50** containing both binding units: benzocrown ether and boronic acid have been reported by Koskela and co-workers [19]. It was found that, the binding of potassium fluoride enhanced the fluorescence of both sensors. In contrast, addition of chloride and bromide salts did not cause any change in the fluorescence intensity. Therefore, the sensors **2.49** and **2.50** have shown the "switches on" upon addition of potassium fluoride.



2.49



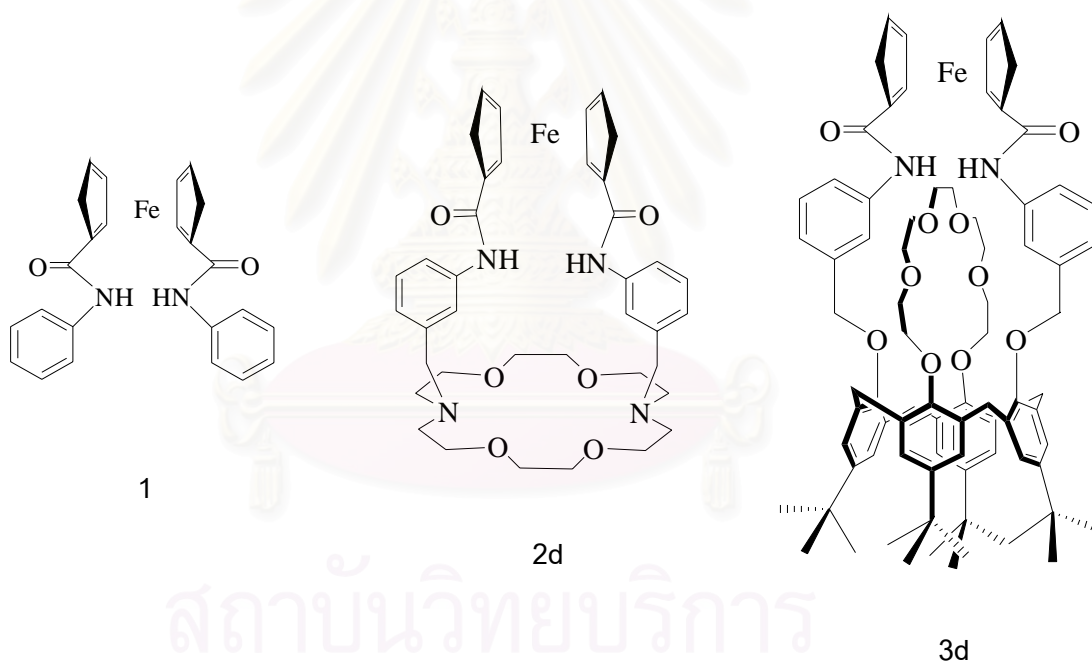
2.50

2.1.8 Objectives of this Research

As outlined, according to the previous reports on electrochemical anion sensors based on calix[4]arenes incorporating amidoferrocene, (compounds 2.39-2.41), which presented the lack of simultaneous binding of cations and anions due to the flexible structure of calix[4]arenes scaffold in solution [74]. It appears to us that if we design the scaffold in which the cation and anion binding sites are in the same side of receptor and relative close to each other then the specific ion-pair interactions should occurred and enhance the binding affinity of anions.

This project has been focused on the synthesis of heteroditopic electrochemical anion sensors containing ferrocene as the sensory unit. The first thing to consider is recognition site of cations. Crown ether is the well-known recognition unit of cationic guest especially alkali metal cations in which the selectivity of complexation depends on the size of the crown ether cavity respect to the size of cationic guest. The final requirement is the hydrogen bonding interactions. This will be provided by amide functional groups of amidoferrocene. We expected that the oxidation from of ferrocene unit (ferrocinium) will support the binding ability of anion as well as provide the electrostatic interactions of the system. Moreover, one of the major goal design was conformational flexibility. As a convenient way of viewing the possible conformations of the host molecules, diaza-crown ether and *p-tert*-butylcalix[4]arenes are the good candidates.

In this research, two heteroditopic electrochemical anion sensors, the amidoferrocene on crown ether (compound **2d**) and *p*-*tert*-butylcalix[4]arene, containing pseudo crown ether (compound **3d**) have been synthesized. The binding abilities and electrochemical properties of the synthetic receptors toward anions in the presence and absence of cations compared to the acyclic monotopic anion sensor **1** were then investigated. We hoped that the benzyl side arms should allow the receptors to preorganize their molecules to be suitable for the second guest binding. The degree of preorganization should depend on the size and shape of both cations and anions when they are interacting.



We expect that the binding affinities of the synthetic heteroditopic sensors towards anions will be enhanced due to strong electrostatic interactions of the doubly positive charge of co-bound metal complexes receptors in the electrochemically oxidized form complementarily with the hydrogen bonds of amide groups to anions.

2.2 Experimental Section

2.2.1 Synthesis of Diaza Crown Ether and Calix[4]arene Derivatives Containing Amidoferrocene

2.2.1.1 General Procedure

2.2.1.1.1 Analytical Measurements

Nuclear magnetic resonance (NMR) spectra were recorded on Variance 400 MHz NMR spectrometer. All chemical shifts were reported in part per million (ppm) using the residual proton or carbon signal in deuterated solvents as internal references. The 2D NMR techniques such as ^1H - ^1H COSY and ^1H - ^{13}C HMQC and ^1H - ^{13}C HMBC have been applied to assign the structure of the receptors.

Elemental analyses were carried out on a Perkin-Elmer CHNO/S analyzer by ignition combustion gas chromatography separated by frontal analyses and quantitatively detected by thermal conductivity detector.

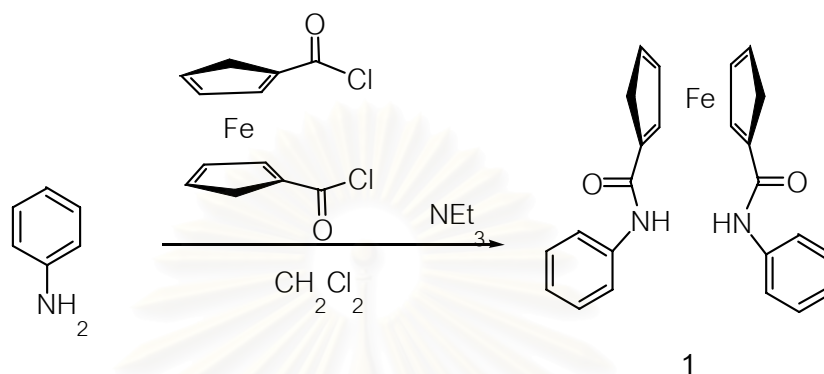
X-Ray data of compound **1** and complex of $[\mathbf{2d.NaCl}].\text{CHCl}_3$ were collected on a KappaCCD area detector diffractometer. Structures were solved by direct method with SIR97 program [86]. All non-hydrogen atoms were refined anisotropically. All structures were solved and refined by full-matrix least-square on F^2 using the computer program SHELXL-97 [87].

2.2.1.1.2 Materials

Unless otherwise noted, the materials and solvents were standard analytical grade and used without purification, purchased from Fluka, Aldrich, Merck, J. T. Baker and Lab Scan. Commercial grade solvents such as acetone, dichloromethane, hexane, methanol and ethyl acetate were purified by distillation. Acetonitrile and dichloromethane were dried over CaH_2 and freshly distilled under nitrogen atmosphere before use. DMF was dried with CaH_2 , distilled under reduced pressure and stored over molecular sieves 3 or 4 Å under N_2 . Column chromatography operations were carried out on silica gel (Kieselgel 60, 0.063-0.200 nm, Merck) and alumina (aluminium oxide 90, 0.063-0.200 nm, Merck.). *p-tert*-Butylcalix[4]arene was prepared according to published procedures [88]. Moreover, the ferrocene derivatives 1,1'-diacetylferrocene, 1,1'-ferrocenedicarboxylic acid and 1,1'-bis(chlorocarbonyl)ferrocene have been synthesized following the literature [89].

2.2.1.2 Synthesis

2.2.1.2.1 Preparation of 1,1'-bis(phenylaminocarbonyl) ferrocene (1)



To a solution of aniline (0.10 mL, 1.09 mmole) and triethylamine (0.38 mL, 2.73 mmole) in 150 mL was added 1,1'-bis(chlorocarbonyl)ferrocene (0.23 g, 0.73 mmole) in dichloromethane 7 mL, and the solution was stirred for 4 hours. The solution was washed with water (3 × 100 mL) and the organic layer was dried over anhydrous Na_2SO_4 and then filtered. The solvent was removed *in vacuo* which was purified by column chromatography on SiO_2 by using 10% EtOAc: CH_2Cl_2 as eluent obtained as orange solid (0.24g, 78% yield).

Characterization data for (1)

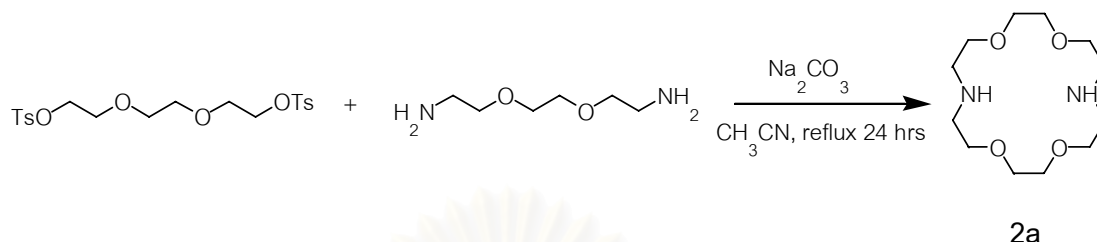
$^1\text{H-NMR}$ spectrum (400 MHz, CDCl_3 , ppm) : δ 8.76 (s, 2H, -NH), 7.88 (d, $J = 8.0$ Hz, 4H, ArH), 7.48 (t, $J = 7.6$ Hz, 4H, ArH), 7.24 (t, $J = 7.2$ Hz, 2H, ArH), 4.75 (s, 4H, o-CpH), 4.58 (s, 4H, m-CpH)

Elemental analysis: Anal. Calcd. For $\text{C}_{24}\text{H}_{20}\text{FeN}_2\text{O}_2$: C, 67.95; H, 4.72; N, 6.61

Found : C,67.85 ; H, 4.63 ; N, 6.51

ESI mass : calcd : 425.28; found: 425.28 $[\text{M}+\text{H}^+]$

2.2.1.2.2 Preparation of diaza-18-crown-6 (2a)



To a mixture of triethylene glycol ditosylate (5.00g, 9.6 mmole) and Na_2CO_3 (10.17 g, 96.0 mmole) in dry acetonitrile 70 mL was slowly added a solution of 2-[2-(2-amino-ethoxy)-ethoxy]-ethylamine (1.41 mL, 9.6 mmol) in acetonitrile 30 mL. The mixture solution was refluxed for 36 hours, then filtered and the solvent was removed *in vacuo*. The crude product that was purified by Al_2O_3 column chromatography by using THF:EtOH 10:1 as eluent. The white solid of **2a** (1.28g, 51% yield) was obtained from addition of hexane to the solution of **2a** in dichloromethane.

Characterization data for (2a)

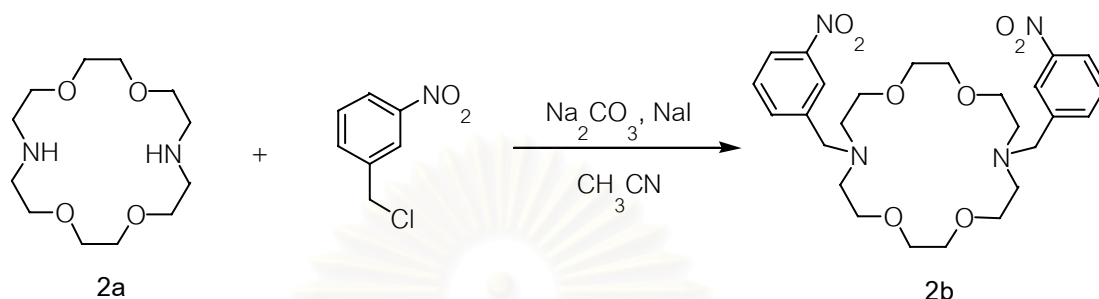
$^1\text{H-NMR}$ spectrum (400 MHz, CDCl_3 , ppm): δ 3.55 (m, 16H, $-\text{NHCH}_2\text{CH}_2\text{O}-$ and $-\text{OCH}_2\text{CH}_2\text{O}-$) 2.83 (m, 8H, $-\text{CH}_2\text{NH}-$), 2.15 (t, $J = 6.0$ Hz, 2H, $-\text{NH}$)

$^{13}\text{C-NMR}$ spectrum (100 MHz, CDCl_3 , ppm) : δ 72.1, 70.6, 50.2

สถาบันวิทยบริการ
จุฬาลงกรณ์มหาวิทยาลัย

2.2.1.2.3 Preparation of *N,N'*-di-(3-nitrobenzyl)-4,13-diaza-18-crown-6

(2b)



A mixture of diaza-18-crown-6 **2b** (0.5g, 1.9 mmole) and anhydrous Na_2CO_3 (1.2 g, 11 mmole) in acetonitrile 70 mL was refluxed for 30 minutes. Then a solution of 3-nitrobenzyl chloride (0.80 g, 4.7 mmole) in acetonitrile 30 mL was slowly added and the reaction mixture was refluxed for 24 hours and filtered to remove Na_2CO_3 . The solvent was removed by a rotary evaporator. The crude product was then purified by column chromatography (SiO_2) using 5% $\text{MeOH}:\text{CH}_2\text{Cl}_2$ to obtain **2b** as white solid (0.74 g, 70% yield).

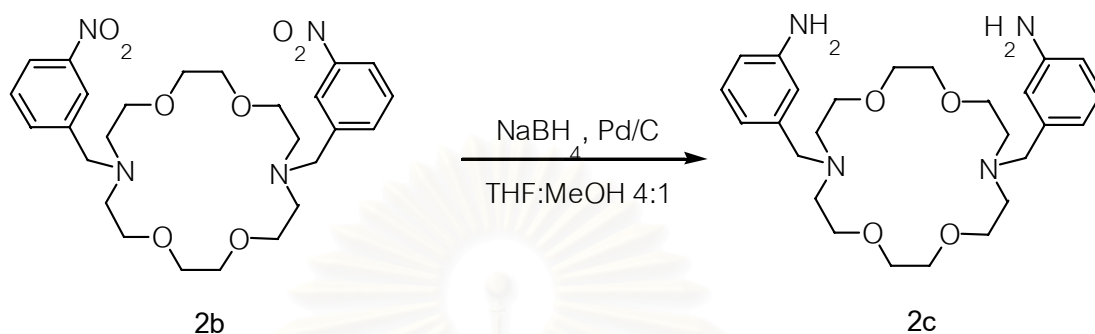
Characterization data for (2b)

$^1\text{H-NMR}$ spectrum (400 MHz, CDCl_3 , ppm): δ 8.26 (s, 2H, *ArH*), 8.27 (d, $J = 8.0$ Hz, 2H, *ArH*), 7.69 (d, $J = 7.6$ Hz, 2H, *ArH*), 7.45 (t, $J = 8.0$ Hz, 2H, *ArH*), 3.80 (s, 2H, $-\text{CH}_2-$), 3.64 (m, 16H, $-\text{NHCH}_2\text{CH}_2\text{O}-$ and $-\text{OCH}_2\text{CH}_2\text{O}-$), 2.83 (t, $J = 6.0$ Hz, 8H, $-\text{CH}_2\text{N}-$)

$^{13}\text{C-NMR}$ spectrum (100 MHz, CDCl_3 , ppm) : δ 148.30, 134.70, 129.01, 123.40, 121.97, 70.76, 69.83, 58.96, 53.94.

2.2.1.2.4 Preparation of *N,N'*-di-(3-aminobenzyl)-4,13-diaza-18-crown-6

(2c)

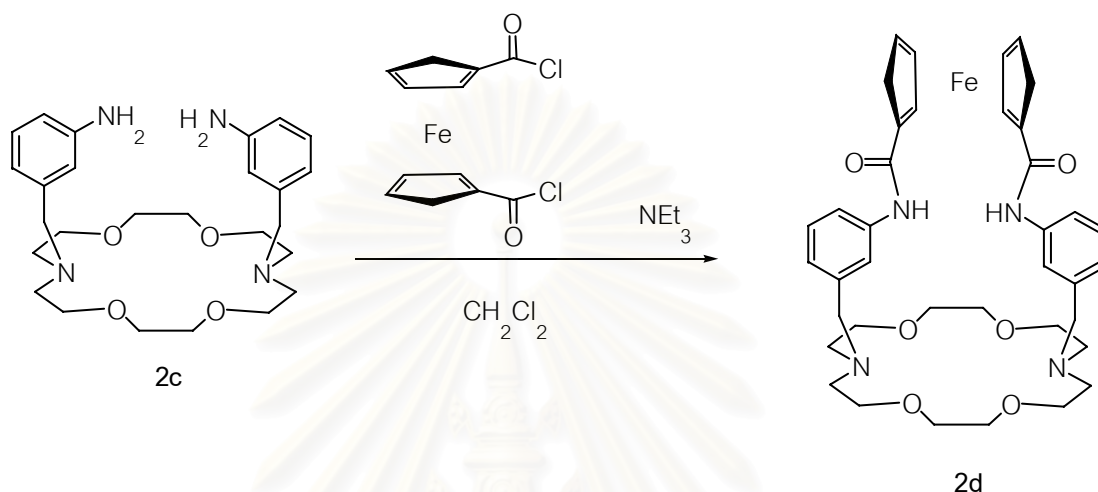


Sodium borohydride (0.055 g, 1.50 mmol) was added to a vigorously stirred suspension of **2b** (1.10g, 2.08 mmol) and palladium on carbon (0.31g, 8.31 mmole) in 4:1 THF:methanol 50 mL. The solution was stirred at room temperature for 20 minutes under nitrogen. Then, the mixture was filtered to remove palladium and the filtrate was dried in *vacuo*. The residual solid was taken up in CH_2Cl_2 and washed with water. The organic layer was dried over anhydrous MgSO_4 . Evaporation of the solvent gave the product, **2c**, as a white solid in a quantitative yield. Compound **2c** was used immediately for the next step.

Characterization data for (2c)

$^1\text{H-NMR}$ spectrum (400 MHz, CDCl_3 , ppm): δ 7.10 (t, $J = 7.6$ Hz, 2H, *ArH*), 6.80 (s, 2H, *ArH*), 6.72 (d, $J = 6.8$ Hz, 2H, *ArH*), 6.58 (d, $J = 8.0$ Hz, 2H, *ArH*), 3.65 (m, 16H, - $\text{NHCH}_2\text{CH}_2\text{O}$ - and $-\text{OCH}_2\text{CH}_2\text{O}$ -), 2.84 (t, $J = 5.6$ Hz, 8H, $-\text{CH}_2\text{NH}$ -)

2.2.1.2.5 Preparation of *N,N*-di-(3-amideferrocenylbenzyl)-4,13-diaza-18-crown-6 (2d)



To a stirred solution of **2c** (0.35 g, 0.73 mmole) and triethylamine (0.26 mL, 1.83 mmole) in 150 mL of CH₂Cl₂ was added a solution of 1,1'-bis(chlorocarbonyl)ferrocene (0.23 g, 0.73 mmole) in dichloromethane 7 mL, and the solution was stirred for 4 hours. The solution was washed with water (3 × 100 mL) and the organic layer was dried over anhydrous Na₂SO₄ and filtered. The solvent was removed *in vacuo* resulted in a red oily residue which was purified by column chromatography on SiO₂ by using 10% EtOAc:CH₂Cl₂ as eluent to obtain an orange solid (0.18 g , 33% yield).

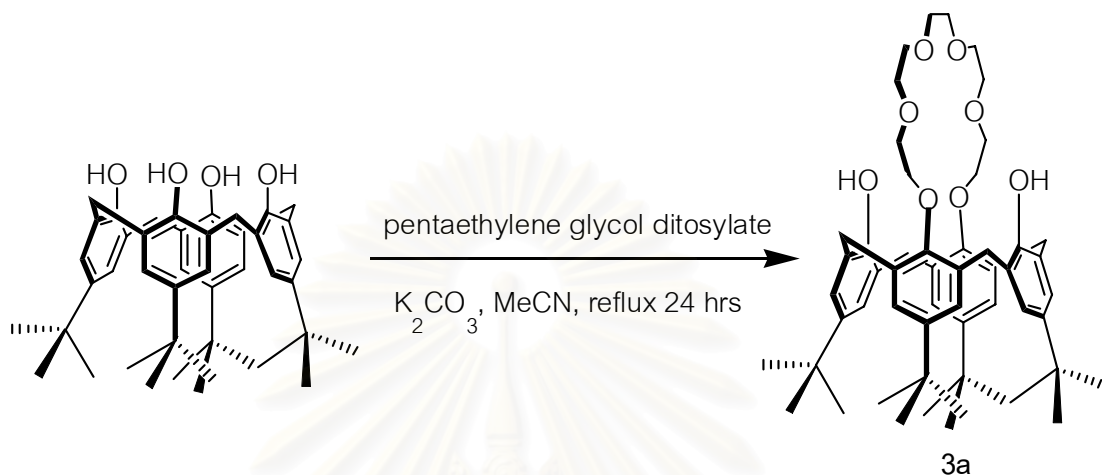
Characterization data for (2d)

¹H-NMR spectrum (400 MHz, CDCl₃, ppm): δ 8.68 (s, 2H, -NH), 7.97 (s, 2H, ArH), 7.58 (d, *J* = 8.0 Hz, 2H, ArH), 7.33 (t, *J* = 7.6 Hz, 2H, ArH), 7.21 (d, *J* = 7.6 Hz, 2H, ArH), 4.71 (s, 4H, *o*-CpH), 4.53 (s, 4H, *m*-CpH), 3.93 (s, 4H, *m*-CpH), 3.67 (t, *J* = 5.2 Hz, 8H, -OCH₂CH₂O-), 3.59 (s, 8H, -NCH₂CH₂O-), 3.01 (s, 8H, -NCH₂CH₂O-)

Elemental analysis: Anal. Calcd. For C₃₆H₄₆FeN₄O₆ : C, 64.24; H, 6.48; N, 7.89.

Found : C,64.37 ; H, 6.52 ; N, 7.56.

2.2.1.2.6 Preparation of 5,11,17,23-tetra-*tert*-butyl-25,27-(dihydroxy) calix[4]arene-crown-6 (3a)



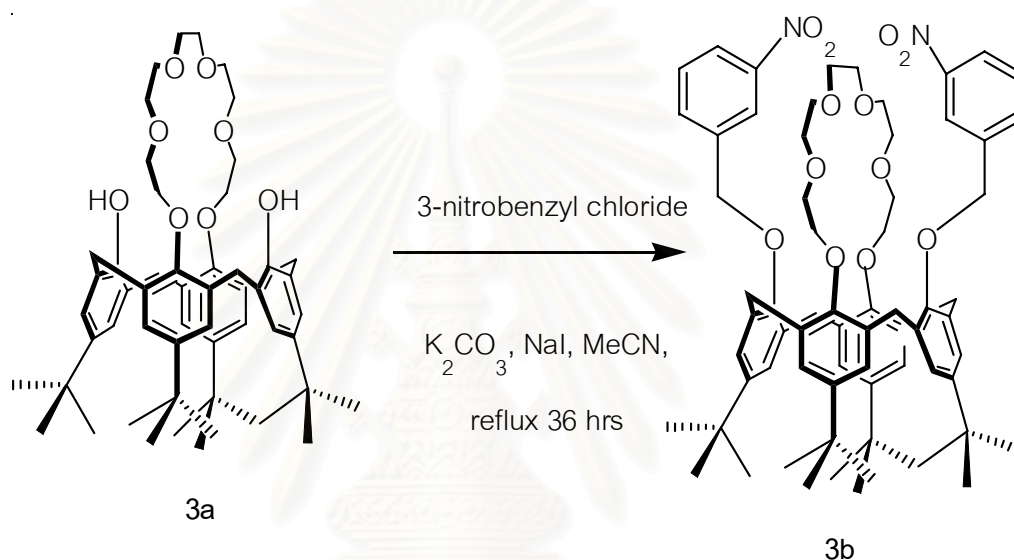
A mixture of *p-tert*-butylcalix[4]arene (5.0 g, 6.75 mmole) and K_2CO_3 (1.06 g, 7.64 mmole) in acetonitrile 300 mL was stirred at room temperature for 1 hour under nitrogen atmosphere. Pentaethyleneglycol ditosylate (3.34 mL, 7.64 mmole) in acetonitrile 50 mL was added dropwise and the mixture was refluxed for 24 hours. After cooling at room temperature, Na_2CO_3 was removed by filtration. The filtrate was evaporated and the residue was dissolved in CH_2Cl_2 100 mL and stirred with 3M HCl 100 mL for 30 minutes. The organic phase was washed with water (3 × 100 mL) and dried over anhydrous MgSO_4 . After removal solvent, the crude product was then purified by column chromatography (SiO_2) using 3% $\text{MeOH}:\text{CH}_2\text{Cl}_2$ as eluent. Compound **3a** was precipitated in hexane as white solid (5.16 g, 90% yield).

Characterization data for (3a)

$^1\text{H-NMR}$ spectrum (400 MHz, CDCl_3 , ppm) : δ 9.42 (s, 2H, -OH), 7.08 (s, 4H, ArH), 6.76 (s, 4H, ArH), 4.37 (d, AB system, $J = 13.2$ Hz, Ar- CH_2 -Ar), 4.12 (m, 4H, - $\text{OCH}_2\text{CH}_2\text{O}$ -), 4.02 (m, 4H, - $\text{OCH}_2\text{CH}_2\text{O}$ -), 3.95 (m, 4H, - $\text{OCH}_2\text{CH}_2\text{O}$ -), 3.86 (m, 4H, - $\text{OCH}_2\text{CH}_2\text{O}$ -), 3.77 (m, 4H, - $\text{OCH}_2\text{CH}_2\text{O}$ -), 3.31 (d, $J = 12.8$ Hz, AB system, Ar- CH_2 -Ar), 1.32 (s, 18H, - $\text{C}(\text{CH}_3)_3$), 0.93 (s, 18H, - $\text{C}(\text{CH}_3)_3$).

^{13}C -NMR spectrum (100 MHz, CDCl_3 , ppm) : δ 150.66, 146.77, 141.24, 132.39, 127.80, 125.44, 125.01, 71.68, 71.06, 71.02, 69.94, 33.82, 33.79, 31.70, 31.28, 30.95.

2.2.1.2.7 Preparation of 5,11,17,23-tetra-*tert*-butyl-25,27-di-(3-nitrobenzyl)calix[4]arene-crown-6 (3b)



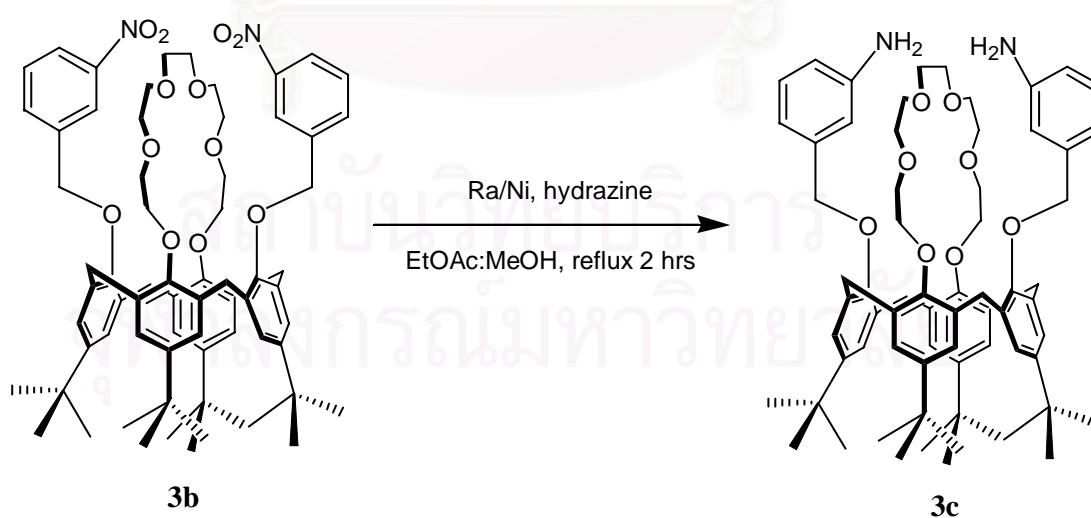
A mixture of **3a** (1.37 g, 1.61 mmole) and anhydrous K_2CO_3 (0.55 g, 4.02 mmole) in acetonitrile 100 mL was stirred at room temperature for 1 hour under nitrogen atmosphere. Then, 3-nitrobenzyl chloride (0.69 g, 4.02 mmole) in acetonitrile 50 mL was added dropwise and the mixture was refluxed for 36 hours. After cooling at room temperature, Na_2CO_3 was removed by filtration. The filtrate was then evaporated and the residue was dissolved in CH_2Cl_2 100 mL and stirred with 3M HCl 100 mL for 30 minutes. The organic phase was washed with water 100 mL for 3 times and dried over anhydrous MgSO_4 . After removal of the solvent, the crude product was purified by column chromatography (SiO_2) using 10% EtOAc: CH_2Cl_2 as eluent. The product was obtained as the white solid (1.31 g, 73% yield).

Characterization data for (3b)

$^1\text{H-NMR}$ spectrum (400 MHz, CDCl_3 , ppm) : δ 8.20 (s, 2H, ArH), 8.19 (s, 2H, ArH), 7.92 (d, $J = 7.2$ Hz, 2H, ArH), 7.59 (t, $J = 7.6$ Hz, 2H, ArH), 6.95 (s, 4H, ArH), 6.55 (s, 4H, ArH), 5.03 (s, 4H, $-\text{OCH}_2\text{Ar}$), 4.24 (d, AB system, $J = 12.4$ Hz, $\text{Ar-CH}_2\text{-Ar}$), 4.03 (t, $J = 6.4$ Hz, 4H, $-\text{ArOCH}_2\text{CH}_2\text{O-}$), 3.85 (t, $J = 7.2$ Hz, 4H, $-\text{OCH}_2\text{CH}_2\text{O-}$), 3.58 (t, $J = 5.2$ Hz, 4H, $-\text{OCH}_2\text{CH}_2\text{O-}$), 3.54 (s, 4H, $-\text{OCH}_2\text{CH}_2\text{O-}$), 3.48 (t, $J = 5.2$ Hz, 4H, $-\text{OCH}_2\text{CH}_2\text{O-}$), 3.01 (d, $J = 12.8$ Hz, AB system, $\text{Ar-CH}_2\text{-Ar}$), 1.22 (s, 18H, $-\text{C}(\text{CH}_3)_3$), 0.91 (s, 18H, $-\text{C}(\text{CH}_3)_3$).

$^{13}\text{C-NMR}$ spectrum (100 MHz, CDCl_3 , ppm) : δ 153.99, 151.07, 147.89, 145.16, 145.04, 139.54, 136.32, 134.41, 132.62, 129.44, 125.40, 124.84, 124.53, 122.97, 75.82, 72.56, 71.04, 70.80, 70.64, 70.00, 33.98, 33.71, 31.56, 31.15.

2.2.1.2.8 Preparation of of 5,11,17,23-tetra-*tert*-butyl-25,27-di-(3-amino benzyl)calix[4]arene-crown-6 (3c)



Compound **3b** (0.82 g, 0.73 mmol) and Raney Ni (0.3g, 4.82 mmole) were suspended in the mixture of ethylacetate 15 mL and MeOH 11 mL under N₂ atmosphere. Hydrazine 1.69 mL was subsequently added and the mixture was refluxed for 2 hours. The rest of Ra/Ni was removed while the solution still warm. The solvent in the filtrate was removed under reduce pressure. The crude product was then dissolved in CH₂Cl₂ 50 mL and washed with water (3 × 50 mL). The organic layer was separated and dried over anhydrous MgSO₄. The solvent was removed *in vacuo* to obtain as white solid of **3c** in a quantitative yield. Compound **3b** was used immediately in the next step.

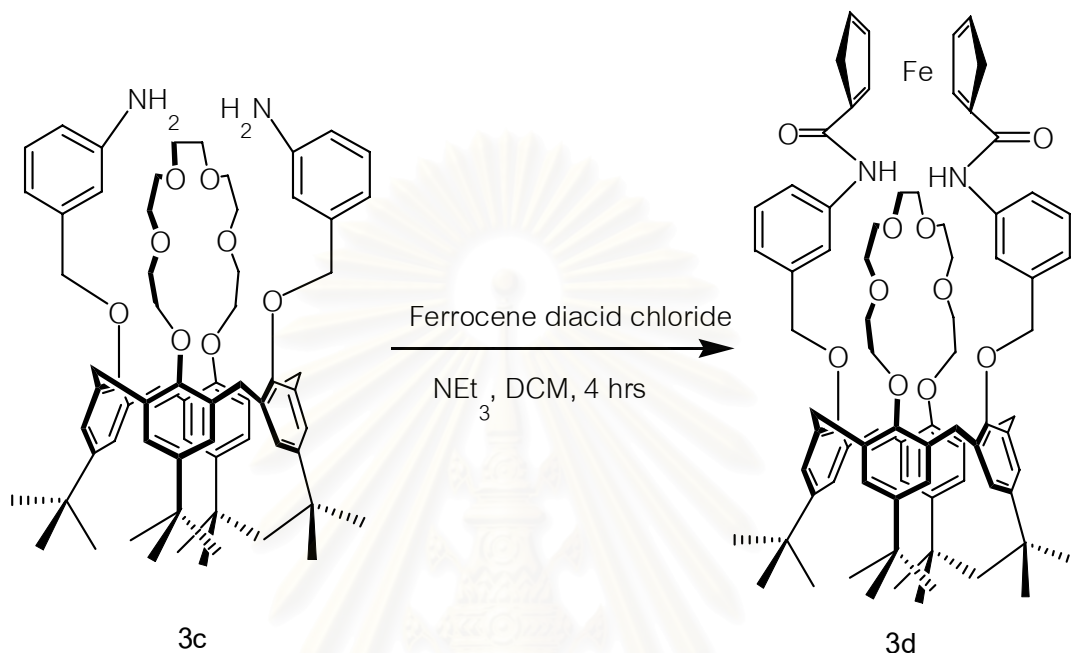
Characterization data for (**3c**)

¹H-NMR spectrum (400 MHz, CDCl₃, ppm) : δ 7.12 (s, 4H, ArH), 6.77 (d, *J* = 7.2 Hz, 2H, ArH), 6.68 (t, *J* = 8.4 Hz, 2H, ArH), 6.44 (s, 4H, ArH), 4.62 (s, 4H, -OCH₂Ar), 4.36 (d, AB system, *J* = 12.8 Hz, Ar-CH₂-Ar), 4.14 (m, 4H, -OCH₂CH₂O-), 3.93 (m, 4H, -OCH₂CH₂O-), 3.64 (s, 4H, -OCH₂CH₂O-), 3.57 (t, *J* = 4.4 Hz, 4H, -OCH₂CH₂O-), 3.62 (t, *J* = 4.8 Hz, 4H, -OCH₂CH₂O-), 3.12 (d, *J* = 12.4 Hz, AB system, Ar-CH₂-Ar), 1.34 (s, 18H, -C(CH₃)₃), 0.82 (s, 18H, -C(CH₃)₃)

¹³C-NMR spectrum (100 MHz, CDCl₃, ppm) : δ 154.52, 152.23, 146.65, 145.14, 144.36, 139.13, 135.41, 131.77, 129.16, 125.57, 124.52, 118.97, 116.17, 115.14, 78.14, 72.03, 70.70, 70.29, 69.36, 33.59, 31.72, 31.12, 30.99

สถาบันวิทยบริการ
จุฬาลงกรณ์มหาวิทยาลัย

2.2.1.2.9 Preparation of 5,11,17,23-tetra-*tert*-butyl-25,27-di-(3-amidoferrocenylbenzyl)calix[4]arene-crown-6 (3d)



To a stirred solution of **3c** (0.80 g, 0.73 mmole) and triethylamine (0.26 mL, 1.83 mmole) in 150 mL of CH_2Cl_2 was added a solution of 1,1'-bis(chlorocarbonyl)ferrocene (0.23 g, 0.73 mmole) in dichloromethane 20 mL, and the solution was stirred for 4 hours. Then, the solution was washed with water (3 × 100 mL) and the organic layer was dried over anhydrous Na_2SO_4 . The solvent was removed by rotary evaporator to give a red oily residue which was purified by column chromatography (SiO_2) by using 50% EtOAc: CHCl_3 as eluent obtained. The orange solid 0.21g (22% yield) was obtained.

Characterization data for (3d)

$^1\text{H-NMR}$ spectrum (400 MHz, CDCl_3 , ppm) : δ 9.03 (s, 2H, -NH), 8.15 (s(br), 2H, ArH), 7.87 (s(br), 2H, ArH), 7.38 (s(br), 2H, ArH), 7.16 (m, 2H, ArH), 7.11 (s, 4H, ArH), 6.50 (s, 4H, ArH), 4.85 (s, 4H, o-CpH), 4.77 (s, 4H-OCH₂Ar), 4.50 (s, 4H, m-CpH), 4.37 (d, AB system, $J = 12.0$ Hz, Ar-CH₂-Ar), 3.98 (s, 4H, -ArOCH₂CH₂O-), 3.87 (s, 4H, -OCH₂CH₂O-), 3.63 (s, 4H, -OCH₂CH₂O-), 3.53 (s, 4H, -OCH₂CH₂O-), 3.40 (s, 4H, -OCH₂CH₂O-), 3.13 (d, $J = 12.0$ Hz, AB system, Ar-CH₂-Ar), 1.33 (s, 18H, -C(CH₃)₃), 0.85 (s, 18H, -C(CH₃)₃)

ESI mass : calcd: 1322.43; found 1322.45 [M+Na⁺]



สถาบันวิทยบริการ
จุฬาลงกรณ์มหาวิทยาลัย

2.2.2 Binding Studies by NMR Titrations

2.2.2.1 General Procedure

2.2.2.1.1 Apparatus

^1H NMR spectra were carried out on a VARIENCE 400 MHz nuclear magnetic resonance spectrometer. All of the experiments were recorded in 5% $\text{CD}_3\text{CN}:\text{CDCl}_3$ and chemical shifts referred to a residue proton signal.

2.2.2.1.2 Chemicals

All materials and solvents were standard analytical grade purchased from Aldrich, and Avacado and used without further purification unless otherwise noted. However, deuterated acetronitrile were stored over 3 Å molecular sieves.

2.2.2.2 Experimental Procedure

2.2.2.2.1 Anion Binding Studies of Receptors 1, 2d and 3d

Typically, a 0.005 M solution of a receptor (2.5×10^{-6} mol) in 5% $\text{CD}_3\text{CN}:\text{CDCl}_3$ 0.5 mL was prepared in NMR tubes. A 0.05 M stock solution of any anionic guest molecules in 5% $\text{CD}_3\text{CN}:\text{CDCl}_3$ was prepared in a small vial. The solution of guest molecules was added into the NMR samples according to the ratio in Table 2.1.

สถาบันวิทยบริการ
จุฬาลงกรณ์มหาวิทยาลัย

Table 2.1 Volume and concentration of guests (as tetrabutylammonium salts) which have been used in the experiments.

Mole ratio Guest : Receptor	Added volume of 0.05 M of guest solution (μL)	Concentration of a guest molecule [M]	Concentration of a receptor [M]
0.0 : 1.0	0	0.00000	0.00500
0.1 : 1.0	5	0.00050	0.00495
0.2 : 1.0	5	0.00098	0.00490
0.3 : 1.0	5	0.00146	0.00485
0.4 : 1.0	5	0.00192	0.00481
0.5 : 1.0	5	0.00238	0.00476
0.6 : 1.0	5	0.00283	0.00472
0.7 : 1.0	5	0.00327	0.00467
0.8 : 1.0	5	0.00370	0.00463
0.9 : 1.0	5	0.00413	0.00459
1.0 : 1.0	5	0.00455	0.00455
1.2 : 1.0	10	0.00536	0.00446
1.4 : 1.0	10	0.00614	0.00439
1.6 : 1.0	10	0.00690	0.00431
1.8 : 1.0	10	0.00763	0.00424
2.0 : 1.0	10	0.00833	0.00417
3.0 : 1.0	50	0.01154	0.00385
4.0 : 1.0	50	0.01429	0.00357

2.2.2.2.2 Cation Binding Studies of Receptors 2d and 3d with NaClO₄ and KPF₆

Typically, a 0.005 M solution of a ligand (2.5×10^{-6} mol) in 5% CD₃CN:CDCl₃ 0.5 mL was prepared in NMR tubes. A 0.05 M stock solution of cationic guest molecules in 5% CD₃CN:CDCl₃ was prepared in a small vial. The solution of cationic guest molecules was added into the NMR samples according to the ratio in Table 2.2.

Table 2.2 Volume and concentration of metal salts (NaClO₄ and KPF₆) which have been used in the experiments.

Mole ratio Guest : Receptor	Added volume of 0.05 M of guest solution (μL)	Concentration of a guest molecule [M]	Concentration of a receptor [M]
0.0 : 1.0	0	0.00000	0.00500
0.1 : 1.0	5	0.00050	0.00495
0.2 : 1.0	5	0.00098	0.00490
0.3 : 1.0	5	0.00146	0.00485
0.4 : 1.0	5	0.00192	0.00481
0.5 : 1.0	5	0.00238	0.00476
0.6 : 1.0	5	0.00283	0.00472
0.7 : 1.0	5	0.00327	0.00467
0.8 : 1.0	5	0.00370	0.00463
0.9 : 1.0	5	0.00413	0.00459
1.0 : 1.0	5	0.00455	0.00455
1.2 : 1.0	10	0.00536	0.00446
1.4 : 1.0	10	0.00614	0.00439
1.6 : 1.0	10	0.00690	0.00431
1.8 : 1.0	10	0.00763	0.00424
2.0 : 1.0	10	0.00833	0.00417
3.0 : 1.0	50	0.01154	0.00385
4.0 : 1.0	50	0.01429	0.00357

2.2.2.2.3 Simultaneous Cation and Anion Binding Studies of Receptors

2d and 3d

Typically, a 0.005 M solution of a receptor (2.5×10^{-6} mol) and cationic guest molecules (3.0×10^{-6} mol) in 5% $\text{CD}_3\text{CN}:\text{CDCl}_3$ 0.5 mL was prepared in NMR tubes. A 0.05 M stock solution of anionic guest molecules in 5% $\text{CD}_3\text{CN}:\text{CDCl}_3$ was prepared in a small vial. The solution of cationic guest molecules was added into the NMR samples according to 0.0-4.0 equivalents in Table 2.3.

Table 2.3 Volume and concentration of guests (as tetrabutylammonium salts) which have been used in the experiments.

Mole ratio Guest : Receptor	Added volume of 0.05 M of a guest solution (μL)	Concentration of a guest molecule [M]	Concentration of a receptor [M]
0.0 : 1.0	0	0.00000	0.00500
0.1 : 1.0	5	0.00050	0.00495
0.2 : 1.0	5	0.00098	0.00490
0.3 : 1.0	5	0.00146	0.00485
0.4 : 1.0	5	0.00192	0.00481
0.5 : 1.0	5	0.00238	0.00476
0.6 : 1.0	5	0.00283	0.00472
0.7 : 1.0	5	0.00327	0.00467
0.8 : 1.0	5	0.00370	0.00463
0.9 : 1.0	5	0.00413	0.00459
1.0 : 1.0	5	0.00455	0.00455
1.2 : 1.0	10	0.00536	0.00446
1.4 : 1.0	10	0.00614	0.00439
1.6 : 1.0	10	0.00690	0.00431
1.8 : 1.0	10	0.00763	0.00424
2.0 : 1.0	10	0.00833	0.00417
3.0 : 1.0	50	0.01154	0.00385
4.0 : 1.0	50	0.01429	0.00357

2.2.3 Electrochemical Studies

2.2.3.1 General Procedure

2.2.3.1.1 Apparatus

Cyclic Voltammetry and Square Wave Voltammetry were performed using AUTOLAB PGSTAT 100 potentiostat. All electrochemical experiments carried out with a three-electrode cell comprising of a working electrode, a counter electrode and a reference electrode at room temperature. The supporting electrolyte is 0.1M tetrabutylammonium hexafluorophosphate (TBAPF₆) in 40% Acetonitrile:CH₂Cl₂. The working electrode was a Pt electrode with a diameter 5 mm embedded in Teflon and the counter electrode was a platinum coil. Ag/AgNO₃ electrodes were used as a reference electrode in 40% CH₃CN:CH₂Cl₂.

The platinum counter electrode was polished with a sandpaper prior to use. A Ag/AgNO₃ electrode was customarily constructed by immersing a silver wire into a solution of 0.01M AgNO₃ in 0.1 M TBAPF₆. The working electrode was polished with slurries of 0.5 μm followed with 1 μm alumina powder, and washed by sonication for 5 minutes in 0.05 M H₂SO₄ and subsequently with a solvent. The appropriate scan rate was found to be 100 mV/s for both cyclic voltammetry and square wave voltammetry.

2.2.3.1.2 Chemicals

All of the guest molecules including tetrabutylammonium salts, supporting electrolyte and metal salts were dried under vacuum overnight. Acet onitrile and dichloromethane were freshly distilled over CaH₂ under nitrogen atmosphere before use.

2.2.3.2 Experimental Procedure

2.2.3.2.1 Anions Binding Studies of Receptors 1, 2d and 3d

Typically, a 0.005 M solution of a receptor (2.5×10^{-5} mol) in 5 mL of supporting electrolyte, was prepared. A 0.50 M stock solution of anionic guests was prepared in supporting electrolyte solution. Upon titration, the solution of anionic guests was added into the solution of ligand following the ratio in the Table 2.4.

Table 2.4 Volume and concentration of guests (as tetrabutylammonium salts) which have been used in the experiments.

Mole ratio Guest : Receptor	Added volume of 0.05 M of a guest solution (μL)	Concentration of a guest molecule [M]	Concentration of a receptor [M]
0.0 : 1.0	0	0.00000	0.00500
0.1 : 1.0	5	0.00050	0.00495
0.2 : 1.0	5	0.00098	0.00490
0.3 : 1.0	5	0.00146	0.00485
0.4 : 1.0	5	0.00192	0.00481
0.5 : 1.0	5	0.00238	0.00476
0.6 : 1.0	5	0.00283	0.00472
0.7 : 1.0	5	0.00327	0.00467
0.8 : 1.0	5	0.00370	0.00463
0.9 : 1.0	5	0.00413	0.00459
1.0 : 1.0	5	0.00455	0.00455
1.2 : 1.0	10	0.00536	0.00446
1.4 : 1.0	10	0.00614	0.00439
1.6 : 1.0	10	0.00690	0.00431
1.8 : 1.0	10	0.00763	0.00424
2.0 : 1.0	10	0.00833	0.00417
3.0 : 1.0	50	0.01154	0.00385
4.0 : 1.0	50	0.01429	0.00357

2.2.3.2.2 Cations Binding Studies of Receptors 2d and 3d

Typically, a 0.005 M solution of a receptor (2.5×10^{-5} mol) in 5 mL of supporting electrolyte was prepared. A 0.50 M stock solution of metal salts was prepared in supporting electrolyte solution as well. Upon titration, the solution of metal salts was added into the solution of ligand following the ratio in the Table 2.5.

Table 2.5 Volume and concentration of metal salts (NaClO_4 and KPF_6) which have been used in the experiments.

Mole ratio Guest : Receptor	Added volume of 0.05 M of a guest solution (μL)	Concentration of guest molecule [M]	Concentration of a receptor [M]
0.0 : 1.0	0	0.00000	0.00500
0.1 : 1.0	5	0.00050	0.00495
0.2 : 1.0	5	0.00098	0.00490
0.3 : 1.0	5	0.00146	0.00485
0.4 : 1.0	5	0.00192	0.00481
0.5 : 1.0	5	0.00238	0.00476
0.6 : 1.0	5	0.00283	0.00472
0.7 : 1.0	5	0.00327	0.00467
0.8 : 1.0	5	0.00370	0.00463
0.9 : 1.0	5	0.00413	0.00459
1.0 : 1.0	5	0.00455	0.00455
1.2 : 1.0	10	0.00536	0.00446
1.4 : 1.0	10	0.00614	0.00439
1.6 : 1.0	10	0.00690	0.00431
1.8 : 1.0	10	0.00763	0.00424
2.0 : 1.0	10	0.00833	0.00417
3.0 : 1.0	50	0.01154	0.00385
4.0 : 1.0	50	0.01429	0.00357

2.2.3.2.3 Simultaneous Cation and Anion Binding Studies of Receptors 2d and 3d

Typically, a 0.005 M solution of a ligand (2.5×10^{-5} mol) and cationic guest (3.0×10^{-5} mol) in supporting electrolyte 5 mL was prepared. A 0.50 M stock solution of anionic guest molecules in supporting electrolyte was prepared. Upon titration, the solution of anionic guest molecules were added into the complex solution following the ratio in the Table 2.6.

Table 2.6 Volume and concentration of anionic guests (as tetrabutylammonium salts) which have been used in the experiments.

Mole ratio Guest : Receptor	Added volume of 0.05 M of a guest solution (μL)	Concentration of a guest molecule [M]	Concentration of a receptor [M]
0.0 : 1.0	0	0.00000	0.00500
0.1 : 1.0	5	0.00050	0.00495
0.2 : 1.0	5	0.00098	0.00490
0.3 : 1.0	5	0.00146	0.00485
0.4 : 1.0	5	0.00192	0.00481
0.5 : 1.0	5	0.00238	0.00476
0.6 : 1.0	5	0.00283	0.00472
0.7 : 1.0	5	0.00327	0.00467
0.8 : 1.0	5	0.00370	0.00463
0.9 : 1.0	5	0.00413	0.00459
1.0 : 1.0	5	0.00455	0.00455
1.2 : 1.0	10	0.00536	0.00446
1.4 : 1.0	10	0.00614	0.00439
1.6 : 1.0	10	0.00690	0.00431
1.8 : 1.0	10	0.00763	0.00424
2.0 : 1.0	10	0.00833	0.00417
3.0 : 1.0	50	0.01154	0.00385
4.0 : 1.0	50	0.01429	0.00357

2.3 Results and Discussion

2.3.1 Synthesis and Solid State Structure of 1,1'-Bis(phenylaminocarbonyl)ferrocene (1)

The compound **1** was synthesized in one step from the reaction of 1,1'-bis(chlorocarbonyl)ferrocene with aniline in the presence of NEt_3 and was obtained in a good yield (87%) as the intense orange solid. The $^1\text{H-NMR}$ spectrum of **1** in CDCl_3 is in agreement with the proposed structure (Figure 2.6). In addition, the NH amide peak was observed and shifted downfield ($\delta = 8.76$ ppm), presumably the intramolecular hydrogen bondings between -NH and CO of the adjacent aniline moieties are being formed and identical in the CDCl_3 solution. The positive ion electrospray mass spectrometry of **1** showed the most intense peak $[\text{Fe}(\text{C}_{24}\text{H}_{20}\text{N}_2\text{O}_2)]$ at $m/z = 424.9$ $[\text{M}+\text{H}^+]$.

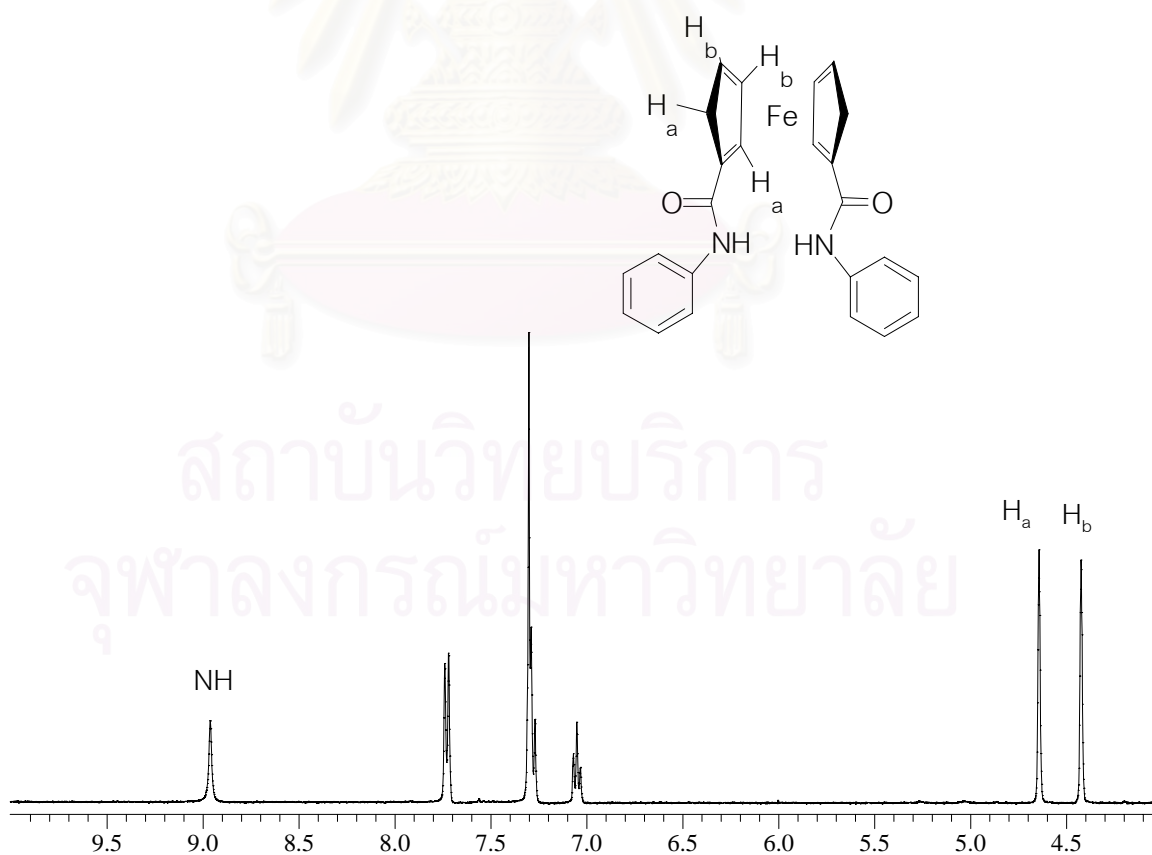


Figure 2.6 $^1\text{H-NMR}$ spectrum of compound **1** in CDCl_3 .

The intramolecular hydrogen bonding between amidoferrocene is not surprising, we have seen this interaction in the crystal structure of calix[4]arene containing amidoferrocene **2.51** which have been observed by Suksai and co-workers [90] (Figure 2.7). In this case, the NH protons were found at 8.5 ppm. Cyclopentadiene rings are eclipsed. The intermolecular hydrogen bond N-H---N is formed with $d(\text{H} \cdots \text{A})$. It can be pronounced that the staggered conformation of this molecule is controlled by the intramolecular hydrogen bond between amidoferrocene.

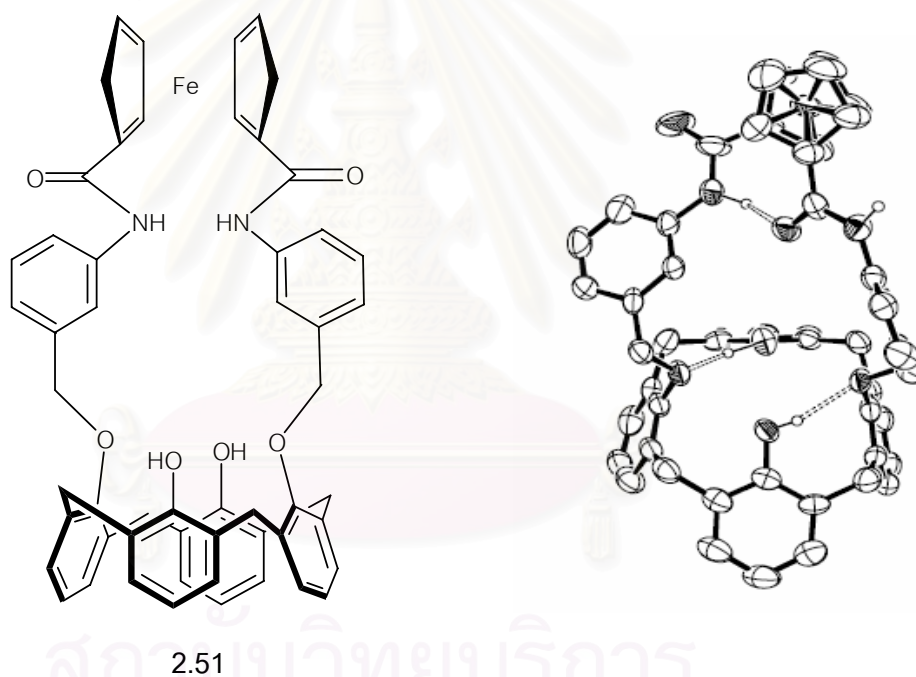


Figure 2.7 X-ray structure of compound **2.51** in 50% probability ellipsoids shows the intramolecular hydrogen bondings of amidoferrocene and of hydroxyl groups at the lower rim of calix[4]arene. Hydrogen atoms of phenyl rings and cyclopentadienyl rings are omitted for clarity.

Orange crystals of compound **1** suitable for X-ray structural investigations were obtained from a CH₂Cl₂:Hexane mixture. Crystallographic data and structure refinement of compound (**1**) are presented in Table 2.7.

Table 2.7 Crystallographic data and structure refinement of compound (**1**).

Empirical formula	C ₇₂ H ₆₀ Fe ₆ N ₆ O ₆
Formula weight	480.12
Temperature	293(2) K
Wavelength	0.71073 Å
Crystal system, space group	Trigonal, P 65
Unit cell dimensions	a = 9.3102(2) Å b = 9.3102(2) Å c = 19.8131(5) Å $\alpha = \beta = 90^{\circ}$ $\gamma = 120^{\circ}$
Volume	1487.31(6) Å ³
Z	3
Density (calculated)	1.608 Mg/m ³
Absorption coefficient	1.487 mm ⁻¹
Theta range for data collection	2.53 to 30.57 ⁰
Limiting indices	-13<=h<=8, -12<=k<=13, -28<=l<=27
Refinement method	Full-matrix least-squares on F ²
Data / restraints / parameters	2888 / 1 / 137
Goodness-of-fit on F ²	1.380
Final R indices [I>2sigma(I)]	R1 = 0.1616, wR2 = 0.3999
R indices (all data)	R1 = 0.2508, wR2 = 0.4349
Largest diff. peak and hole	0.899 and -2.212 e.Å ⁻³

Table 2.8 Selected bond lengths [Å] and angles [°] for compound (1).

Bond lengths [Å]			
C(1)-Fe(1)	1.869(12)	C(4)-Fe(1)#1	1.923(14)
C(2)-Fe(1)	1.979(14)	C(5)-Fe(1)#1	2.023(10)
C(3)-Fe(1)	2.15(2)	Fe(1)-C(1)#2	2.149(12)
C(4)-Fe(1)	2.220(17)	Fe(1)-C(2)#2	2.089(18)
C(5)-Fe(1)	2.049(12)	Fe(1)-C(3)#2	2.042(18)
C(1)-Fe(1)#1	2.149(12)	Fe(1)-C(4)#2	1.923(14)
C(2)-Fe(1)#1	2.089(18)	Fe(1)-C(5)#2	2.023(10)
C(3)-Fe(1)#1	2.042(18)		
Bond angles [°]			
C(1)-Fe(1)-C(2)	45.9(9)	Fe(1)#1-C(4)-Fe(1)	107.1(10)
C(5)-Fe(1)-C(3)	65.3(6)	Fe(1)#1-C(5)-Fe(1)	110.1(5)
C(1)-Fe(1)-C(5)	40.6(5)	C(4)#2-Fe(1)-C(3)	146.8(10)
C(1)-Fe(1)-C(4)	66.7(5)	C(4)#2-Fe(1)-C(2)	174.6(11)
C(2)-Fe(1)-C(4)	62.4(11)	C(4)#2-Fe(1)-C(5)	114.6(6)
C(2)-Fe(1)-C(5)	68.8(5)	C(4)#2-Fe(1)-C(4)	123.0(7)
C(1)-Fe(1)-C(3)	69.8(7)	C(5)#2-Fe(1)-C(3)	163.8(8)
C(2)-Fe(1)-C(3)	38.0(10)	C(3)#2-Fe(1)-C(3)	113.3(7)
C(5)-Fe(1)-C(4)	39.3(5)	C(3)#2-Fe(1)-C(4)	109.1(7)
C(3)-Fe(1)-C(4)	35.1(8)	C(2)#2-Fe(1)-C(4)	122.8(6)
Fe(1)-C(1)-Fe(1)#1	112.1(7)	C(1)#2-Fe(1)-C(4)	159.6(7)
Fe(1)-C(2)-Fe(1)#1	110.2(8)	C(2)#2-Fe(1)-C(3)	103.2(6)
C(1)-Fe(1)-C(4)#2	133.7(8)	C(5)#2-Fe(1)-C(4)	161.0(7)
C(1)-Fe(1)-C(5)#2	112.4(5)	C(5)#2-Fe(1)-C(5)	127.4(4)
C(2)-Fe(1)-C(5)#2	131.8(11)	C(3)#2-Fe(1)-C(5)	129.6(10)
C(1)-Fe(1)-C(3)#2	168.8(10)	C(5)#2-Fe(1)-C(2)#2	67.2(5)
C(2)-Fe(1)-C(3)#2	142.8(9)	C(3)#2-Fe(1)-C(2)#2	38.2(10)
C(1)-Fe(1)-C(1)#2	120.8(6)	C(4)#2-Fe(1)-C(2)#2	65.8(11)
C(2)-Fe(1)-C(1)#2	107.8(8)	C(5)#2-Fe(1)-C(3)#2	67.8(6)
C(5)-Fe(1)-C(1)#2	157.8(5)	C(2)#2-Fe(1)-C(1)#2	41.5(9)
C(3)-Fe(1)-C(1)#2	126.2(7)	C(5)#2-Fe(1)-C(1)#2	38.2(5)
C(1)-Fe(1)-C(2)#2	152.9(12)	C(3)#2-Fe(1)-C(1)#2	66.9(8)
C(2)-Fe(1)-C(2)#2	112.6(7)	C(4)#2-Fe(1)-C(1)#2	67.4(6)
C(5)-Fe(1)-C(2)#2	160.7(9)	C(4)#2-Fe(1)-C(3)#2	38.7(9)
Fe(1)#1-C(3)-Fe(1)	105.6(10)	C(4)#2-Fe(1)-C(5)#2	42.8(5)

Symmetry transformations used to generate equivalent atoms:

#1 y,-x+y,z+1/6 #2 x-y,x,z-1/6

Table 2.9 Hydrogen bond length [\AA] and angle [$^{\circ}$] for compound (1).

D-H...A	d(D-H)	d(H...A)	d(D...A)	$\angle(\text{DHA})$
N(1)-H(10)...O(1)#2	0.848(9)	2.261(9)	2.883(13)	130.4(7)

Symmetry transformations used to generate equivalent atoms: #2 x-y,x,z-1/6

Interestingly, we have found that the proposed compound forms “polymeric multiple-decker” of ferrocene in solid state (Figure 2.8). As far as we know, this is the first example where an η^5 -Cp ring of the ferrocene unit is bounded to another Fe^{2+} metal center of the adjacent ferrocene unit without any bridging metals. The propensity to form a polymeric structure is more likely to be induced by the intramolecular hydrogen bonding between NH and CO from the adjacent cyclopentadienyl rings, *vide infra*.

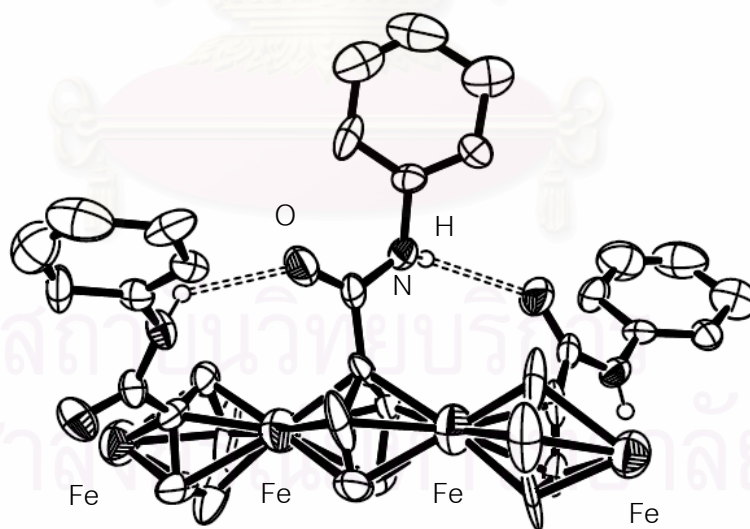


Figure 2.8 Part of the polymeric chain of receptor 1. Ellipsoids represent 50% probability; hydrogen atoms are omitted for clarity.

As far as we know, cyclopentadiene can form polymeric multiple-decker complexes, particularly with alkali metal cations (Li^+ , Na^+ and K^+) and their structures were investigated by powder diffraction methods using high-resolution synchrotron radiation [91]. It has shown that $[\text{LiC}_5\text{H}_5]_n$ and $[\text{NaC}_5\text{H}_5]_n$ form the “supersandwich” or “strings of pears” structure consisting of stacked metal-ring unit in an almost linear arrangement (Figure 2.9a). In contrast, the crystal structure of $[\text{KC}_5\text{H}_5]_n$ differs significantly from that of $[\text{LiC}_5\text{H}_5]_n$ and $[\text{NaC}_5\text{H}_5]_n$. It consists of polymeric zigzag chains containing bent metallocene units with a $\text{K}'\text{-K-K}''$ angle 138.0° (Figure 2.9b).

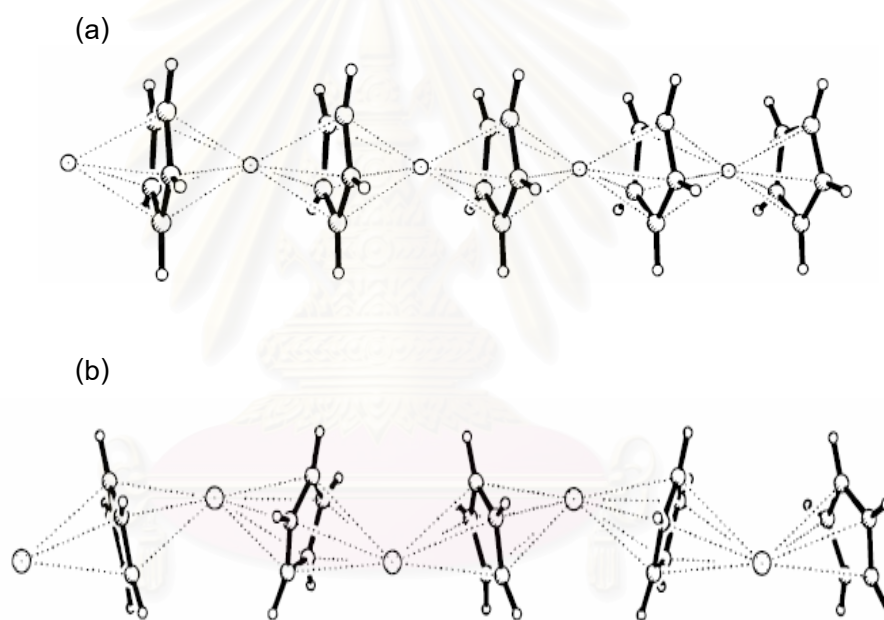
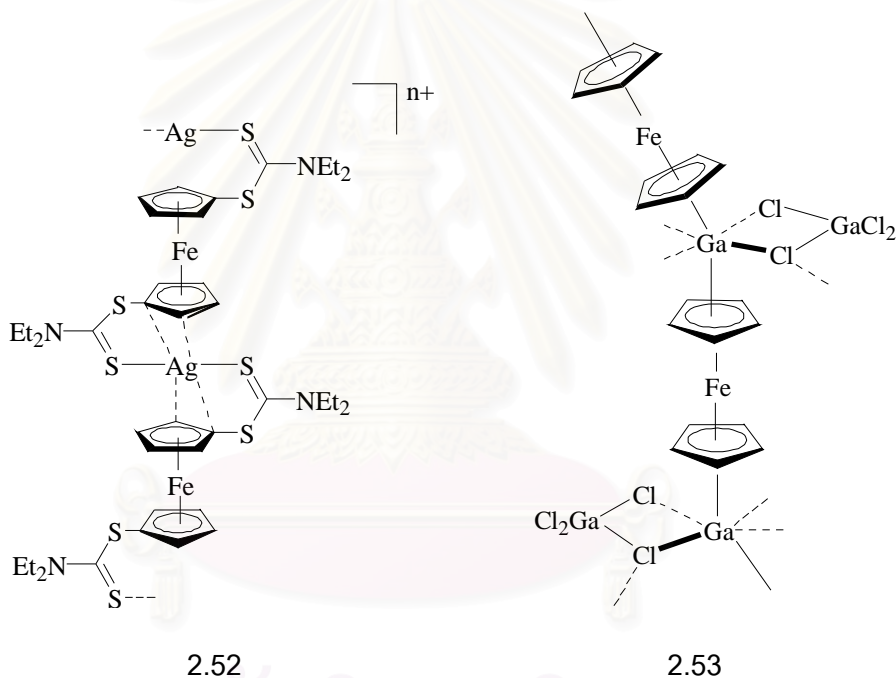


Figure 2.9 Plot of polymeric structures of (a) LiCp and (b) KCp.

Although, cyclopentadienyl complexes with alkali metal cations have been presented to form the polymeric structure. However, there are few examples which showed η^5 -cyclopentadienyl rings of ferrocene would share with another metal atoms giving polymeric multiple-decker sandwich complexes. For example, the multiple-decker sandwich complexes of $[\text{Fe}_2(\text{C}_5\text{H}_5)_3]^+$ and clusters of the general formula $\text{V}_n[\text{Fe}(\text{C}_5\text{H}_5)_2]_{n+1}$ ($n = 1-3$) have been only detected in the gas phase [92]. In 1998 Lagma and co-workers [93] reported the first crystal structure of a double sandwich

silver(I) complex with 1,1'-bis(diethyldithiocarbamate)ferrocene, **2.52**. This ligand-supported polymer represented the first isolable compound where η^5 -cyclopentadienyl ring of ferrocene was shared with another metal atom *via* the π system. More recently, Llkhechi and co-workers published the synthesis and X-ray crystal structure analysis of **2.53** consisting of a ligand-supported array of alternating Ga(I) and Fe(II) ions connected by η^5 - μ -[C₅H₅]⁻ moieties [94,95].



In our system, compound **1** crystallizes in the P6(5) space group of the trigonal system. The crystal structure of **1** shows a slightly bent multiple-decker in which $\text{Cp}_{\text{centroid}}\text{-Fe-Cp}'_{\text{centroid}}$ is 153.45° and $\text{Fe}'\text{-Fe-Fe}''$ is 171.69° . Moreover, the two Cp rings presented distorted staggered conformation whereas the Fe atoms are slightly distorted from a position on a crystallographic centre of inversion. The Fe-C bond lengths are deviated in the wide range $1.896(12)$ (Å) – $2.220(17)$ (Å), as well as the observed $\text{Fe-Cp}_{\text{centroid}}$ distance is much longer 1.688 (Å) than the previously report [96].

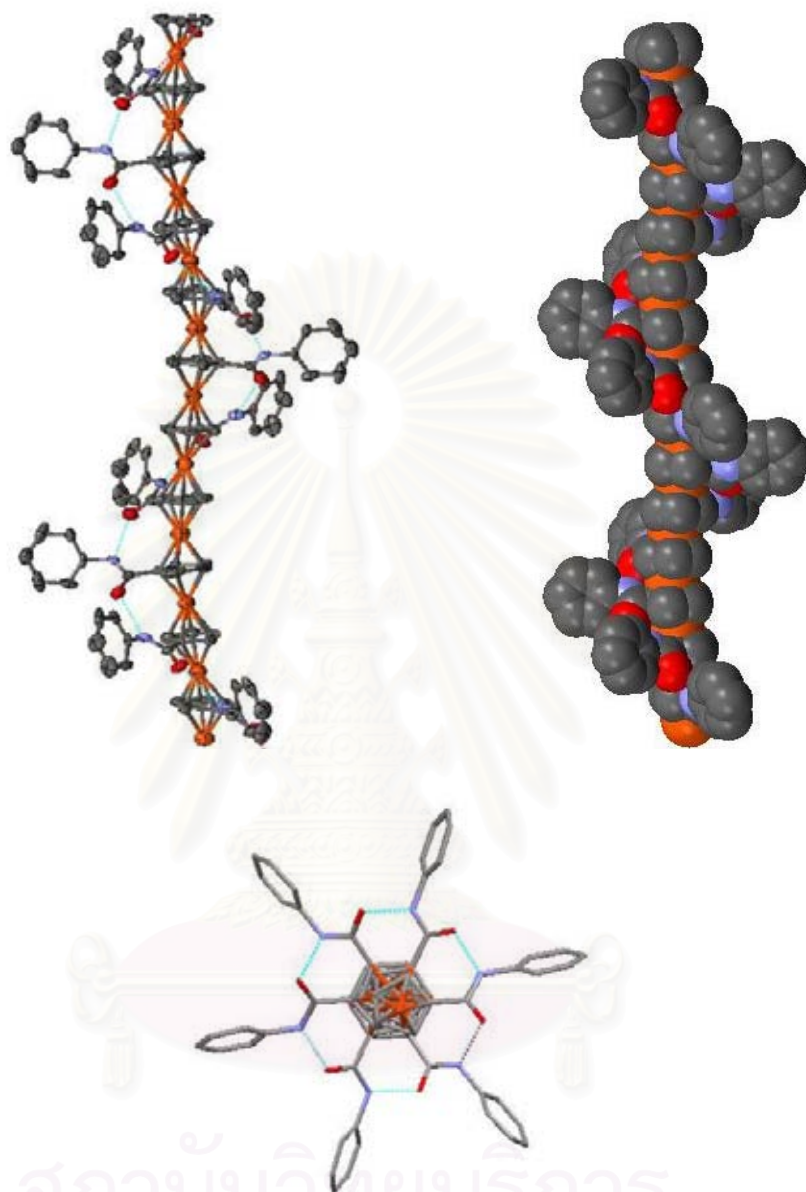
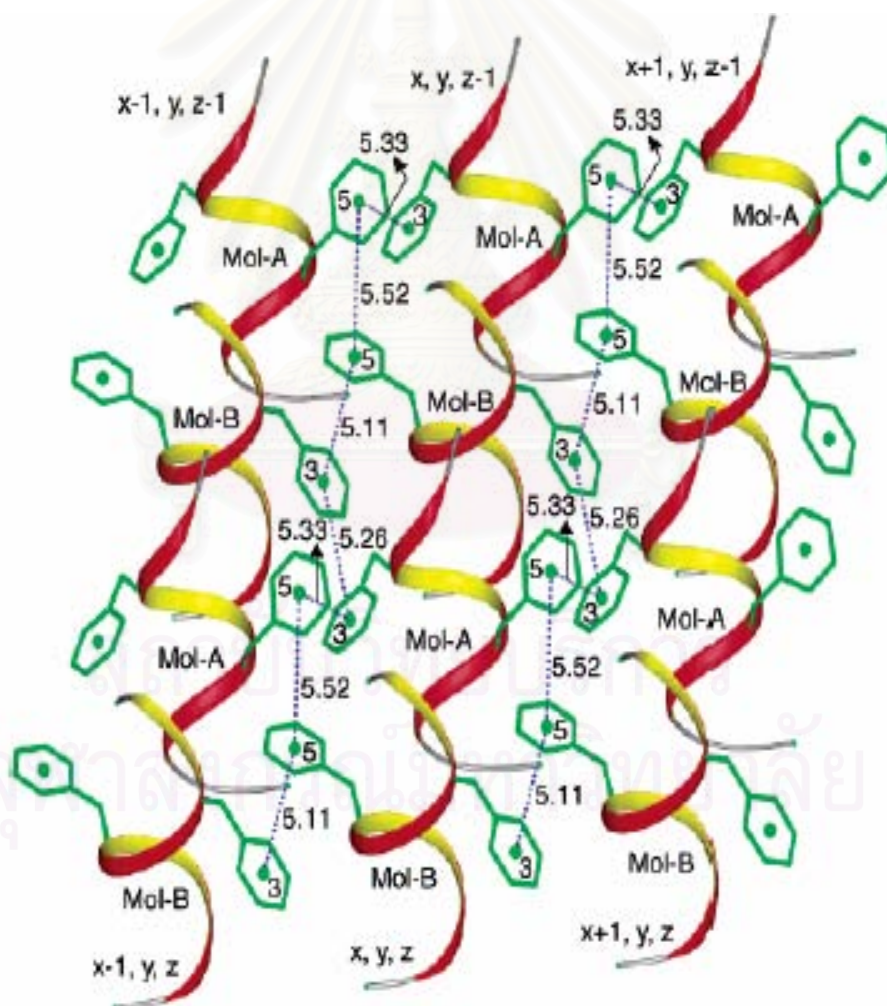


Figure 2.10 Presented the helical structure and pseudo hexagonal structure of compound 1.

The structure of compound 1 is very interesting for several reasons. Obviously, a striking feature is that 1 is found to be packed in a helical molecular arrangement in which the symmetrical intramolecular hydrogen bonding between CO and NH of the adjacent amide group ; $N(1)-H(10)\cdots O(1)\#2$ is formed with $d(H\cdots A)$ is 2.261 Å), induce the highly ordered structure resulting in a pseudo hexagonal

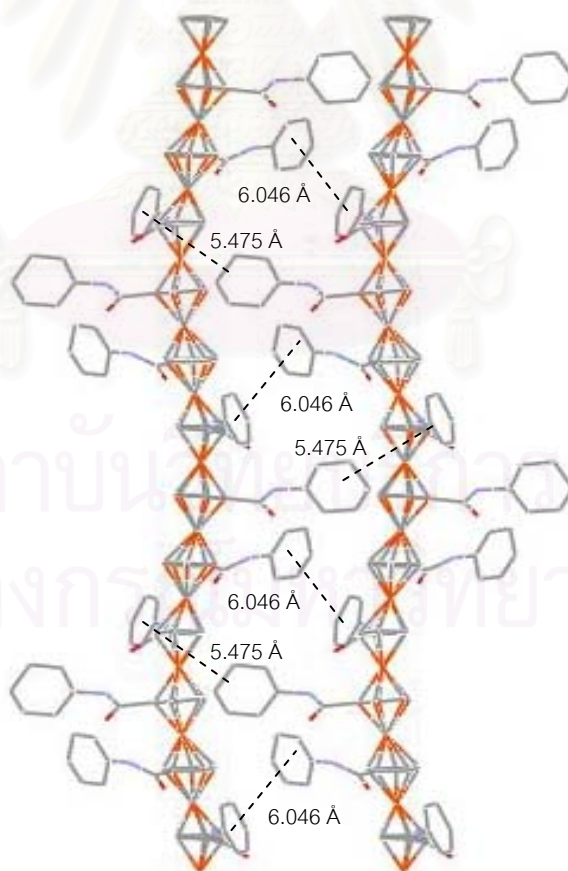
arrangements (Figure 2.10). The NH of the aniline in this conformation is available for participating in intramolecular hydrogen bonding with CO adjacent to the ferrocene unit, creating the highly organized self assembly in the crystal packing. Interestingly, the top view of the helix structure of polymer 1 clearly shows that the phenyl side arms protrude from the helix along 6 directions which is considered to be one of the factors that control the crystal packing and permit the helical assembly. Moreover, the adjacent helical columns are packed in parallel fashion. No evidence for intermolecular hydrogen bonding between each helix array was observed. This is the clear indication that specific arrangements of hydrogen bonding stabilize the helical structure.



Scheme 2.5 Schematic view of the Phe-Phe interactions in the crystal of peptides. The centroid distances (Å) are indicated

The present system of **1** is likely to be related to helical peptide containing phenylalanine moieties in which the interhelix arrays in peptide packing were suggested to be stabilized by aromatic-aromatic interactions of phenylalanine side chains (Scheme 2.5). Normally, phenyl ring centroids (R_{cen} : centroid-centroid distance) are separated by a preferential distance between 4.5 to 7 Å [97].

Considering the crystal packing of **1**, a particular interesting consequence of the intermolecular aromatic-aromatic interactions between adjacent helical columns are presented ($R_{\text{cen}} = 5.045$ Å and 6.046 Å) (Scheme 2.6). This is the clear indication that specific arrangements of the aromatic rings stabilize interhelix packing and no evidence for intramolecular aromatic-aromatic interactions were observed in the crystal packing because the distance is quite long (about 7.373 Å).



Scheme 2.6 Schematic view in the crystal packing of **1** shows the aromatic-aromatic interactions between the interhelix arrays.

Indeed, we can isolate a sandwich compound of **1** from aprotic solution (mixture of CH_2Cl_2 :Hexane), instead obtained a polymeric multiple-decker sandwich complex. We anticipate that in polar solvent such as methanol, compound **1** would be presented in the non-helical structure. Presumably, the high polar solvent can break the intramolecular hydrogen bonds in the helical structure of compound **1** and give a discrete ferrocene bis-amide complex.

After we have attempted to grow the crystal of compound **1** in the methanol solution, the cubic orange crystals were obtained. The X-ray analysis presented the non-helical sandwich complex structure as shown in Figure 2.11. In this system, compound **1** crystallizes in Pbn21 space group of the orthorhombic system (Tables 2.10 and 2.11). Interestingly, the phenyl side chains are pointing away from each other in which one of the phenyl rings is coplanar and the other is perpendicular to the cyclopentadiene ring. The phenyl side chains must be in a trans conformation to reduce steric hindrance.

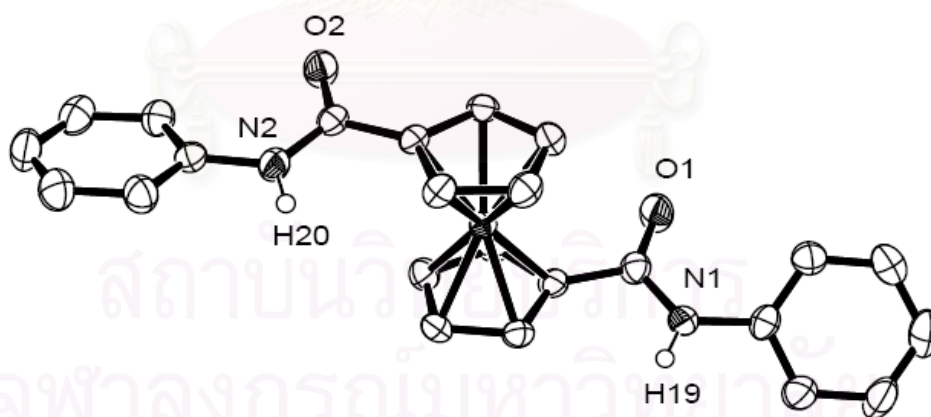


Figure 2.11 ORTEP plots of (**1**) with 50% probability thermal ellipsoids. Hydrogen atoms of phenyl rings and cyclopentadiene rings are omitted for clarity.

Table 2.10 Crystallographic data and structure refinement of compound (1) after recrystallization in MeOH.

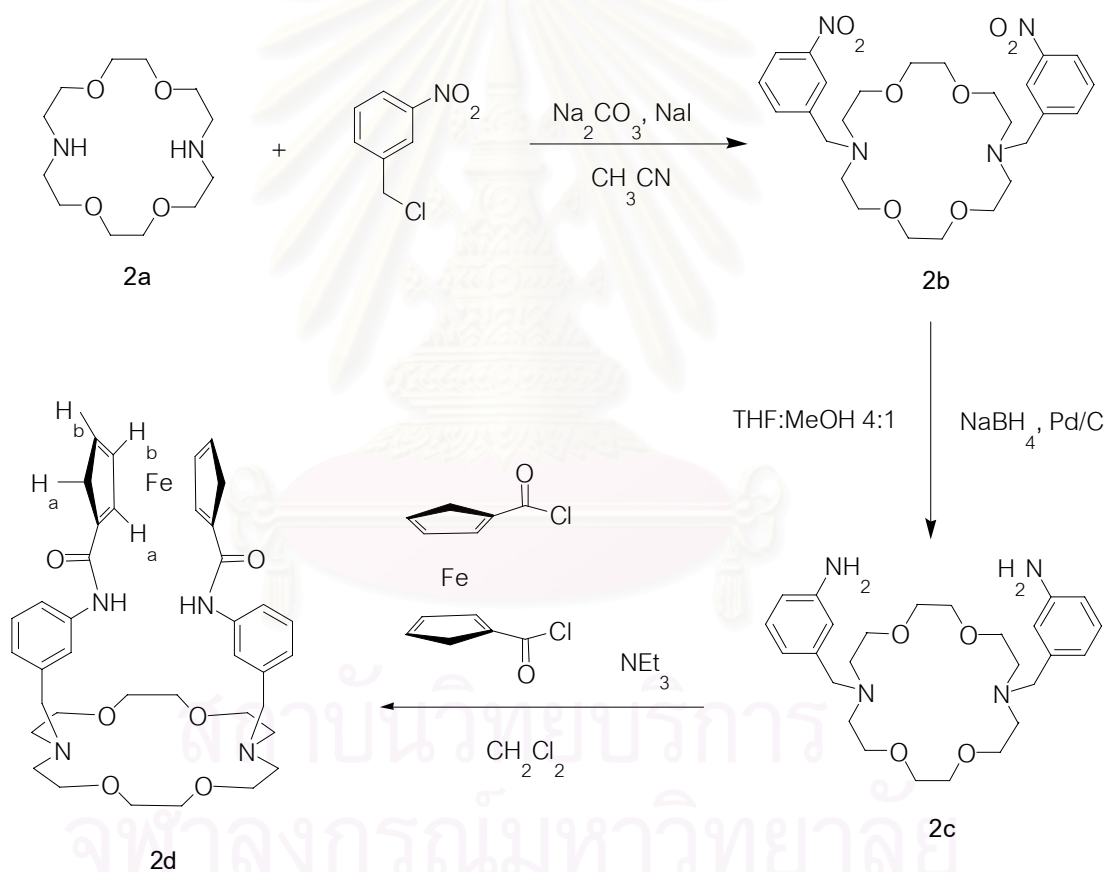
Empirical formula	$C_{24}H_{20}FeN_2O_2$
Formula weight	424.27
Temperature	293(2) K
Wavelength	0.71073 Å
Crystal system, space group	Orthorhombic, Pbn21
Unit cell dimensions	$a = 5.6007(2)$ $b = 12.7730(3)$ $c = 26.1521(7)$ $\alpha = \beta = \gamma = 90^\circ$
Volume	$1870.86(9) \text{ \AA}^3$
Z, Calculated density	4, 1.506 Mg/m ³
Absorption coefficient	0.830 mm^{-1}
F(000)	880
Theta range for data collection	1.56 to 30.42
Limiting indices	$-7 \leq h \leq 7, -18 <$
Reflections collected / unique	12758 / 4195
Refinement method	Full-matrix least-square on F^2
Data / restraints / parameters	4195 / 1 / 270
Goodness-of-fit on F^2	1.106
Final R indices [$I > 2\sigma(I)$]	$R1 = 0.0358, wR2 = 0.0677$
R indices (all data)	$R1 = 0.0499, wR2 = 0.0735$
Largest diff. peak and hole	0.246 and $-0.306 \text{ e.\AA}^{-3}$

Table 2.11 Selected bond length [Å] and angle [°] for compound (1) after recrystallized in MeOH.

Bond lengths [Å]			
C(1)-Fe(1)	2.049(2)		
C(2)-Fe(1)	2.048(3)		
C(3)-Fe(1)	2.048(3)		
C(4)-Fe(1)	2.056(3)		
C(5)-Fe(1)	2.064(3)		
C(6)-Fe(1)	2.055(3)		
C(7)-Fe(1)	2.054(2)		
C(8)-Fe(1)	2.046(3)		
C(9)-Fe(1)	2.043(3)		
C(10)-Fe(1)	2.053(3)		
Bond angles [°]			
C(9)-Fe(1)-C(8)	41.12(11)	C(8)-Fe(1)-C(6)	40.53(10)
C(3)-Fe(1)-C(1)	68.30(10)	C(7)-Fe(1)-C(6)	40.43(11)
C(3)-Fe(1)-C(2)	40.40(10)	C(10)-Fe(1)-C(6)	68.37(11)
C(1)-Fe(1)-C(2)	40.81(10)	C(3)-Fe(1)-C(4)	67.88(12)
C(9)-Fe(1)-C(7)	68.20(11)	C(1)-Fe(1)-C(4)	41.02(10)
C(8)-Fe(1)-C(7)	68.12(11)	C(2)-Fe(1)-C(4)	68.43(12)
C(9)-Fe(1)-C(10)	40.73(10)	C(3)-Fe(1)-C(5)	40.30(11)
C(8)-Fe(1)-C(10)	68.71(11)	C(1)-Fe(1)-C(5)	68.26(11)
C(7)-Fe(1)-C(10)	40.46(11)	C(2)-Fe(1)-C(5)	67.98(11)
C(9)-Fe(1)-C(6)	68.57(11)	C(4)-Fe(1)-C(5)	40.12(11)

2.3.2 Synthesis and Characterization of Receptor 2d

The synthesis of receptor **2d** is described in Scheme 2.7. The pathway begins with coupling 18-diaza crown ether **2a** with 3-nitrobenzyl chloride to produce **2b** in 70% yield. Catalytic hydrogenation of **2b** affords the corresponding diamine **2c** in a quantitative yield and used without purification for subsequently coupling with 1,1'-bis(chlorocarbonyl)ferrocene giving the final product **2d** as the yellow solid in 33% yield.



Scheme 2.7 Synthetic pathway for receptor **2d**.

The ^1H NMR spectra of receptor **2d** shows the two sharp singlet peaks of cyclopentadiene rings at 4.5 - 4.7 ppm (Figure 2.12). The NH of amidoferrocene protons appear at 8.65 ppm, probably the intramolecular hydrogen bond between two amide groups occurred as receptor **1**.

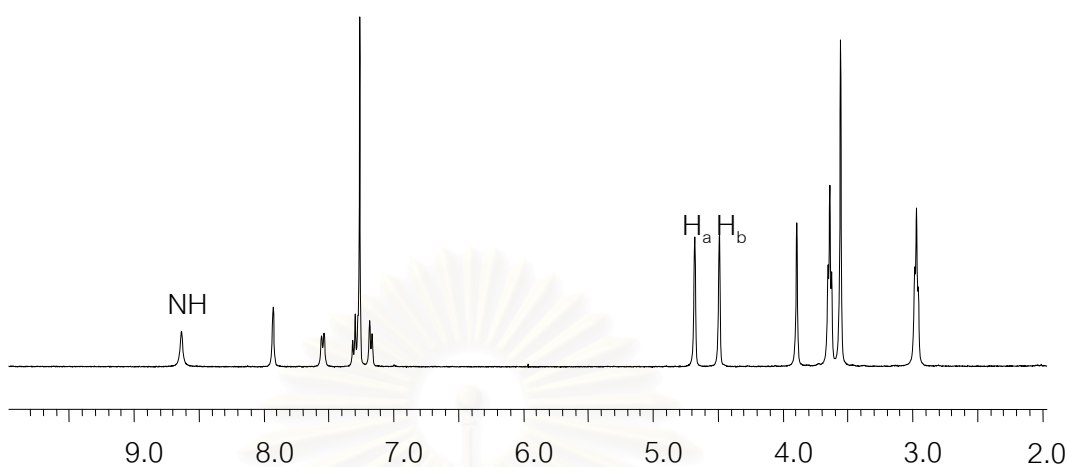
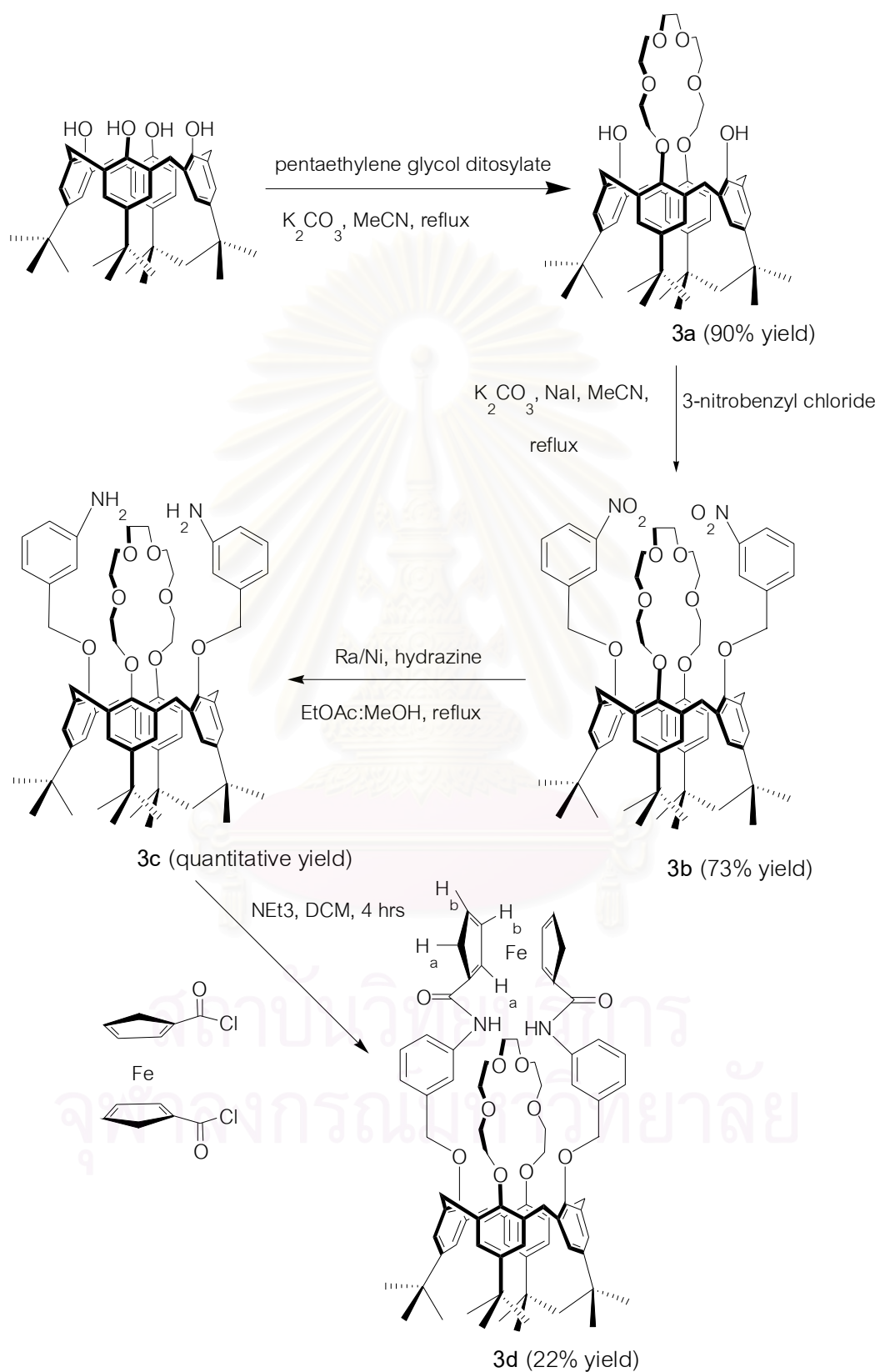


Figure 2.12 ^1H NMR spectrum of receptor **2d** in CDCl_3 .

2.3.3 Synthesis and Characterization of Receptor **3d**

Crown ether ring formation by reaction of *p*-*tert*-butylcalix[4]arene with pentaethylene glycol ditosylate and base was more difficult than anticipated. It was reported that direct ring formation by reaction of *p*-*tert*-butylcalix[4]arene with pentaethylene glycol ditosylate and *t*-BuOK in benzene gave only 38% yield [98]. However, following Zhou's report [99] by refluxing *p*-*tert*-butylcalix[4]arene and pentaethylene glycol ditosylate in CH_3CN using exactly one equivalent of K_2CO_3 gave *p*-*tert*-butylcalix[4]arene-crown-6, **3a**, in 90% yield. The ^1H -NMR spectrum of **3a** showed a cone conformation according to the ArCH_2Ar signals, which appears as a pair of doublets (AB system) at 4.37 and 3.31 ppm.

The *p*-*tert*-butylcalix[4]arene-crown-6 **3a** was then reacted with 3-nitrobenzyl chloride in the presence of Na_2CO_3 in acetonitrile at reflux to give the cone conformer of di-(3-nitrobenzyl)-*p*-*tert*-butylcalix[4]arene-crown-6, **3b**, in 73% yield. The ^1H -NMR spectrum of **3b** supported this conformation. Subsequent reduction with Raney/Ni and hydrazine in $\text{EtOAc}:\text{MeOH}$ gave cone di-(3-aminobenzyl)-*p*-*tert*-butylcalix[4]arene-crown-6, **3c** quantitatively. Finally, the corresponding diamine-calix[4]arene **3c** derivative was reacted with 1,1'-bis(chlorocarbonyl)ferrocene to give the final product **3d** in 22% yield (Scheme 2.8).



Scheme 2.8 Synthetic pathway for receptor 3d.

The cone conformation of the product was confirmed by $^1\text{H-NMR}$ spectrum as shown in Figure 2.13. A typical AB pattern was observed for the methylene bridge (ArCH_2Ar) protons at 4.37 and 3.13 ppm ($J = 12.0$ Hz). The $\text{OCH}_2\text{C}(\text{O})$ protons for cone conformers gave singlet peak at 4.77 ppm. Similar to receptor **2d**, the NH amide protons were found at 9.05 ppm, due to the formation of strong intramolecular hydrogen bonding of amidoferrocene unit presumably with the oxygen atom donors of crown ether. The positive ion electrospray mass spectrometry of **3** shows the mother peak [$\text{Fe}(\text{C}_{80}\text{H}_{94}\text{N}_2\text{O}_{10})$] at $m/z = 1321.63$ [$\text{M}+\text{Na}^+$].

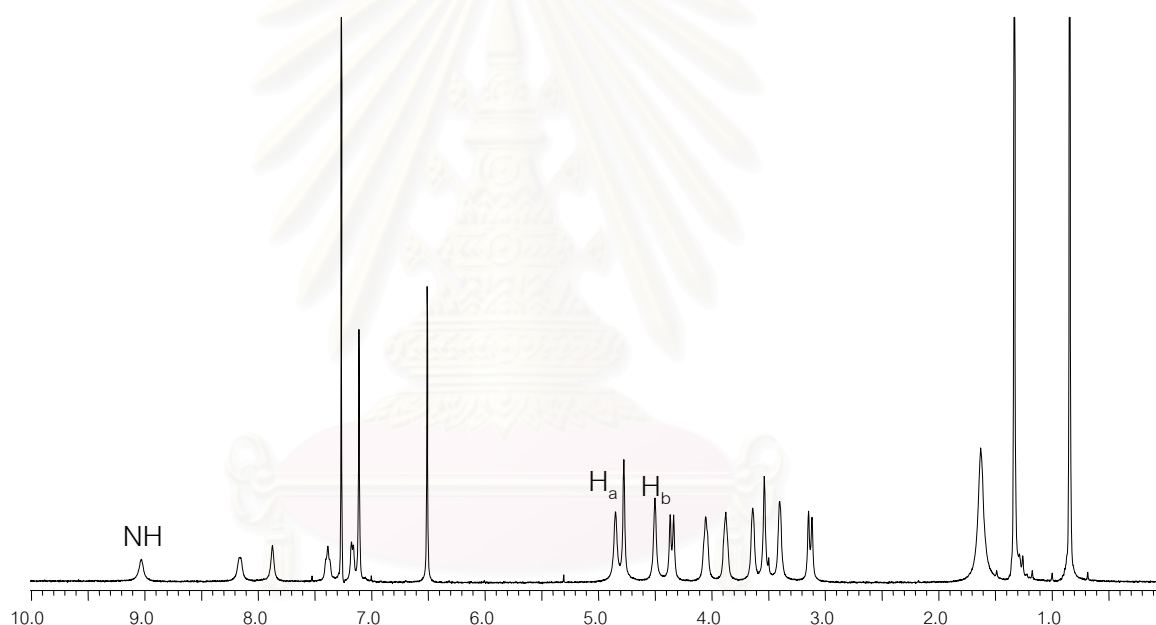


Figure 2.13 ^1H NMR spectrum of receptor **3d** in CDCl_3 .

2.3.4 Binding Properties of Receptors **2d** and **3d** towards Alkali Metal Cations by NMR Studies

The choice of solvent for all of the experiments was limited because all possible species that might exist in the titration experiment (receptor, ion-pair salts, cation-anion-receptor complexes) need to be soluble in the selected solvent. Also, ideally the metal cation must be bound strongly so as to minimize ion-pairing outside the receptor. Taking this into account, the cation and anion coordination properties of **1**, **2d** and **3d** were investigated by $^1\text{H-NMR}$ titration experiments in 5% $\text{CD}_3\text{CN}:\text{CDCl}_3$.

The addition of variable amount of NaClO_4 and KPF_6 to a solution of both receptors **2d** and **3d** in 5% $\text{CD}_3\text{CN}/\text{CDCl}_3$, showed quantitative 1:1 complexation of both receptors with Na^+ or K^+ in which the complexation occur under slow exchange conditions, therefore both complexes and free species are distinguishable in the spectrum. Binding constants were determined by direct integrations of host and complex resonances in the ^1H NMR spectrum which described by Macomber [100] and the binding constants are presented in Table 2.10.

The stoichiometry between both receptors and alkali metal cations was 1:1 as judged by the disappearance of the old set of signals as well as the rise of the new set of NMR peaks at 1 equivalent of metal cation in the ^1H -NMR spectrum. The stability constants could be determined from the variation of the integration ratio between complex and ligand at various amount of the cationic guest. When a 1:1 complex formation between receptor and each cationic guest takes place, the stability constant (K) for the equilibrium is expressed as:

$$K = \frac{[\text{HG}]}{([\text{H}]_0 - [\text{HG}])([\text{G}]_0 - [\text{HG}])}$$

$$K = \frac{n_{\text{hg}}/[\text{H}]_0}{(1-n_{\text{hg}})(R-n_{\text{hg}})}$$

Where $[\text{H}]_0$ represents the initial concentration of the host

$[\text{G}]_0$ represents the initial concentration of the guest

$[\text{HG}]$ represents concentration of the complex

$$[\text{HG}] = n_{\text{hg}}[\text{H}]_0$$

$$n_{\text{hg}} = \frac{I_{\text{hg}}}{I_{\text{hg}} + I_{\text{h}}}$$

Where I_{hg} represents the integration of the complex

I_{h} represents the integration of the host

and,

$$R = \frac{[G]_0}{[H]_0}$$

According to the expression above, the binding constants of receptors and alkali metal cations can be calculated and several interesting results have been observed as follows. The $^1\text{H-NMR}$ spectra of receptors **2d** and **3d** upon addition of Na^+ and K^+ cations display some similarities. For instance, as the concentration of metal cations increased the signals of free receptors **2d** and **3d** decreased and new signals of co-bound metal complexes appeared. Furthermore, the chemical shift of crown ether in receptor **2d** and pseudo-crown ether and CH_2 bridging methylene protons at the lower rim of receptor **3d** shifted upfield indicating that the alkali metal cations have been encapsulated in the cavity of crown ether of the proposed receptor molecules and the complexes are in slow exchange in the NMR time scale (Figures 2.14 and 2.15).

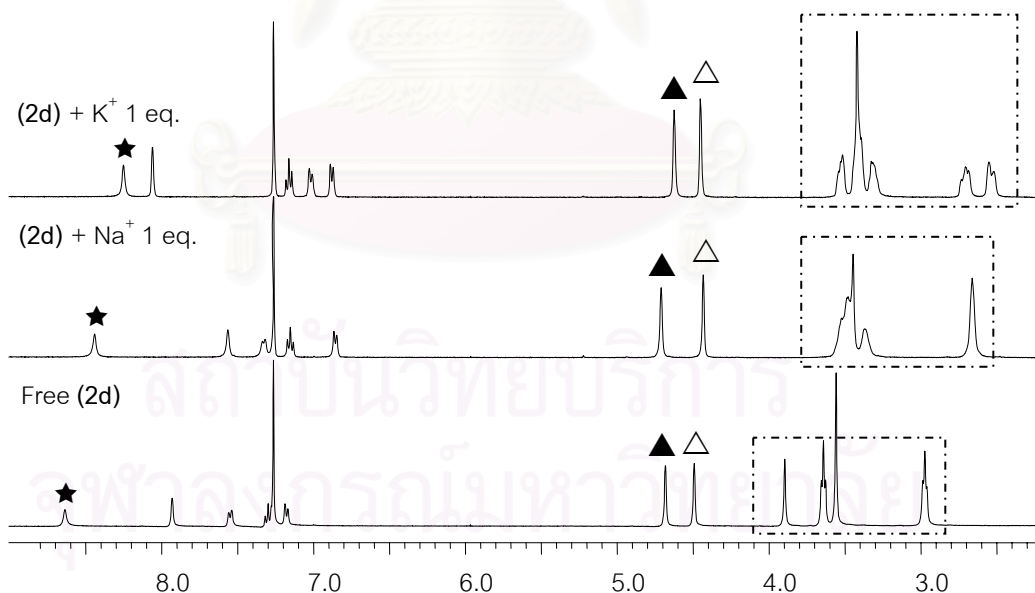


Figure 2.14 $^1\text{H-NMR}$ spectra of receptor **2d** with NaClO_4 and KPF_6 at 1 equivalent in $5\%\text{CD}_3\text{CN}/\text{CDCl}_3$, where ★ is NH protons ▲ and △ are H_a and H_b protons of ferrocene. The peaks in the square refer to CH_2 of crown ether part.

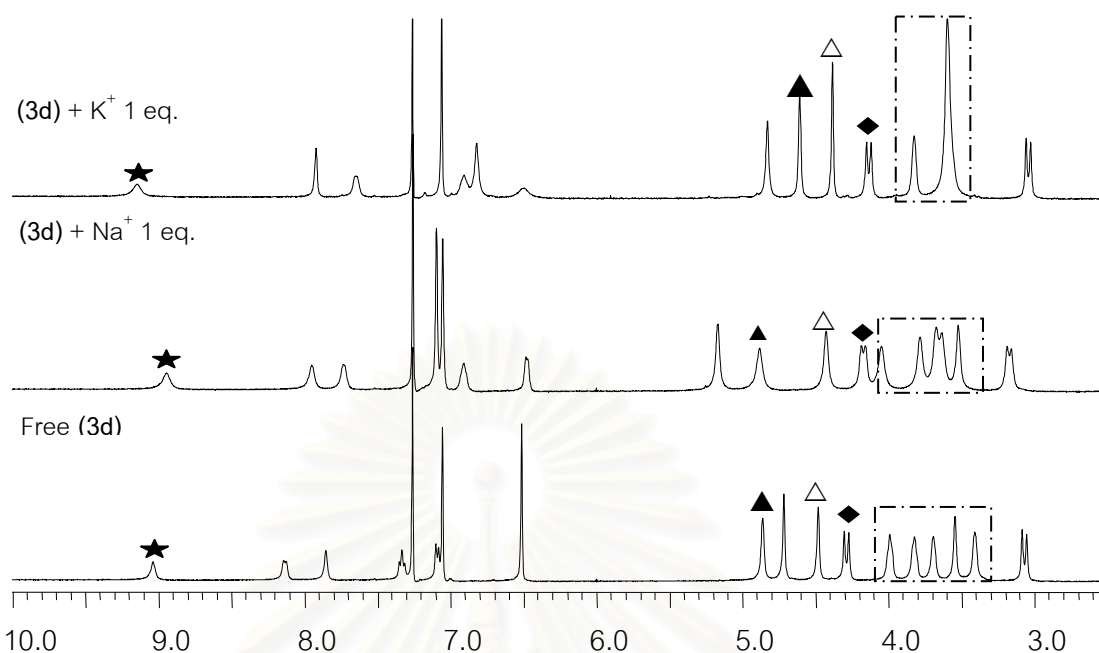


Figure 2.15 $^1\text{H-NMR}$ spectra of receptor **3d** with NaClO_4 and KPF_6 at 1 equivalent in $5\%\text{CD}_3\text{CN}/\text{CDCl}_3$, where ★ is NH protons, ▲ and △ are H_a and H_b protons of ferrocene and ◆ is CH_2 bridging methylene protons. The peaks in the square refer to CH_2 protons of crown ether part.

However, there are also some interesting differences, most notably the position of NH amidoferrocene protons of cobound complexes when compared to the free receptors. In receptor **2d**, the addition of both metal salts also resulted in a large upfield shift ($\Delta\delta = -0.198$ and -0.387 ppm for Na^+ and K^+ , respectively) of the amide protons. Whereas in receptor **3d**, it has shifted upfield ($\Delta\delta = -0.090$ ppm) upon complexation with Na^+ , but in the K^+ complex it appears downfield ($\Delta\delta = +0.109$ ppm). This opposite effect on the chemical shift of amido protons can be rationalized to the strengthening and weakening intramolecular hydrogen bonding of the amidoferrocene moieties. However, the results suggested that alkali cation was encapsulated in the cavity which effected the strength of the intramolecular hydrogen bonding between two amide groups. Not only the changing of NH amide protons but also the acidic protons of ferrocene (H_a) have been slightly shifted as well, which can be referred to the complexation-induced conformational changes as well. The proposed structures of the complexes between receptors **2d** and **3d** with Na^+ and K^+ are shown in Figure 2.16.

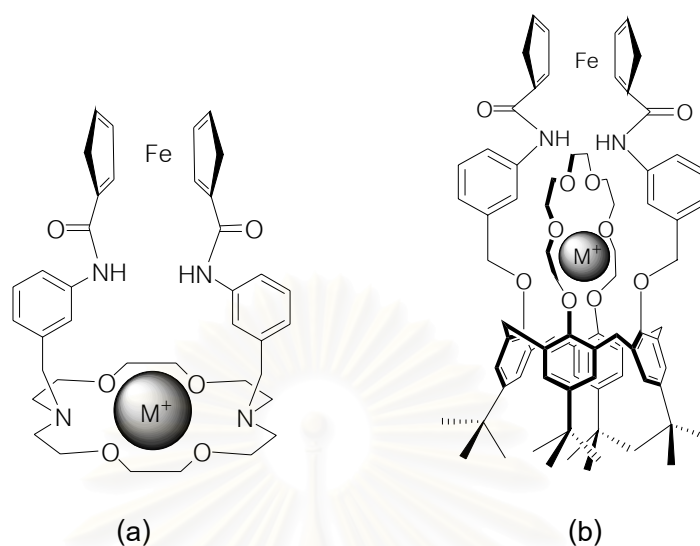


Figure 2.16 Proposed complex structures of (a) **2d** and (b) **3d** with alkali metal cations.

According to the results in Table 2.12, receptors **2d** and **3d** were found to bind Na^+ markedly better than K^+ . The results are pertinent to other crown ether or crown ether-like structures [101]. This was attributed to hard/soft acid interactions of metal cations and oxygen atoms of the crown ether complementary with the size of cations relate to the cavity size of the crown ether part. It should be noted that, the more steric hindrance of receptor **3d** molecule limits the binding of metal cations in the pseudo-crown cavity resulting in the low stability constants compared to receptor **2d**. In addition, the reason that why receptor **3d** has the highly selective binding towards bromide only in the presence of Na^+ can be rationalized to the steric hindrance of the host molecule **3d** and the bigger size of K^+ (1.36 Å) comparable to Na^+ (1.02 Å) [102].

Table 2.12 Binding constants (K) for Na^+ and K^+ cations complexes with receptors **2d** and **3d** in 5% $\text{CD}_3\text{CN}:\text{CDCl}_3$.

Receptors	Binding Constant, K^a (M^{-1})	
	$\text{Na}^{+(a)}$	$\text{K}^{+(b)}$
2d	764	387
3d	522	222

^a Na^+ cations added as NaClO_4 . ^b K^+ cations added as KPF_6 .

2.3.5 Binding Properties of Receptors 1, 2d and 3d with Anionic Guests in the Absence and Presence of Alkali Metal Cations by NMR Studies

To determine the association constants for the synthetic receptors 1, 2d and 3d with anionic guests in the absence and presence of alkali metal cations (Na^+ and K^+), the ^1H -NMR titration technique was employed to monitor the chemical shift change of amide protons in 5% $\text{CD}_3\text{CN}/\text{CDCl}_3$. EQNMR program [103] was used to analyze the binding isotherms and the results were shown in Table 2.13.

In the absence of alkali metal cations, upon addition of the corresponding anionic guests to the solution of free receptors resulted in slightly downfield shifts of NH amide protons indicating that the amide protons participate in an authentic hydrogen-bonded complex (Figure 2.17). Titration isotherms obtained from these changes in the chemical shifts of the host NH signals were fit to 1:1 (receptor/anion) binding model (Figure 2.18). Obviously, all of the receptors were found to be able to bind with Cl^- spherical anions and acetate Y-shaped anions. This is due to the basicity of chloride and acetate anions.

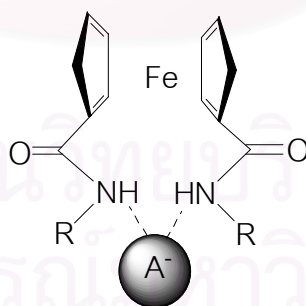


Figure 2.17 The proposed structures of amidoferrocene unit with anions.

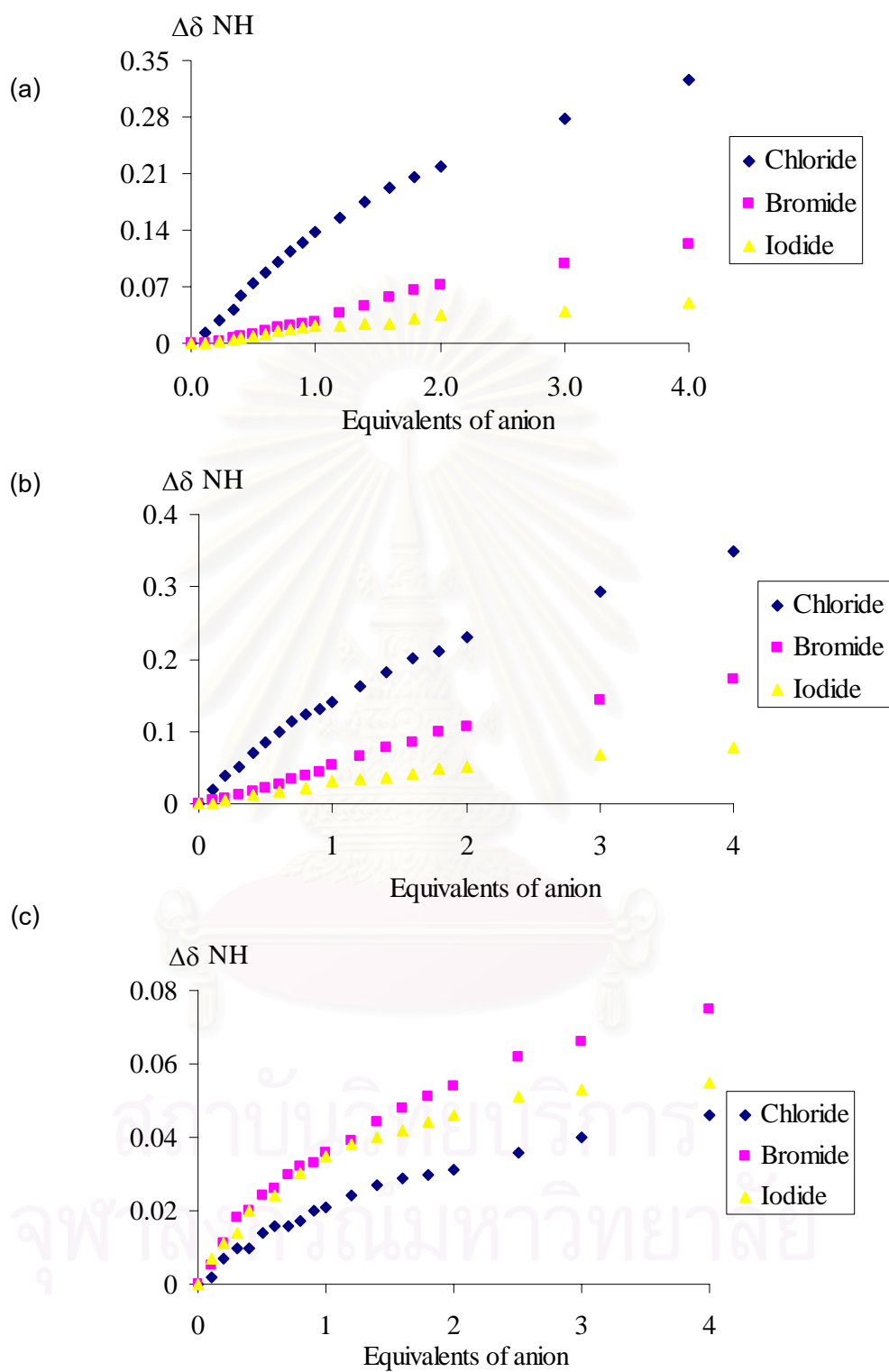


Figure 2.18 Titration curves of receptors (a) 1, (b) 2d and (c) 3d with various halide anions (as tetrabutylammonium salts) in 5% $\text{CD}_3\text{CN}:\text{CDCl}_3$.

Table 2.13 Binding constants (K) for receptors **1**, **2d** and **3d** with anionic guests (as tetrabutylammonium salts) in 5% $\text{CD}_3\text{CN}:\text{CDCl}_3$.

Receptors	Binding Constant, K^a (M^{-1})				
	Cl^-	Br^-	I^-	AcO^-	BzO^-
1	60	^b	^b	120	80
2d	35	^b	^b	90	82
[2d.Na⁺]^c	^d	16,096	93	^d	^d
[2d.K⁺]^c	^d	^d	39	^d	^d
3d	40	^b	^b	92	77
[3d.Na⁺]^c	^d	1,110	^d	1,046	^d
[3d.K⁺]^c	^d	^d	^d	^d	^d

^a Maximum error estimated to be $\pm 10\%$. ^b Values are very small and errors are more than 10%. ^c The alkali metal cations were added at 1 equivalent as their perchlorate or hexafluorophosphate salts. ^d Cannot be calculated due to ion-pair formation between bound metal cations and added anions.

The proposed binding structure of receptor **1** can be referred to the X-ray structure of complex of cobaltocenium receptor **2.52** with bromide anion [104]. X-ray analysis showed that bromide anion was hydrogen bonded to the $-\text{NH}$ amide, cyclopentadiene (cp H) and aryl (aryl H) protons, Figure 2.19. The two cyclopentadienyl rings are almost eclipsed and one phenyl group is almost coplanar to the Cp ring whilst the other is perpendicular. It is more likely that the anion complex consists of one bromide anion per receptor molecule, with each bromide anion hydrogen bonded to two amide protons, one from each of two different molecules.

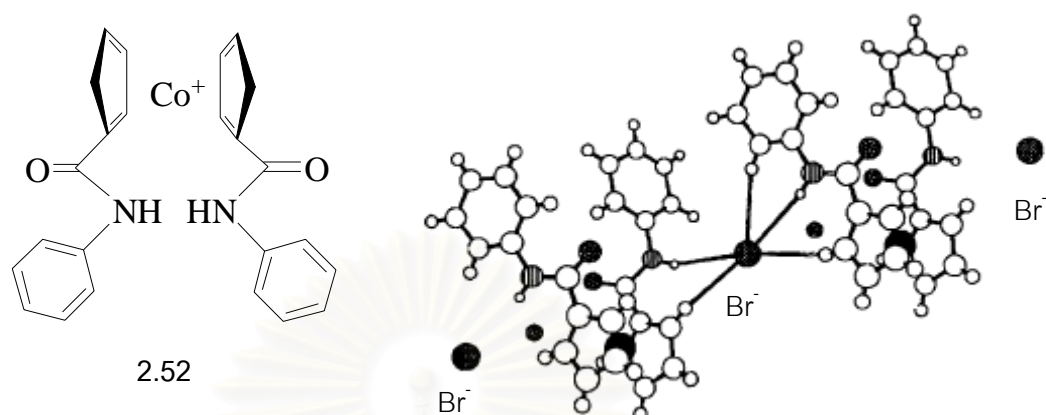


Figure 2.19 Cobaltocenium receptor 2.52 and crystal structure of 2.52 complex with Br⁻.

In the presence of alkali metal cations, the results in Table 2.13 can be categorized into two groups-negative and positive effects. Firstly, the negative binding means the binding constants of the second guest is decreased by the first guest binding with the host molecule. In this work, we have found that in the systems of [2d.Na⁺]/Cl⁻, [2d.K⁺]/Cl⁻, [2d.K⁺]/Br⁻, [3d.Na⁺]/Cl⁻, [3d.K⁺]/Cl⁻, [3d.K⁺]/Br⁻, [3d.Na⁺]/I⁻ and [3.K⁺]/I⁻ show the negative binding behaviour. Obviously from Figure 2.20, addition of 0-1 equivalent of anions to the co-bound receptor solutions resulted in very slightly downfield shift of NH protons indicating that the presence of those anions have little effect on the binding despite the formation of the stable ion-pair complexes with co-bound metal cations as described by Branda [105] and Tumcharern *et al.* [106]. Further addition of anions, the progressive chemical shift of NH protons were observed. This is consistent to the complex formation between receptors and anions *via* hydrogen bonds. It can be implied that the binding constants of co-bound metal complexes with unbound anion is stronger than co-bound ion-pairing (cobound cation-anion) complexes. The proposed binding steps of the negative binding are shown in Scheme 2.9.

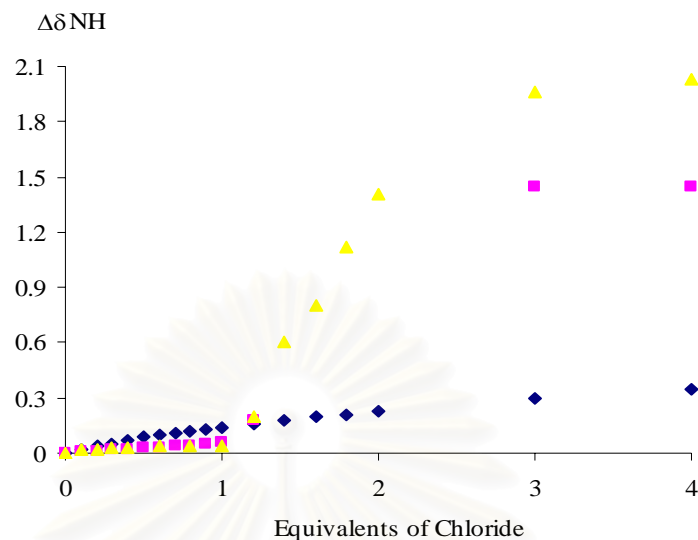
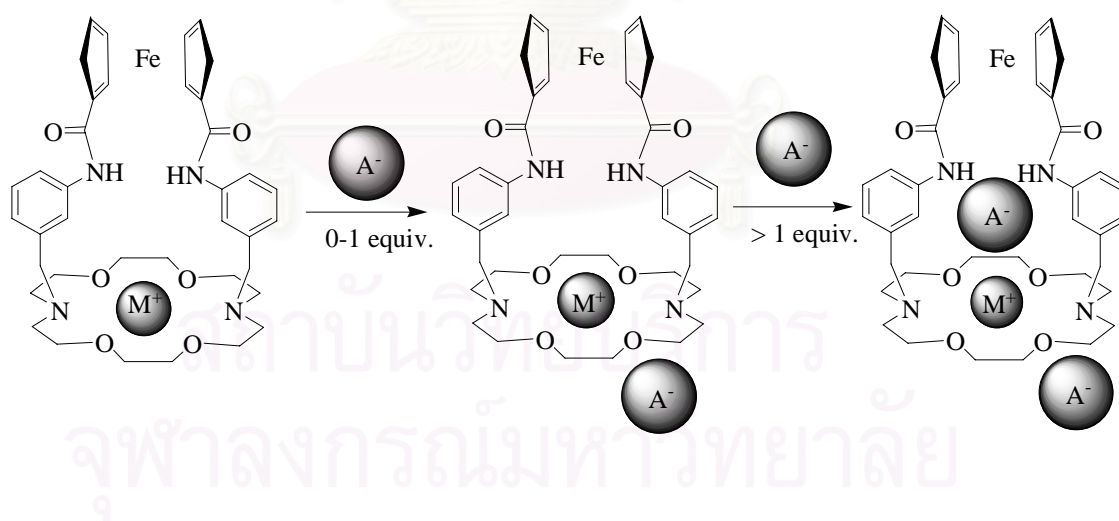


Figure 2.20 Change in NH chemical shift ($\Delta\delta_{\text{NH}}$) of receptor **2d** as a function of increasing of TBA chloride, where \blacklozenge free **2d**, \blacksquare presence of Na^+ 1 equivalent and \blacktriangle presence of K^+ 1 equivalent in 5% $\text{CD}_3\text{CN}:\text{CDCl}_3$.



Scheme 2.9 Proposed binding steps for negative binding of heteroditopic receptor **2d**.

Secondly, the positive binding means the binding constants of the second guest with the host molecule will be enhanced by the first guest binding. In this work, the systems of $[\mathbf{2d}.\text{Na}^+]/\text{Br}^-$, $[\mathbf{2d}.\text{Na}^+]/\text{I}^-$, $[\mathbf{2d}.\text{K}^+]/\text{I}^-$ and $[\mathbf{3d}.\text{Na}^+]/\text{Br}^-$ were found to have the cooperative behavior. Upon addition of halide anions the titration isotherms

illustrated the NH amide protons had a large downfield shift due to hydrogen bonding formation with anions directly (Figures 2.22, 2.25, 2.27 and 2.29).

Considering receptor **2d** system, the binding affinities of Br^- and I^- anions were markedly enhanced in the presence of Na^+ , whereas in the presence of K^+ , iodide binding affinity was enhanced. In contrast, the binding affinity of receptor **3d** with Br^- and AcO^- were observed and enhanced in the presence of Na^+ . It should be noted that besides hydrogen bonding with NH of amidoferrocene, the weakly anion interactions of acidic Cp's CH and aromatic's CH which adjacent to amide were also observed to shift downfield (Figures 2.21, 2.23, 2.24, 2.26 and 2.28).

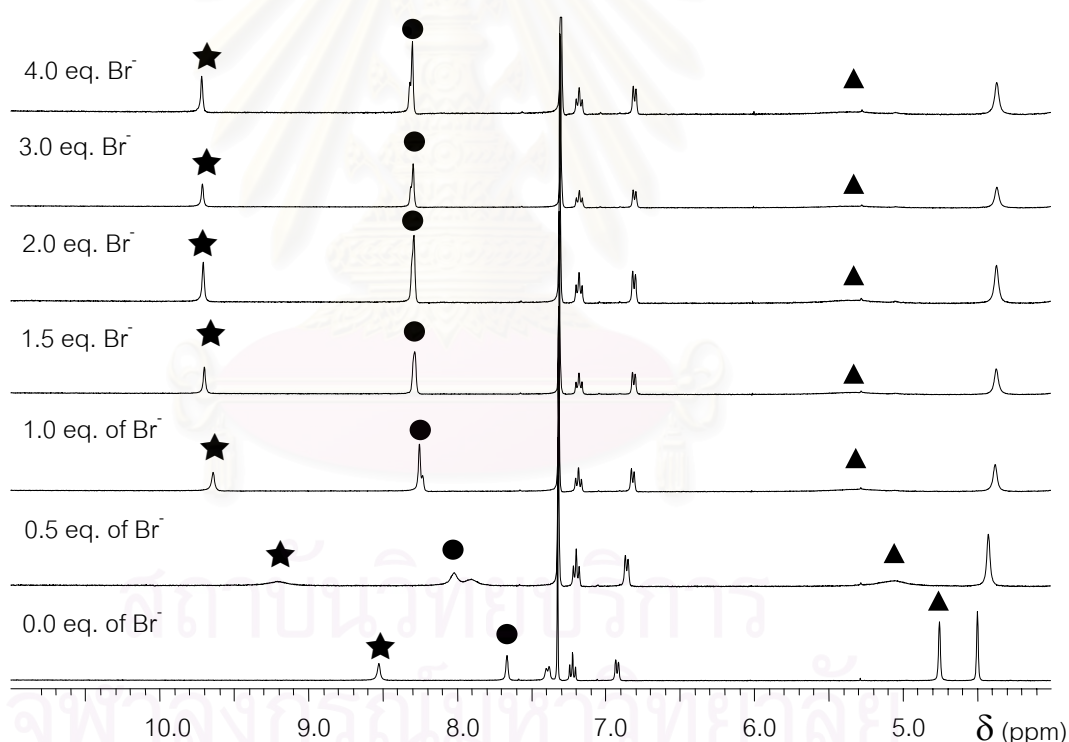


Figure 2.21 $^1\text{H-NMR}$ titration spectra of $[\mathbf{2d.Na}^+]$ with TBA bromide at room temperature in 5% $\text{CD}_3\text{CN}/\text{CDCl}_3$, where \star is NH proton, \bullet is *ortho* protons to amide groups and \blacktriangle is H_a protons of cyclopentadienyl rings.

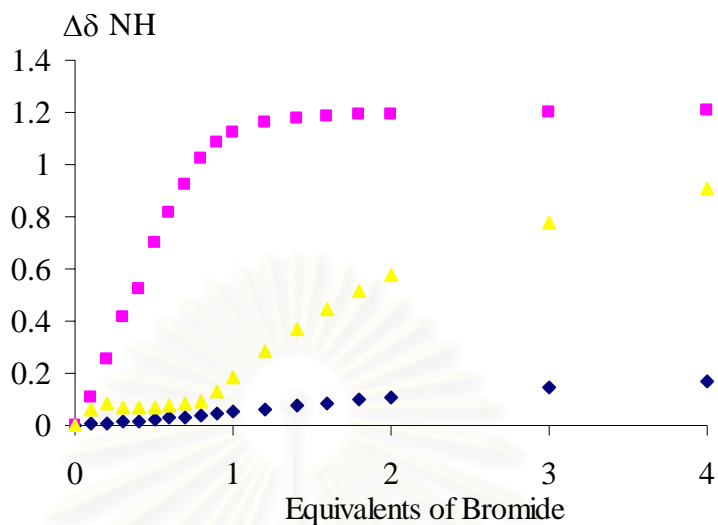


Figure 2.22 Change in NH chemical shift ($\Delta\delta_{\text{NH}}$) of receptor **2d** as a function of increasing of TBA bromide, where \blacklozenge free **2d**, \blacksquare presence of Na^+ 1 equivalent and \blacktriangle presence of K^+ 1 equivalent in 5% $\text{CD}_3\text{CN}:\text{CDCl}_3$.

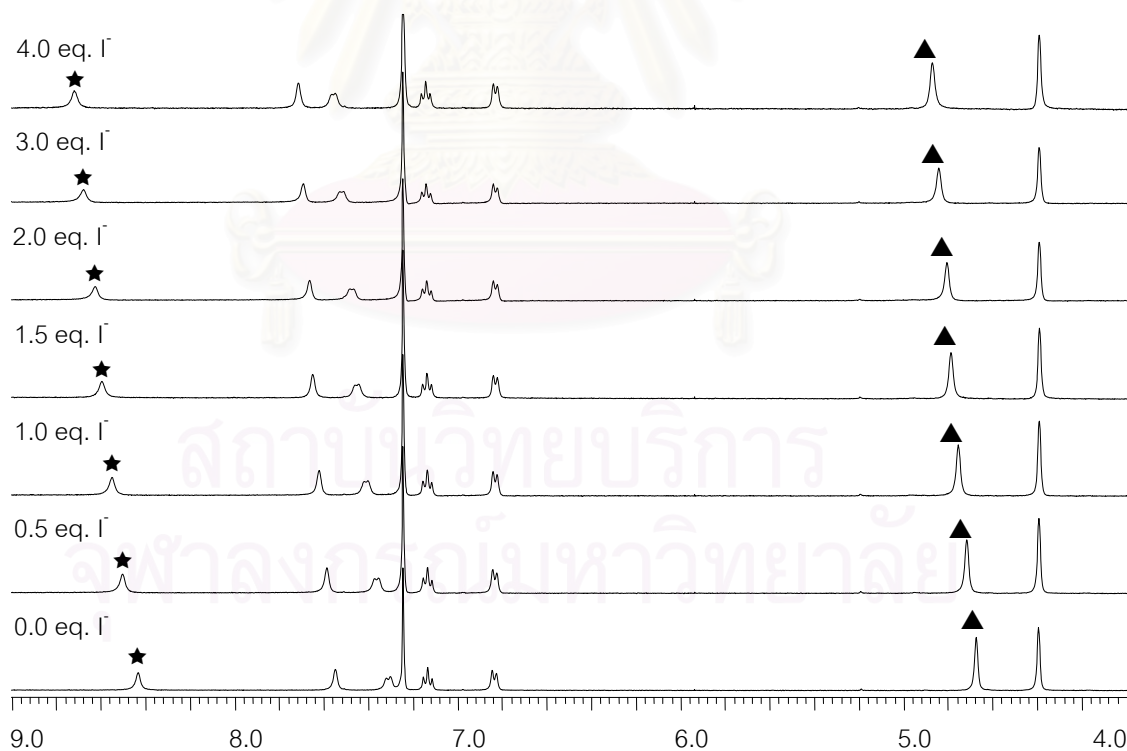


Figure 2.23 $^1\text{H-NMR}$ titration of $[\mathbf{2d.Na}^+]$ with TBA iodide at room temperature in 5% $\text{CD}_3\text{CN}/\text{CDCl}_3$, where \star is NH protons, and \blacktriangle is H_a protons of cyclopentadienyl rings.

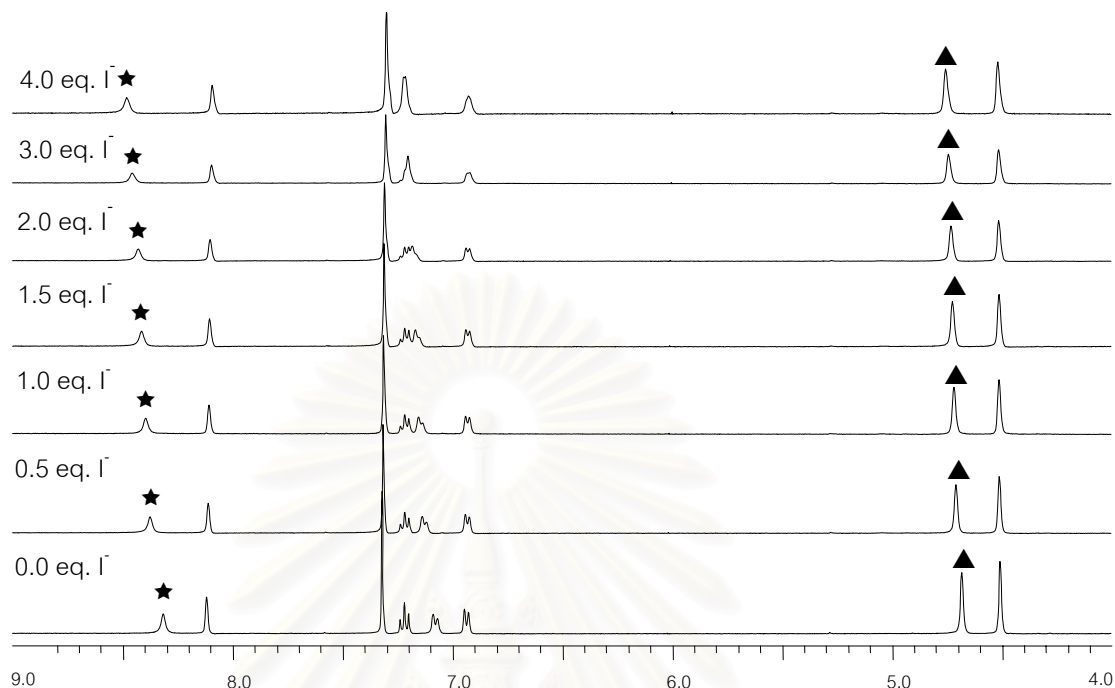


Figure 2.24 $^1\text{H-NMR}$ titration of $[\text{2d.K}^+]$ with TBA iodide at room temperature in 5% $\text{CD}_3\text{CN}/\text{CDCl}_3$, where ★ is NH protons, and ▲ is H_a protons of cyclopentadienyl rings.

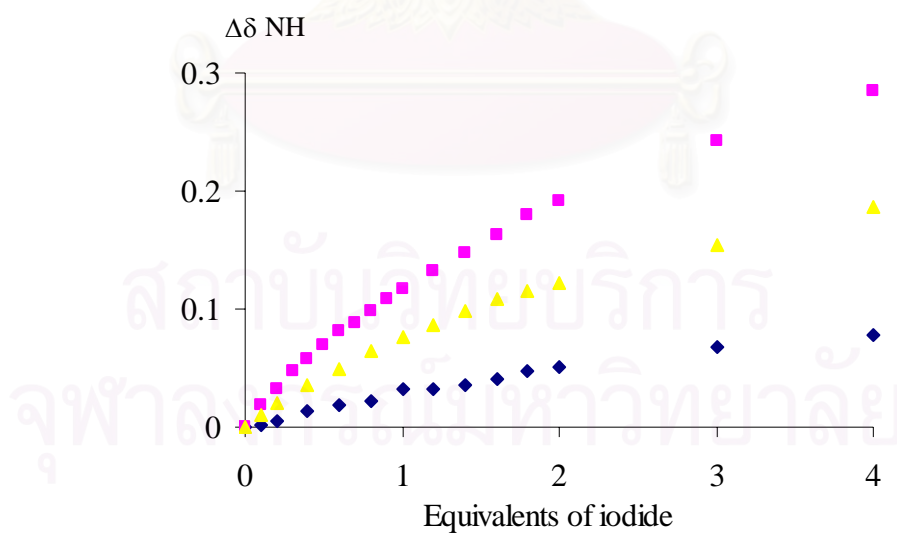


Figure 2.25 Change in NH chemical shift (ΔNH) of receptor 2d as a function of increasing TBA bromide, where ◆ free 2d, ■ presence of Na^+ 1 equivalent and ▲ presence of K^+ 1 equivalent in 5% $\text{CD}_3\text{CN}:\text{CDCl}_3$.

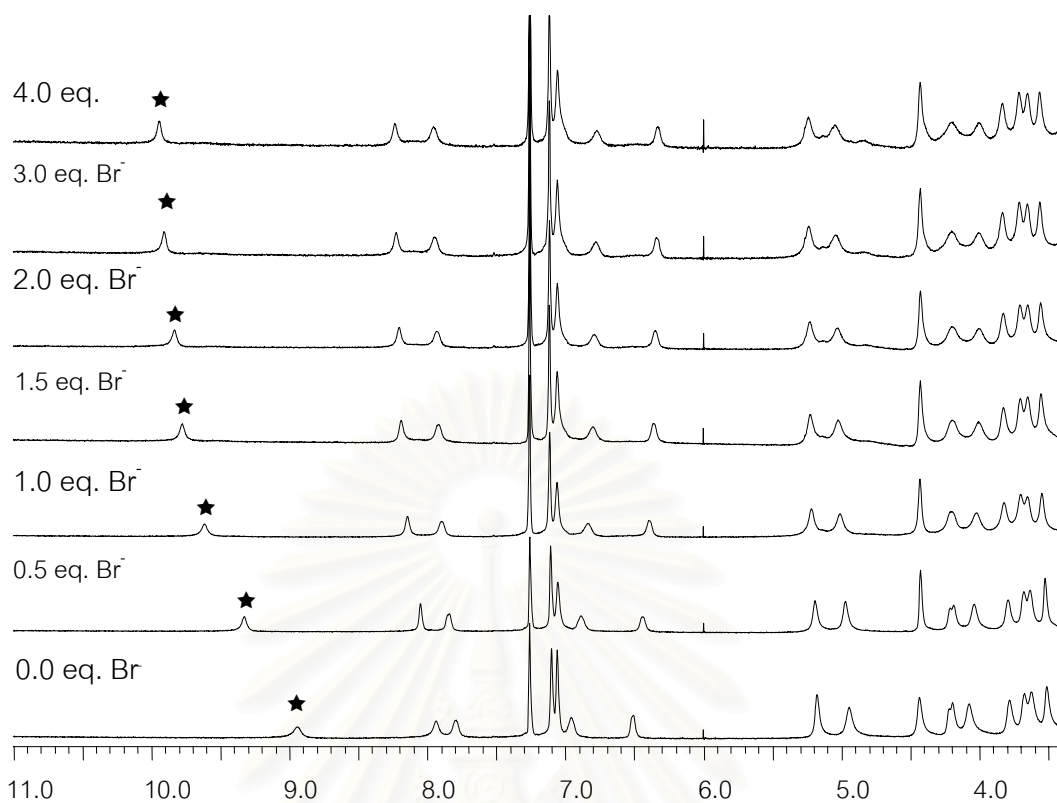


Figure 2.26 $^1\text{H-NMR}$ spectrum of $[\text{3d.Na}^+]$ with TBA bromide in $5\%\text{CD}_3\text{CN}/\text{CDCl}_3$, where ★ is NH amide protons.

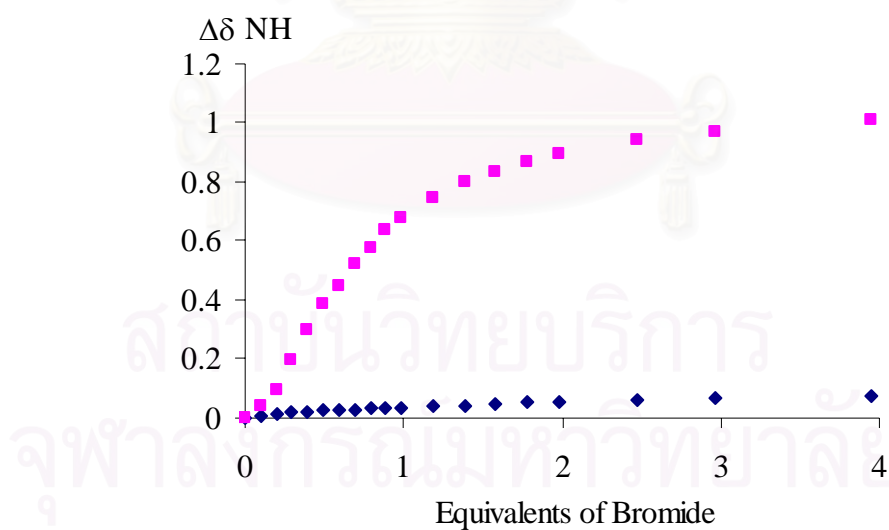


Figure 2.27 Change in NH chemical shift (ΔNH) of receptor **3d** as a function of increasing TBA bromide, where ◆ free **3d** and ■ presence of Na^+ 1 equivalent in $5\%\text{CD}_3\text{CN}:\text{CDCl}_3$.

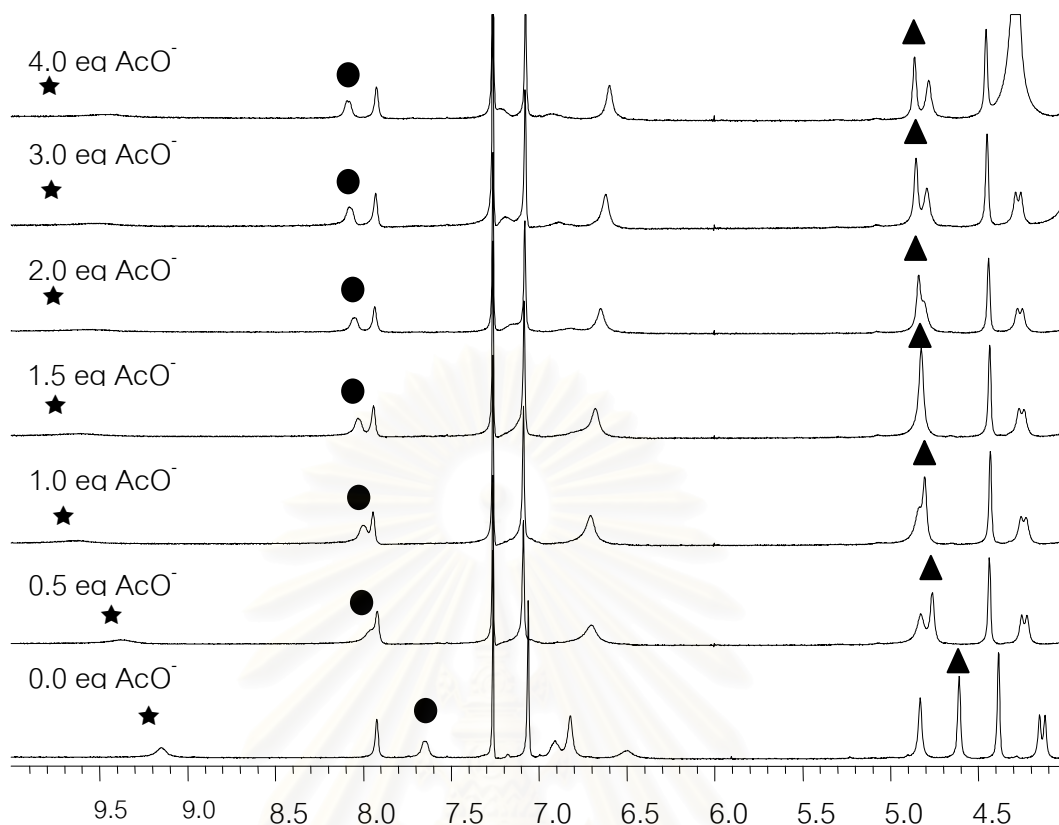


Figure 2.28 $^1\text{H-NMR}$ spectrum of $[\mathbf{3d.Na}^+]$ with TBA acetate in $5\%\text{CD}_3\text{CN}/\text{CDCl}_3$, where ★ is NH amide protons.

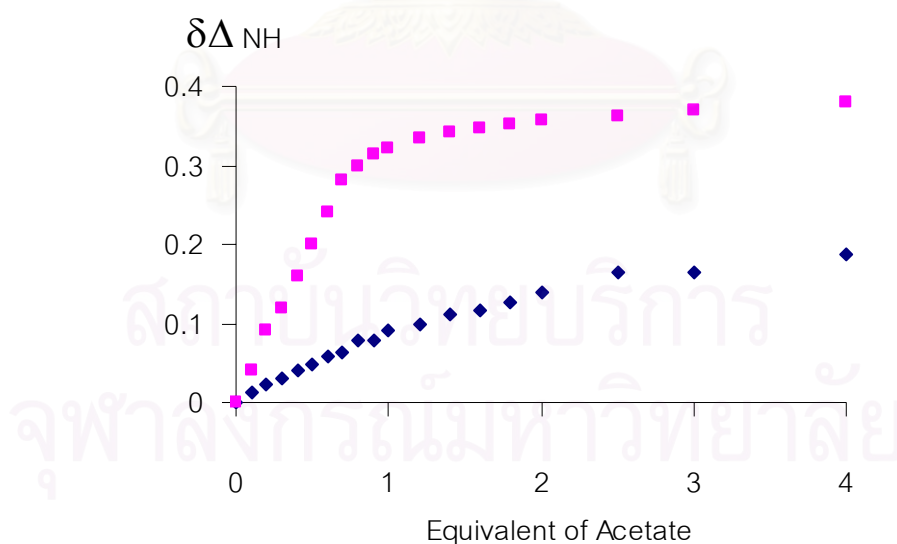


Figure 2.29 Change in NH chemical shift (ΔNH) of receptor $\mathbf{3d}$ as a function of increasing TBA acetate, where ◆ free $\mathbf{3d}$ and ■ presence of Na^+ 1 equivalent in $5\%\text{CD}_3\text{CN}:\text{CDCl}_3$.

Obviously, it can be seen that Na^+ illustrates the “switch on” bromide bindings in both receptors **2d** and **3d** and “switch on” acetate binding in receptor **3d**. Furthermore, receptor **2d** acts “switch on” iodide binding in the presence of Na^+ as well. These positive cooperative binding may be attributed to electrostatic of metal cations and anions co-bound interactions and preorganization effects of receptors **2d** and **3d** when metal cations encapsulate in crown ether cavity. The proposed structures of the contact ion-pair complexes are presented in Figure 2.30.

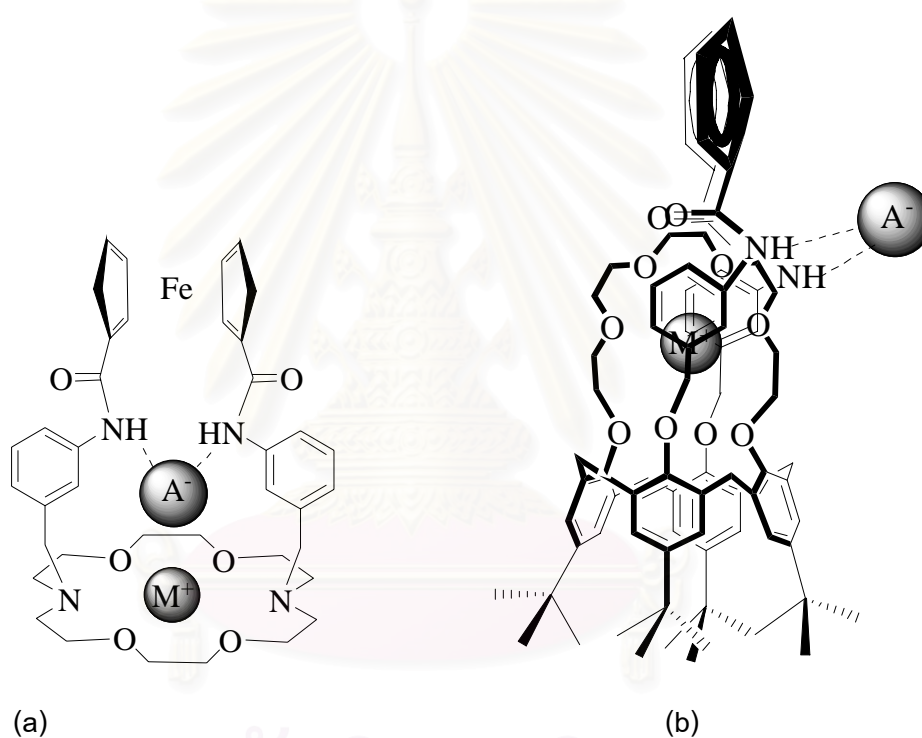


Figure 2.30 The proposed structures of the contact ion-pair complexes of receptors (a) **2d** and (b) **3d**.

Interestingly, we have found that the complex structures of receptor **2d** show the twisting of phenylamidoferrocene in which the degree of twisting depends on size of anions respect to the cavity of the binding sites of co-bound complex molecules, *vide infra*. Whereas in receptor **3d** complex, we expected that the amido protons are hydrogen bonded to bromide anion, while the carbonyl of amide are pointing away from the bromide atom to avoid steric hindrance from crown ether part. This phenomena is supported by X-ray structure of bridge-cobaltocenium amide calix[4]arene (Figure 2.31) [107].

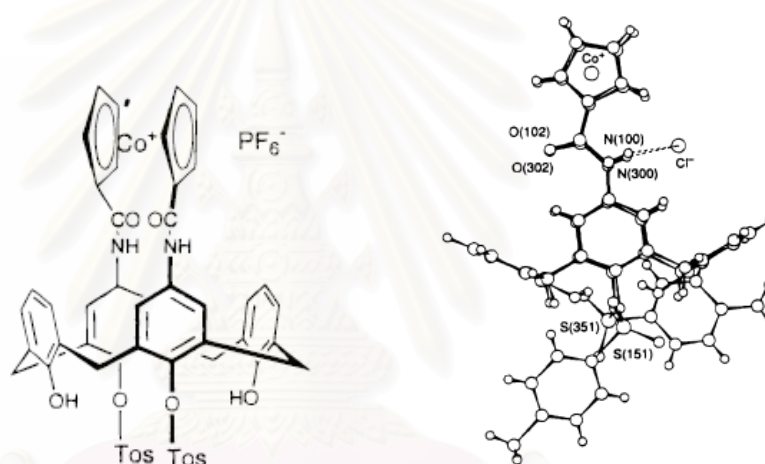


Figure 2.31 X-ray structure of bridge-cobaltocenium amide calix[4]arene upon complexes with chloride anion.

It should be mentioned that upon addition of small anionic guests, especially chloride anion, to the co-bound metal complexes of receptor **2d** the broadening peak of the acidic H_a protons of cyclopentadienyl rings are observed (Figure 2.32). This behavior is more likely to be the rotation of ferrocene moieties are being form when the co-bound metal complexes bind to the guest molecules. VT 1H -NMR technique was applied to confirm this result. As seen in Figure 2.33, upon cool down the temperature the broadening peaks of cyclopentadiene rings are being sharper which means that at lower temperature the rotation of ferrocene unit is slow.

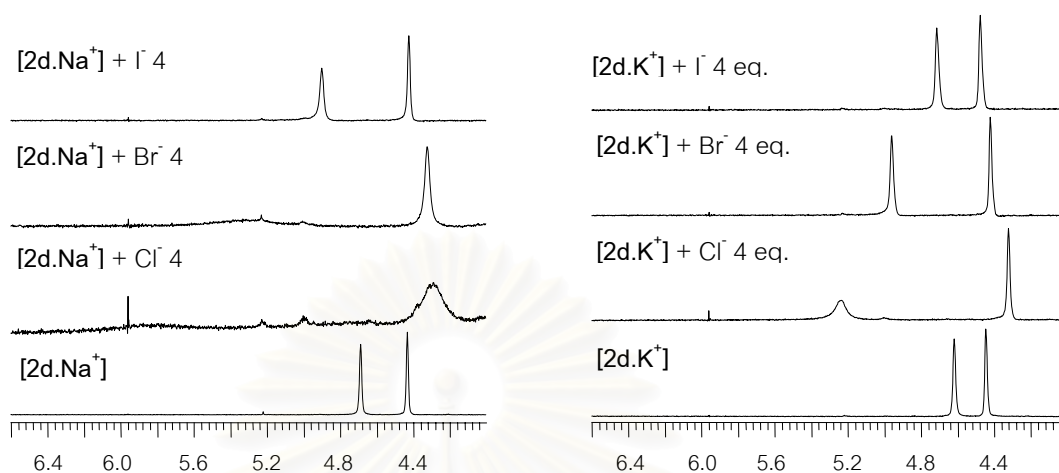


Figure 2.32 Partial $^1\text{H-NMR}$ spectra of co-bound metal complexes of receptor **2d** in the presence of 4 equivalents of halide anions at room temperature in 5% $\text{CD}_3\text{CN}:\text{CDCl}_3$.

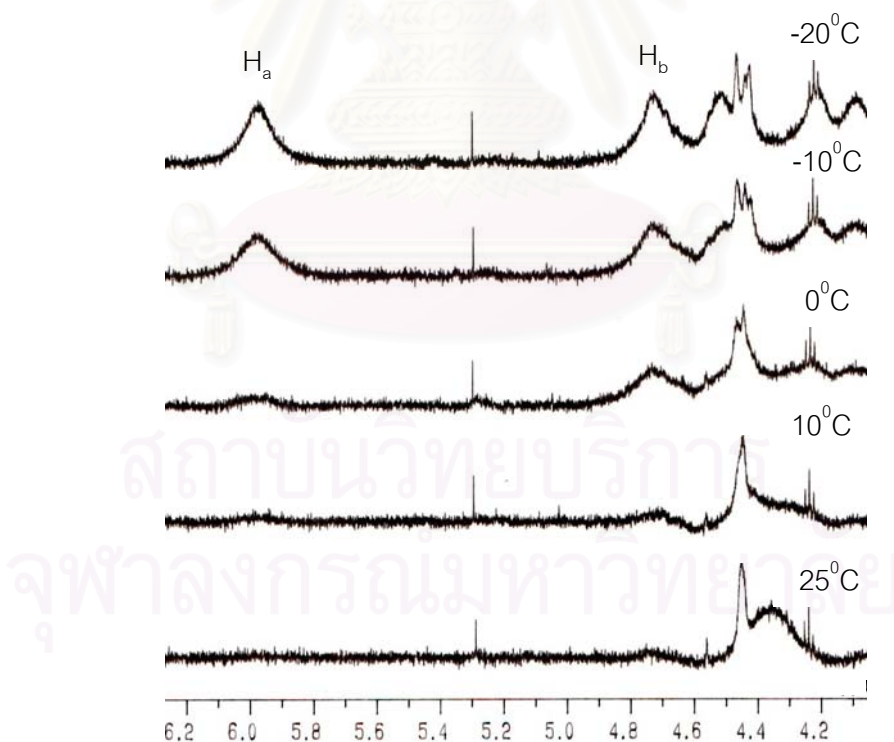


Figure 2.33 Partial variable temperature $^1\text{H-NMR}$ spectra of receptor $[\mathbf{2d.Na}^+]$ in the presence of TBA chloride 4 equivalent in 5% $\text{CD}_3\text{CN}:\text{CDCl}_3$.

As we can see from Figure 2.32, the next question is why the broadening peaks of acidic protons of ferrocene disappeared especially in MCl complexes of receptor **2d** only? The rationalized of this question can be explained in the terms of the size of anions related to the cavity of the binding site and the rigidity of the receptor molecule. Firstly, considering to the size of anions Cl^- (1.67 Å), Br^- (1.96 Å) and I^- (2.06 Å), chloride is the smallest anion among this series [102]. Compared to the cavity size of the receptor **2d**, it seems to be that upon chloride binding the receptor molecule has to arrange molecule itself to bind the small guest molecule. Then, the small guest molecule will have more effect to the rotation of the binding part (fast rotation) as well as the twist of the host molecule, resulting in the broadening peak in the $^1\text{H-NMR}$ spectrum (this hypothesis can be confirmed by X-ray structure in the next part). While the big guest molecule results in the slow rotation and showing the sharper peak.

Secondly, the rigidity of the host molecule, it's obvious to see that calix[4]arene has more rigidity than crown ether. If the molecule has to have rotation or movement, then the crown ether platform could be easily organized than calix[4]arene. This is the strong reason why the broadening peak of acidic ferrocene protons were only found in the crown ether receptor **2d** not in calix[4]arene receptor **3d**.

In conclusion, the proposed heteroditopic receptors can simultaneously bind alkali metal cations and halide anions as the contact ion-pair in which the cation complexation induces a structural change that is prerequisite for anion complexation. An augmentation in stability constant can be ascribed to (i) an increase in acidity of the amide NH proton due to electron withdrawing effect of the bound cation; (ii) rigidification of the crown ether and calixarene units through cation complexation and (iii) an electrostatic attraction between bound cations and anions.

2.3.6 Solid State Structure of [2d.NaCl] Complex

Further insight into the binding process was gained by X-ray crystallography. Although receptor **2d** showed the negative binding effect to Cl^- in the presence of Na^+ . However in the excess of Cl^- , co-bound metal complex of receptor **2d** are hydrogen bonded to Cl^- directly as show in the titration curve in Figure 2.20 [108]. Single crystal of $[\mathbf{2d.NaCl}].\text{CHCl}_3$ complexes were obtained by slowly evaporation of CHCl_3 solution of **2d** saturated with NaCl. The crystal data and refinement $[\mathbf{2d.NaCl}].\text{CHCl}_3$ are presented in Table 2.14 and selected bond lengths and bond angles are presented in Table 2.15. As expected, receptor **2d** binds NaCl as a contact ion-pair. The Na^+ can be encapsulated in crown ether cavity and Cl^- bind with two NH amide protons via hydrogen bonds, Figure 2.34. Remarkably, an explanation of why Na^+ shows negative cooperative Cl^- binding can be provided by X-ray structure. Not only the Na-Cl distance is 2.624 Å is shorter than the Na-Cl distance in crystalline sodium chloride (2.81 Å) [109], but also the Cl-N distances (3.396 Å) is larger than the other heteroditopic receptors showing the positive cooperative Cl^- binding [80,83,110]. Moreover, the average distances from the four diazacrown ether oxygen donors to the Cl^- is 4.053 Å, which is markedly closer to Cl^- that can be effected to ion-dipole repulsion between diazacrown ether and Cl^- ion [80,83,110]. Therefore, these results can be confirmed that in the presence of Na^+ shows the negative cooperative binding of Cl^- .

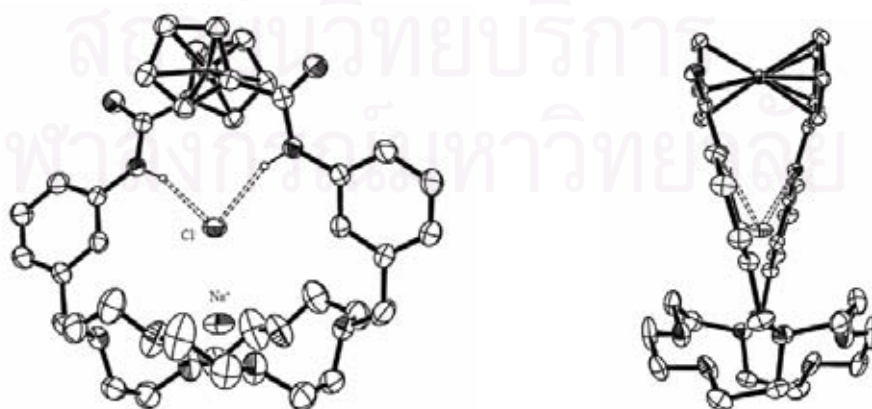


Figure 2.34 Front and side view of the X-ray crystal structure of $[\mathbf{2d.NaCl}].\text{CHCl}_3$.

Table 2.14 Crystallographic data and refinement of [2d.NaCl].CHCl₃.

Empirical formula	C ₄₀ H ₅₁ FeNaN ₄ O ₆
Formula weight	940.519
Temperature	298 K
Wavelength	0.71073 Å
Crystal system, space group	Orthorhombic, Pbcn
Unit cell dimensions	$a = 16.7076(8)$ Å $b = 19.0501(8)$ Å $c = 14.8949(4)$ Å $\alpha = \beta = \gamma = 90^\circ$
Volume	4740.8(3) Å ³
Z	4
Density (calculated)	1.412 Mg/m ³
Absorption coefficient	0.60 mm ⁻¹
Theta range for data collection	22.08°
Limiting indices	-17 ≤ h ≤ 7, -20 ≤ k ≤ 20, -15 ≤ l ≤ 15
Refinement method	Full-matrix least-squares on F ²
Data / restraints / parameters	2918 / 0 / 269
Goodness-of-fit on F ²	1.051
Final R indices [I > 2σ(I)]	R1 = 0.0733, wR2 = 0.2101
R indices (all data)	R1 = 0.1014, wR2 = 0.2383
Largest diff. peak and hole	0.355 and -0.468 e.Å ⁻³

Table 2.15 Selected bond lengths [\AA] and bond angles [$^\circ$] of $[2d.NaCl].CHCl_3$.

Bond Length			
Fe1—C10	2.014 (6)	Na3—O13 ⁱ	2.336 (6)
Fe1—C5	2.022 (6)	Na3—O13	2.336 (6)
Fe1—C5 ⁱ	2.022 (6)	Na3—O19 ⁱ	2.461 (7)
Fe1—C16	2.030 (7)	Na3—O19	2.461 (7)
Fe1—C16 ⁱ	2.030 (7)	Na3—C28 ⁱ	3.075 (10)
Fe1—C11	2.037 (7)	Cl2—Na3	2.625 (5)
Fe1—C11 ⁱ	2.037 (7)	N6—H6	0.9601
Fe1—C18	2.041 (7)		
Bond Angles			
C10 ⁱ -Fe1-C10	106.6 (4)	C11 ⁱ -Fe1-C11	129.7 (4)
C10 ⁱ -Fe1-C5	114.9 (3)	C10 ⁱ -Fe1-C18	168.4 (3)
C10-Fe1-C5	42.0 (3)	C10-Fe1-C18	68.2 (3)
C10 ⁱ -Fe1-C5 ⁱ	42.0 (3)	C5-Fe1-C18	68.8 (3)
C5-Fe1-C5 ⁱ	148.7 (4)	C5 ⁱ -Fe1-C18	129.5 (3)
C10 ⁱ -Fe1-C16	129.5 (3)	C16-Fe1-C18	40.0 (3)
C10-Fe1-C16	40.6 (3)	C16 ⁱ -Fe1-C18	150.6 (3)

Symmetry codes: (i) $1/2+x, 1/2+y, 1/2-z$.

สถาบันวิทยบริการ
จุฬาลงกรณ์มหาวิทยาลัย

2.3.7 Electrochemical Properties of Receptors 1, 2d and 3d and Their Electrochemical Sensing towards Cationic and Anionic Guests

As we mentioned before, proposed synthetic receptors **1**, **2d** and **3d** consist of ferrocene unit which is capable of electrochemical sensing for both cations and anions. Therefore, the binding abilities of these receptors can be studied by electrochemical method. We have investigated the electrochemical response of the synthetic heteroditopic receptors **2d** and **3d** towards halide anions in the presence and absence of alkali metal cations compared to the monotopic anion receptor **1** by cyclic voltammetry (CV) and square wave voltammetry (SWV).

The cyclic voltammetry and square wave voltammetric studies of receptors **1**, **2d** and **3d** were performed using 0.1 M Bu_4NPF_6 in 40% $\text{CH}_3\text{CN}:\text{CH}_2\text{Cl}_2$ as supporting electrolyte. The system contained three electrodes in which a Pt electrode was used as a working electrode, a Ag/Ag^+ was used as a reference electrode and a Pt wire was used as a counter electrode. All solutions were purged with N_2 before measurements. The potential was scanned in the range of 0.1 to 0.8 V at a scan rate of 100 mV/s. The electrochemical data of three receptors are presented in Table 2.16. From Figure 2.35, the cyclic voltammograms of receptors **1** and **3d** exhibited a reversible wave of Fc/Fc^+ redox couple, whereas receptor **2d** showed one quasi-reversible behavior of Fc/Fc^+ and other irreversible peak at a more negative potential at $E_{\text{pa}} = 0.420$ V.

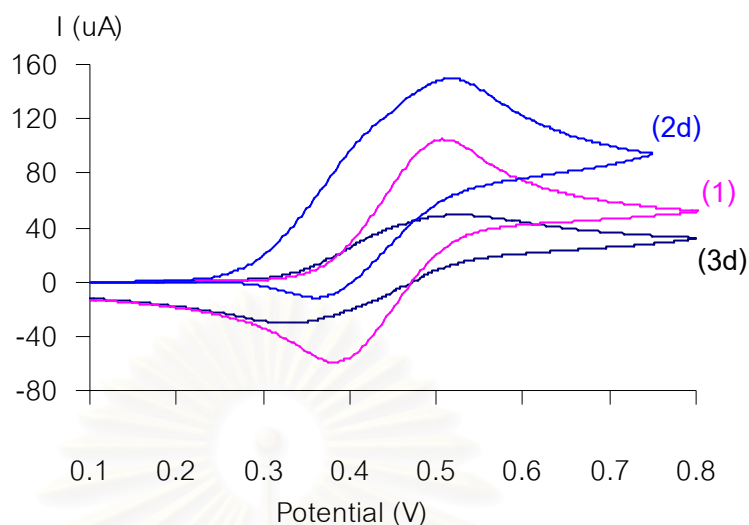


Figure 2.35 Cyclic voltammogram of receptors **1**, **2d** and **3d** in 40% CH₃CN:CH₂Cl₂ with 0.1 M TBAPF₆ at scan rate 100 mV/s.

The quasi-reversible feature of receptor **2d** may be due to an effect from the two tertiary amines of receptor **2d** itself. It has been reported that analogous molecules of other ferrocene derivatives containing amine moieties also showed this quasi-reversible wave which can be attributed to the combination effects of the lone pair electron on the nitrogen atom of the tertiary amines [111], which is capable to stabilize the Fc⁺ cation and the slow oxidation of these amines with weak product adsorption of cation radical (amine during oxidation losses one electron to produce a cation radical) [112-114]. Normally, it should be noted that upon protonation or metal cation complexation these phenomena are eliminated with a great improvement of the reversibility of the CV of receptor **2d** (see Figure 2.40). In our case, we expected that the irreversible peak at more negative potential of receptor **2d**, E_{pa} = 0.420 V, should belong to the oxidation peak of tertiary amines to cationic radical because this peak disappeared during increasing the amount of metal cation concentration. The actual redox couple of Fc/Fc⁺ in receptor **2d** cannot be measured, because the redox couple which have been reported here (E_{app}) is effected from the cationic radical as well. Then, the E_{pa} of ferrocene in this molecule will be shifted to more positive potential than usual.

Moreover, receptor **3d** shows the lowest oxidation currents compared to those of receptors **1** and **2d** at the same concentration, indicating a decrease in the diffusion coefficient, due to the much larger size of receptor **3d** [115].

Table 2.16 Electrochemical data (Fc/Fc⁺ redox couple) of receptors **1**, **2d** and **3d** in 40% CH₃CN/CH₂Cl₂ with 0.1 M TBAPF₆ at scan rate 100 mV/s.

Receptors	E _{pa}	E _{pc}
1	0.480	0.395
2d	0.529 ^a	0.385
3d	0.520	0.437

^a E_{app} contains the contributions from the electropositive repulsion between cationic radical and ferrocenium cation during the oxidation process.

Cyclic voltammograms of free receptors **1** and **3d** at various scan rates with 0.1M TBAPF₆ in 40% CH₃CN/CH₂Cl₂ are presented in Figure 2.36 and the correlation between current (I_p) and square root of scan rates (V^{1/2}) are shown in Figure 2.37. It was found that the proportion of I_p and V^{1/2} displays the non-diffusion system due to the linear lines do not pass through the origin.

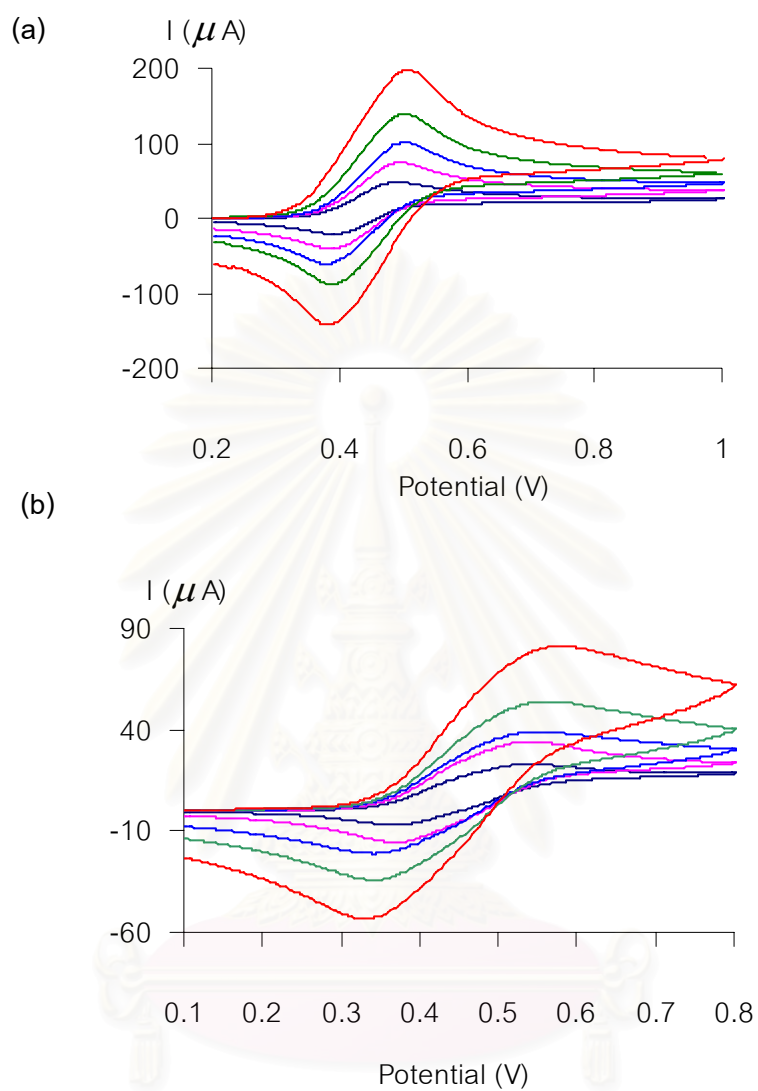


Figure 2.36 Cyclic voltammogram of receptors (a) 1 and (b) 3d with 0.1 M TBAPF₆ in 40% CH₃CN:CH₂Cl₂ at scan rates of 20, 100, 200, 500 and 1000 mV/s.

จุฬาลงกรณ์มหาวิทยาลัย

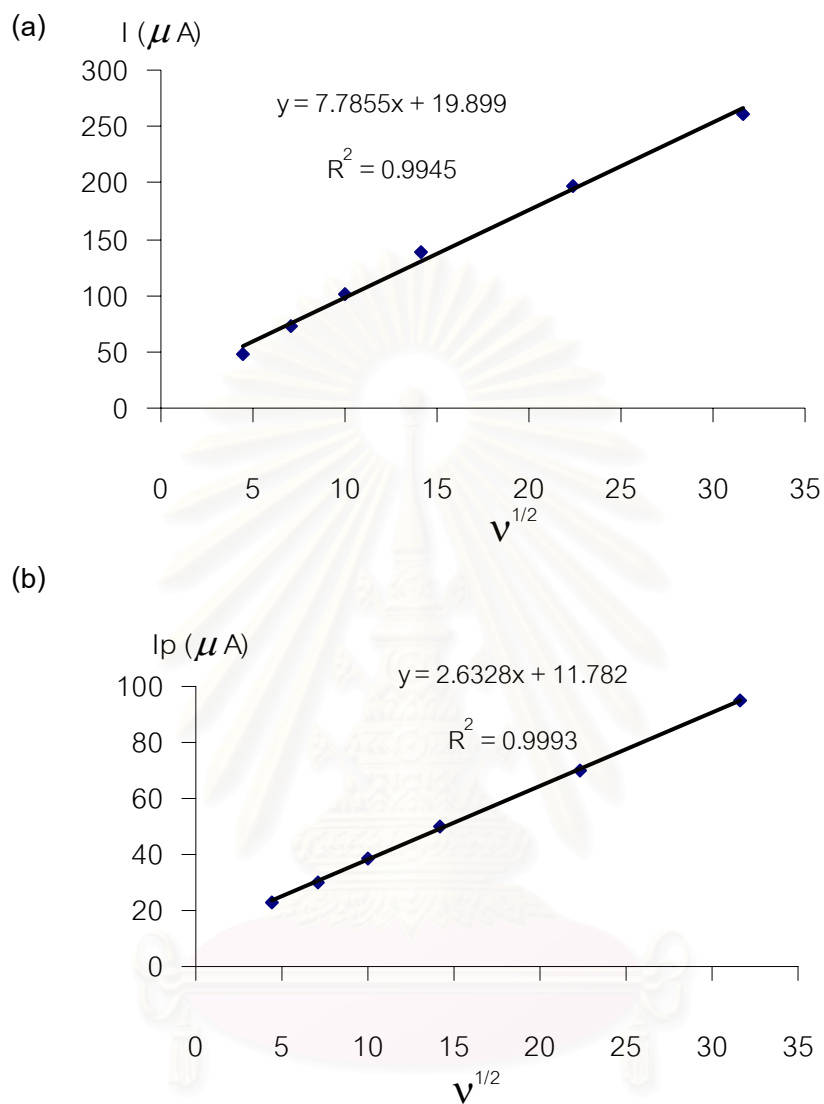


Figure 2.37 Plots of currents (I_p) and square root of scan rate ($V^{1/2}$) of receptors 1 and 3d in 40% $\text{CH}_3\text{CN}:\text{CH}_2\text{Cl}_2$ with 0.1 M TBAPF_6 .

Additionally, upon increasing the scan rate to the solution of receptor 2d, the E_{app} 's shifted to more negative potentials (Figure 2.38). It means that the redox process in this receptor depends on the scan rate.

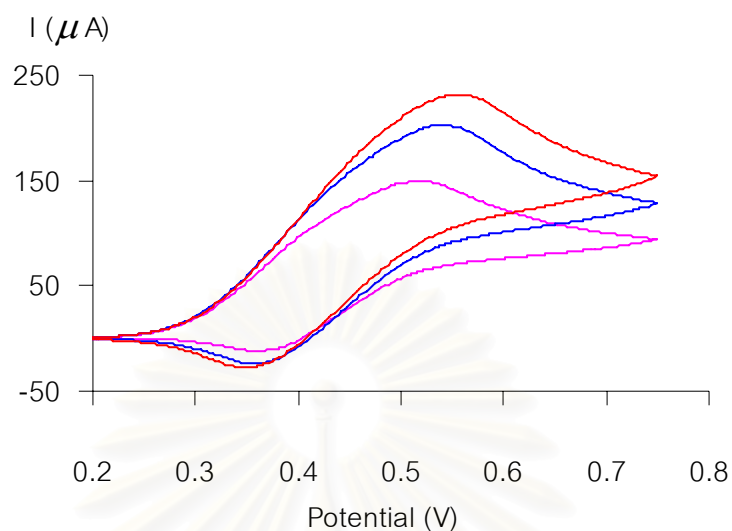
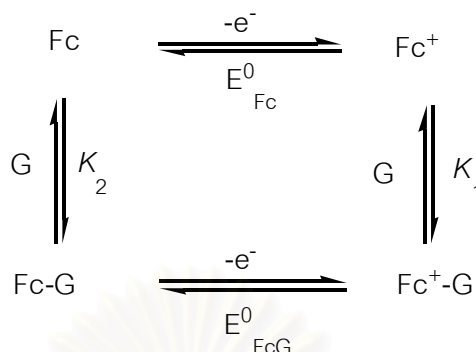


Figure 2.38 Cyclic voltammogram of receptor **2d** with 0.1 M TBAPF₆ in 40% CH₃CN:CH₂Cl₂ at scan rate of 50, 100 and 200 mV/s.

Upon the addition of guest molecules, either cations or anions, to the ferrocene containing receptor the electrochemical properties of ferrocene unit were perturbed. The receptors were designed to recognize guest species and must be able to respond to the binding of the guest with a significant change in their redox potentials. The simple electrochemical response pathway during guest binding to the receptor can be described by the scheme of squares as shown in Scheme 2.10, where Fc, G and FcG represents the receptor, guest and the complex species, respectively. E^0 is the formal potential of the electron transfer reaction and K is the stability constant [116].



Scheme 2.10 Schematic representation for guest binding (G) and electron transfer in electrochemical sensing of ferrocene containing receptor (Fc).

The four reactions in Scheme 2.10 constitute a cycle route; therefore the total Gibbs free energy change in this cycle is zero. If we consider equilibrium to be approached via a clockwise route starting from Fc, then the relationship between E^0 and K can be expressed mathematically in Eq. (2.1).

$$\sum \Delta G = \Delta G_{Fc} + \Delta G_{Fc^+} + \Delta G_{Fc^+G} + \Delta G_{FcG} = 0$$

$$nF(E - E^0_{Fc}) - RT \ln(K_1) + nF(E^0_{FcG} - E) + RT \ln(K_2) = 0 \quad (2.1)$$

$$-nF(E^0_{FcG} - E^0_{Fc}) = RT \ln(K_1/K_2) \quad (2.2)$$

Rearranging Eq. (2.1) to Eq. (2.2), then the stability constants K_1 and K_2 of a complex can be observed from different oxidation potential of receptor (E^0_{Fc}) and receptor-guest (E^0_{FcG}) complex species. The quotient K_1/K_2 is a useful parameter because it allows not only the calculation of K_1 if K_2 is known, but also the evaluation of the effect of electron transfer on the complexation during the guest binding. Some scientists have termed K_1/K_2 to the “*Binding Enhancement Factor*”(BEF) [117]. However, guest binding through a redox active molecular receptor is not always enhanced upon electron transfer, but it's decreased occasionally, *vide infra*. Then, the “*Reaction Coupling Efficiency*” (RCE) has been proposed by Beer and co-workers instead [118].

2.3.8 Electrochemical Studies of Receptors 2d and 3d towards Cationic Guests

Normally, when the ferrocene is oxidized to ferrocenium ion, then an electrostatic repulsion is created between the ferrocenium ion of the host and the cationic guest. This chemical changes diminishes the binding capacity of the synthetic host molecules which offers the possibility of creating a redox sensor and/or a cation switch.

The interactions of alkali metal cations (Na^+ and K^+) with receptors **2d** and **3d** were then investigated by cyclic voltammetry and the results can be categorized into two groups. Firstly, as we mentioned before, receptor **2d** has one irreversible and one quasi-reversible corresponding to the oxidation of lone pair electron of two tertiary amines to cationic radical and Fc/Fc^+ redox couple, respectively. Therefore, after addition of metal cations to a solution of receptor **2d** resulted in the disappearance of the amine oxidation peak due to metal coordination. If we compare the E_{app} of Fc/Fc^+ redox couple of receptor **2d** in the absence and presence of metal cations, obviously we can see that E_{pa} of the later system are shifted to less positive position than the former one, Figure 2.39. It is implied that the electropositive repulsions between the ferrocenium cation and metal cations are weaker than the repulsion of the cationic radical and ferrocenium cation. Moreover, in the presence of a metal ion, the oxidation of the amine to radical could be suppressed.

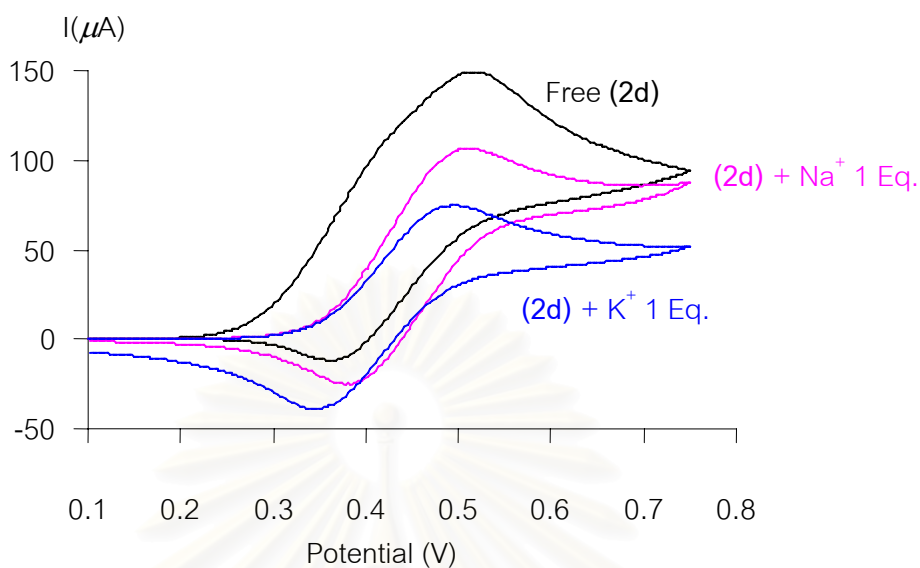


Figure 2.39 Cyclic voltammogram of receptor **2d** in the presence of 1 equivalent of NaClO_4 and KPF_6 in 40% $\text{CH}_3\text{CN}:\text{CH}_2\text{Cl}_2$ with 0.1 M TBAPF_6 at scan rate 100 mV/s.

Secondly, upon the addition of the corresponding metal cations to the receptor **3d** solution resulted in the anodic shift of the Fc/Fc^+ redox couple (Figure 2.40). It is also implied that during the oxidation process the electrostatic repulsion between the complexed cation and the electrogenerated positive charge ion on the oxidized form of the ferrocene subunit (ferrocenium) are generated. Since the oxidation of the metal complexes take place at more positive potentials than the oxidation of the free ligand, then we can conclude that the ferrocenium form of the complex is destabilized by repulsive electrostatic interactions with the bound-cation. These results were supported by the work of Saji and co-workers, who first reported the anodic shifts of cryptand containing ferrocene upon addition of alkali cations [119].

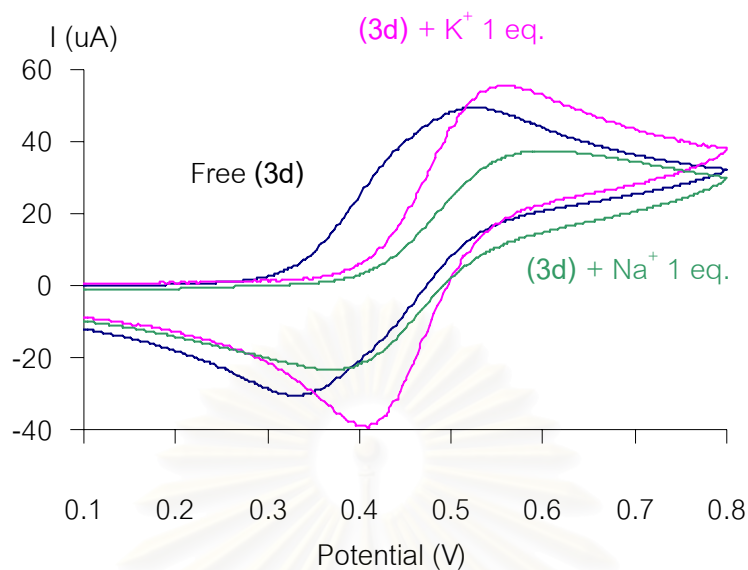
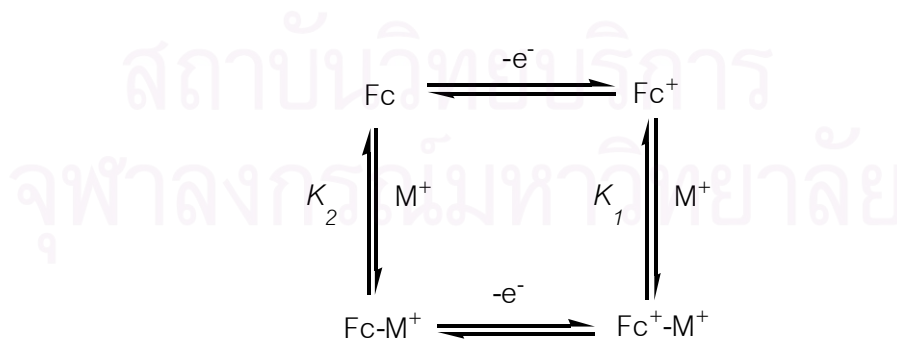


Figure 2.40 Cyclic voltammogram of receptor **3d** in the presence of 1 equivalent of NaClO_4 and KPF_6 in 40% $\text{CH}_3\text{CN}:\text{CH}_2\text{Cl}_2$ with 0.1 M TBAPF_6 at scan rate 100 mV/s.

The oxidation mechanism of free and co-bound complexes of receptor **3d** upon cationic guest binding can be represented by Scheme 2.11, for which K_1 would be expected to be less than K_2 , due to electrostatic repulsion as we mentioned so far. Then, quantitative values of the *reaction coupling efficiency* (K_1/K_2) (RCEs), for each cation can be calculated from the Eq. (2.3). The difference of formal redox potentials (ΔE) is the shift in the reduction potential caused by the complexation with metal cations and n represents the number of electrons involved in the redox process.



Scheme 2.11 The mechanism of electrochemical process during metal cation (M^+) binding through a ferrocenyl receptor (Fc).

$$K_1 = K_2 e^{[-nF(\Delta E)/RT]} \quad (2.3)$$

Table 2.17 Cyclic voltammetric data and calculated binding constants (K_1) of the co-bound complexes **2d** and **3d** with Na^+ and K^+ in 40% $\text{CH}_3\text{CN}:\text{CH}_2\text{Cl}_2$ with 0.1 M TBAPF_6 at scan rate 100 mV/s.

	Receptor 2d		Receptor 3d	
	$[\text{2d.Na}^+]^b$	$[\text{2d.K}^+]^c$	$[\text{3d.Na}^+]^b$	$[\text{3d.K}^+]^c$
ΔE^a	- ^e	- ^e	40	25
K_2^d	764	387	522	122
K_1	- ^f	- ^f	61	84
RCE ^g	- ^f	- ^f	0.12	0.68

^a ΔE is defined as $E_{\text{pa}}(\text{complex}) - E_{\text{pa}}(\text{receptor})$. ^b Added as NaClO_4 . ^c Added as KPF_6 . ^d Calculated from NMR titration experiments. ^e Could not measure. ^f Could not be calculated. ^g Reaction Coupling Efficiency (K_1/K_2).

According to Table 2.17, the difference between the E_{pa} of the free ligand and the complex increases in the order $\text{Na}^+ > \text{K}^+$ as expected from the increasing charge-to-size ratios of those cations [68]. Considering in ΔE of the proposed receptors, however, it was showed that the ΔE values in this work are smaller than cryptand containing ferrocene unit, receptor **2.53** (the ΔE was found to be 188 mV) [120]. This is probably due to the distance between the iron atom and the bound cations in the cryptand structure is more closer (see Figure 2.41) than our host molecules giving in the strong electrostatic repulsion between ferrocenium ion and a bound cation.

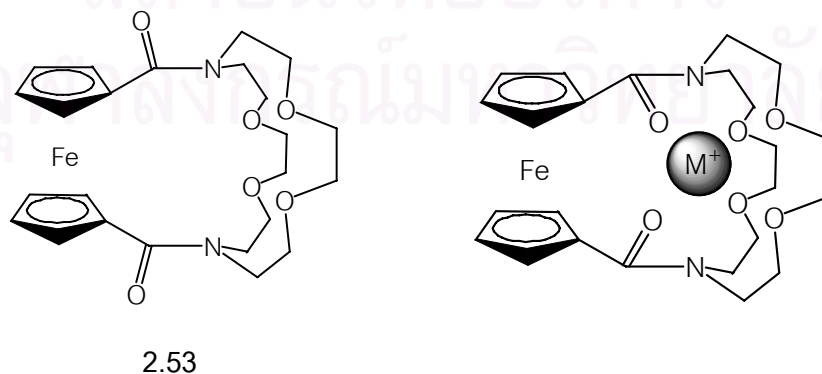
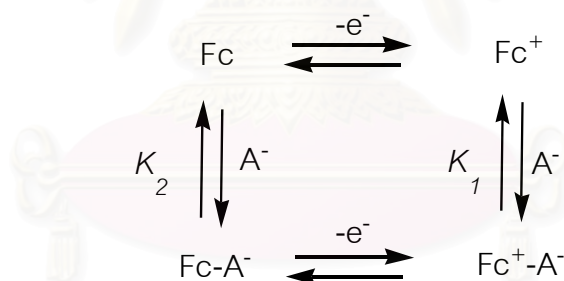


Figure 2.41 Receptor **2.53** and proposed the binding structure of its complex with alkali metal cations.

2.3.9 Electrochemical Sensing of Receptors 1, 2d and 3d towards Anionic Guests in the Absence and in the Presence of Alkali Metal Cations

An important feature of monotopic receptor **1** and novel heteroditopic receptors **2d** and **3d** the incorporation of amidoferrocene as the electrochemical anion-binding site. It is well-known that upon oxidation, amidoferrocene and its derivatives can bind anions more effectively than its reduced form as a consequence of electrostatic interactions between the ferrocenium group and the bound anion [121]. This give rise to a shift in the redox potential to the less positive (cathodic shift). It can thus be assumed that the oxidation of ferrocene in the vicinity of amide groups increases the acidity of the amide protons and makes hydrogen bonding stronger, leading to a synergy between ion pairing of $[R^+ \cdot A^-]$ and hydrogen bonds. In general, redox and complexation equilibria for a ferrocene based host in the presence of a given anion can be summarized by a simple square scheme as shown in Scheme 2.12.



Scheme 2.12 The mechanism of electrochemical response during anion binding (A^-) through a ferrocenyl receptor (Fc).

In this case, we can expect that K_1 would be higher than K_2 rising from electrostatic interactions between anions and ferrocenium cation complementarily with the strong hydrogen bonding through the NH amide functional group. In other words, since anion binds more strongly to the cationic ferrocenium form of the receptor, the neutral receptor becomes easier to oxidize and the potential of the ferrocene/ferrocenium system shifts negatively. The more the interactions are reinforced through oxidation of the receptor, the more the potential shifts negatively upon

complexation. Then, the binding enhancement factor (BEF) in anion binding strength on the introduction of the positive charge can be directly related to the redox shift induced by addition of anions.

Normally, the results obtain on the stepwise addition of substoichiometry amounts of the appropriate anionic guest species to the receptor solutions revealed two different electrochemical behaviors, depending on the receptor and anion are interacting. Firstly, “*two wave behavior*” means the growth of a new distinct voltammetric curve which develops a second wave at more negative potential, together with the corresponding to the free receptor one upon progressive addition of the guest species. The two wave behavior is linked to a very strong increase anion-receptor interactions following the oxidation of the receptor. Secondly, “*shifting behavior*” means a second redox waves showing negatively shifted compared to the free receptor [122]. Indeed, negative shifts in the potential values on the addition of a guest anion are owing to ion-pairing interactions between the anions and the oxidized, positively charged receptor leading to the stabilization of ferrocene moieties. It should be noted that during the redox cycling, ion-pairing associations are accompanied by adsorption phenomena owing to the weak solubility of the ion pairs in electrolyte. This is revealed in the CV waves by a loss of reversibility of the Fc/Fc^+ redox wave [123]. Table 2.16, summarizes the potential shifts measurements of receptors **1**, **2d** and **3d** towards halide anions both in the presence and absence of metal cations.

In this work, the interactions of three receptors with chloride and bromide anions were investigated electrochemically. Attempts were made to investigate the binding of iodide anion electrochemically, unfortunately, the redox process corresponding to iodide oxidation overlaps with the ferrocene redox wave, and therefore anion binding could not be monitored essentially. However, we have found that upon addition of chloride and bromide anions to a solution of receptors **1**, **2d** and **3d** a slight progressive cathodic shift of the response of ion-pairing $\text{R}^+ + \text{A}^-$ system, associated with an increase in its intensity and a marked trend in irreversibility are observed, somehow,

partially overlapped with that of the free receptors, for example see Figure 2.42. These systems show the shifting behavior in electrochemical sense. Obviously, chloride invoked a larger electrochemical response than bromide probably because of the higher negative charge density. As already mentioned, the observed negative shift result from a reinforcement of strong electrostatic interactions between the anion and the oxidized ferrocenium positively charged in which stabilized the ferrocenium moieties.

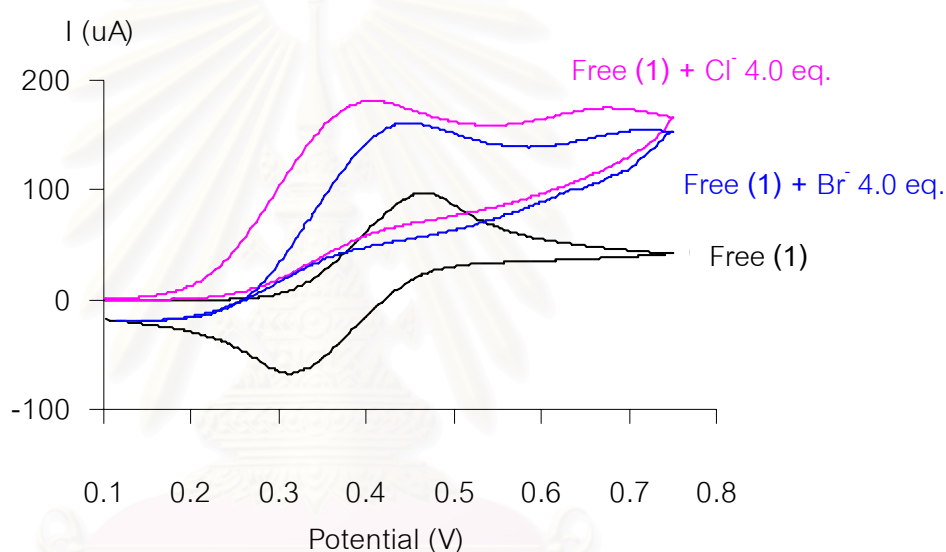
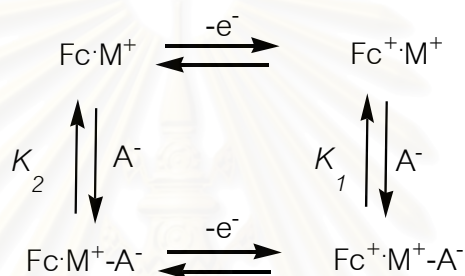


Figure 2.42 Cyclic voltammogram of receptor 1 with TBA chloride and bromide 4.0 equivalent in 40% $\text{CH}_3\text{CN}:\text{CH}_2\text{Cl}_2$ with 0.1 M TBAPF_6 as supporting electrolyte at a scan rate of 100 mV/s.

The electrochemical response becomes fully irreversible and the shoulder reaches full development when an excess of anions have been added. This behavior is characteristic of an EC mechanism with product absorption [123], suggesting that the complex species of oxidized positively charged R^+ receptor with halide anions form insoluble ion-pairs that remain strongly adsorbed onto the electrode surface and cannot be reduced in the reverse scan. As a matter of fact, no redox signal is detected during the second scan, which shows that an insulating layer is coated onto the electrode surface from the first anodic scan.

The addition of increasing amounts of anionic guests to the co-bound complex solution, $[\text{Fc}\cdot\text{M}^+]$, cause in both shifting and appearing of CV waves. The electrochemical sensing pathway would be presented in Scheme 2.12. We can expected that K_1 in this system will be higher than its neutral form due to the strong electrostatic interaction between doubly positively charge of receptor $[\text{Fc}^+\cdot\text{M}^+]$ in oxidized form and negatively charge of anion complementarily with the formation of strong hydrogen bonds of anions through amide groups as well.



Scheme 2.12 The mechanism of electrochemical process during anion (A^-) binding to heteroditopic electrochemical anion receptor ($\text{Fc}\cdot\text{M}^+$).

In the presence of metal cations, the shifting behaviors were found in the system of $[\text{2d.Na}^+]/\text{Cl}^-$, $[\text{2d.Na}^+]/\text{Br}^-$, $[\text{3d.Na}^+]/\text{Cl}^-$ and $[\text{3d.K}^+]/\text{Cl}^-$ as shown in Figure 2.43. The cyclic voltammograms of these systems display larger cathodic shift in Fc/Fc^+ redox coupling than their free forms (Table 2.18), indicating the strong interactions of the corresponding guests to the oxidized co-bound metal complexes. As mentioned previously, an insoluble $[\text{R}^+\cdot\text{M}^+]-\text{A}^-$ ion-pairs are adsorbed strongly onto the electrode surface resulting in the loss of reversibility of the redox couple of Fc/Fc^+ couple. Unfortunately, there are some precipitation problems in the systems of $[\text{2d.K}^+]/\text{Br}^-$, $[\text{3d.Na}^+]/\text{Br}^-$ and $[\text{3d.K}^+]/\text{Br}^-$.

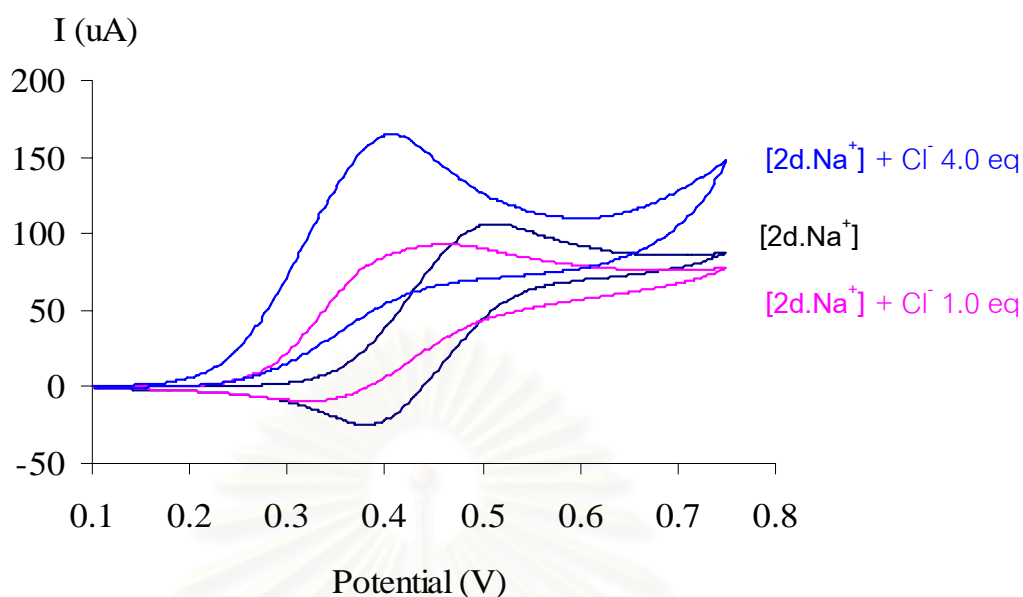


Figure 2.43 Cyclic voltammograms of $[2d.Na^+]$ titrate with TBA chloride 1.0 equivalent and 4.0 equivalent in 40% $CH_3CN:CH_2Cl_2$ with 0.1 M $TBAPF_6$ as supporting electrolyte at scan rate 100 mV/s.

Table 2.18 Electrochemical recognition data (ΔE)^a for receptors 1, 2d and 3d towards Cl^- and Br^- in 40% $CH_3CN:CH_2Cl_2$ with 0.1 M $TBAPF_6$ at scan rate 100 mV/s.

Receptors	ΔE (mV)			
	Cl^-	Br^-	AcO^-	BzO^-
1	58	10	140	100
2d	<107	> 28	> 28	> 80
$[2d.Na^+]^b$	122	46	- ^d	- ^d
$[2d.K^+]^c$	153	- ^d	- ^d	- ^d
3d	82	- ^d	90	70
$[3d.Na^+]^b$	110	- ^d	250	- ^d
$[3d.K^+]^c$	138	- ^d	- ^d	- ^d

^a ΔE is defined as E_{pa} (free receptor) – E_{pa} (complex). ^b Added as $NaClO_4$. ^c Added as KPF_6 . ^d Precipitation occurred.

In contrast, in the systems of $[2d.K^+]/Cl^-$ and $[3d.Na^+]/AcO^-$ display the two-wave behavior in which the progressive appearance of a new wave at the less potential and a progressive disappearance of the initial wave are observed (Figure 2.44). The results obtained by the stepwise addition of anions revealed the appearance of a second irreversible wave corresponding to the ferrocene redox couple of the double positively charged complexed receptor $[R^+.M^+]+A^-$, together with the corresponding to the co-bound receptor. Its position with respect to the wave corresponding to the uncomplexed receptor, $[2d^+.K^+]$ ($\Delta E = 153$ mV) and $[3d^+.Na^+]$ ($\Delta E = 250$ mV) reflect a more favorable oxidation process for the ferrocene moiety in the complexed species during guest binding. The new redox peak reaches full development until 2 equivalents of anions are added. This “two wave behavior” is diagnostic of a large equilibrium constant for chloride binding by the doubly positively charged co-bound receptor $[R^+.M^+]$. The observed negative shift is due to a reinforcement of the interaction between anions and co-bound metal complexes in its oxidized state following the establishment of strong electrostatic interactions between the anion and the oxidized doubly positively charged $[R^+.M^+]$ as well as leading to a stabilization of the ferrocenium moieties. As previously mentioned, the co-bound ion-pair complexes show irreversible electrochemical behavior resulting from the absorption of ion-pairs $[R^+.M^+]\cdot A^-$ onto the electrode surface as well.

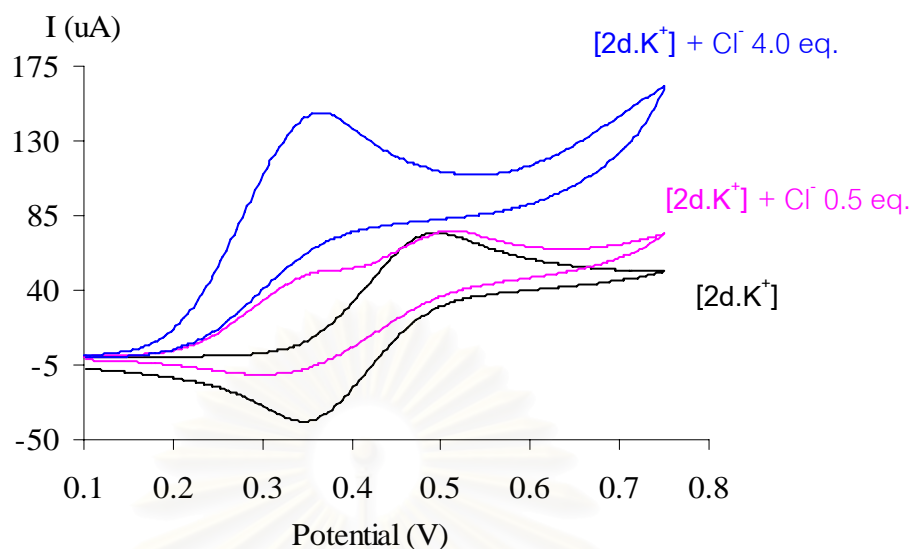


Figure 2.44 Cyclic voltammograms of $[2d.K^+]$ titrate with TBA chloride 0.5 and 4.0 equivalent in 40% $CH_3CN:CH_2Cl_2$ with 0.1 M $TBAPF_6$ as supporting electrolyte at scan rate 100 mV/s.

A clear two-wave behavior was observed in SWV experiments as shown in Figures 2.45 and 2.46 After addition of more than two equivalents of anions (Cl^- and AcO^-), only the peak corresponding to the oxidation of $[2d^+ \cdot K^+] + Cl^-$ and $[3d^+ \cdot Na^+] + AcO^-$ complex are seen on the SWV curve.

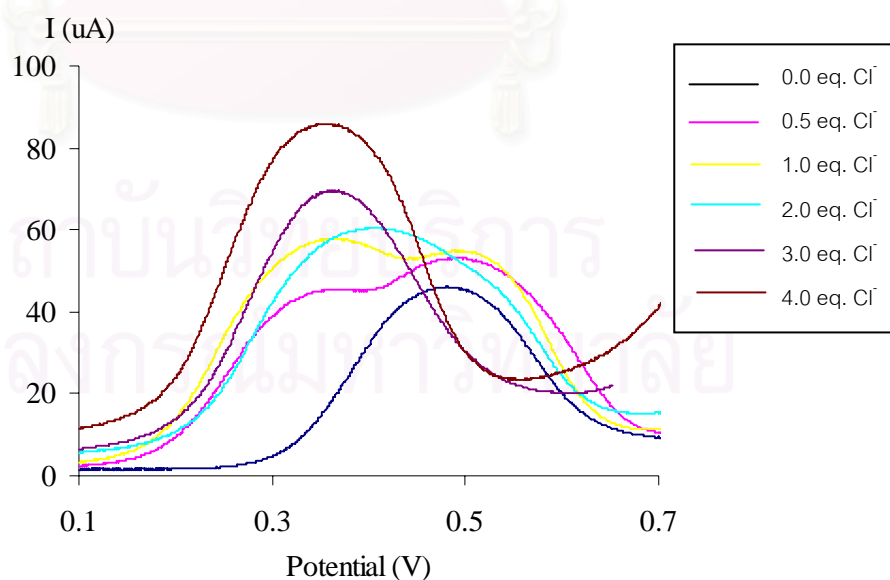


Figure 2.45 Square wave voltammograms of $[2d.K^+]$ titrate with TBA chloride in 40% CH_3CN/CH_2Cl_2 with 0.1 M $TBAPF_6$ as supporting electrolyte at scan rate 100 mV/s.

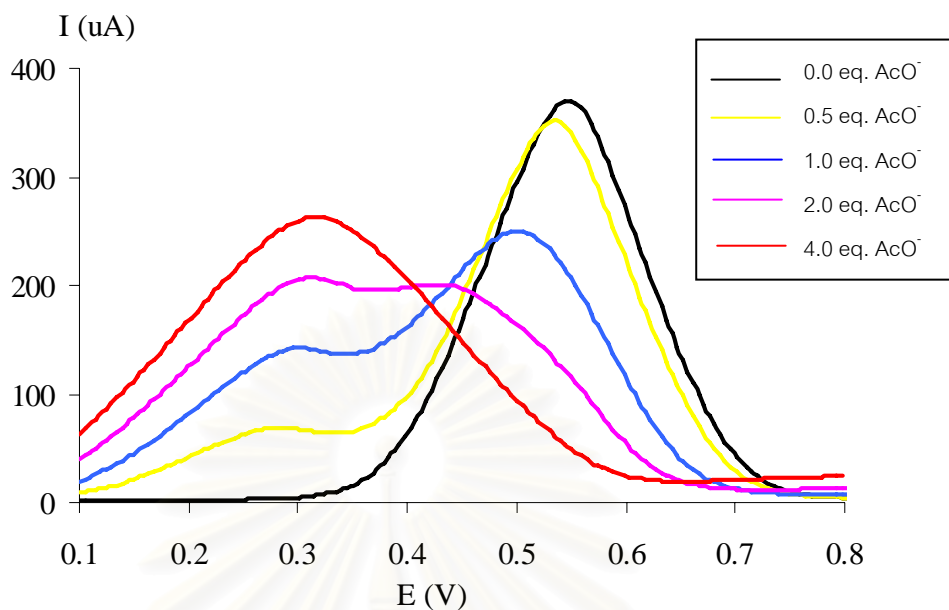


Figure 2.46 Square wave voltammograms of $[3d.Na^+]$ titrate with TBA acetate in $40\%CH_3CN/CH_2Cl_2$ with $0.1 M TBAPF_6$ as supporting electrolyte at scan rate $100 mV/s$.

Although, we cannot calculate BEF of $[2d^+.K^+]/Cl^-$ in this system because K_2 could not be observed from NMR titration experiments (as we discussed before in the system of $[2d.K^+]/Cl^-$ the result showed the negative binding). However, we expected that the BEF of $[2d.K^+]/Cl^-$ should be absolutely enhanced, which means that the binding of chloride to the oxidized form of co-bound complex $[2d.K^+]$ is definitively stronger than its reduced form. In another word, the oxidized form of co-bound complex $[2d.K^+]$ prefers to bind chloride anion, while the reduced form is not.

In general point of view, the electrochemical anion sensing properties of ferrocene-based receptors **1**, **2d** and **3d** are due to the formation of a complex between the selected anion and the receptors in its oxidized form, complexation that is reinforced in the oxidized, ferricinium form of the receptors. Receptor **1** can interact with anions through hydrogen bonding interactions. In addition, for receptors **2d** and **3d** the recognition behavior can be explained in terms of hydrogen bonding complexation, and the magnitude of the electrochemical sensing is essentially dependent on the strength of ion-pairing interactions. It is not surprising that the best results have been obtained in the systems of co-bound cation receptors.

In conclusion, in the presence of metal cations the interactions of heteroditopic receptors **2d** and **3d** towards anions are higher than its free forms. Actually, this is the case of the synergy between the electrostatic effect between double positive charge (from ferrocenium and metal cation) of co-bound complex and anions complementarily to the hydrogen bonding between amidoferrocene and anionic guest. Then, we can conclude that both synthetic heteroditopic receptors can act as electrochemical anion sensors for halide anions.



สถาบันวิทยบริการ
จุฬาลงกรณ์มหาวิทยาลัย

CHAPTER 3

CONTROLLING THE MORPHOLOGY OF AGGREGATES OF AN AMPHIPHILIC SYNTHETIC RECEPTOR THROUGH HOST-GUEST INTERACTIONS

3.1 Introduction

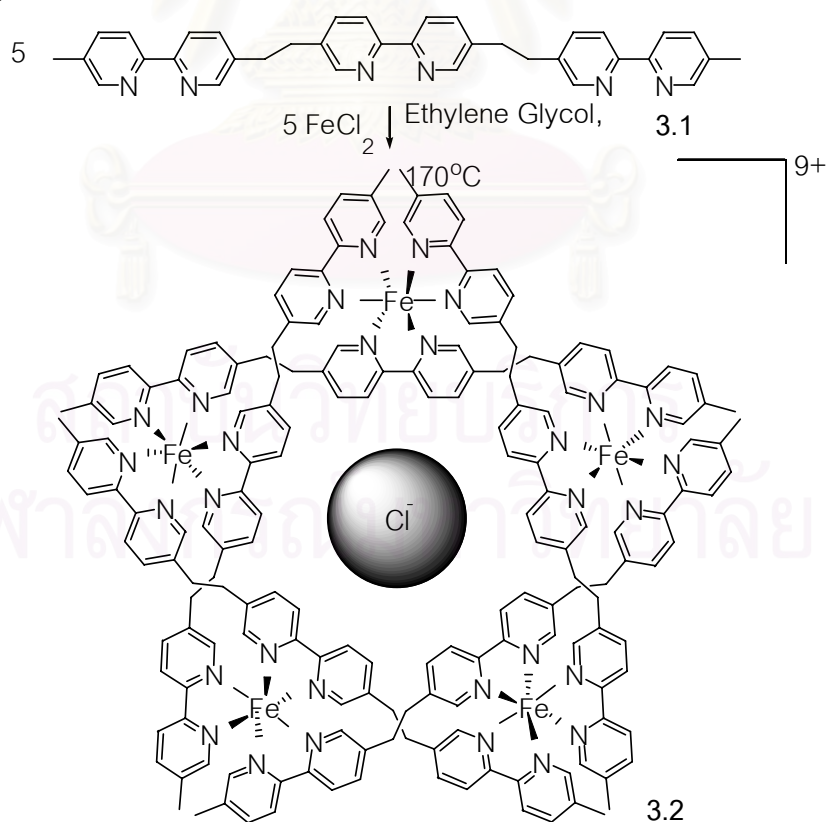
3.1.1 Template Effect: Thermodynamic and Kinetic Approaches

A template is a molecule or ion that can form a supramolecular complex with the reagents or products of a reaction, and thus influence its outcome. The effects of templates can be divided into two types – kinetic and thermodynamic [124].

Thermodynamic effects is the outcome of reversible templated reactions [125], whereas **kinetic effects** control irreversible reactions. A template may be a small molecules or ions which gathers the reactants around, a large molecule that surrounds the reactants like a host, or a molecule with similar dimensions to that of the reactants for example single-stranded DNA acting as a template for a second strand. In kinetic templating control, the outcome of irreversible reactions, regards to reaction outside equilibria whereas the thermodynamic control, the outcome of reversible reactions, refers to the stability of the entirely products at equilibrium.

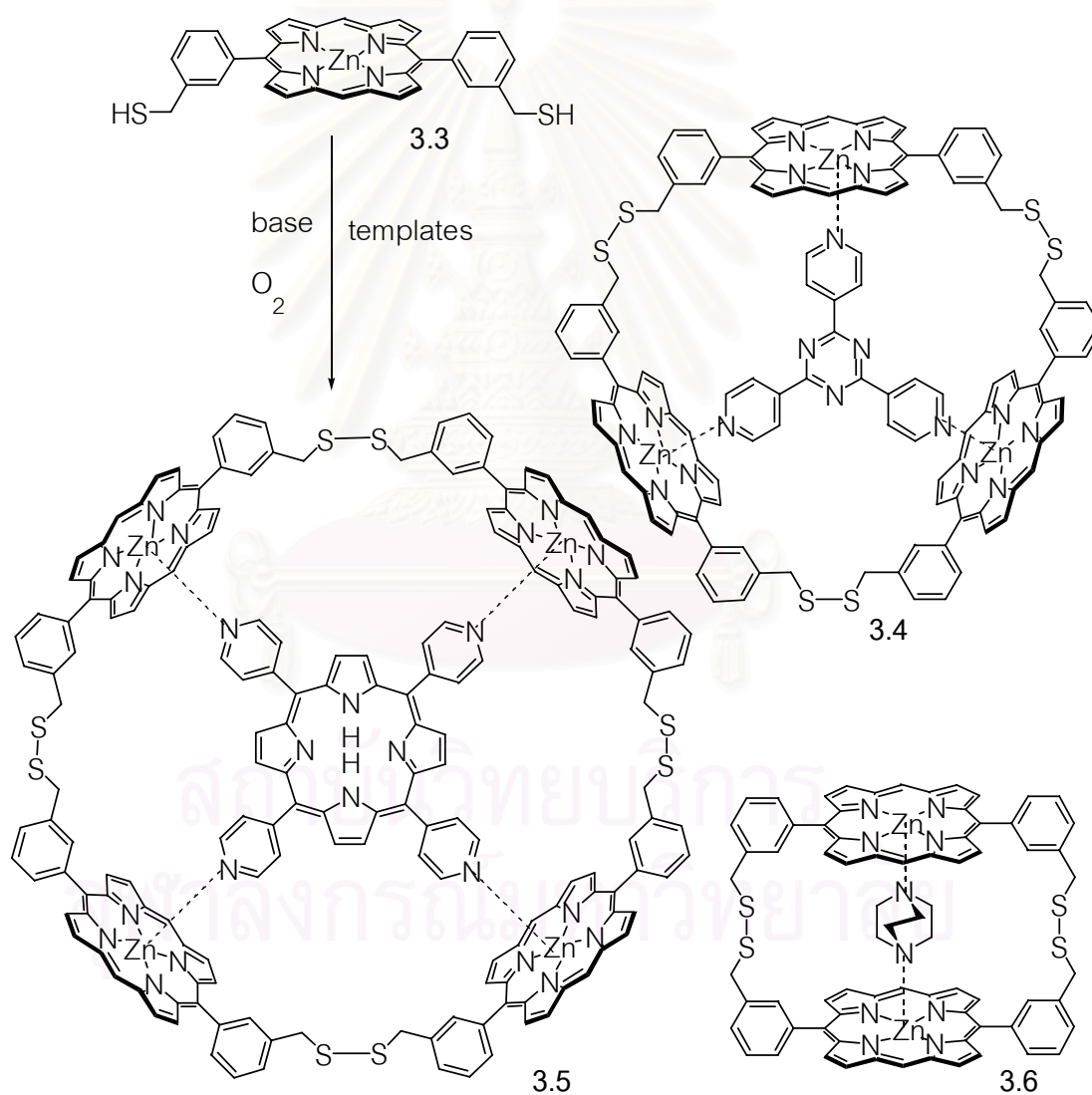
These effects are highly important in biological systems. Many enzymes can be thought of as templates as well as catalysts [126], and the synthesis of nucleic acids and proteins is controlled by the template effect [127]. For example, DNA acts as a template for itself and RNA, and RNA acts as a template for proteins. The self-templating effect employed in DNA replication has been imitated in a number of artificial self-replicators, including an intriguing system of mesoscopic objects held together by magnetic interactions.

The most striking examples of template effect is to create transition metal helicates, using chains of 2,2'-bipyridine ligands, such as **3.1** which was presented by Lehn and co-workers [128]. Indeed, each bipyridine moiety in the molecule would chelate a different transition metal ion, allowing two or three ligand molecules to join together to form a double or triple helix. When iron (II) chloride was used to generate helices, a cyclic double helicate, consisting of five ligand chains and five metal ions, was formed, compound **3.2** as shown in Scheme 3.1. An X-ray crystal structure of the complex revealed the presence of a chloride ion acts as the template in the centre. The structure generated was found to be dependent on the nature of the transition metal salt used. Using NiCl_2 resulted in the production of a linear triple helicate, whereas $\text{Fe}(\text{BF}_4)_2$ gave rise to a hexameric species. A later study was to find that hexamers were also formed using other counterions, and that a tetramer could be formed using a more flexible ligand chain. This dependence on not just the metal ion, but also the counterion led to a key observation.



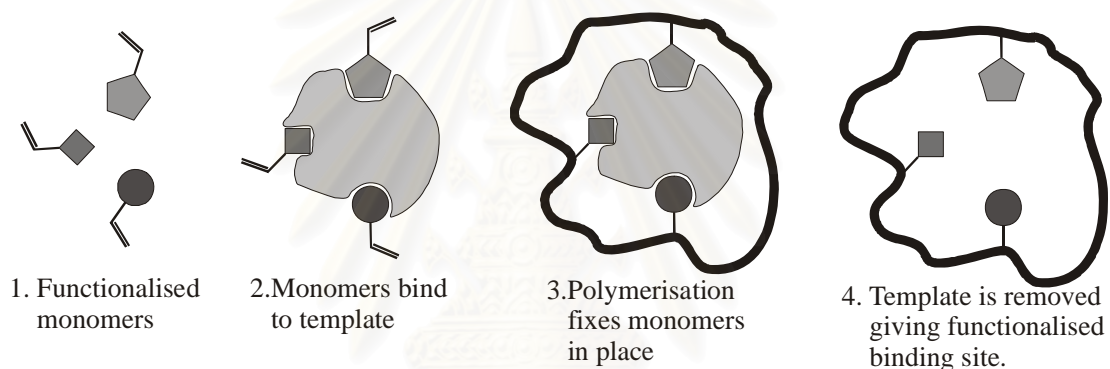
Scheme 3.1 A cyclic double helicate templated by a chloride anion.

The formation of macrocyclic porphyrin oligomers by Sanders and co-workers, which uses three different pyridine-based ligands as templates for three different oligomers [129]. The porphyrin **3.3** is oligomerised by Glaser coupling reactions to form **3.4**, **3.5** or **3.6** in the presence of specific templates (Scheme 3.2). Interestingly, the templates bind any linear dimers that are formed as intermediates, and either encourage or prevent cyclisation, thus giving the desired products.



Scheme 3.2 A template effect to form porphyrin oligomers.

Another intriguing approach is to use templates in polymer synthesis. If the monomers are appropriately chosen to have the right functionality to bind to the templates, then by synthesising the polymer in the presence of the template and then removing the template, a polymer bearing binding sites can be made [130], Scheme 3.3. This approach of *imprinting* has been used to make selective chromatographic media and even artificial catalysts, using transition-state analogues as the template. However, the materials produced by this method are hard to analyse, and the binding sites produced are not likely to be homogeneous.



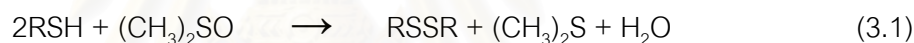
Scheme 3.3 Formation of imprinted polymers.

สถาบันวิทยบริการ
จุฬาลงกรณ์มหาวิทยาลัย

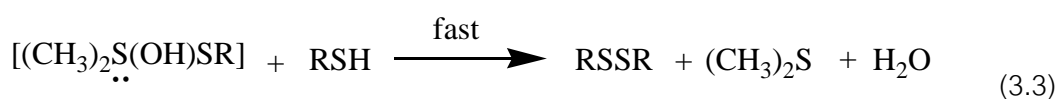
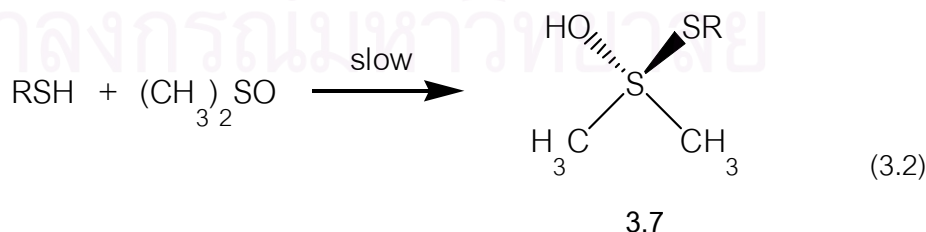
3.1.2 Oxidation of Thiols to Disulfides

It is well known that, the oxidation of thiol (-SH) to disulfide (-SS-) can be taken place in the aqueous and non-aqueous systems in the presence of the oxidizing agents such as nitric acid, hydrogen peroxides, oxygen, and dimethylsulfoxide. In the aqueous system, the oxidation of thiol to disulfide can be occurred very easily in the presence of oxygen at pH 8-9.

In the other hand, oxidation of thiol to disulfides can be occurred in organic solvent media such as dimethylsulfoxide (DMSO) as well. Yiannios and Karabinos [131] reported that thiols were selectively oxidized by DMSO to the corresponding disulfide in high yield with the concomitant reduction of DMSO to dimethylsulfide (Eq.3.1).

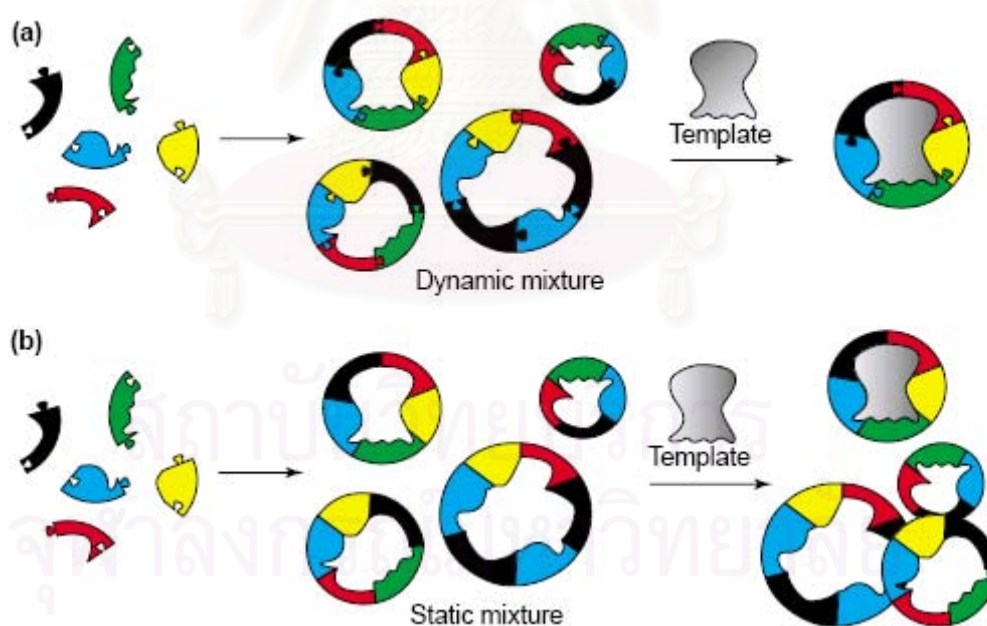


Wallace and co-workers have showed that the rate of oxidation depends on the acidity of thiol [132,133]. In addition, they proposed that the rate determination step is the formation of the intermediate adduct **3.7** followed by a fast reaction with a second molecule of thiol (Eq. 3.2 and 3.3). The oxidation of thiols with dimethylsulfoxide presents several attractive features like the simplicity of the reaction, the high yield and the selectivity of disulfide formation.



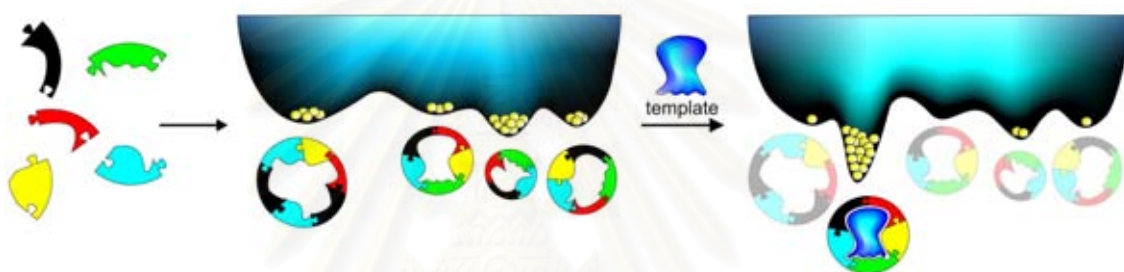
3.1.3 Dynamic Combinatorial Chemistry (DCC)

The main difference between dynamic combinatorial chemistry and traditional combinatorial chemistry is that the reaction that links the building blocks together in dynamic combinatorial chemistry is reversible [134,135]. There is a continuous interchange of building blocks between the different members of the dynamic combinatorial library (DCL) and so the composition of the library is governed by thermodynamics rather than kinetics. A DCL is therefore able to respond to external influences. More specifically, molecular recognition events selective for one member of the library will stabilize this member, thereby inducing a shift of the equilibrium towards the formation of this species and away from the species that are not recognized (Scheme 3.4).



Scheme 3.4 Schematic representation of (a) dynamic combinatorial chemistry and (b) traditional combinatorial chemistry.

Considering in dynamic combinatorial system, when a guest molecule is introduced into a dynamic library of potential hosts it will select and bind the best host. The binding event introduces a new equilibrium in the system adding an additional free energy well, Scheme 3.5. If this well is sufficiently deep, the equilibria will shift in the direction of the best host at the expense of unfit hosts. The resulting amplification of the ideal host will facilitate identification. Moreover, template synthesis under the same reversible conditions should provide quick and easy access to large amounts of material.



Scheme 3.5 A small dynamic combinatorial library and its free energy landscape showing the effect of adding a template that strongly and selectively binds to one of the equilibrating species.

For a reaction to be suitable for use in dynamic combinatorial chemistry, it must have several features. It must be reversible, and fast enough in both directions. There must be no irreversible side reactions fast enough to remove significant amounts of the building blocks from the library. The functional groups involved must be compatible with the body of the building blocks, and with the template. Finally, there must be some way of stopping the reaction, to allow stable products to be produced. Several different reversible reactions that fulfill these conditions have been adapted for use with dynamic combinatorial libraries as shown in Figure 3.1.

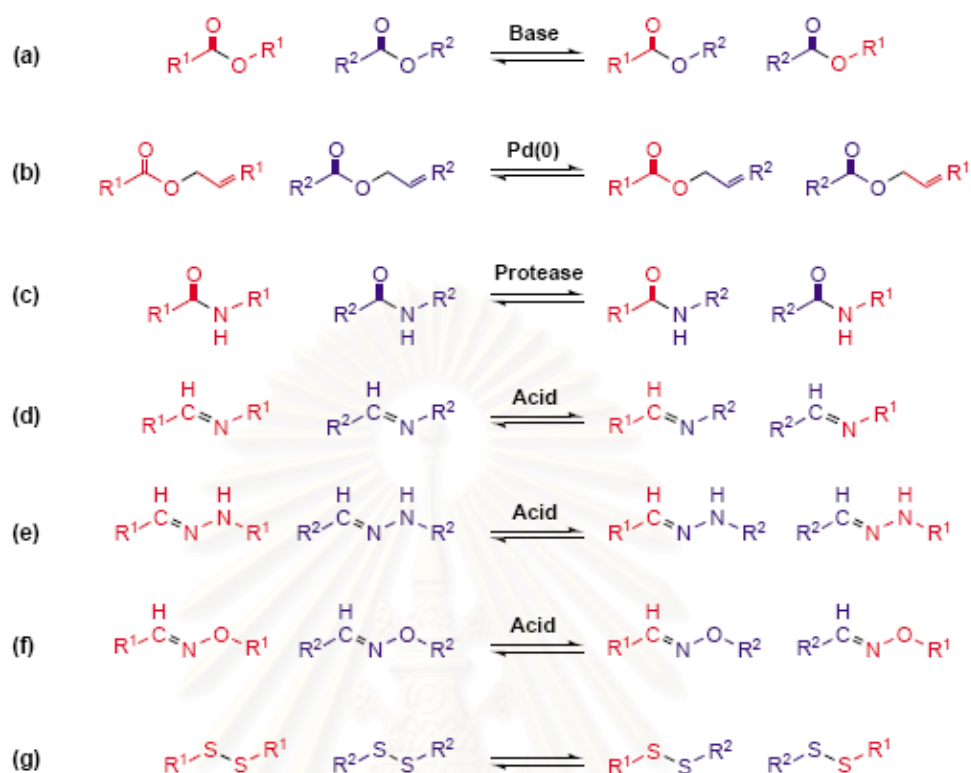
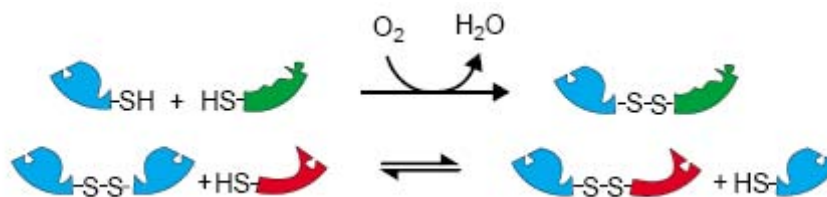


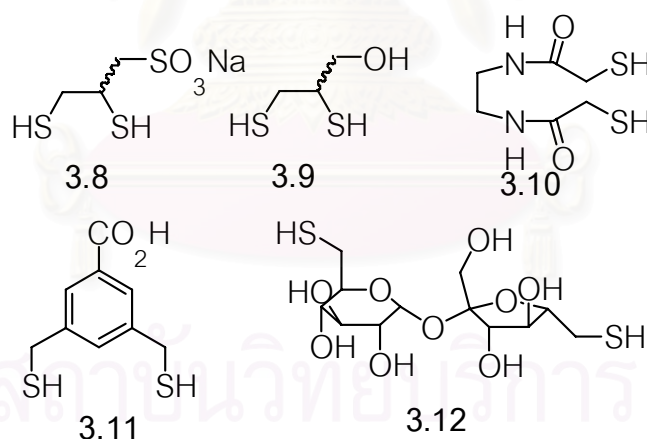
Figure 3.1 Reversible reactions used in dynamic combinatorial chemistry.

In this thesis, we have been focused in DCL of disulfide exchange because the reaction is easy to operate and it can quench in mild condition (acid condition). Disulfide exchange, along with imine [136,137] and hydrazone exchange [138-140], is one of the major reactions in dynamic combinatorial chemistry. The true exchange reaction is thiol-disulfide exchange, whereby a thiolate anion displaces another thiolate anion from a disulfide (Scheme 3.6). However, in many cases it is simpler to think of this as an exchange reaction between disulfides, mediated by thiolate anions. As these anions are required for exchange, acidification of a mixture of disulfides will freeze any exchange. Disulfide exchange may also be accompanied by disulfide formation, by the oxidation of thiols using either oxygen from the air or another oxidising agent. This may be carried out in conditions compatible with disulfide exchange, allowing the formation and equilibration of a DCL in a single step. It should be noticed that the oxidation of thiol to disulfide can be taken place in DMSO as we described so far.

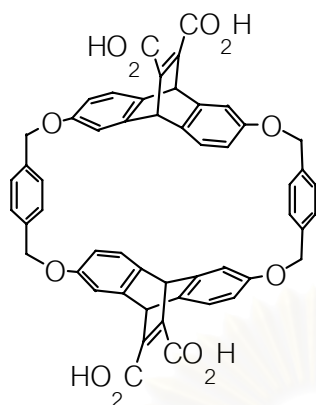


Scheme 3.6 Reversible disulfide exchange from dithiols building blocks.

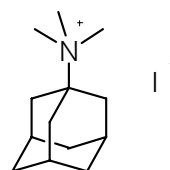
A series of DCLs on the discovery of host molecules from disulfide DCLs have been constructed by Otto and co-workers. A number of dithiols building blocks **3.8-3.12**, and various libraries were constructed by allowing them to oxidise and equilibrate in aqueous solution at pH 7.5 and the resulting libraries were analysed by mass spectrometry [141]. For each library, all of the expected masses corresponding to species up to a certain size, ranging from pentamers to octamers, were observed. A DCL made from **3.8**, **3.9**, **3.10** and **3.11** was found to contain 119 different macrocyclic product masses, including 56 out of the expected 66 tetrameric and smaller masses.



Moreover, Otto and co-workers have demonstrated the amplification of host molecules from a DCL with a host-guest system by Dougherty and co-workers [142] was selected, **3.13-3.14**. Host **3.13** contains an aromatic cavity in which the cationic guest **3.14** binds in this cavity, by a mixture of hydrophobic and cation- π interactions, with a binding constant of $2.4 \times 10^5 \text{ M}^{-1}$. Consequently, based on parts of this host the building blocks **3.14** and **3.15** were designed [143].



3.13



3.14

In the absence of templates, an initial DCL was formed by mixing the building blocks 3.15 and 3.16 with the structurally related 3.17 in water at pH 8-9. An ESI-MS study was conducted on the resulting mixture, revealing disulfides of 45 different masses, many more different macrocycles, due to sequence isomerism and diastereoisomerism. After separation by HPLC the two main compounds were shown by ESI-MS to be $(3.15)_2$ and $(3.15) \cdot (3.16) \cdot (3.17)$. In the presence of the template 3.18, ESI-MS analysis of these peaks showed them to be the heterotrimer 3.20 as a mixture of two diastereomers. Whereas a larger template 3.19 was used in an attempt to elicit that host, but instead, the homotrimer 3.21 was amplified as a mixture of diastereomers (Figure 3.2).

ITC studies confirmed that the correct hosts were selected by the template. Macrocycle 3.20 was found to bind to 3.18 with $K_a = 2.5 \times 10^5 \text{ M}^{-1}$, and 3.21 to 3.19 with $K_a = 7.1 \times 10^5 \text{ M}^{-1}$. The templates did not bind as strongly to the hosts that they did not select in which macrocycle 3.20 bound to guest 3.19 with $K_a = 4.5 \times 10^4 \text{ M}^{-1}$ and 3.21 bound to 3.18 with $K_a = 2.8 \times 10^4 \text{ M}^{-1}$. Furthermore, they provide an extensible system from which other discoveries can be made for example catalysis.

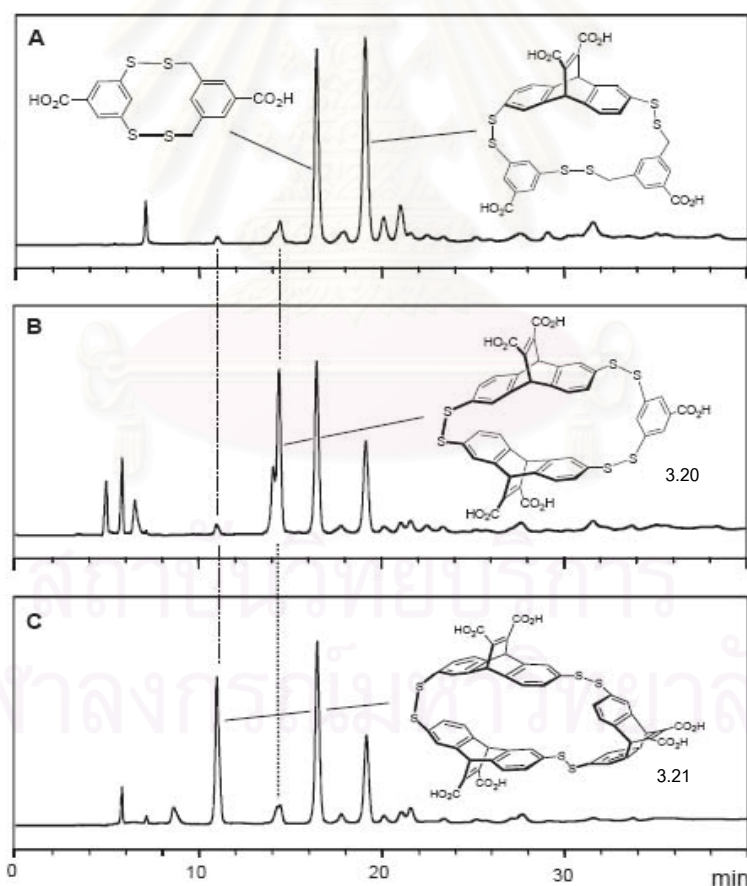
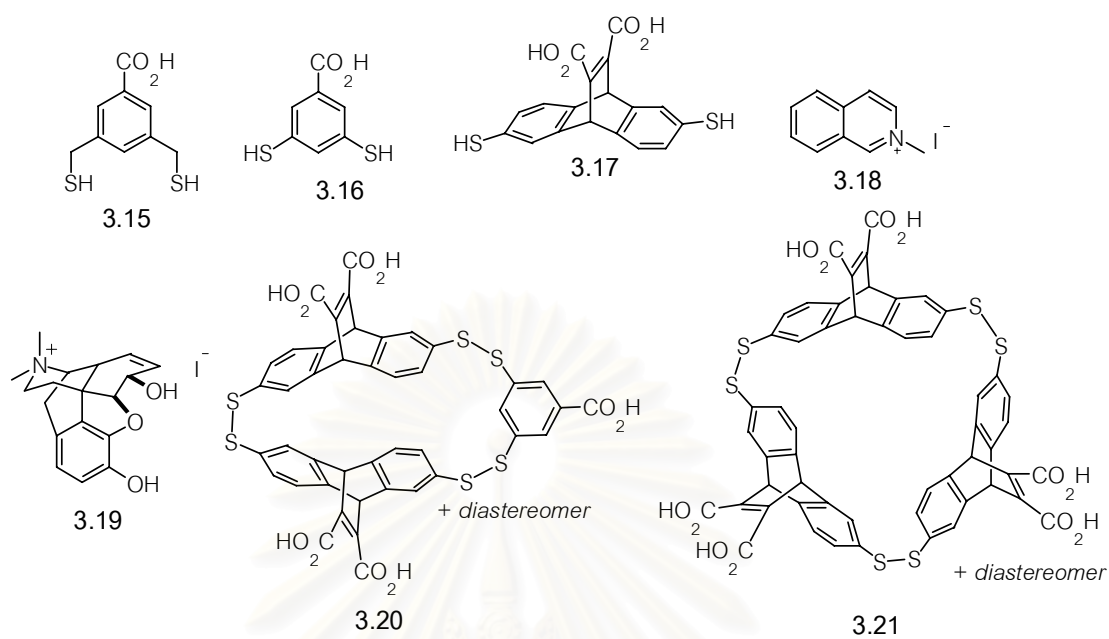
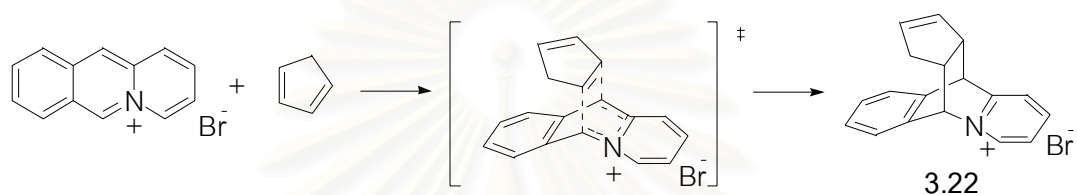


Figure 3.2 HPLC analyses of the DCL made from dithiols 3.15, 3.16, and 3.17 (A) in the absence of any template; (B) in the presence of 3.18 inducing the amplification of host 3.20; and (C) in the presence of morphine derivative 3.19 leading to the amplification of host 3.21.

The Diels-Alder reaction shown in Scheme 3.7 was chosen as a candidate for catalyst development [144]. It has the useful feature that the product **3.22** of the reaction is analogous to the transition state, allowing it to be used as a template. Therefore, DCLs containing **3.15**, **3.16** and **3.17** were made, and used **3.22** was found to amplify both **3.20** and **3.21**. In kinetic studies of the Diels-Alder reaction, **3.21** showed a modest rate acceleration for the reaction, and also some degree of catalytic turnover.



Scheme 3.7 Diels-Alder reaction, catalysed by a library member from a DCL.

In conclusion, since dynamic combinatorial chemistry has developed substantially in the first papers in 1996 [145]. The basic DCL concepts of library formation through reversible reactions, and of template-driven amplification have been proven in many different systems, and strong template effects have been demonstrated in some systems. A range of building block, template and exchange chemistries have been shown to be useful. Several different architectures and methodologies have been explored, and a few related approaches to the DCL method have emerged.

สถาบันวิทยบริการ
จุฬาลงกรณ์มหาวิทยาลัย

3.1.4 Aggregation of Amphiphilics : Micelles Formation

A surfactant is a molecule contains two distinct zones with extremely different solubilities. The *hydrophilic zone* is highly water-soluble, while the *lipophilic* portion of the molecule is soluble in organic media and is highly hydrophobic. Because of this dual behavior, surfactants are then often referred to as *amphiphiles*. Amphiphilics containing two tails usually form bilayer structures called vesicles, and those containing a single tail usually form micelles. These self-assemblies have been widely exploited in diverse areas such as catalysis [146], biochemistry [147] and pharmaceutical industries [148].

As we mentioned before, the single-chain amphiphilic molecules usually form micelles rather than vesicles. When the concentrations of amphiphilic molecules exceed the critical micelle concentration (cmc) in water, micelles are formed as aggregates of these molecules. In normal micelles, the hydrophobic hydrocarbon chains of the amphiphilic molecules are oriented toward the interior of the micelle, and the hydrophilic groups are in contact with the surrounding aqueous medium. On the other hand, reverse micelles are formed in nonaqueous medium where the hydrophilic headgroups are directed toward the core of the micelles and the hydrophobic groups are directed outward. In this case the hydrophilic groups are sequestered in the micelle core and the hydrophobic groups remain solvent-exposed on the surface of the micelle. These reverse micelles are extremely difficult to form from surfactants with charged head groups, since hydrophilic sequestration would create highly unfavorable electrostatic interactions.

The formation of micelles can be understood using thermodynamics: micelles can form spontaneously because of a balance between entropy and enthalpy. In water, the hydrophobic effect is the driving force for micelle formation, despite the fact that assembling surfactant molecules together reduces their entropy. Broadly speaking, above the CMC, the entropic penalty of assembling the surfactant molecules is less than the entropic penalty of the caging water molecules. Also important are enthalpic considerations, such as the electrostatic interactions that occur between charged (or ionic) surfactants.

When surfactants are present above the CMC, they can act as emulsifiers that will solubilize a compound normally insoluble in the solvent being used. This occurs because the insoluble species can be incorporated into the micelle core, which is itself solubilized in the bulk solvent by virtue of the head groups' favorable interactions with solvent species. The most common example of this phenomenon is detergents, which clean poorly soluble hydrophobic material (such as oil, grease, or dirt) that cannot be cleaned by water alone. Detergent also helps clean by lowering the surface tension of water, making it easier to remove dirt from a surface. The emulsifying ability of surfactants is also the basis for emulsion polymerization.

Normally, the size and shape of micelles are dictated by the molecular size, composition, architecture, and the concentration of the amphiphile. Understanding the connection between supramolecular microstructure and molecular structure is essential for a wide range of technical applications in which the desired function of a complex fluid is made possible through the precise control of the self-assembled microstructure.

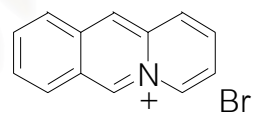
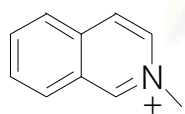
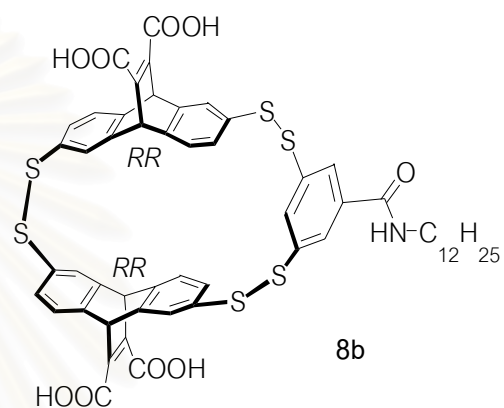
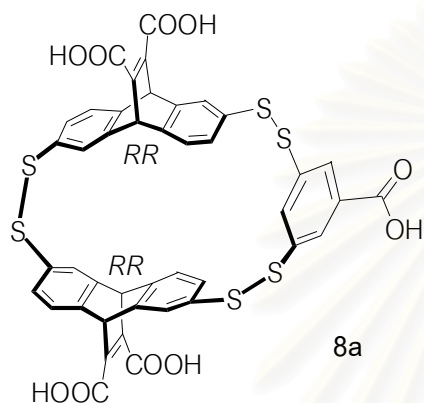
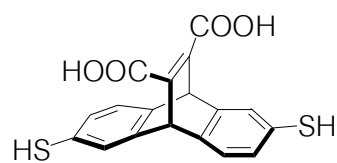
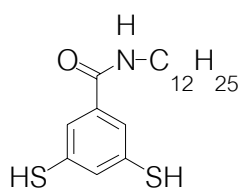
3.1.5 Objectives of this Research

One of supramolecular chemistry approach is control the molecular assembly. According to the knowledge of host-guest interactions, we are interested in how to apply specific host-guest interaction to control the morphology transformation of self-assembly molecules. According to highly self-organization properties of amphiphiles, then the amphiphilic molecule is a reasonable candidate to serve that purpose.

In this work, we have investigated the aggregation behavior of a synthetic amphiphilic receptor **8b** (the analogue of water soluble macrocyclic receptor **8a**), which contains the long C_{12} hydrocarbon chain, in the presence of guest **9** and **10**. We expected to see how effect of guest molecules to conduct the transformation of assembly structure of receptor **8b**.

In the first stage of this work, the strategy was to synthesize receptor **8b** probably using the dynamic combinatorial method, like receptor **8a**, by starting from dithiols building blocks **5** and **6**. The host-guest interactions of receptor **8b** with guest **9** and **10** can be investigated by ITC (Isothermal Titration Calorimetric Studies). To investigate the microstructure of aggregates, we have performed transmission electron microscopic (TEM) to studies.

สถาบันวิทยบริการ
จุฬาลงกรณ์มหาวิทยาลัย



สถาบันวิทยบริการ
จุฬาลงกรณ์มหาวิทยาลัย

3.2 Experimental Section

3.2.1 Synthesis of Dithiols Building Blocks and Guests Molecules

3.2.1.1 General Procedure

3.2.1.1.1 Analytical Measurements

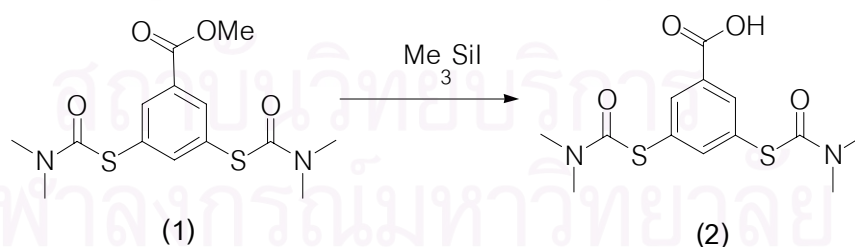
$^1\text{H-NMR}$ and 2D-NMR spectra were recorded on a Bruker ATM 500 MHz Spectrometer at room temperature. Variable Temperature $^1\text{H-NMR}$ spectra were recorded on a Bruker DPX 500 MHz spectrometer.

3.2.1.1.2 Materials

All materials and solvents were standard analytical grade, purchased from Fluka, Aldrich, Alfa Aesar and Avocado and were used without further purification. The dithiol building block **1** [140], **6** [140], **7** [140], receptor **8a** [140], cationic guests **9** [142] and **10** [149] were prepared following the literature procedures.

3.2.1.2 Synthesis

3.2.1.2.1 Preparation of 3,5-bis-dimethylcarbamoylsulfanyl benzoic acid (**2**)



A mixture of 3,5-bis-dimethylcarbamoylsulfanylbenzoic acid methyl ester **1** (2.8g, 8.18 mmol) and Me₃SiH (6.22 mL, 45 mmol) was refluxed at 105^o C for 15 hours. Diethyl ether (200 mL) was added and the solution was washed with 10% NaOH and dried over anhydrous Na₂SO₄. A white solid **2** was obtained in 90% yield after removing the diethyl ether.

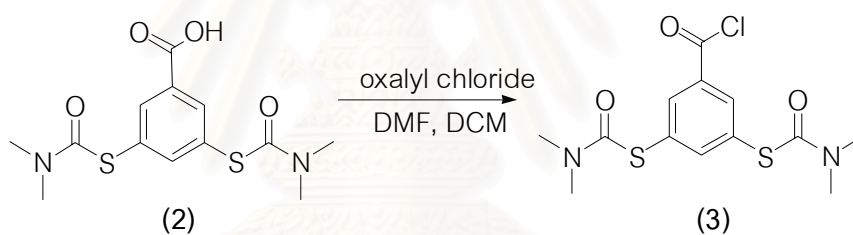
Characterization data for (2)

$^1\text{H-NMR}$ spectrum (400 MHz, CDCl_3 , ppm): δ 8.19 (s, 2H, *ArH*), 7.85 (s, 1H, *ArH*), 3.09 (m, 12H, $-\text{N}(\text{CH}_3)_2$)

$^{13}\text{C-NMR}$ spectrum (100 MHz, CDCl_3 , ppm) : δ 166.68, 164.12, 144.85, 135.73, 128.90, 128.05, 34.98.

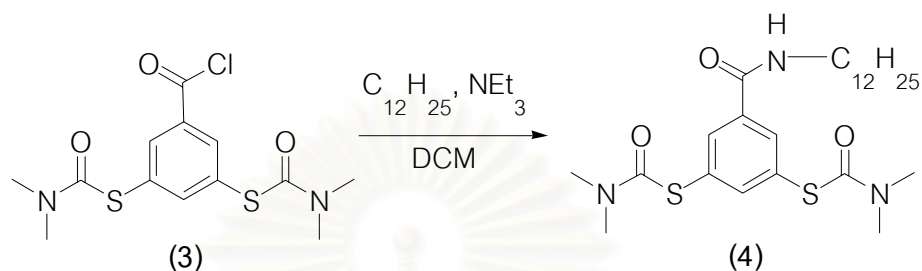
Exact mass: calcd: 329.0630; found: 329.0630 $[\text{M}+\text{H}^+]$.

3.2.1.2.2 Preparation of 3,5-bis-dimethylcarbamoylsulfanyl benzoyl chloride (3)



Oxalyl chloride (1.3 mL, 15mmol) was added to a solution of 2 (0.98 g; 3 mmol) in 8 mL of dry dichloromethane with 4 drops of DMF under a nitrogen atmosphere. The solution was stirred at room temperature for 3 hours. The solvent was removed under vacuum and the crude product was used in the next step without purification.

3.2.1.2.3 Preparation of *N*-dodecyl-3,5-dimethylcarbamoyl sulfanyl benzamide (4)



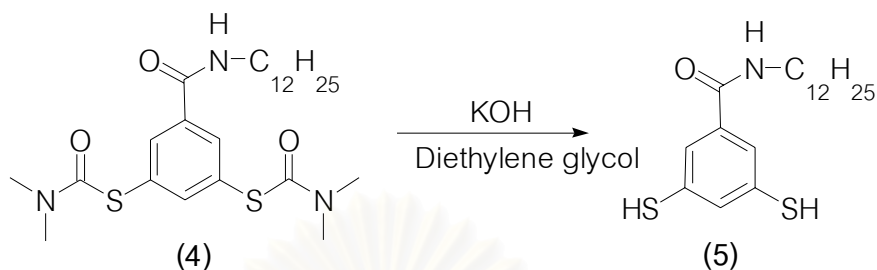
To a solution of dodecylamine (0.64 g, 3.5 mmol) and triethylamine (0.55 mL, 4 mmol) in dry dichloromethane (50 mL) was added a solution of acid chloride **3** (1.09 g; 3 mmol) in dry dichloromethane (15 mL) and stirred at room temperature for 15 hours. Then, the solution was washed with 10% HCl and water, respectively. After removal of the solvent, the residue was recrystallised from MeOH, giving a white solid of **4** in 85% yield.

Characterization data for (4)

$^1\text{H-NMR}$ spectrum (400 MHz, CDCl_3 , ppm) : δ 7.86 (s, 2H, *ArH*), 7.73 (s, 1H, *ArH*), 6.22 (m, 1H, -NH-), 3.39 (q, $J = 6$ Hz, 2H, -NHCH₂-), 3.05 (m, 12H, -N(CH₃)₄), 1.59 (m, $J = 7.6$ Hz, 2H, -NHCH₂CH₂-), 1.25 (m, 18H, -(CH₂)₉-), 0.87 (t, $J = 6.8$ Hz, 3H, -CH₃).

$^{13}\text{C-NMR}$ spectrum (100 MHz, CDCl_3 , ppm) : δ 164.89, 143.42, 135.19, 133.51, 129.12, 44.78, 39.25, 35.98, 30.90, 28.61, 28.53, 28.32, 25.99, 21.67, 13.10.

Exact mass: calcd: 518.2487; found: 518.2487 [M+Na⁺].

3.2.1.2.4 Preparation of *N*-dodecyl-3,5-dimercaptobenzamide (5)

Compound 4 (0.3 g; 0.060 mmol) was dissolved in 35 mL of degassed 1.75 M KOH in diethylene glycol and heated at 105^oC for 30 min under a nitrogen atmosphere. The solution was cooled to room temperature and 250 mL of degassed H₂O was added rapidly, followed by 10% HCl (30 mL). The white precipitate 5 was obtained in 97% yield after filtered and extensively washed with water.

Characterization data for (5)

¹H NMR (CDCl₃, 400 MHz, ppm): δ 7.39 (s, 1H, *ArH*), 7.26 (d, J = 7.2 Hz, 2H, *ArH*), 5.9 (m, 1H, -NH-), 3.42 (q, J = 7.2 Hz, 2H, -NHCH₂-), 1.55 (m, 2H, -NHCH₂CH₂-), 1.25 (m, 18H, *alkyl chain* CH₂), 0.87 (t, J = 7.2 Hz, 3H, -CH₃).

¹³C NMR (CDCl₃, 400 MHz, ppm): δ 166.99, 135.66, 132.14, 130.65, 123.89, 39.41, 31.05, 28.77, 28.73, 28.68, 28.46, 26.13, 21.82, 13.25.

Exact mass: calcd: 354.1925; found: 354.1925 [M+H⁺].

3.2.2 Preparation and Purification of Receptor 8b

Receptor **8b** was prepared by stirring a mixture of building blocks **6** (6.67 mM), **5** (3.33 mM) and template **9** (10 mM) in DMSO for 24 h at room temperature. The receptor was isolated by using a Gilson preparative HPLC. Aliquots of 2 mL of the solution were chromatographed using a Nucleodur C₁₈ preparative column (25.0 cm × 2.1 cm, 100 Å, 5 μm) with a Nucleodur C₁₈ guard column (5.0 cm × 2.1 cm, 100 Å, 5 μm), at a flow rate 20 mL/min, using 75:25:0.1 acetonitrile:water:trifluoroacetic acid as mobile phase. The chromatography was performed at 45 °C by immersing the column, the guard column and a length of HPLC tubing (to ensure heat exchange) into a water bath. Retention times were 35-40 minutes for the major *rac* diastereomer. The collected fraction of 10 runs were combined and dried *in vacuo*, and redissolved in 2 mL of DMSO and rechromatographed only 1 injections. The collected product was dried *in vacuo*, filtered and washed extensively with water (250 mL).

Characterization data for (8b)

¹H NMR of **8b** *rac* (D₂O:CD₃CN 1:1, 500 MHz, ppm) δ 8.59 (s, 1H, *ArH*), 8.10 (m, 6H, *ArH*), 7.78 (d, *J* = 7.5 Hz, 2H, *ArH*), 7.69 (m, 4H, *ArH*), 7.55 (m, 2H, *ArH*), 6.37 (s, 2H, -*CH*-), 6.29 (s, 2H, -*CH*-), 3.78 (q, *J* = 6.6 Hz, 2H, -NHCH₂-), 2.02 (t, *J* = 6.1 Hz, 2H, -NHCH₂CH₂-), 1.63 (m, 18H, -CH₂-), 1.21 (t, *J* = 7.1 Hz, 3H, -CH₃).

¹H NMR of **8b** *meso* (D₂O:CD₃CN 1:1, 500 MHz, ppm) δ 8.28 (s, 2H, *ArH*), 8.06 (s, 2H, *ArH*), 8.02 (s, 2H, *ArH*), 7.98 (s, 1H, *ArH*), 7.74 (d, *J* = 7.5 Hz, 2H, *ArH*), 7.66 (m, 4H, *ArH*), 7.55 (d, *J* = 7.5 Hz, 2H, *ArH*), 6.33 (s, 2H, -*CH*-), 6.27 (s, 2H, -*CH*-), 3.82 (q, *J* = 6.5 Hz, 2H, -NHCH₂-), 2.05 (t, *J* = 7.0 Hz, 2H, -NHCH₂CH₂-), 1.75 (m, 18H, -CH₂-), 1.11 (t, *J* = 7.5 Hz, 3H, -CH₃).

3.2.3 Analytical HPLC

Analytical HPLC was carried out on a Hewlett Packard 1100 coupled to a UV analyser, set to 250 nm. The data was processed using HP Chemstation software. Separations were performed using a Nucleodur C₁₈ column (4.6 cm × 250 mm, 100 Å, 5 μm), flow rate 1 mL/min, 75:25:0.1 acetonitrile:water:trifluoroacetic acid as mobile phase at 45⁰ C.

3.2.4 LC-MS Method and Parameters

LC was performed using an Agilent 1100 series HPLC equipped with an online degasser, binary pump, autosampler, heated column compartment and diode array detector. MS was performed using an Agilent XCT ion trap MSD mass spectrometer. The mixture of the dithiol building blocks and guest molecule in DMSO was analyzed by injecting 10 μl of the solution onto a Nucleodur C₁₈ column (4.6 cm × 250 mm, 100 Å, 5 μm) using a 75:25:0.1 acetonitrile:water:trifluoroacetic acid mixture as the mobile phase at a flow rate of 1 mL/min. Mass spectra (negative ion mode) were acquired in ultra scan mode using a drying temperature of 350⁰C, a nebuliser pressure of 55.00 psi, a drying gas flow of 121 mL/min, a capillary voltage of 4000 V and an ICC target of 200,000 ions. We tuned for a target mass of 1200 m/z.

3.2.5 Isomer Discrimination of Receptor 8b

Each diastereomer of receptor **8b** was isolated by preparative HPLC and dissolved in 1:1 solvent mixture of 10 mM borate buffer pH 9: acetonitrile (0.1 mg/mL of major or minor isomer). To this solution was added 1 equivalent of dithiol building block **7**. The build up of small amounts of the expected **8a** isomers was monitored with time by HPLC. Separations were achieved by injecting 5 μl of the mixture onto a Nucleodur C₁₈ column (4.6 cm × 250 mm, 100 Å, 5 μm) at 45⁰C using a flow rate 1 mL/min. The following gradient was shown in Table 3.1.

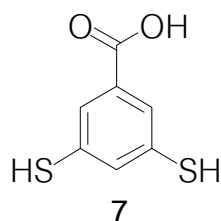


Table 3.1 HPLC Conditions for isomers discrimination of receptor **8b**.

Time (min.)	Acetonitrile +0.1% Trifluoroacetic acid	H ₂ O + 0.1% Trifluoroacetic acid
0	50	50
20	50	50
25	75	25
60	75	25
65	50	50
75	50	50

3.2.6 Isothermal Titration Calorimetry

Isothermal titration calorimetry was performed at 25 °C using a MCS isothermal titration calorimeter (MicroCal, Northampton, MA, USA). All solutions were degassed before titrations. Titrations were performed in 10 mM borate buffer pH 9. The host concentration in the cell was 0.075 mM and the guest (0.75 mM) was titrated in 10 μ L steps using 30 injections spaced at intervals of 200 seconds with a syringe stirring speed at 300 rpm. The binding constants were analyzed by using the one-site binding model using ORIGIN software (version 2.9).

3.2.7 Dynamic Light Scattering Studies

Dynamic light scattering measurements were performed on a Malvern Instruments Zetasizer Nano ZS. Stock solution of receptor **8b** *rac* and guest molecules were filtered through a membrane filter (0.45 μ m) prior to measurements to remove any dust particles.

3.2.8 Transmission Electron Microscopy (TEM)

TEM was conducted on a Philips CM100 electron microscope operating at 80 kV. A 300 mesh carbon-coated copper grid was placed on top of a drop of sample solution (0.1 mg/mL) for 30 minutes and then gently blotted with filter paper. The specimen was negatively stained using a drop of 2% PTA (phosphotungstic acid) pH 7 solution, incubated for 5 minutes, finally gently blotted and dried at room temperature.

3.2.9 Nile Red Solubilisation

Nile red (0.10 mg) was added to 3 mL of a solution of **8b**·**10** in 10 mM borate buffer pH 9 and equilibrated by stirring at room temperature for 2 hours. The solution was filtered through membrane filtered (0.45 μm) before measurements. UV-Vis experiments were carried on a Hewlett Packard 8452A spectrophotometer. Fluorescence experiments were measured on an Aminco-Bowman spectrometer.

3.2.10 NMR Titration : Micelles Formation

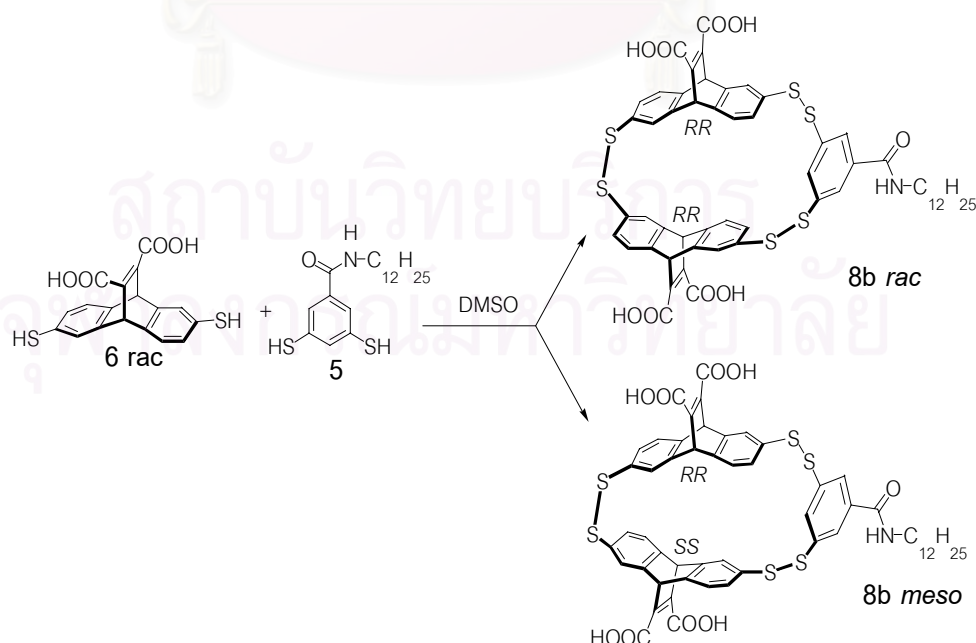
The ^1H NMR titrations are performed by the addition of 10 μL aliquots of the guest **10** (22.6 mM), which corresponds to 0.5 equivalents of receptor **8b** *rac*, to the solution of receptor **8b** *rac* 1.0 mM in D_2O pD 8.7 at 330 K until 4 equivalents of guest **10**.

สถาบันวิทยบริการ
จุฬาลงกรณ์มหาวิทยาลัย

3.3 Results and Discussion

3.3.1 Preparation of Macrocyclic Receptor 8b

In the programmed on dynamic combinatorial chemistry [134,135], Otto and co-workers have developed a number of disulfide-based receptors [140] that bind organic ammonium ions such as guests **9** and **10** with micromolar affinity in water including macrocycle **8a**. We have now produced an amphiphilic version of **8a** by a templated synthesis starting from **5** and previously described **6** [140]. The n-dodecyl building block **5** was prepared in six steps from methyl 3,5-dihydroxybenzoate and dodecylamine. Macrocycle **8b** was generated in one step by mixing the constituent dithiol building blocks and template **9** in DMSO solution, as shown in Scheme 3.8. Due to the low water solubility of **5** precludes the use of aqueous conditions. Using DMSO as solvent as well as oxidizing agent gave the best results. HPLC and LC-MS analysis of the crude product mixture indicated a 95 % conversion into two diastereomers of **8b**: 25% of the minor *meso* isomer (*RR/SS*) and 70% of the major isomer (*RR/RR* and *SS/SS* as a racemic mixture; see Figure 3.3 and 3.4). The major isomer was isolated giving 47% yield by preparative HPLC.



Scheme 3.8 Thiol oxidation to form receptor **8b** as a mixture of stereoisomers.

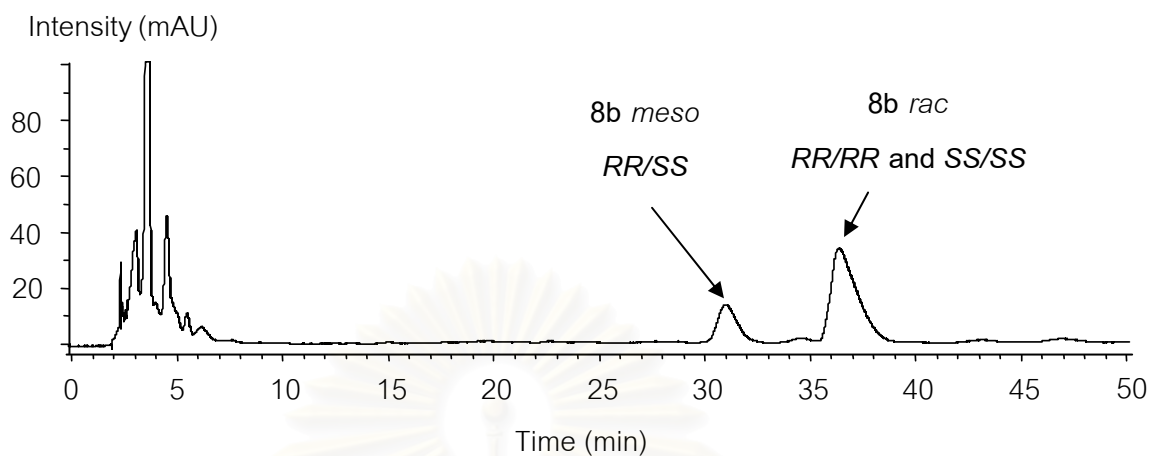


Figure 3.3 HPLC analysis of the solution obtained 24 h after mixing building blocks 6 (6.67 mM), 5 (3.33 mM) and template 9 (10 mM) in DMSO.

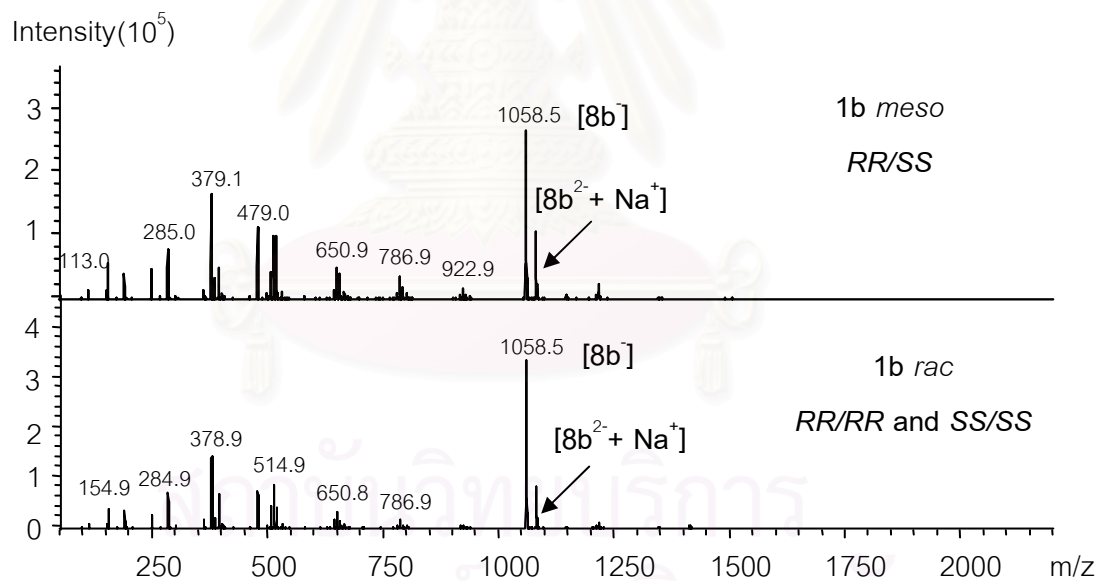
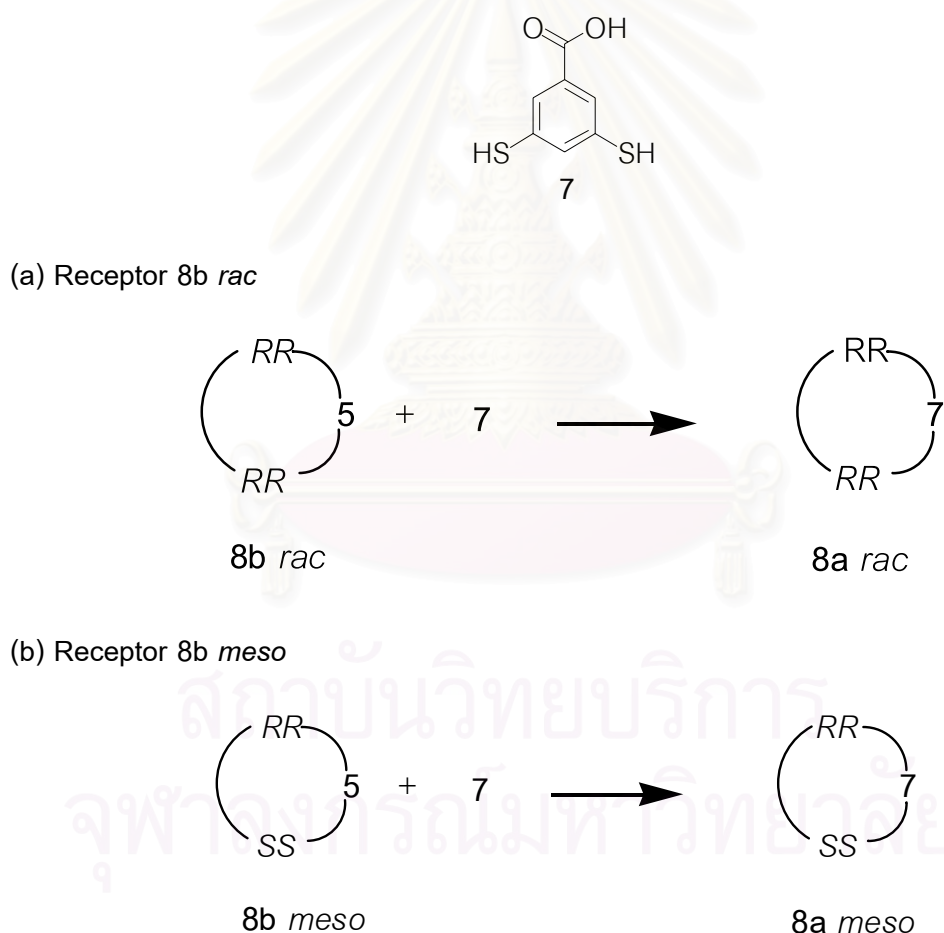


Figure 3.4 A mass spectrum retention time 31 min (top) and 36.5 min (bottom) for receptor **8b meso** and **8b rac**, respectively.

3.3.2 Isomers Discrimination of Receptor 8b

To assign the diastereomers of receptor **8b** (*rac RR/RR* and *SS/SS*, *meso RR/SS*), we have studied the early stages of the re-equilibration of **8b** and its transformation into receptor **8a** of which we have previously assigned the diastereomers [150]. The results were compared with the HPLC analysis of an independently generated mixture made from building blocks **6rac** and building block **7**, which contains all stereoisomers of the building blocks which we have assigned previously (Scheme 3.9 and Figure 3.5).



Scheme 3.9 Correlation between the diastereomers of **8b** with those of **8a** that are formed in the early stages of re-equilibration of receptor **8b** with building block **7**.

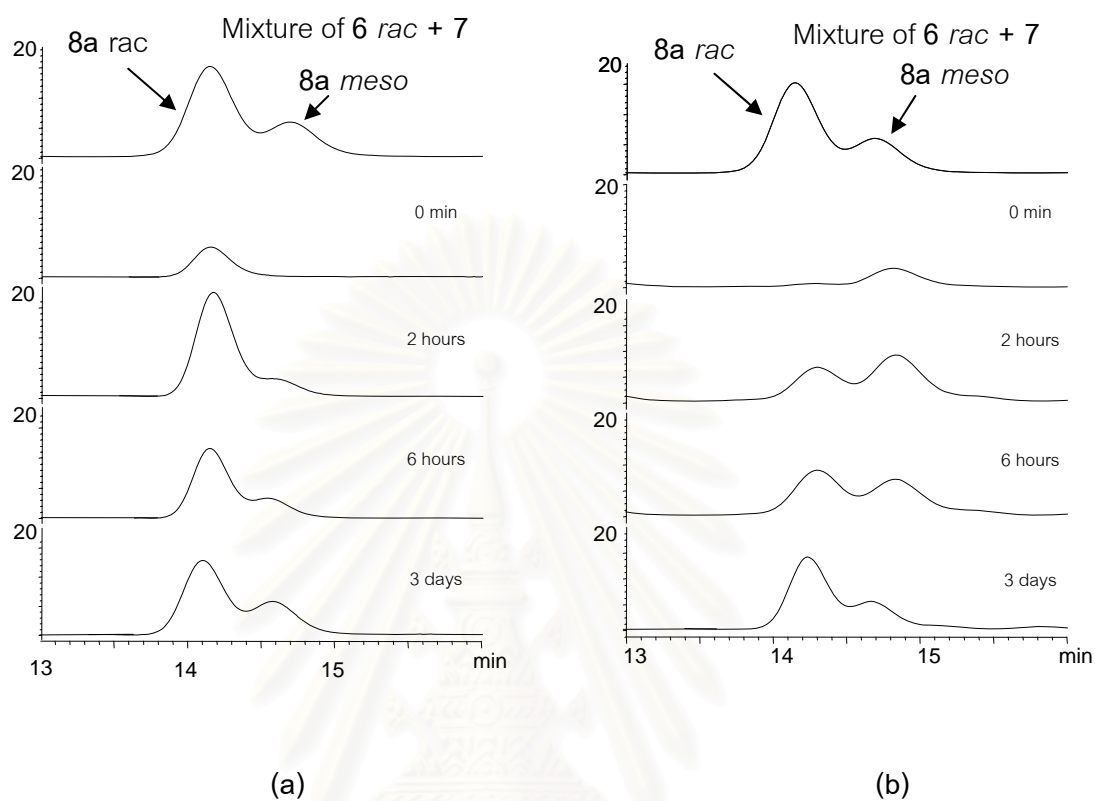


Figure 3.5 HPLC chromatograms of the product mixture obtained upon re-equilibration of (a) receptor **8b** (major *rac* isomer; 0.1 mM) and, (b) receptor **8b** (minor *meso* isomer; 0.1 mM) in the presence of building block **7** (1 equivalent) in H₂O(pH 9):CH₃CN 1:1. The top traces represent the HPLC analysis of an independently generated mixture made from building blocks **6** *rac* and **7**, which contains all stereoisomers of macrocycle **8a** which we have assigned previously.

3.3.3 Binding Studies of Receptor **8b**

We have used isothermal titration calorimetry to study binding behaviors of **8b** with monovalent isoquinolinium guest **9** and monovalent acridizinium guests **10** comparing with water soluble macrocycle **8a**, Figure 3.6. Surprisingly, we failed to detect any binding of **9** in aqueous solutions containing 0.075 mM of **8b**, despite the fact that the same guest binds strongly to **8a** ($K = 2.5 \times 10^5 \text{ M}^{-1}$) as presented in Table 3.2. We were able to measure the binding of **10** to **8b** ($K_{app} = 2.4 \times 10^4 \text{ M}^{-1}$), but also for this guest, binding to **8b** is much less (27 times) efficient than binding to **8a**. Noteworthy, the binding of guests **10** to amphiphilic receptor **8b** are accompanied by a change in aggregate morphology. The apparent binding constant (K_{app}) therefore contains contributions from the interactions between host and guest as well as contributions associated with the reorganization of the aggregates.



Considering the structures of macrocycle **8a** and **8b**, it is possible that the alkyl side chain of **8b** is sitting inside the cavity and inhibiting the binding of isoquinolinium-monovalent guests. Then, we can imagine that the alkyl side chain can be replaced from the cavity by using hydrophobic guest **10**. These observations might be illustrated that the specific hydrophobic interactions play the crucial role of molecular recognition processes.

Table 3.2 Thermodynamic data^(a) for the binding of macrocycles **8a** and **8b** with guest **9** and **10** in 10 mM borate buffer pH 9 at 298 K.

		9	10
8a	$K[M^{-1}]$	$2.3 \times 10^{5(3)}$	$6.4 \times 10^{5(4)}$
	ΔG^0 [kJ/mol]	-30.1	-33.1
	ΔH^0 [kJ/mol]	-40.6	-40.6
	$T\Delta S^0$ [kJ/mol]	-10.5	-7.5
8b	$K_{app}[M^{-1}]$	No binding detectable	2.4×10^4
	ΔG^0 [kJ/mol]		-25.0
	ΔH^0 [kJ/mol]		-8.3
	$T\Delta S^0$ [kJ/mol]		16.7

^(a) Equilibrium constants (K), Gibbs energies (ΔG^0), Enthalpies (ΔH^0) and Entropies ($T\Delta S^0$) of the binding of guests **9** and **10** to macrocycles **8a** and **8b** (major diastereomer) were determined by using isothermal titration microcalorimetry.

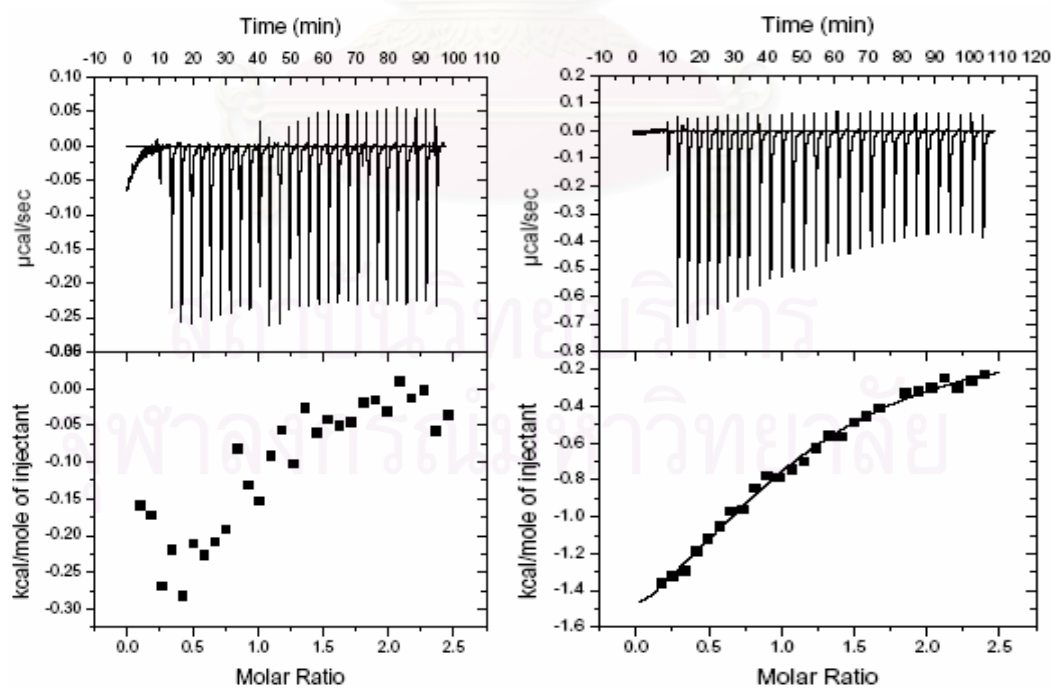


Figure 3.6 Isothermal titration isotherms of receptor **8b** with guest **9** (left) and guest **10** (right) in 10 mM borate buffer pH 9.

3.3.4 Self-Assembly of Amphiphilic Receptor **8b**

The surprising drop in affinity turned out to be a result of the alkyl side chain of **8b** occupying the hydrophobic cavity of the receptor and inhibiting the binding of the guest. This inclusion behaviour was evident from $^1\text{H-NMR}$ spectroscopy (Figure 3.7). The $^1\text{H-NMR}$ of **8b** was recorded in $\text{D}_2\text{O}/\text{CD}_3\text{CN}$ (Figure 3.7a) and in D_2O at pD 8.7 (Figure 3.7a). Comparison of the two spectra showed that in D_2O the protons of the alkyl chain are shifted upfield (up to -1.6 ppm), presumably as a result of the aromatic-ring currents that they experience inside the hydrophobic cavity of **8b**.

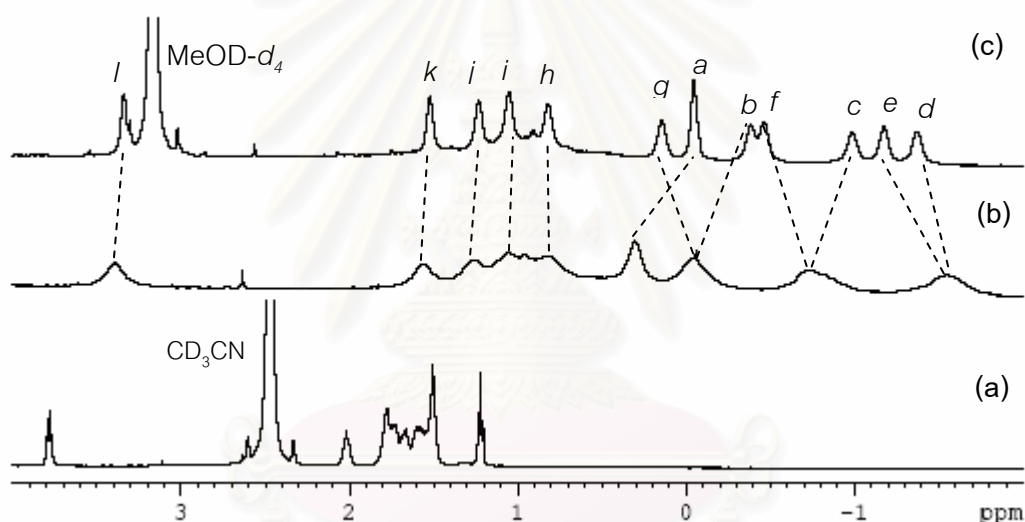


Figure 3.7 Part of the $^1\text{H-NMR}$ spectra of amphiphilic receptor **8b** in (a) $\text{D}_2\text{O}:\text{CD}_3\text{CN}$ 1:1; (b) D_2O (pD 8.7) and (c) D_2O (pD 8.7): $\text{MeOD-}d_4$ 2:1 at room temperature.

Remarkably, we have found that upon addition of CD_3OD (Figure 3.8 or Figure 3.9) at higher temperatures the spectrum sharpened up, and small changes in chemical shifts occurred, which allowed us to observe all 11 methylene groups as separate signals (Figure 3.7c).

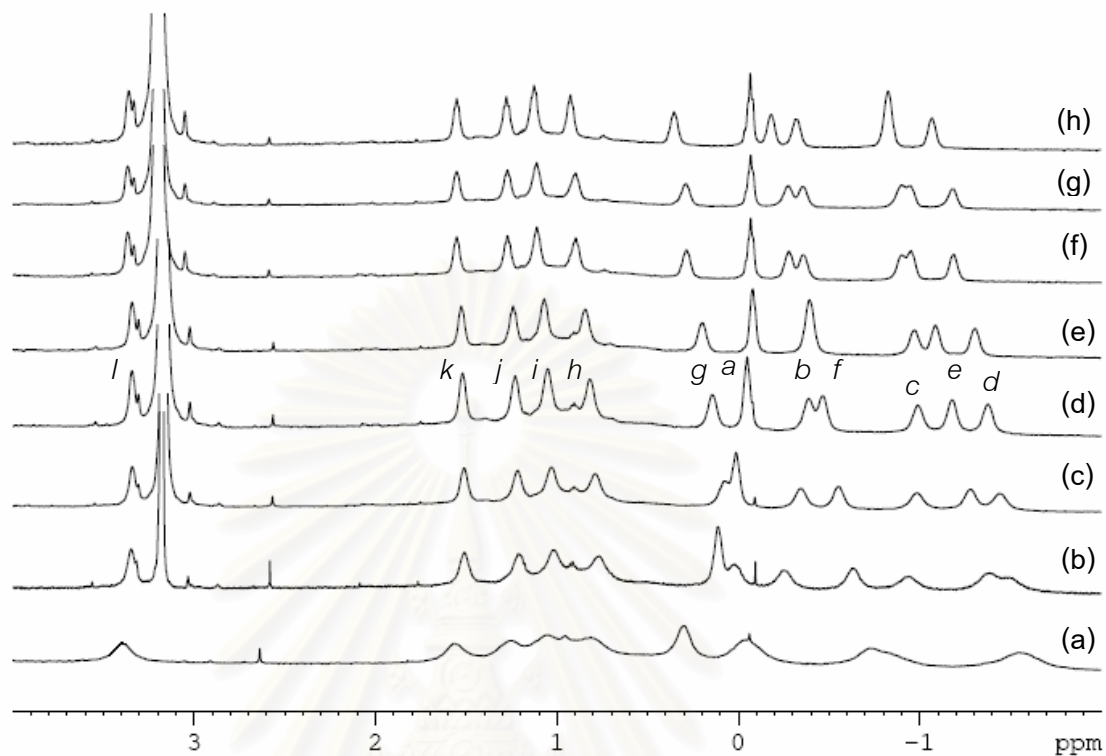


Figure 3.8 Part of the ^1H -NMR titration of $\text{MeOD-}d_4$ into a solution of receptor **8b** *rac* (1 mM in D_2O (pD 8.7)). The volume ratio of D_2O (pD 8.7) to $\text{MeOD-}d_4$ was: (a) 1:0, (b) 1:0.16, (c) 1:0.32, (d) 1:0.5, (e) 1:0.64, (f) 1:0.8, (g) 1:1, and (h) 1:1.16.

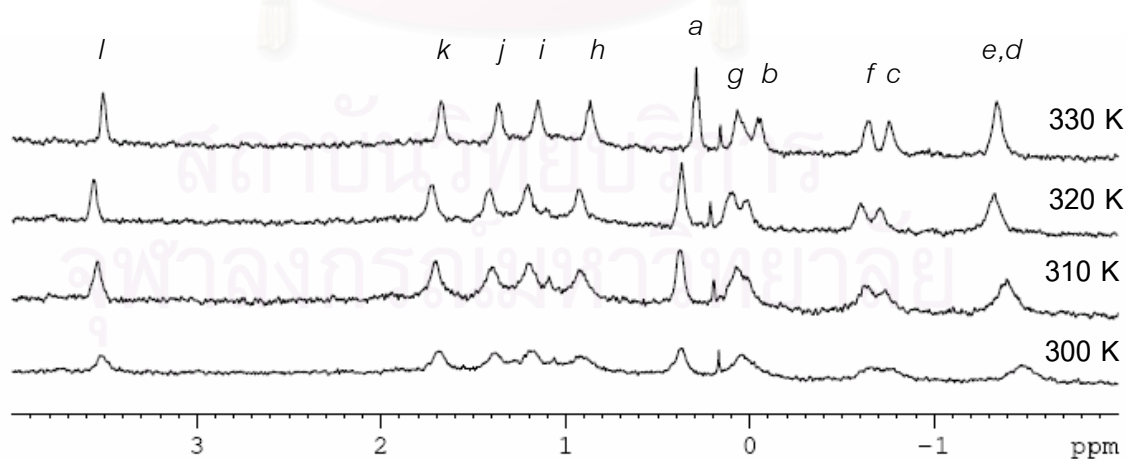


Figure 3.9 Part of the VT- ^1H -NMR of receptor **8b** *rac* 1 mM in D_2O pD 8.7.

A TOCSY spectrum recorded in the presence of methanol enabled us to assign all signals of the alkyl chain. Correlation with the spectrum in D_2O indicated that in this solvent the strongest shifts are experienced by six methylene groups *b-g* (Figure 3.10). It's not surprising, the inclusion behavior of the alkyl side chains of macrocycles have been reported by Petter [151,152] and Binkowski [153].

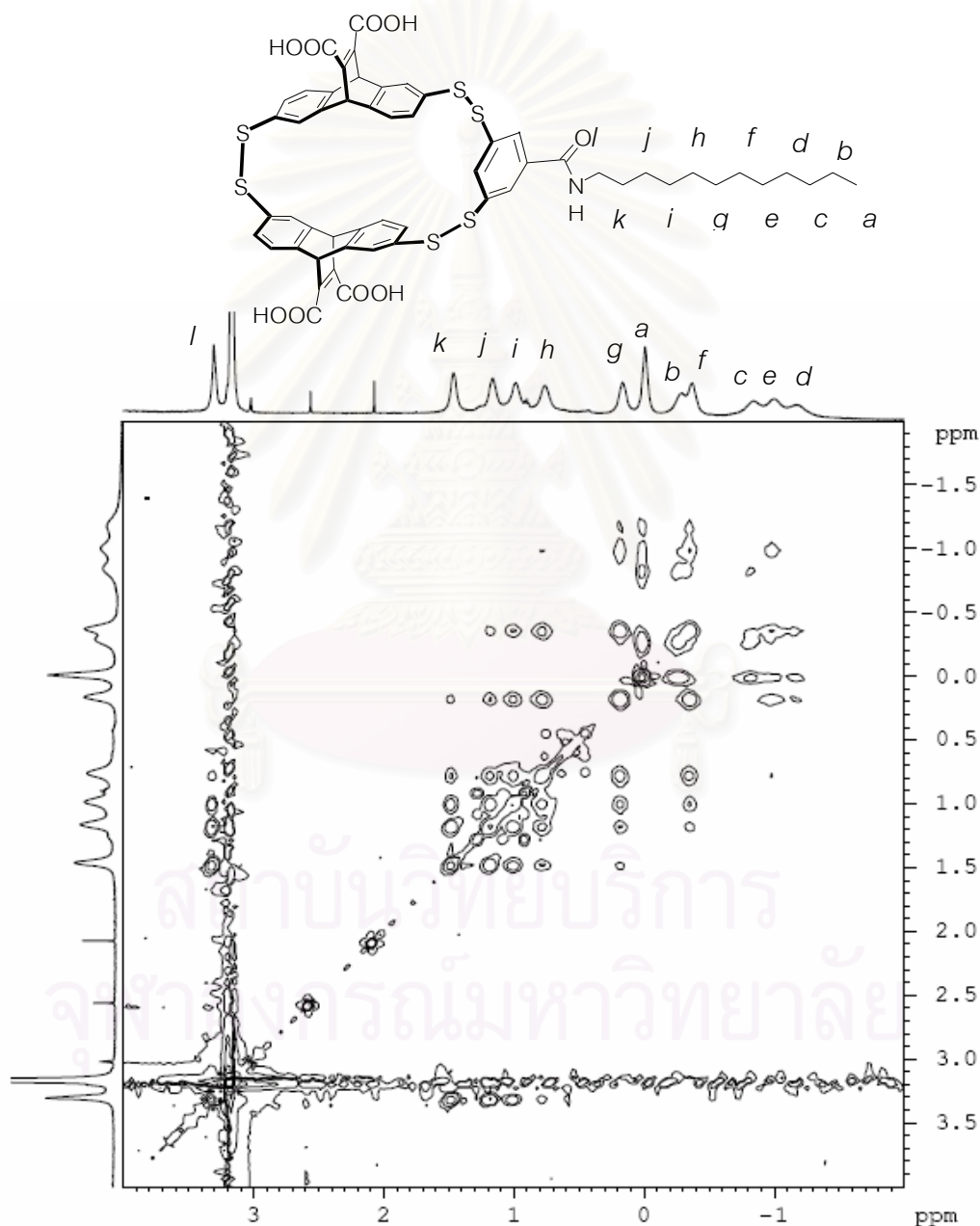


Figure 3.10 Part of the TOCSY NMR spectrum of receptor **8b rac** (0.6 mM in D_2O (pD 8.7) : MeOD- d_4 2:1 ratio).

While significant parts of the alkyl chain of **8b** appear to spend a significant fraction of their time inside the aromatic cavity, the compound nevertheless forms large aggregates in aqueous solution as evident from dynamic light scattering (DLS) and electron microscopy. Analysis of the DLS data of a 0.1 mg/mL solution of **8b** in 10 mM borate buffer pH 9 suggested the presence of aggregates with a diameter around 100 nm. Negative staining transmission electron microscopy showed the well-defined tubular structures (Figure 3.11), having a diameter of 60 nm and lengths ranging from 250 nm to 2.5 μm . (Note : The discrepancy between the results from DLS and electron microscopy is most likely an artifact from the analysis of the DLS data, which is based on the assumption that the aggregates are spherical. Electron microscopy shows this assumption is not valid in this case.) Obviously, these tubular structures come from the packing of inclusion of receptor **8b**.

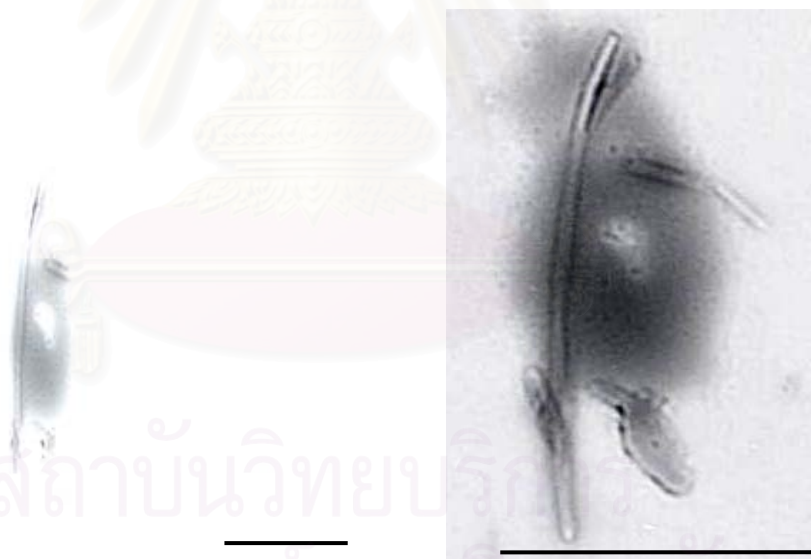


Figure 3.11 Transmission electron micrograph of negatively stained (2% PTA: phosphotungstic acid) assemblies of amphiphilic receptor **8b** (0.1 mg/mL) in 10 mM borate buffer pH 9, scale bar represents 1 μm .

Thus, in the aggregates, the terminus of the alkyl chain of **8b** is included inside the hydrophobic cavity of the macrocycle. One possibility would be that the alkyl chain would loop back into the cavity of the same molecule (Figure 3.12a). Alternatively, the alkyl chain could insert itself into the cavity of a neighboring receptor leading to dimerization (Figure 3.12b) or the formation of 'daisychains' (Figure 3.12c). Discriminating between these arrangements (if indeed a single of these arrangements is preferred) is challenging and experiments in this direction have thus far been inconclusive. However, irrespective of the exact mechanism of inclusion, we speculate that the result will be an arrangement in which the cross-sectional area of the alkyl chain region is effectively doubled, either by looping back (Figure 3.12a and 3.12b) or by interdigitation (Figure 3.12c) of the chains. Such an arrangement is more likely to result in a bilayer-type organization rather than in micelles.

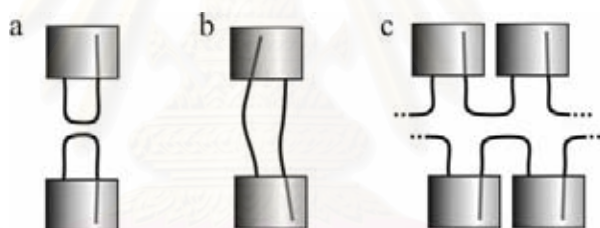
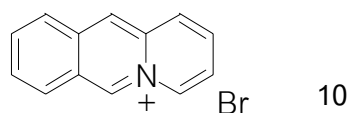


Figure 3.12 Cartoon representations of different modes of inclusion of the alkyl chain in the cavity of **8b**.

3.3.5 Micelles Formation

Our binding data suggests that guest **10** is able to displace the alkyl chain from the cavity of receptor **8b**. This was confirmed by the changes observed in the $^1\text{H-NMR}$ spectrum of the alkyl chain upon titrating with **10** into a solution of **8b** (Figure 3.13). The upfield shifted methylene resonances disappeared and were replaced by resonances at 1-2 ppm, which corresponds to the normal region for the unsubstituted alkanes (cf. Figure 3.7a).



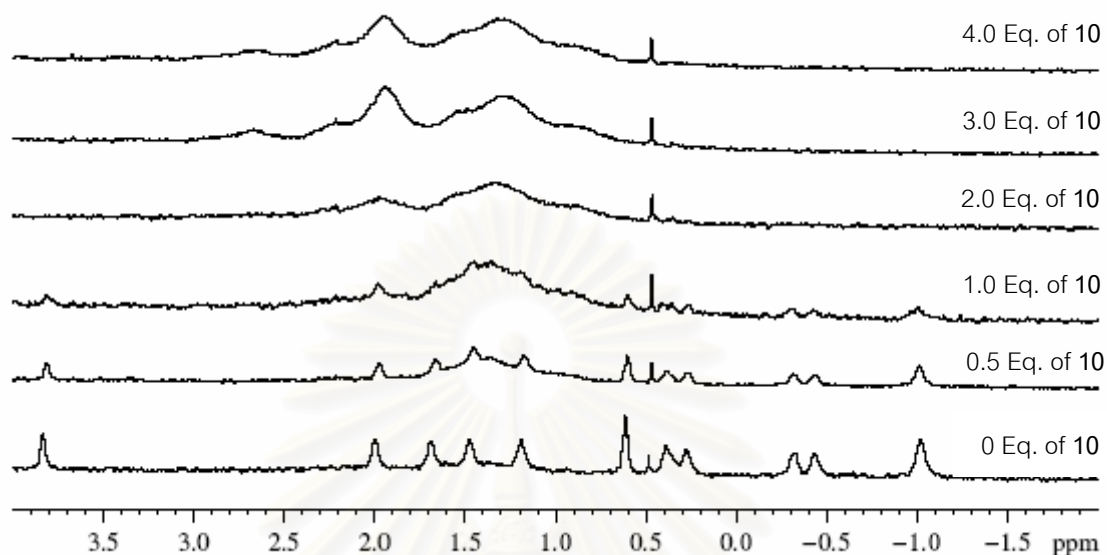
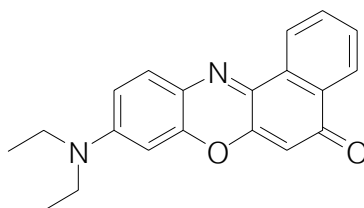


Figure 3.13 Part of the ^1H -NMR spectra of amphiphilic receptor **8b** upon addition guest **10** at 330 K in D_2O pD 8.7.

Analysis of the resulting solution by DLS indicated that after addition of **8b** the size of aggregates was reduced to around 10 nm, which is close to the size expected for micellar aggregates. Further support for a guest-induced transition to micelles was obtained by studying the solubilization of the hydrophobic dye Nile Red **3.23** [154-156]. Because, it has long been known that the dye solubility or dye entrapment, hydrophobic dye, in the micelle core is the one of the important characteristic of micelles.



3.23

Obviously, Figure 3.14(a) shows the absorbance spectrum of a solution of Nile Red ($\lambda_{\text{max}} = 570 \text{ nm}$) in a solution of **8b**, **10** and **8b·10**. The dye is only significantly solubilized in the solution of **8b·10**. This is the strong evidence that the micelles can form in our system. Moreover, we have studied the solubilization of Nile Red as a function of the concentration of **8b·10** in order to determine the critical micelle concentration (cmc). The curve in Figure 3.14 (b) shows the fluorescence intensity of different solutions of **8b·10** which were stirred for 2 hrs in the presence of Nile Red and then filtered to remove unsolubilized dye. The cmc of this system was estimated to be around $35 \mu\text{M}$. The tendency of **8b·10** to form micelles is perhaps not surprising, given that single-chain surfactants generally form micelles as a result of the large polar head group compared with the relatively small single nonpolar tail, giving an overall conically shaped molecule.

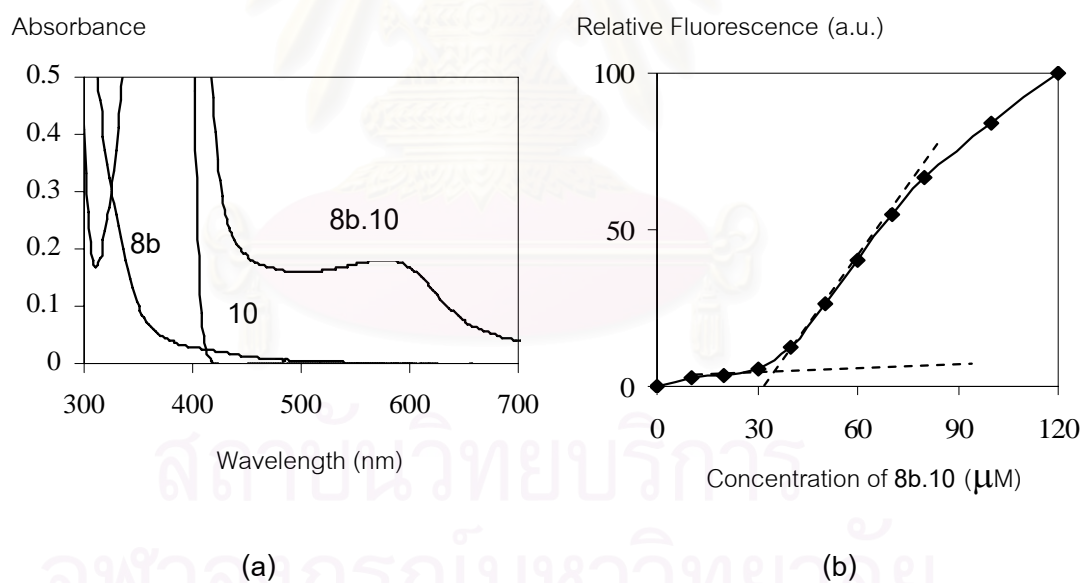


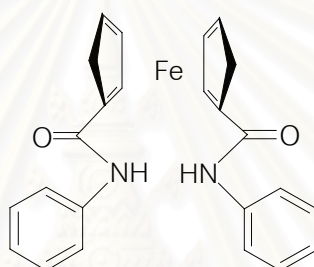
Figure 3.14 (a) Absorption spectra of Nile Red in the solution of 0.1 mM of **8b** in the absence and presence of 0.4 mM of **10**. (b) Emission intensity of different saturated solutions of Nile Red at 640 nm ($\lambda_{\text{ex}} = 570 \text{ nm}$) versus concentration of **8b·10** in 10 mM borate buffer pH 9.

CHAPTER 4

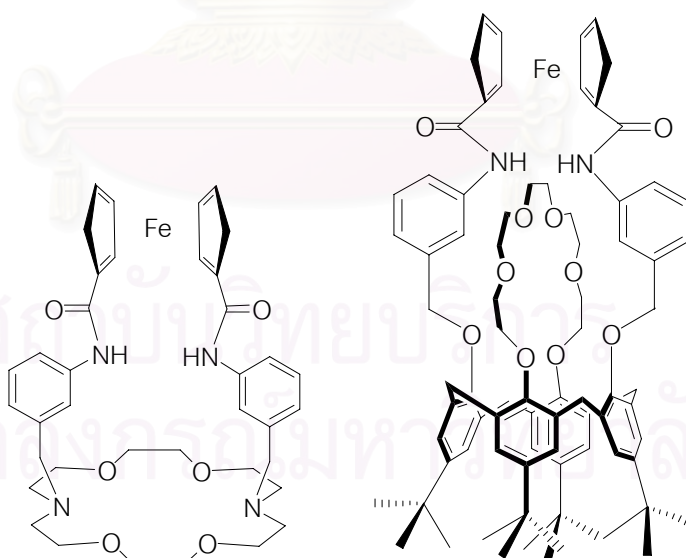
CONCLUSIONS

4.1 Halide Anions Sensing by Heteroditopic Electrochemical Anion Sensors

From the unexpected result, we found that in the solid state structure the monotopic receptor **1** showed the helical structure of polymeric multiple-decker ferrocene complex. In this case we believe that the intramolecular hydrogen bonding interactions between NH amide protons and oxygen carbonyl atoms of the adjacent phenyl side arms are the most important driving force.



1



2d

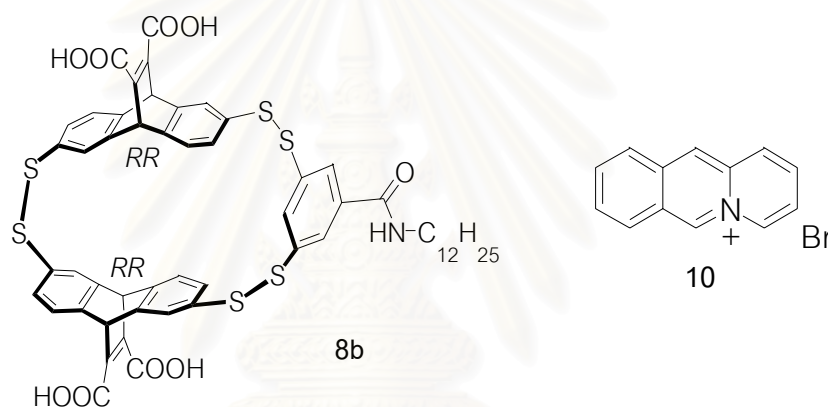
3d

From $^1\text{H-NMR}$ studies, receptor **1** can interact with anions through hydrogen bonding interactions only. Whereas receptors **2d** and **3d** can simultaneously complex the alkali metal salt in the ion-pair fashion in which metal cations are encapsulated in crown ether cavity and anions are hydrogen bonded to amide protons. In addition, the cation complexation induces a structural change that is appropriate for anion complexation which can be confirmed by X-ray crystallography for receptor **2d**. Interestingly, the proposed heteroditopic receptors possessed the highest selectivity for Br^- in the presence of Na^+ , (especially for receptor **2d**). Interestingly, receptor **3d** shows the high selectivity to acetate anion in the presence of Na^+ whereas receptor **2d** is not. From these results we can conclude that, the rigidity and steric hindrance as well as the size of binding cavity of the receptors also have an important effect on the complexation and the recognition properties. Then, the binding constants of the more flexible structure and less steric hindrance of receptor **2d** with spherical halide anions are higher than the more rigid *p-tert-butylcalix[4]arene* structure **3d**. Whereas, only receptor **3d** possessed the high selectivity with Y-shaped acetate anion.

It is noteworthy that even when the association constant between the neutral receptor and the anion is too weak to be measurable, for example in the system of $[\mathbf{2d.M}^+]/\text{Cl}^-$, the redox property can be used to sense anions. In electrochemical sensing process, we have found that in the presence of metal cations the interactions of heteroditopic receptors **2d** and **3d** towards anions, especially with Cl^- and acetate are higher than its free forms. This stemmed from the synergy between the electrostatic interactions between double positive charge (from ferrocenium and metal cation) of co-bound complex and anions and hydrogen bonding interactions between amidoferrocene and the anionic guest. Therefore, both synthetic heteroditopic receptors **2d** and **3d** can act as electrochemical sensors for halide and acetate anions.

4.2 Controlling the Morphology of Aggregates of an Amphiphilic Synthetic Receptor through Host-Guest Interactions

From the knowledge of non-covalent supramolecular chemistry, we have reported a new synthetic amphiphilic receptor **8b** based on a disulfide macrocycle and show how specific host-guest interactions can induce a dramatic change in the morphology of the assemblies formed by this synthetic receptor, from nanotubes in the absence of a guest to much smaller micellar assemblies in the presence of hydrophobic guest **10**.



We have found that in the absence of any guest, amphiphilic receptor **8b** aggregates into nanotubes as a result of the self-inclusion of the alkyl part of the molecule inside the nonpolar cavity of the polar headgroup. While this leads to a reduction in the efficiency with which these receptors bind their guests, complexation of a suitable guest molecule is still achievable. This creates the possibility of controlling aggregate morphology through specific host-guest interactions. Indeed, we have demonstrated that the addition of a guest induces a dramatic change in the morphology of aggregates formed by the amphiphilic receptor. Studies are underway to elaborate on the resulting organized receptor assemblies for the construction of well-defined nanosized objects through noncovalent surface functionalization including the use of multivalent interactions.

4.3 Suggestions for Future Works

From a practical point of view the synthesized heteroditopic electrochemical anion sensors **2d** and **3d** might be incorporated into the suitable amperometric devices. These two compounds will be immobilized the sensors to the electrode surface and use such electrode for determination of chloride anion.



สถาบันวิทยบริการ
จุฬาลงกรณ์มหาวิทยาลัย

REFERENCES

1. Lehn, J.-M. Supramolecular Chemistry. Germany: Federal Republic of Germany, 1995.
2. Steed, J. W.; and Atwood, J. L. Supramolecular Chemistry. England: John Wiley & Sons, Ltd, 2002.
3. Fiedler, D.; Leung, D. H.; Bergman, R. G.; and Raymond, K. N. Selective molecular recognition, C-H bond activation, and catalysis in nanoscale reaction vessels. Acc. Chem. Res. 38 (2005): 349-358.
4. Kang, J.; and Rebek, J., Jr. Acceleration of a Diels–Alder reaction by a self-assembled molecular capsule. Nature 385 (1997): 50-52.
5. Kang, J.; Santamaria, J.; Hilmersson, G.; and Rebek, J., Jr. Self-assembled molecular capsule catalyzes a Diels-Alder reaction. J. Am. Chem. Soc. 120 (1998): 7389-7390.
6. Cram, D. J.; and Cram, J. M. Host-guest chemistry: Complexes between organic compounds simulate the substrate selectivity of enzymes. Science 183 (1974): 803-809.
7. Hartley, J. H.; James, T. D.; and Ward, C. J. Synthetic receptors. J. Chem. Soc., Perkin Trans. 1 (2000):3155-3184.
8. Lavigne, J. L.; and Anslyn, E. V. Sensing a paradigm shift in the field of molecular recognition: From selective to differential receptors. Angew. Chem. Int. Ed. 40 (2001): 3118-3130.
9. Fabbrizzi, L.; and Poggi, A. Sensors and switches from supramolecular chemistry. Chem. Soc. Rev. 23 (1995): 197-202.
10. Gawley, R. E.; Pinet, S.; Cardona, C. M.; and Leblanc, R. M. Chemosensors for the marine toxin saxitoxin. J. Am. Chem. Soc. 124 (2002): 13448-13453.
11. Beer, P. D.; Hopkins, P. K.; and McKinney, J. D. Cooperative halide, perchlorate anion-sodium cation binding and pertechnetate extraction and transport by a novel tripodal tris(amido benzo-15-crown-5) ligand. Chem. Commun. (1999): 1253-1254.

12. Trapani, G.; Laquintana, V.; Latrofa, A.; Ma, J.; Reed, K.; Serra, M.; Biggio, G.; Liso, G.; and Gallo, J. M. Peripheral benzodiazepine receptor ligand-Mmelphalan conjugates for potential selective drug delivery to brain tumors Bioconjugate Chem. 14 (2003): 830-839.
13. Fages, F.; Desvergne, J.-P.; and Bouas-Laurent, H. Synthesis, structural, spectroscopic, and alkali-metal cations complexation studies of a bis-anthracenediyl macrotricyclic ditopic receptor. J. Org. Chem. 59 (1994): 5264-5271.
14. Prez-Inestrosa, E.; Desvergne, J.-P.; Bouas-Laurent, H.; Rayez, J.-C.; Rayez, M.-T.; Cotrait, M.; and Marsau, P. Barium cation complexation by flexible mono- and ditopic receptors, studied by UV absorption and fluorescence spectroscopy. Eur. J. Org. Chem. (2002): 331-334.
15. Arduini, A.; Brindani, E.; Giorgi, G.; Pochini, A.; and Secchi, A. Recognition of guests bearing donor and receptor hydrogen bonding groups by heteroditopic calix[4]arene receptors. Tetrahedron 59 (2003): 7587-7594.
16. Pelizzi, N.; Casnati, A.; Friggeri, A.; and Ungaro, R. Synthesis and properties of new calixarene-based ditopic receptors for the simultaneous complexation of cations and carboxylate anions. J. Chem. Soc. Perkin Trans.2 (1998): 1307-1311.
17. Amendola, V.; Esteban-Gómez, D.; Fabbrizzi, L.; Licchelli, M.; Monzani, E.; and Sancenón, F. Metal-enhanced H-bond donor tendencies of urea and thiourea toward anions: ditopic receptors for silver(I) salts. Inorg. Chem. 44 (2005): 8690-8698.
18. Lankshear, M. D.; Cowley, A. R.; and Beer, P. D. Cooperative AND receptor for ion-pairs. Chem. Commun. (2006): 612-614.
19. Koskela, S. J. M.; Fyles, T. M.; and James, T. D. A ditopic fluorescence sensor for potassium fluoride. Chem. Commun. (2005): 945-947.
20. Otón, F.; Tárraga, A.; Velasco, M. D.; and Molina, P. A ferrocene-based heteroditopic ligand for electrochemical sensing of cations and anions. Chem. Commun. (2005): 1159-1161.

21. Lehn, J.-M. Toward complex matter: Supramolecular chemistry and self-organization. Proc. Natl. Acad. Sci. USA 99 (2002): 4763-4768.
22. Whitesides, G. M.; Mathias J. P.; and Seto, C. T. Molecular self-assembly and nanochemistry: a chemical strategy for the synthesis of nanostructures. Science 254 (1991): 1312-1319.
23. Tecilla, P.; Dixon, R. P.; Slobodkin, G.; Alavi, D. S.; Waldeck, D. H.; and Hamilton, A. D. Hydrogen-bonding self-assembly of multichromophore structures. J. Am. Chem. Soc. 112 (1990): 9408-9410.
24. Kunitake, T. Synthetic bilayer membranes: Molecular design, self-organization, and application. Angew. Chem. Int. Ed. Engl. 31 (1992): 709-726.
25. Johnsson, M.; Wagenaar, A.; and Engberts, J. F. B. N. Sugar-based gemini surfactant with a vesicle-to-micelle transition at acidic pH and a reversible vesicle flocculation near neutral pH. J. Am. Chem. Soc. 125 (2003): 757-760.
26. Hu, Z. J.; Jonas, A. M.; Varshney, S. K.; and Gohy, J. F. Dilution-induced spheres-to-vesicles morphological transition in micelles from block copolymer/surfactant complexes. J. Am. Chem. Soc. 127 (2005): 6526-6527.
27. Yin, H.; Huang, J.; Lin, Zhang, Y.; Qiu, S.; and Ye, J. Heating-induced micelle to vesicle transition in the cationic-anionic surfactant systems: Comprehensive study and understanding. J. Phys. Chem. B 109 (2005): 4104-4110.
28. Beer, P. D.; and Gale, P. A. Anion recognition and sensing: The state of the art and future perspectives. Angew. Chem. Int. Ed. 40 (2001): 486-516.
29. Bowman-James, K. Alfred Werner revisited: The coordination chemistry of anions. Acc. Chem. Res. 38 (2005): 671-678.
30. Schmidtchen, F. P.; and Berger, M. Artificial organic host molecules for anions. Chem. Rev. 97 (1997): 1609-1646.
31. Gale, P. A. Anion coordination and anion-directed assembly: highlights from 1997 and 1998. Coord. Chem. Rev. 199 (2000): 181-233.
32. Gale, P. A. Anion receptor chemistry: highlights from 1999. Coord. Chem. Rev. 213 (2001): 79-128.

33. Fitzmaurice, R. J.; Kyne, G. M.; Douheret, D.; and Kilburn, J. D. Synthetic receptors for carboxylic acids and carboxylates. J. Chem. Soc., Perkin Trans. 1, 7 (2002): 841-864.
34. Llinares, J. M.; Powell, D.; and Bowman-James, K. Ammonium based anion receptor. Coord. Chem. Rev. 240 (2003): 57-75.
35. Linton, B.; and Hamilton, A. D. Formation of artificial receptors by metal-templated self-assembly. Chem. Rev. 97 (1997): 1669-1680.
36. Bondy, C. R.; and Loeb, S. J. Amide based receptors for anions. Coord. Chem. Rev. 240 (2003): 77-99.
37. Sessler, J. L.; Camiolo, S.; and gale, P. A. Pyrrolic and polypyrrolic anion binding agents Coord. Chem. Rev. 240 (2003): 17-55.
38. Park C. H.; and Simmons, H. E. Macrobicyclic amines. III. Encapsulation of halide ions by in,in-1,(k + 2)-diazabicyclo[k.l.m.]alkane ammonium ions. J. Am. Chem. Soc. 90 (1968): 2431-2432.
39. Kavallieratos, K.; Bertao, C. M.; and Crabtree, R. H. Hydrogen bonding in anion recognition: A family of versatile, nonpreorganized neutral and acyclic receptors. J. Org. Chem. 64 (1999): 1675-1683.
40. Niikura, K.; Bisson, A. P.; and Anslyn, E.V. Optical sensing of inorganic anions employing a synthetic receptor and ionic colorimetric dyes. J. Chem. Soc. Perkins Trans. 2 (1999): 1111-1114.
41. Metzger, A.; and Anslyn, E. V. A chemosensor for citrate in beverages. Angew. Chem. Int. Ed. 37 (1998): 649-652.
42. Lazzarotto, M.; Sansone, F.; Baldini, L.; Casnati, A.; Cozzini, P.; and Ungaro, R. Synthesis and properties of upper rim C-linked peptidocalix[4]arenes. Eur. J. Org. Chem. 2001 (2001): 595-602.
43. Sansone, F.; Baldini, L.; Casnati, A.; Lazzarotto, M.; Ugozzoli, F.; and Ungaro, R. Supramolecular Chemistry And Self-assembly Special Feature: Biomimetic macrocyclic receptors for carboxylate anion recognition based on C-linked peptidocalix[4]arenes. Proc. Natl. acad. Sci. USA 99 (2002): 4842-4847.

44. Camiolo, S.; Gale, P.A.; Hursthouse, M. B. and Light, M. E. Nitrophenyl derivatives of pyrrole 2,5-diamides: Structural behaviour, anion binding and colour change signalled deprotonation. Org. Biomol. Chem. 1 (2003): 741-744.
45. El Drubi Vega, I.; Gale, P. A.; Hursthouse, M. B. and Light, M. E. Anion binding properties of 5,5'-dicarboxamido-dipyrrolylmethanes. Org. Biomol. Chem. 2 (2004): 2935-2941.
46. Camiolo, S.; Gale, P. A.; Hursthouse, M. B.; Light, M. E. and Shi, A. J. Solution and solid-state studies of 3,4-dichloro-2,5-diamidopyrroles: formation of an unusual anionic narcissistic dimer. Chem. Commun. (2002): 758-759.
47. Gale, P. A.; Camiolo, S.; Tizzard, G. J.; Chapman, C. P.; Light, M. E.; Coles, S. J. and Hursthouse, M. B. 2-Amidopyrroles and 2,5-diamidopyrroles as simple anion binding agents. J. Org. Chem. 66 (2001): 7849-7853.
48. Camiolo, S.; Gale, P. A.; Hursthouse, M. B. and Light, M. E. Confirmation of a 'cleft-mode' of binding in a 2,5-diamidopyrrole anion receptor in the solid state. Tetrahedron Lett. 43 (2002): 6995-6996.
49. Sessler, J. L.; Cho, W.-S.; Gross, D. E.; Shriver, J. A.; Lynch, V. M. and Marquez, M. Anion binding studies of fluorinated expanded calixpyrroles. J. Org. Chem. 70 (2005): 5982-5986.
50. Sessler, J. L.; Jayawickramarajah, J.; Gouloumis, A.; Torres, T.; Guldi, D. M.; Maldonado, S.; and Stevenson, K. J. Synthesis and photophysics of a porphyrin–fullerene dyad assembled through Watson–Crick hydrogen bonding. Chem. Commun. (2005): 1892-1894.
51. Lee, C.-H.; Lee, J.-S.; Na, H.-K.; Yoon, D.-W.; Miyaji, H.; Cho, W.-S. and Sessler, J. L. Cis- and trans-strapped calix[4]pyrroles bearing phthalamide linkers: synthesis and anion-binding properties. J. Org. Chem. 70 (2005): 2067-2074.
52. Kubik, S.; Goddard, R.; Kirchner, R.; Nolting, D.; and Seidel, J. A cyclic hexapeptide containing L-proline and 6-aminopicolinic acid subunits binds anions in water. Angew. Chem. Int. Ed. 40 (2001): 2648-2651.

53. Otto, S.; and Kubik, S. Dynamic combinatorial optimization of a neutral receptor that binds inorganic anions in aqueous solution. J. Am. Chem. Soc. 125 (2003): 7804-7805.
54. Kubik, S.; Goddard, R.; Otto, S.; Pohl, S.; Reyheller, C. and Stowe, S. Optimization of the binding properties of a synthetic anion receptor using rational and combinatorial strategies" Biosensors Bioelectronics. 20 (2005): 2364-2375.
55. Suksai, C.; and Tuntulani, T. Chromogenic anion sensors. Chem. Soc. Rev. 32 (2003): 192-202.
56. Suksai, C.; and Tuntulani, T. Chromogenic anion sensors. Top. Curr. Chem. 255 (2005): 163-198.
57. Martinez-Manez, R.; and Sancenon, F. Fluorogenic and chromogenic chemosensors and reagents for Anions. Chem. Rev. 103 (2003): 4419-4476.
58. Beer, P. D. Redox responsive macrocyclic receptor molecules containing transition metal redox centers. Chem. Soc. Rev. 18 (1989): 409-450.
59. Snowden, T. S.; and Anslyn, E. V. Anion recognition: Synthetic receptors for anions and their application in sensors. Current Opinion in Chemical Biology. 3 (1999): 740-746.
60. Kato, R.; Nishizawa, S.; Hayashita, T. and Teramae, N. A thiourea-based chromoionophore for selective binding and sensing of acetate. Tetrahedron Lett. 42 (2001): 5053-5056.
61. Piatek, P.; and Jurczak, A selective colorimetric anion sensor based on an amide group containing macrocycle. J. Chem. Commun. (2002): 2450-2451.
62. Beer, P. D.; Drew, M. G. B.; Graydon, A. R.; Smith, D. K.; and Stokes, S. E. Quantitative and Structural investigations of hydrogen-bonding interactions in anion binding of mono- and 1,1'-bis-substituted aryl cobaltocenium receptors. J. Chem. Soc. Dalton Trans. (1995): 403-408.

63. Beer, P. D.; Heseck, D.; Kingston, J. E.; Smith, D. K.; Stokes, S. E. Anion recognition by redox-responsive ditopic bis-cobaltocenium receptor molecules including a novel calix[4]arene derivative that binds a dicarboxylate dianion. Organometallics 14 (1995): 3288-3295.
64. Nielsen, K. A.; Cho, W.-S.; Lyskawa, J.; Levilain, E.; Lynch, V. M.; Sessler, J. L.; Jeppesen, J. O. Tetrathiafulvalene-calix[4]pyrroles: Synthesis, anion binding, and electrochemical properties. J. Am. Chem. Soc. 128 (2006): 2444-2451.
65. Brooks, S. J.; Birkin, P. R.; and Gale, P. A. Electrochemical measurements of switchable hydrogen bonding in an anthraquinone-based anion receptor. Electrochemistry Communications 7 (2005): 1351-1356.
66. Togni, A.; and Hayashi, T. Ferrocenes. New York: VCH Publishers, 1995.
67. Plenio, H.; and Diodone, R. Complexation of Na^+ in redox-active ferrocene crown ethers, a structural investigation, and an unexpected case of Li^+ selectivity. Inorg. Chem. 34 (1995): 3964-3972.
68. Medina, J. C.; Goodnow, T. T.; Bott, S.; Atwood, J. L.; Kaifer, A. E.; and Gokel, G. W. Ferrocenyldimethyl-[2.2]-cryptand: Solid state structure of the external hydrate and alkali and alkali-earth-dependent electrochemical behaviour. J. Chem. Soc., Chem. Commun. (1991): 290-292.
69. Chen, Z.; Pilgrim, A. J.; and Beer, P. D. Novel voltammetric responses of a 1,1'-ferrocene bis(methyleneaza-18-crown-6) receptor to group 1 and 2 metal cations in acetonitrile. J. Electroanal. Chem. 444 (1998): 209-217.
70. Doorn, A. R. V.; Bos, M.; Harkema, S.; Eerden, J. V.; Verboom, W.; and Reinhoudt, D. N. Novel ferrocene receptors for barbiturates and ureas. Chem. Commun. (2001): 555-556.
71. Carr, J. D.; Lambert, L.; Hibbs, D. E.; Hursthouse, M. B.; Malik, K. M. A.; and Tucker, J. H. R. Novel electrochemical sensors for neutral molecules. Chem. Commun. (1997): 1649-1650.
72. Beer, P. D.; and Cadman, J. Electrochemical and optical sensing of anions by transition metal based receptors. Coord. Chem. Rev. 205 (2000): 131-155.

73. Beer, P. D.; and Hayes, E. J. Transition metal and organometallics anion complexation agents. Coord. Chem. Rev. 240 (2003): 167-189.
74. Tomapatanaget, B.; Tuntulani, T.; and Chailapakul, O. Calix[4]arenes containing ferrocene amide as carboxylate anion receptors and sensors. Org. Lett. 5 (2003): 1539-1542.
75. Scheerder, J.; van Duynhoven, J. P. M.; Engbersen, J. F. J.; Reinhoudt, D. N. Solubilization of NaX salts in chloroform by bifunctional receptors. Angew. Chem. Int. Ed. Engl. 35 (1996): 1090-1093.
76. Macchioni, A. Ion pairing in transition-metal organometallic chemistry Chem. Rev. 105 (2005): 2039-2074.
77. Davilleva, M. G.; Lü, J.-M.; Lindeman, S. V.; and Kochi, J. K. Crystallographic distinction between "contact" and "separated" ion pairs: Structural effects on electronic/ESR spectra of alkali-metal nitrobenzenides. J. Am. Chem. Soc. 126 (2004): 4557-4565.
78. Sasaki, S.-I.; Hashizume, A.; Citterio, D.; Fujii, E.; and Suzuki, K. Fluororeceptor for zwitterionic form amino acids in aqueous methanol solution. Tetrahedron Lett. 43 (2002): 7243-7245.
79. Gale, P.A. Anion and ion-pair receptor chemistry: highlights from 2000 and 2001. Coord. Chem. Rev. 240 (2003): 191-221.
80. Deetz, M. J.; Shang, M.; and Smith, B. D. A macrocyclic receptor with versatile recognition properties: Simultaneous binding of an ion pair and selective complexation of dimethylsulfoxide. J. Am. Chem. Soc. 122 (2000): 6201-6207.
81. Robertson, A.; and Shinko, S. Cooperative binding in selective sensors, catalyst and actuators. Coord. Chem. Rev. 205 (2000): 157-199.
82. Mahoney, J. M.; Nawaratna, G. U.; Beatty, A. M.; Duggan, P. J.; and Smith, B. D. Transport of alkali halides through a lipid organic membrane containing a ditopic salt-building receptor. Inorg. Chem. 43 (2004): 5902-5907.

83. Mahoney, J. M.; Marshall, R. A.; Beatty, A. M.; Smith, B. D.; Camiolo, S.; and Gale, P. A. Complexation of alkali chloride contact ion-pairs using a 2,5-diamidopyrrole crown macrobicyclic. J. Supramolecular Chem. 1 (2001): 289-292.
84. Custelcean, R.; delmau, L. H.; Moyer, B. A.; Sessler, J. L.; Cho, W.-S.; Gross, D.; Bates, G. W.; Brooks, S. J.; Light, M. E.; and Gale, P. A. Calix[4]pyrrole: An old yet new ion-pair receptor. Angew. Chem. Int. Ed. 44 (2005): 2537-2542.
85. Miyaji, H.; Collinson, S. R.; Prokeš, I.; and Tucker, J. H. R. A ditopic ferrocene receptor for anions and cations that functions as a chromogenic molecular switch. Chem. Commun. (2003): 64-65.
86. Altomare, A.; Burla, M. C.; Camalli, M.; Cascarano, G. L.; Giacovazzo, C.; Guagliardi, A.; Moliterni, A. G. G.; and Spagna, R. SIR-97. J. Appl. Cryst. 32 (1999): 115-119.
87. Sheldrick, G. M. SHELXL-97. A program for the refinement of crystal structures: Universität Göttingen, Germany. 1997.
88. C. David Gutsche, C. D.; and Bauer, L. J. Calixarenes. 13. The conformational properties of calix[4]arenes, calix[6]arenes, calix[8]arenes, and oxacalixarenes. J. Am. Chem. Soc. 107 (1985): 6052-6059.
89. Knobloch, F. W.; and Rauscher, W. H. Condensation polymers of ferrocene derivatives. J. Polymer Sci. 54 (1961): 651-656.
90. Suksai, C.; Jennigs, C.; Kongsaree, P.; and T. Tuntulani. To be submitted.
91. Dinnebier, R. E.; Behrens, U. and Olbrich, F. Solid state structures of cyclopentadienyllithium, -sodium, and -potassium. Determination by high-resolution powder diffraction. Organometallics 16 (1997): 3855-3858.
92. Nagao, S.; Kato, A.; and Nakajima, A. Multiple-decker sandwich poly-ferrocene clusters. J. Am. Chem. Soc. 122 (2000): 4221-4222.
93. Crespo, O.; Gimeno, C. G.; Jones, P. G.; Laguna, A.; and Sarroca, C. A double sandwich silver(I) polymer with 1,1'-bis(diethyldithiocarbamate)-ferrocene. Chem. Commun. (1998): 1481-1482.

94. Scholz, S.; Green, J. C.; Lerner, H.-W.; Bolte, M.; and Wagner, M. A novel multidecker sandwich complex from the reaction of ferrocene with GaCl₃. Chem. Commun. (2002): 36-37.
95. Ilkechi, A. H.; Scheibitz, M.; Bolte, M.; lerner, H.-W.; Wagner, M. On the way to ferrocene-based multiple-decker sandwich complexes. Polyhedron 23 (2004): 2597-2604.
96. Bucher, C.; Devillers, C. H.; Moutet, J.-C.; Pécaut, J.; royal, G.; Saint-Aman, E.; and Thomas, F. Calix[4]phyrin based redox architectures: towards new molecular tools for electrochemical sensing. Dalton Trans. 22 (2005): 3620-3631.
97. Aravinda, S.; Shamala, N.; Das, C.; Sriranjini, A.; Karle, I. L.; Balaram, P. Aromatic-aromatic interactions in crystal structures of helical peptide scaffolds containing projecting phenylalanine residues. J. Am. Chem. Soc. 125 (2003): 5308-5315.
98. Ghidini, E.; Ugozzoli, F.; Ungaro, R.; Harkeme, S.; Abu El-Fadl, A.; and Reinhoudt, D. N. Complexation of alkali metal cations by conformationally rigid, stereoisomeric calix[4]arene crown ethers: a quantitative evaluation of preorganization. J. Am. Chem. Soc. 112 (1990): 6979-6985.
99. Zhou, H.; Surowiec, K. Purkiss, D. W.; and Bartsch, R. A. Proton di-ionizable *p*-*tert*-butylcalix[4]arene-crown-6 compounds in cone, partial-cone and 1,3-alternate conformations: synthesis and alkaline earth metal cation extraction. Org. Biomol. Chem. 3 (2005): 1676-1684.
100. Macomber, R. S. An introduction to NMR titration for studying rapid reversible complexation. J. Chem. Edu. 69 (1992): 375-377.
101. Lockhart, J. C.; Robson, A. C.; Thompson, M. E.; Tyson, P. D. and Wallace, I. H. M. Ligands for the alkali metals. Part 4. Nuclear magnetic resonance of crown ethers with alkali metal ions. J. Chem. Soc. Dalton Trans. (1978): 611-617.
102. Shriver, D. F.; and Atkins, P. W. Inorganic Chemistry. English: Oxford University Press, 1994.

103. Hynes, M. J. EQNMR: a computer program for the calculation of stability constants from nuclear magnetic resonance chemical shift data. J. Chem. Soc., Dalton Trans. (1993), 311–312.
104. Beer, P. D.; Drew, M. G. B.; Graydon, A. R.; Smith, D. K.; and Stokes, S. E. Quantitative and structural investigations of hydrogen-bonding interactions in anion binding of mono- and 1,1'-bis-substituted aryl cobaltocenium receptors. J. Chem. Soc. Dalton Trans. (1995): 403-408.
105. Al-Sayah, M. H.; and Branda, N. R. Protons as the triggers to regulate hydrogen-bonding receptors. Org. Lett. 4 (2002): 881-884.
106. Tumchareon, G.; Tuntulani, T.; Coles, S. J.; Hursthouse, M. B.; and Kilburn, J. D. A novel ditopic receptor and reversal of anion binding selectivity in the presence and absence of bound cation. Org. Lett. 5 (2003): 4971-4974
107. Beer, P. D.; Heseck, D.; and Nam, K. C. Anion recognition properties of new upper-rim cobaltocenium calix[4]arene receptors. Organometallics 18 (1999): 3933-3943.
108. Suksai, C.; Leeladee, P.; Jainuknan, D.; Tuntulani, T.; Muangsin, N.; Chailapakul, O.; Kongsaree, P.; and Pakawatchai, C. A new heteroditopic receptor and sensor highly selective for bromide in the presence of a bound cation. Tetrahedron Lett. 46 (2005): 2765-2769.
109. Wells, A. F. Structural Inorganic Chemistry. England: Oxford University Press, 1984.
110. Mahoney, J. M.; Beatty, A. M.; and Smith, B. D. Selective recognition of an alkali halide contact ion-pair. J. Am. Chem. Soc. 123 (2001): 5847-5848.
111. Chen, Z.; Pilgrim, A. J.; and Beer, P. D. Novel voltammetric responses of a 1,1'-ferrocene bis(methylene aza-18-crown-6) receptor to group 1 and 2 metal cations in acetonitrile. J. Electroanal. Chem. 444 (1998): 209-217.
112. Lindsay, J. R. L.; and Masheder, D. Amine oxidation. Part IX. The electrochemical oxidation of some tertiary amines: the effect of structure on reactivity J. Chem. Soc., Perkin Trans. 2. (1976): 47 - 51

113. Deinhammer, R. S.; Ho, M.; Anderegg, J. W.; and Porter, M. D. Electrochemical oxidation of amine-containing compounds; A route to the surface modification of glassy carbon electrodes. Langmuir. 10 (1994): 1306-1313.
114. Hathoot, A. A. Electrochemical behavior of poly 8-(3-acetylrimino-6-methyl-2,4-dioxopyran)-1-aminonaphthaline in aqueous and non aqueous media. Bull. Korean. Chem. Soc. 24 (2003): 1609-1612.
115. Jin, S.; Jin, X.; Wang, D.; Cheng, G.; Peng, L.; and Chen, G. Z. Voltammetric studies of through-space and through-bond electrostatic interactions in alkyl linked ferrocene and benzoaza-15-crown-5 receptor molecules in acetonitrile. J. Phys. Chem. B 109 (2005): 10658-10667.
116. Beer, P. D.; Gale, P. A.; and Chen, G. Z. Mechanisms of electrochemical recognition of cations, anions and neutral guest species by redox-active receptor molecules. Coord. Chem. Rev. 185-186 (1999): 3-36.
117. Medina, J. C.; Goodnow, T. T.; Rojas, M. T.; Atwood, J. L.; Lynn, B. C.; Kaifer, A. E.; and Gokel, G. W. Ferrocenyl iron as a donor group for complexed silver in ferrocenyldimethyl[2.2]cryptand: a redox-switched receptor effective in water. J. Am. Chem. Soc. 114 (1992): 10583-10595.
118. Beer, P. D.; Gale, P. A.; and Chen, G. Z. Electrochemical molecular recognition: pathways between complexation and signalling. J. Chem. Soc., Dalton Trans. (1999): 1897-1909.
119. Saji, T.; and Kinoshita, J. Electrochemical ion transport with ferrocene functionalized crown ether. J. Chem. Soc., Chem. Commun. (1986): 716-717.
120. Hall, C. D.; and Chu, S. Y. F. Cyclic voltammetry of cryptands and cryptates containing the ferrocene unit. J. Organomet. Chem. 498 (1995): 221-228.
121. Beer, P. D. Anion selective recognition and optical/electrochemical sensing by novel transition-metal receptor systems. Chem. Commun. (1996): 689-696.

122. Miller, S. R.; Gustowski, D. A.; Chen, Z. H.; Gokel, G. W.; Echegoyen, L.; Kaifer, A. E. Rationalization of the unusual electrochemical behavior observed in lariat ethers and other reducible macrocyclic systems. Anal. Chem. 60 (1988): 2021-2024.
123. Wopschall, R. H.; and Shain, I. Effects of adsorption of electroactive species in stationary electrode polarography. Anal. Chem. 39 (1967): 1514-1526.
124. Alexander, V. Design and synthesis of macrocyclic ligands and their complexes of lanthanides and actinides. Chem. Rev. 95 (1995): 273-342.
125. Furlan, R. L. E.; Otto, S.; and Sanders, J. K. M. Supramolecular templating in thermodynamically controlled synthesis. Proc. Natl. Acad. Sci. USA 99 (2002): 4801-4804.
126. Arman, S. A. V.; and Czarnik, A. W. A general fluorescence assay for enzyme catalyzed polyanion hydrolysis based on template directed excimer formation. Application to heparin and polyglutamate. J. Am. Chem. Soc. 112 (1990): 5376-5377.
127. Voet, D.; and Voet, J. G. Biochemistry. United State of America: John Wiley & Sons, Inc., 2004
128. Hasenknopf, B.; Lehn, J.-M.; Kneisel, B. O.; Baum, G.; and Fenske, D. Angew. Chem. Int. Ed. Engl. 35 (1996): 1838-1840.
129. Kieran, A. L.; Bond, A. D.; Belenguer, A. M.; and Sanders, J. K. M. Dynamic combinatorial libraries of metalloporphyrins: templated amplification of disulfide-linked oligomers. Chem. Commun. (2003): 2674-2675.
130. Haupt, K.; and Mosbach, K. Molecularly Imprinted Polymers and Their Use in Biomimetic Sensors. Chem. Rev. 100 (2000): 2495-2504.
131. Yannios, C. N.; and Karabinos. J. V. Oxidation of thiols by dimethyl sulfoxide. J. Org. Chem. 28 (1963): 3246-3248.
132. Wallace, T. J.; and Mahon, J. J. Reactions of thiols with sulfoxides. II. Kinetics and mechanistic implications. J. Am. Chem. Soc. 86 (1964): 4099-4103.

133. Wallace, T. J.; and Mahon, J. J. Reactions of thiols with sulfoxides. III. Catalysis by acids and bases. J. Org. Chem. 30 (1965): 1502-1506.
134. Otto, S.; Furlan, R. L. E.; and Sanders, J. K. M. Dynamic combinatorial chemistry. Drug Discov. Today 7 (2002): 117-125.
135. Otto, S.; Furlan, R. L. E.; and Sanders, J. K. M. Recent developments in dynamic combinatorial chemistry. Current Opinion in Chemical Biology 7 (2002): 321-327.
136. Epstein, D. M.; Choudhary, S.; Churchill, M. R.; Keil, K. M.; Eliseev, A. V.; and Morrow, J. R. Chloroform-soluble schiff-base Zn(II) or Cd(II) complexes from a dynamic combinatorial library. Inorg. Chem. 40 (2001): 1591-1596.
137. Katayev, E. A.; Pantos, G. D.; reshetova, M. D.; Khrustalev, V. N.; Lynch, V. M.; Ustynyuk, Y. A.; and Sessler, J. L. Anion-induced synthesis and combinatorial selection of polypyrrolic macrocycles. Angew. Chem. Int. Ed. 44 (2005): 1-5.
138. Furlan, R. L. E.; Ng, Y.-F.; Otto, S.; and Sanders, J. K. M. A new cyclic pseudopeptide receptor for Li⁺ from a dynamic combinatorial library. J. Am. Chem. Soc. 123 (2001): 8876-8877.
139. Roberts, S. L.; Furlan, R. L. E.; Otto, S.; and Sanders, J. K. M. Metal-ion induced amplification of three receptors from dynamic combinatorial libraries of peptide-hydrazones. Org. Biomol. Chem. 1 (2003): 1625-1633.
140. Lam, R. T. S.; Belenguer, A.; Roberts, S. L.; Naumann, C.; Jarrosson, T.; Otto, S.; and Sanders, J. K. M. Amplification of acetylcholine-binding catenanes from dynamic combinatorial libraries. Science 308 (2005): 667-669.
141. Otto, S.; Furlan, R. L. E.; and Sanders, J. K. M. Dynamic combinatorial libraries of macrocyclic disulfides in water. J. Am. Chem. Soc. 122 (2000): 12063-12064.
142. Petti, M. A.; Sheppard, T. J.; Barrans, R. E.; and Dougherty, D. A. "Hydrophobic" binding of water-soluble guests by high-symmetry, chiral hosts. An electron-rich receptor site with a general affinity for quaternary ammonium compounds and electron-deficient .pi. systems. J. Am. Chem. Soc. 10 (1988), 6825-6840.

143. Otto, S.; Furlan, R. L. E.; and Sanders, J. K. M. Selection and amplification of hosts from dynamic combinatorial libraries of macrocyclic disulfides. Science 297 (2002): 590-593.
144. Brisis, B.; Sanders, J. K. M.; and Otto, S. Selection and amplification of a catalyst from a dynamic combinatorial library. Angew. Chem. Int. Ed. 42 (2003): 1270-1273.
145. Brady, P. A.; Bonar-Law, R. P.; Rowan, S. J.; Suckling, C. J.; and Sanders, J. K. M. 'Living' macrolactonisation: Thermodynamically-controlled cyclisation and interconversion of oligocholates. Chem. Commun. (1996): 319-320
146. Anoardi, L.; and Tonellato, U. Catalysis of amide hydrolysis due to micelles containing imidazole and hydroxy functional groups J. Chem. Soc., Chem. Commun. (1977):401-402.
147. Kono, K.; Torikoshi, Y.; Mitsutomi, M.; Itoh, T.; Emi, N.; Yanagei, H.; Takagishi, T. Novel gene delivery systems: complexes of fusigenic polymer-polymer-modified liposomes and lipoplexes. Gene Therapy 8 (2001): 5-12.
148. Elizabeth, R.; Gillies, J. M.; and Fréchet, J. A new approach towards acid sensitive copolymer micelles for drug delivery. Chem. Commun. (2003):1640-1641
149. van der Wel, G. K.; Wijnen, J. W.; and Engberts, J. F. B. N. Solvent effects on a diels-alder reaction involving a cationic diene: consequences of the absence of hydrogen-bond interactions for accelerations in aqueous media. J. Org. Chem. 61 (1996): 9001-9005.
150. Peter, C.; Sanders, J. K. M.; and Otto, S. unpublished data.
151. Petter, R. C.; and Salek, J. S. Cooperative binding by an amphipathic host. J. Am. Chem. Soc. 109 (1987): 7897-7899.
152. Petter, R. C.; and Salek, J. S. Cooperative binding by aggregated mono-6-(alkylamino)-.beta.-cyclodextrins. J. Am. Chem. Soc. 112 (1990): 3860-3868.

153. Binkowski, C.; Hapiot, F.; Lequart, V.; Martin, P. and Monflier, E. Evidence of a self-inclusion phenomenon for a new class of mono-substituted alkylammonium- β -cyclodextrins. Org. Biomol. Chem. 6 (2005): 1129.
154. Jiang, J.; Tong, X.; and Zhao, Y. A new design for light-breakable polymer micelles. J. Am. Chem. Soc. 127 (2005): 8290-8291.
155. Wagner, B. D.; Boland, P. G.; Lagona, J.; and Isaacs, L. A cucurbit[6]uril analogue: Host properties monitored by fluorescence spectroscopy. J. Phys. Chem. B 109 (2005): 7686-7691.
156. Goodwin, A. P.; Mynar, J. L.; Ma, Y.; Fleming, G. R.; and Fréchet, J. M. J. Synthetic micelle sensitive to IR light via a two-photon process. J. Am. Chem. Soc. 127 (2005): 9952-9953.



สถาบันวิทยบริการ
จุฬาลงกรณ์มหาวิทยาลัย



APPENDICES

สถาบันวิทยบริการ
จุฬาลงกรณ์มหาวิทยาลัย



APPENDIX A

สถาบันวิทยบริการ
จุฬาลงกรณ์มหาวิทยาลัย

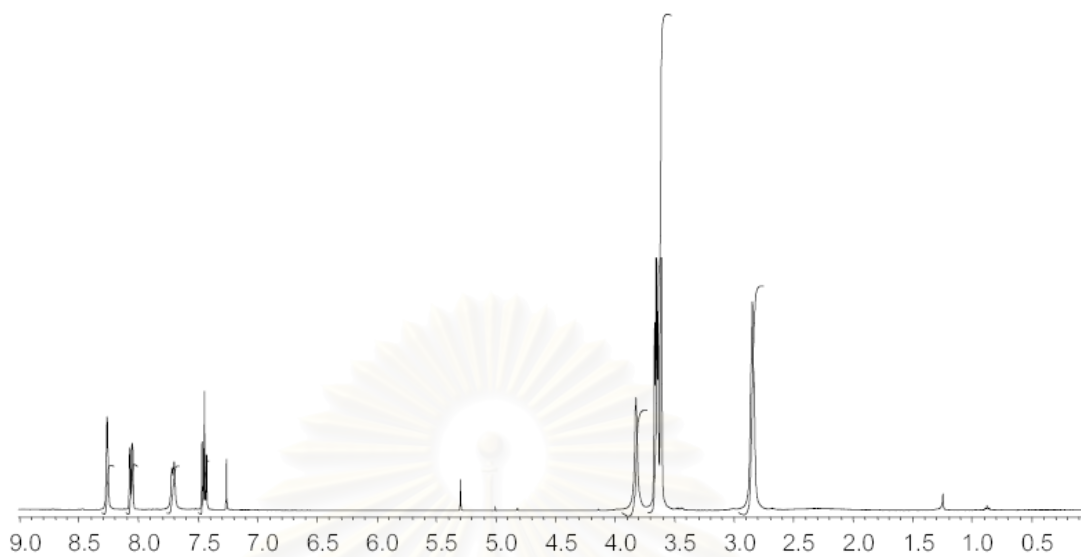


Figure A1. ^1H NMR spectra of *N,N'*-di-(3-aminobenzyl) 4,13-diaza-18-crown-6 (2c).

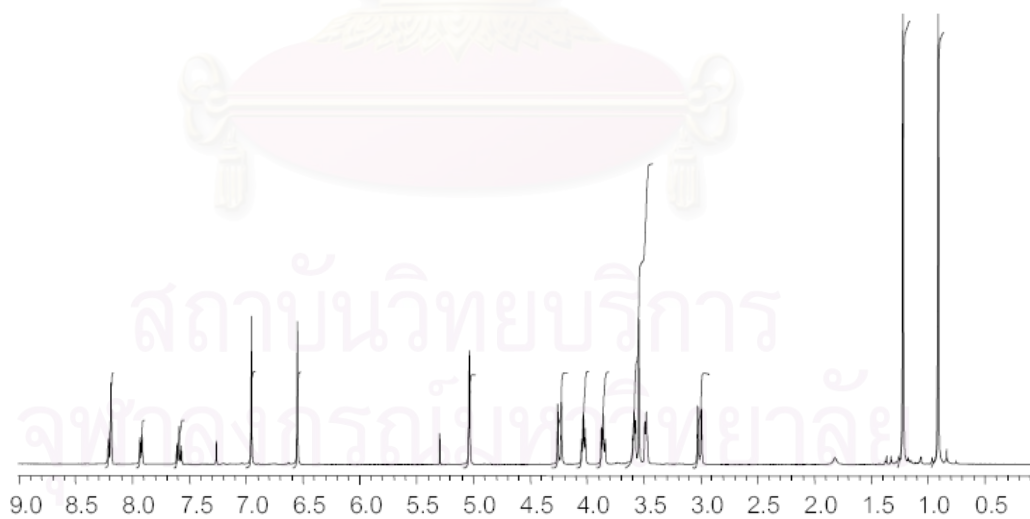


Figure A2. ^1H -NMR spectra of 5,11,17,23-Tetrakis(1,1-dimethyl ethyl)-25,27-di(3-nitrobenzyl) calix[4]arene-crown-6 (3b).

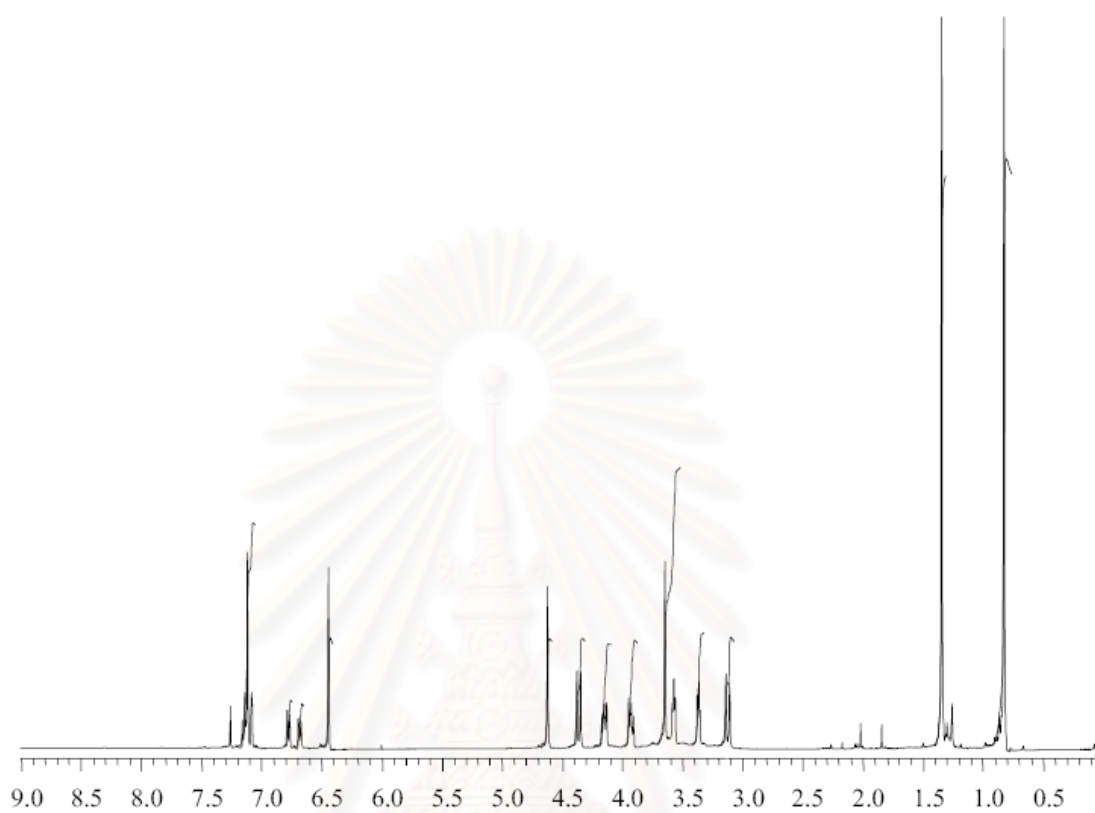


Figure A3. ^1H NMR spectra of 5,11,17,23-Tetrakis(1,1-dimethyl ethyl)-25,27-di(3-amino benzyl) calix[4]arene-crown-6 (3c).

สถาบันวิทยบริการ
จุฬาลงกรณ์มหาวิทยาลัย



APPENDIX B

สถาบันวิทยบริการ
จุฬาลงกรณ์มหาวิทยาลัย

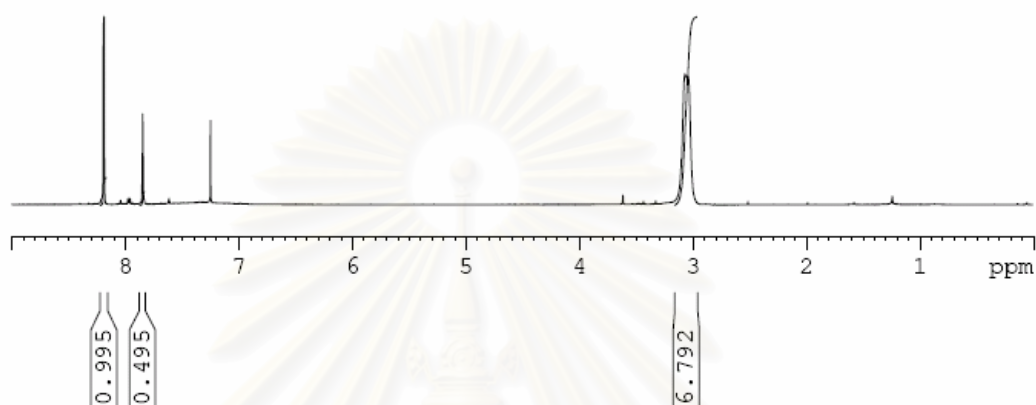


Figure B1. ^1H NMR spectrum of 3,5-bis-dimethylcarbamoylsulfanyl benzoic acid.

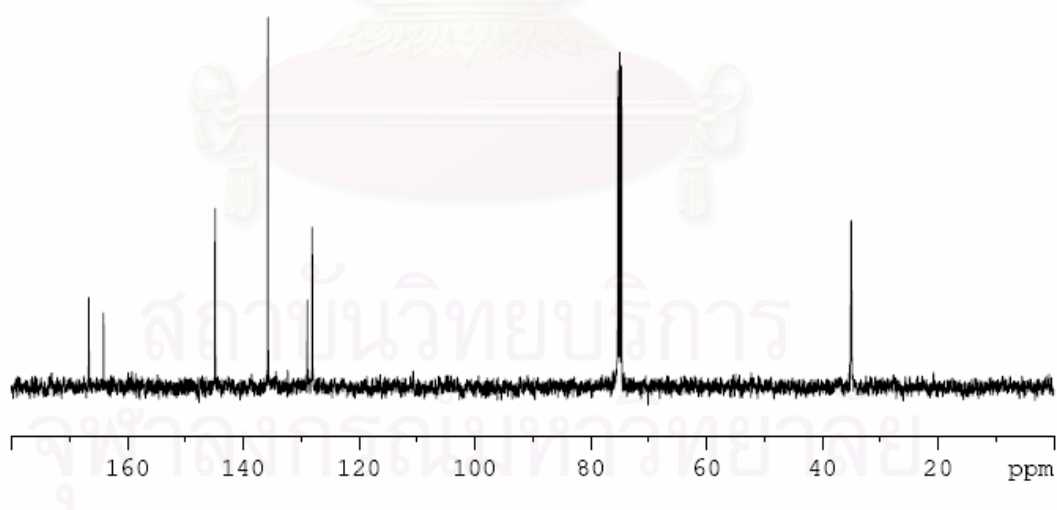


Figure B2. ^{13}C NMR spectrum of 3,5-bis-dimethylcarbamoylsulfanyl benzoic acid.

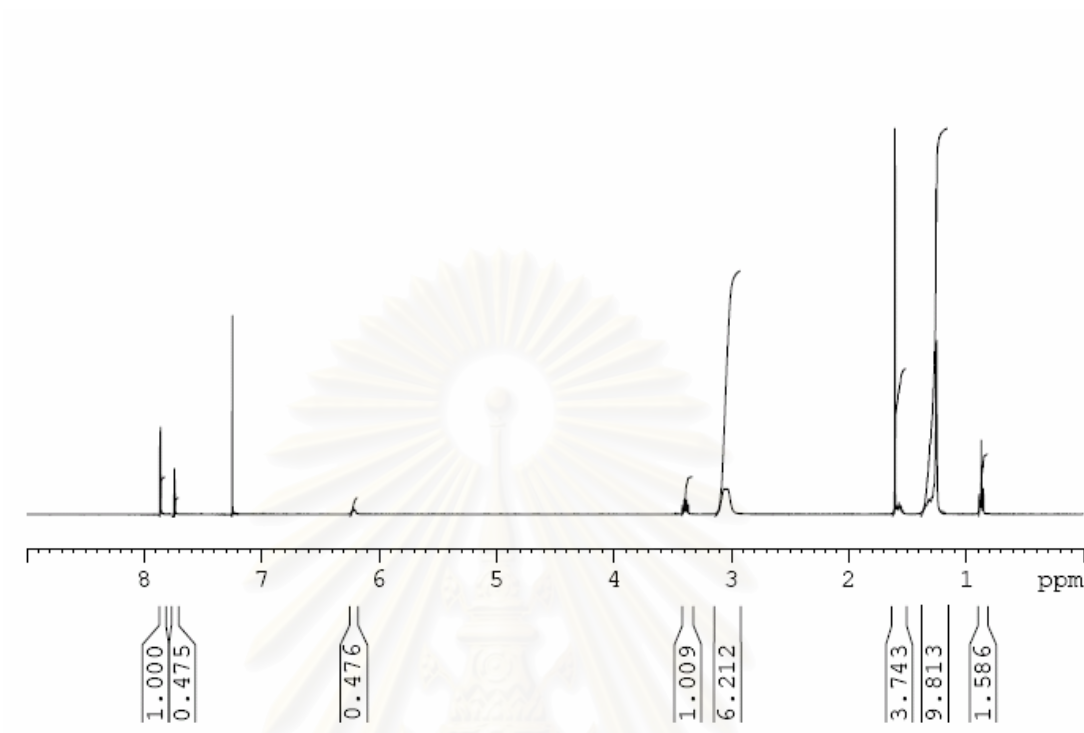


Figure B3. ^1H NMR spectrum of *N*-dodecyl-3,5-dimethylcarbamoyl sulfanyl benzamide.

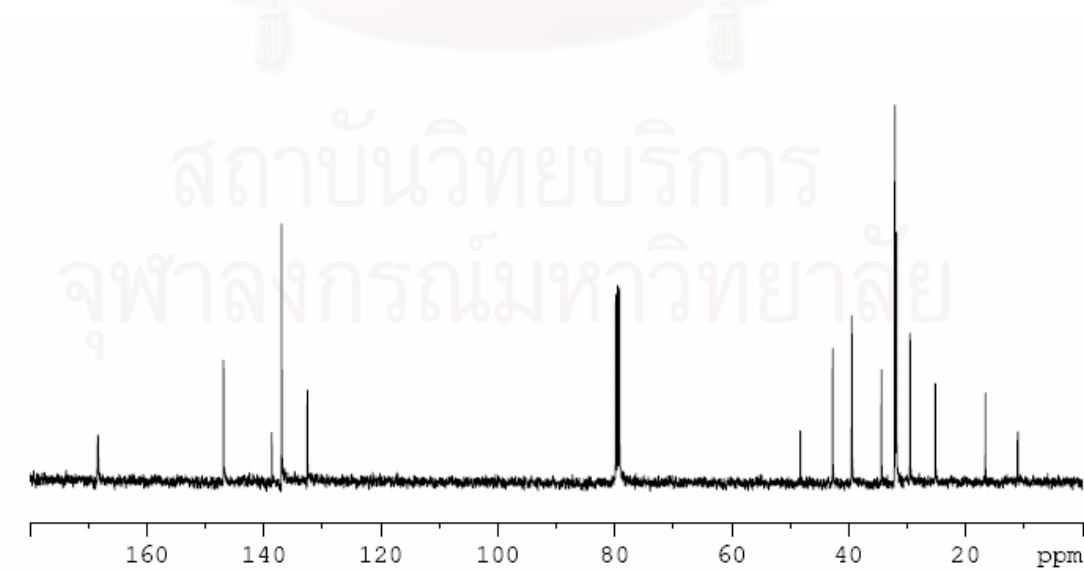


Figure B4. ^{13}C NMR spectrum of *N*-dodecyl-3,5-dimethylcarbamoyl sulfanyl benzamide.

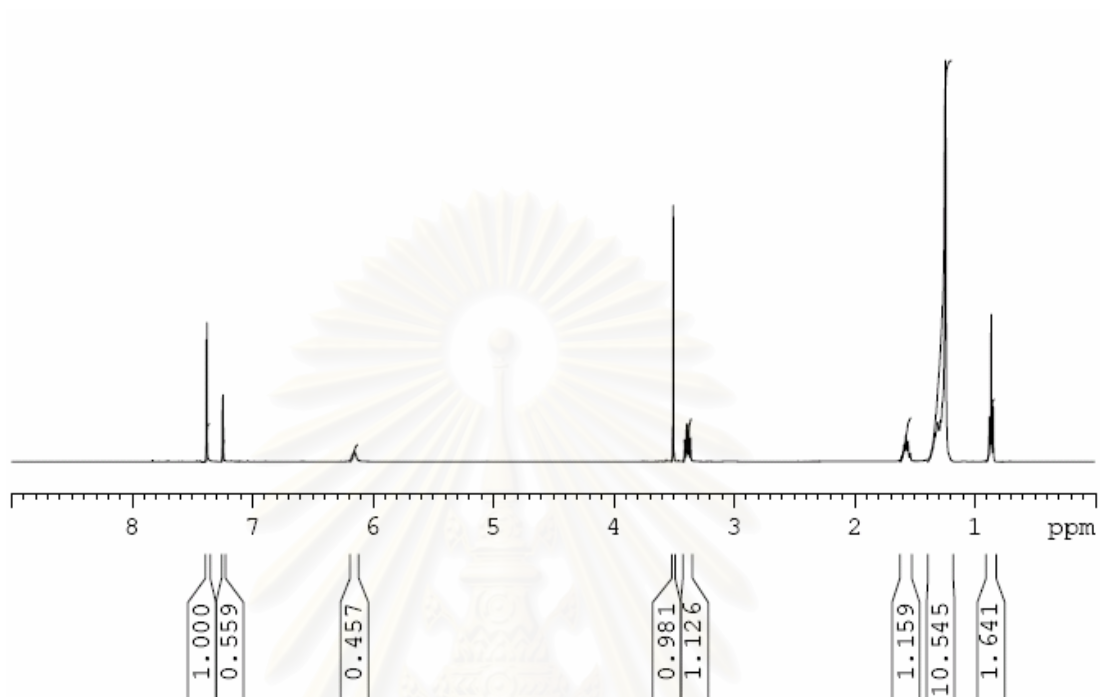


Figure B5. ^1H NMR spectrum of *N*-dodecyl-3,5-dimercaptobenzamide.

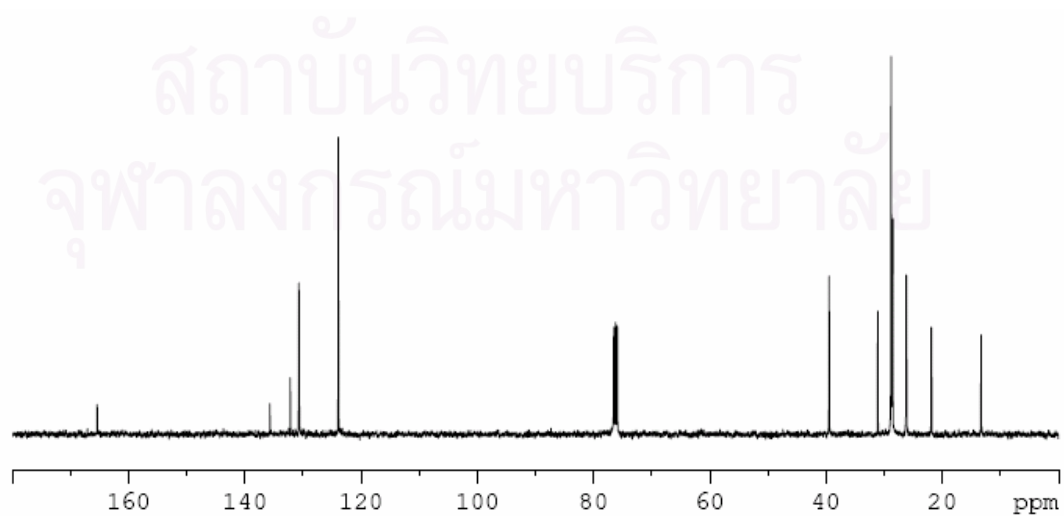


Figure B6. ^{13}C NMR spectrum of *N*-dodecyl-3,5-dimercaptobenzamide.

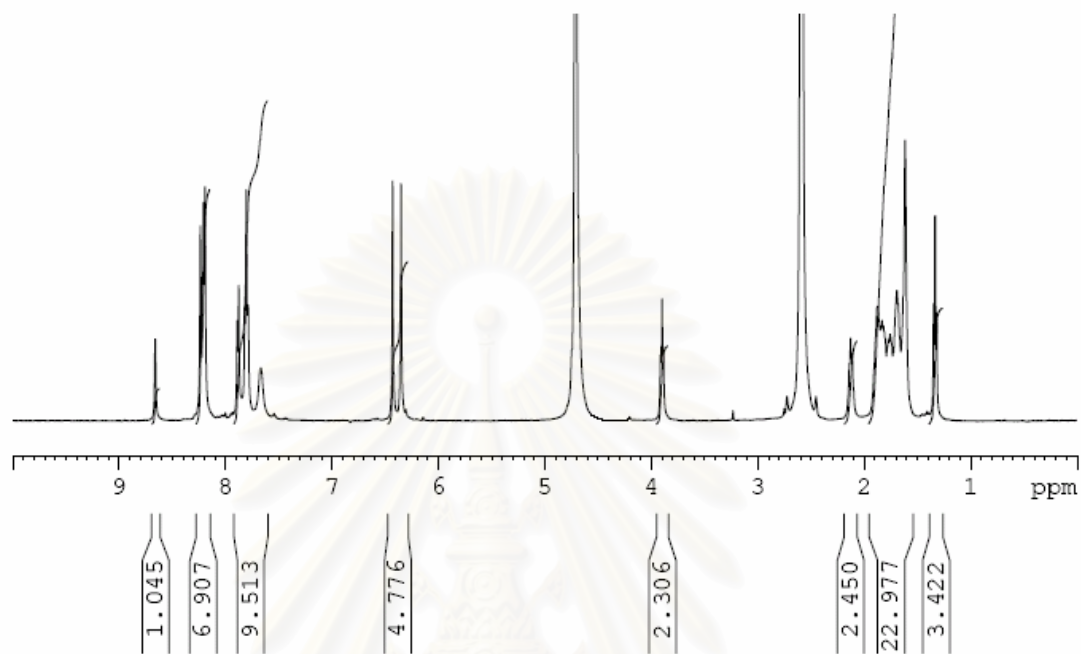


Figure B7. ^1H NMR spectrum of receptor **8b** rac isomer.

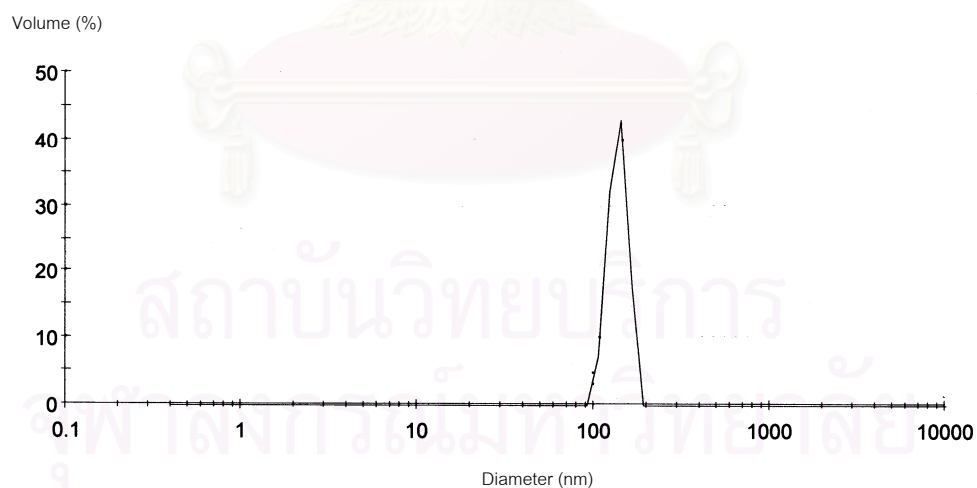


Figure B8. Dynamic Light Scattering data for a solution of **8b** (0.1 mg/mL in 10 mM borate buffer pH 9). The graph represents the volume average taken over 14 measurements.

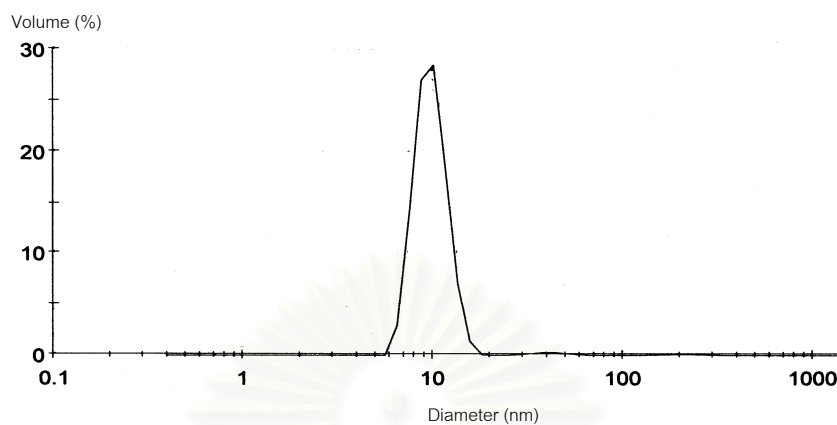


Figure B9. Dynamic Light Scattering data for a solution of **8b**·**10** (0.1 mg/mL of **8b** and 4 equivalent of guest **10**) in 10 mM borate buffer pH 9. The graph represents the volume average taken over 14 measurements.

สถาบันวิทยบริการ
จุฬาลงกรณ์มหาวิทยาลัย

VITA

Miss Chomchai Suksai was born in July 16, 1976 in Chonburi, Thailand. She graduated with high school from Chongyunanukul School, Chonburi in 1994. She received her Bachelor's degree of Science in Chemistry from Burapha University in 1998. Then, she received her Master's degree of Science in Applied Analytical and Inorganic Chemistry from Mahidol University in 2002. Since then she has been a postgraduate student studying inorganic chemistry and become a member of Supramolecular Chemistry Research Unit under the supervision of Associate Professor Thawatchai Tuntulani. During this period, her financial support is granted by "The Royal Golden Jubilee (RGJ)" from the Thailand Research Fund (TRF). She had an opportunity to do the research under the supervision of Dr. Sijbren Otto at the University of Cambridge, England in 2004-2005 with the financial support from RGJ and EPSRC grants. She graduated with a doctorate degree in chemistry in the academic year 2006.

Publications

1. Suksai, C.; Gómez, S. F.; Chhabra, A.; Liu, J.; Skepper, J. N.; Tuntulani, T.; and Otto, S. Controlling the morphology of aggregates of an amphiphilic synthetic receptor through host-guest interactions. Langmuir 22 (2006): 5994-5997.
2. Suksai, C.; Leeladee, P.; Jainuknan, D.; Tuntulani, T.; Muangsin, N.; Chailapakul, O.; Kongsaree, P.; and Pakavatchai, C. A new heteroditopic receptor and sensor highly selective for bromide in the presence of a bound cation. Tetrahedron Lett. 46 (2005): 2765-2769.
3. Suksai, C.; and Tuntulani, T. Chromogenic anion sensors. Top. Curr. Chem. 255 (2005): 163-198.
4. Suksai, C.; and Tuntulani, T. Chromogenic anion sensors. Chem. Soc. Rev. 32 (2003): 192-202.